The Examination of Mechanisms Underlying Meiotic Chromosome Segregation

by

Gloria Ann Brar
B.A. Molecular and Cellular Biology,
University of California, Berkeley

SUBMITTED TO THE DEPARTMENT OF BIOLOGY IN PARTIAL FULFILLMENT OF THE REQUIREMENTS FOR THE DEGREE OF

DOCTOR OF PHILOSOPHY IN BIOLOGY
AT THE
MASSACHUSETTS INSTITUTE OF TECHNOLOGY

ARCHIVES

MAY 2008

Signature of Author:_____
Department of Biology
May 23, 2008

Certified by:_____
Angelika Amon
Professor of Biology
Thesis Supervisor

Accepted by:_____
Stephen P. Bell
Professor of Biology
Chair, Committee for Graduate Students

The Examination of Mechanisms Underlying Meiotic Chromosome Segregation

by

Gloria Ann Brar

Submitted to the Department of Biology
on May 23, 2008 in Partial Fulfillment of the
Requirements for the Degree of Doctor of Philosophy in Biology

ABSTRACT

Meiosis is the cell division by which gametes are produced. Meiotic chromosome segregation differs from Mitotic segregation in that one DNA replication phase is followed by two chromosome segregation phases. This allows generation of haploid products from a diploid precursor cell and depends on a number of cellular specializations that allow completion of a reductional segregation phase, in which homologous chromosomes segregate apart. I have investigated several mechanisms that contribute to meiotic segregation, including stepwise loss of meiotic cohesion, proper prophase progression and homolog pairing. I have found that stepwise cohesion loss is regulated by multiple mechanisms, including bulk phosphorylation of the meiotic cohesin Rec8. I also find that homolog linkage resulting from recombination regulates stepwise cohesion loss. Additionally, I present data that Rec8 plays an additional cellular role that is separable from its function as a cohesin. Rec8 is important for assembly of the Synaptonemal Complex (SC) and meiotic prophase progression. Like Rec8's cohesin role, this prophase role appears to be influenced by Rec8 phosphorylation. Finally, I present a basic characterization of the process of homolog pairing in early meiosis. I find that pairing is independent of DNA replication, but depends on cohesins, actin filaments, SC components and DSBs.

Thesis Supervisor: Angelika Amon
Title: Professor of Biology

This thesis is dedicated to my parents, Dorothy Watson Brar and Gurdip Singh Brar and my brother Victor Watson Brar

Acknowledgements:

The work in this thesis would not have been possible without past and present members of the Amon lab: Britt Adamson, Michelle Attner, Monica Boselli, Ilana Brito, Thomas Carlile, Leon Chan, Georgette Charles, Jenny Cimino, Damien D'Amours, Katie D'Aquino, Ly-sha Ee, Sheryl Elkin, Nina Glazier, Christian Gonzales, Alexi Goranov, Andreas Hochwagen, Karen Hunter, Ashwini Jambhekar, Brendan Kiburz, Annie Kloimwieder, Brian Lee, Adele Marston Matt Miller, Fernando Monje-Casas, Vineet Prabhu, Jocelyn Provost, Rami Rahal, Vladimir Reiser, Jeremy Rock, Anupama Seshan, Tanya Sokolsky, Frank Stegmeier, Yun-Chi Tang, Brett Tomson, Eduardo Torres, Elcin Unal, Rosella Visintin, Bret Williams. They have all contributed significantly to my graduate work and my life. I am especially grateful to Andreas, Brendan and Brian, who were great scientific influences in my time in the lab and Brett, Monje, Anu, Leon, Matt and Michelle, who have shown me extraordinary friendship.

Collaborators were essential to the work described within, particularly Forest White and his lab. I am also grateful to Scott Keeney, Shirleen Roeder, Franz Klein, Nancy Hollingsworth, Michael Lichten, Doug Koshland, Andrew Murray, Nancy Kleckner, and Steve Bell for strains and reagents.

Special thanks to my thesis committee of Phil Sharp, Steve Bell and Gerry Fiink for their input and support and Jim Haber for his participation in my thesis defense.

I would also like to acknowledge members of the MIT community, including the Biograd class of 2002, with special thanks to Ann Cheung and Keara Lane.

My family and friends have contributed immensely to my life throughout my time in grad school. Thanks to Lisa Anusasunanan, Adrienne Rand, Lyndsey Yoshino, and Jenny Velasco. Emphatic thanks to my parents, Dorothy and Gurdip, my brother, Victor, and Dan Mulcahy for their support and love.

Finally, I am hugely indebted to Angelika for her constant support, brilliance and humor.

Table of contents

Chapter 1:

Introduction

Abstract

In meiosis, chromosomes undergo two rounds of chromosome segregation with no intervening DNA replication step. This variation from mitotic segregation, in which DNA replication and chromosome segregation alternate, requires meiotic specializations including attachment of homologs through recombination, coorientation of sister kinetechores, and differential regulation of the meiotic cohesin Rec8 at the two meiotic divisions. The remarkable conservation of meiotic mechanisms has allowed rapid progress in meiosis research. Many significant mysteries remain, however, including how homologous chromosomes find each other in early prophase. Addressing these and other questions, will likely be important to better understand human conditions based on meiotic defects, such as aneuploidy and infertility. This thesis describes work towards understanding mechanisms of meiotic chromosome segregation. I will describe characterization of the multiple roles of the meiotic cohesin Rec8 and its phosphorylation in meiotic progression, as well as a basic characterization of the mechanism by which homologs pair in prophase.

Why meiose?

An important property of life is the ability to reproduce. Countless early life-like forms likely perished without passing along their newly evolved characteristics. A breakthrough in the evolution of life came when cells gained the ability to divide clonally through a process that has presumably been modified over generations to become mitosis. Mitosis allows single-celled organisms to reproduce asexually and allows multi-cellular organisms to develop complex body plans. For cells to divide mitotically they must first replicate their DNA, then segregate this genetic matter to create two cells with identical DNA content to each other and the precursor cell. Due to impressive efforts by numerous investigators, we now understand much of how these cellular goals are achieved on a molecular level and ongoing research continues to illuminate elegant mechanisms by which mitotsis is performed accurately.

Mitosis is not, however, the only mechanism developed by organisms to pass on their genetic information. The likely later-evolved and less studied process of meiosis allows for sexual reproduction, such that organisms can pass on their genetic information while simultaneously creating new genetic combinations and potentially increasingly robust or specialized offspring. Meiosis is the process by which a single cell divides to form products with identical amounts of DNA to each other, but a halved genome with respect to the (generally) diploid precursor cell. Meiotic products, called gametes in complex organisms, are not necessarily genetically identical. Two gametes,

frequently from different parental organisms, can thus fuse to produce unique offspring with a unique genetic makeup. Meiosis is therefore not just an alternative mechanism by which organisms can reproduce, it is a process central to modern biological diversity.

Based on the many conserved factors and mechanisms between meiotic and mitotic events, meiosis almost certainly evolved as a modified mitotic division. To halve the genome in meiosis, one DNA replication phase is followed by two DNA segregation phases, rather than the single segregation step seen in mitosis (Figure 1). Achieving two stages of DNA segregation involves a number of meiotic specializations, which will be discussed in detail here. First, however, we will take a walk through meiosis, touching on major events that occur as cells execute the meiotic program and highlighting the importance of regulation of meiotic timing and order (Marston and Amon 2004).

Figure 1

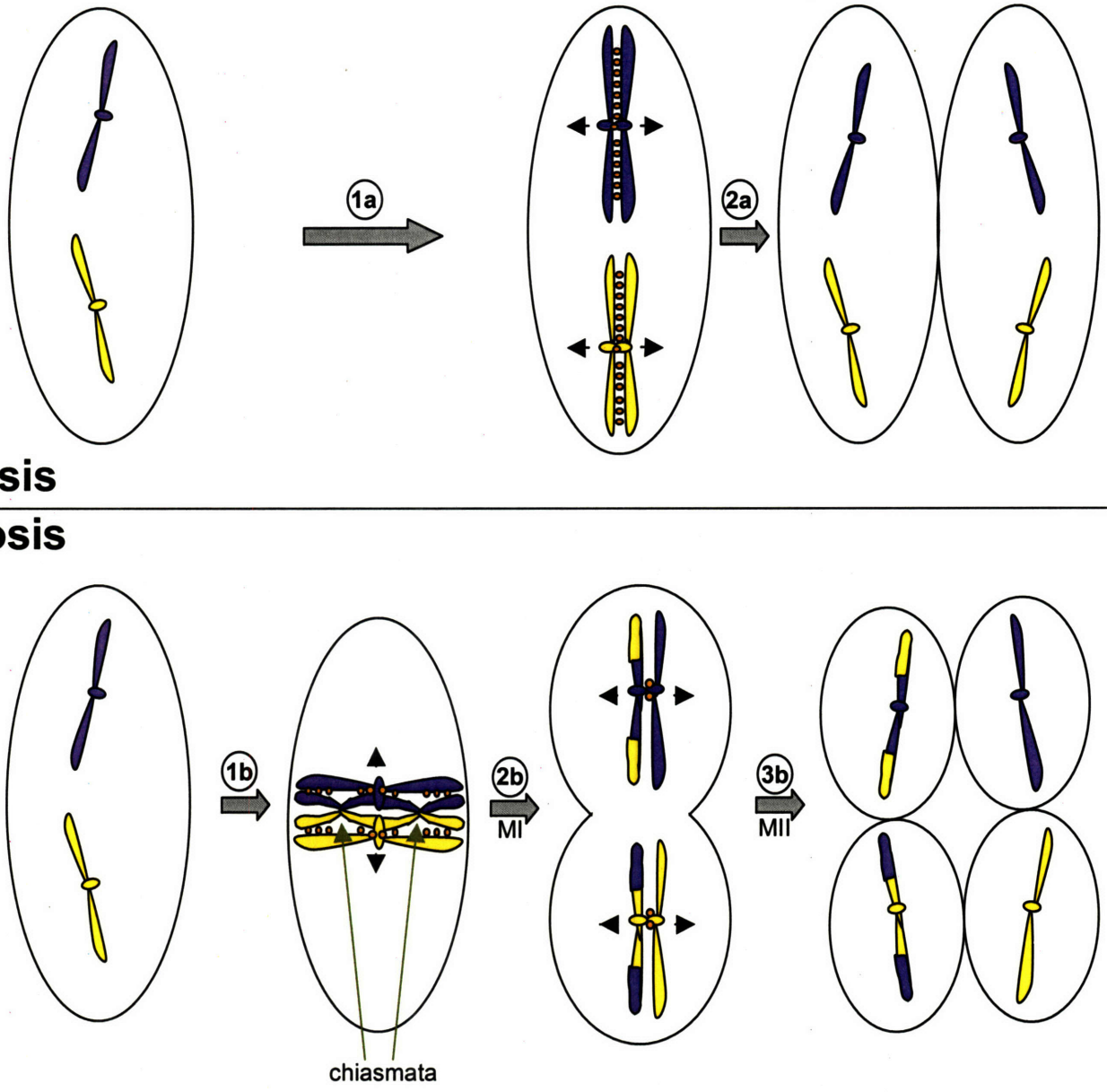

Figure 1: Mitotic versus Meiotic Segregation
Mitotic cells undergo a single round of DNA replication (1a) followed by a single round of chromosome segregation (2a). Meiotic cells also undergo one round of DNA replication (1b), but this is followed by two rounds of chromosome segregation (2b, 3b). At Meiosis I (2b), linked homologous chromosomes segregate apart in a reductional segregation. In Meiosis II (3b), sister chromatids segregate in an equational division much like that seen in meiosis (2b). There is no intervening DNA replication round between MI and MII so that meiosis creates four haploid products from one diploid progenitor. Note that this figure only follows one pair of homologs for simplicity, with the "dad chromosome" in yellow and the "mom chromosome" in blue (Marston and Amon 2004).

A walk through meiosis in budding yeast

Entry into meiosis and DNA replication

Meiotic mechanisms are highly conserved throughout nature. For the introduction to meiosis presented here, I will focus primarily on meiosis in the budding yeast *Saccharomyces cervisiae*, as this organism is highly tractable for genetic and molecular studies and is the organism in which I have performed my thesis work. From my work and the investigations of many other investigators, the meiotic program of *S. cerevisiae* has now been relatively well studied, providing a coherent framework upon which to base future studies.

Meiosis in diploid *S. cerevisiae* cells is initiated upon nitrogen starvation and lack of a fermentable carbon source. Primary regulation occurs at the transcriptional level with the presence of both a and ∝ mating types, the absence of nitrogen and a fermentable carbon source all feeding in to transcriptional regulation of the master regulator of meiosis, *IME1* (Inducer of Meiosis 1). Ime1 is itself a transcription factor that is responsible for activating a number of early meiotic genes including factors required for DNA replication and prophase events (Kassir, Adir et al. 2003).

Meiotic DNA replication occurs shortly following meiotic initiation. The mechanism of meiotic replication appears to be very similar to mitotic replication. The ORC (Origin Recognition Complex) binds origins of DNA replication and recruits a number of factors including Cdc6 (Cell Division Cycle

6) and MCM (Mini Chromosome Maintenance) hexamers, which act as the replication helicases. These factors together form the pre-Replicative Complex (pre-RC). CDK (Cyclin Dependent Kinase) activity, specifically through CDK association with B-type cyclins Clb5 and Clb6, activates origins, resulting in the initiation of DNA replication. Newly created sister chromatids are immediately tethered to each other through establishment of sister chromatid cohesion by the cohesin complex (Dirick, Goetsch et al. 1998; Stuart and Wittenberg 1998; Smith, Penkner et al. 2001).

The cohesin complex consists of four core subunits. Three of these components- Smc1 (Structural Mainenance of Chromosomes 1), Smc3, Scc3 (Sister Chromatid Cohesion 3)- are identical in mitotic and meiotic cohesin, while one component- Scc1 in mitosis- is replaced by Rec8 (Recombination factor 8) in meiosis. The cohesin complex forms a ring-like structure that seems to be loaded onto a given genome region as that region is replicating (Figure 2) (Uhlmann 2003). It has been shown that a factor required for establishment of cohesion, Eco1 (Establishment of cohesion 1) interacts with the replication machinery including DNA polymerase, indicating that cohesin is loaded in conjunction with DNA replication (Ivanov, Schleiffer et al. 2002; Skibbens, Maradeo et al. 2007). Interestingly, whereas cohesin loading appears to depend on the DNA replication machinery, the efficiency of replication also appears to depend on the presence of Rec8, indicating some mechanistic interdependence between these two processes (Cha, Weiner et al. 2000). The method by which this newly-loaded cohesin holds sisters together is the subject of some

controversy. Based on studies to date, it is not clear whether a cohesin ring envelopes both sister chromatids or whether each sister is encircled by a single cohesin ring at a given site, and then two cohesin rings click together to create cohesion (Huang, Milutinovich et al. 2005; Ivanov and Nasmyth 2005; Nasmyth 2005; Nasmyth and Haering 2005). In either case, the establishment of sister chromatid cohesion is, along with DNA replication, a similarly vital event in meiotic and mitotic S phase.

Meiotic S-phase versus mitotic S-phase

It has been shown that cells utilize largely similar origins, the same core replication factors, and that replication itself occurs at a similar rate in both mitosis and meiosis. Paradoxically, studies show that meiotic S-phase lasts approximately twice as long as mitotic S phase in every organism examined thus far (Forsburg 2002). Therefore, it seems likely that there are meiotic replication specializations that have not yet been explained. One difference between meiotic and mitotic DNA replication is based on Clb specificity. In mitosis, cells can replicate relatively normally even in the absence of the so-called S-phase cyclins, Clb5 and Clb6. It appears that other cyclins are capable of activating pre-RCs in conjunction with CDK under these circumstances (Schwob and Nasmyth 1993). In contrast, meiotic cells do not undergo DNA replication in the absence of Clb5 and Clb6 (Smith, Penkner et al. 2001). The reason for this meiotic variation is unclear, although recent work shows other cases of increased cyclin specificity in meiosis relative to mitosis (Carlile and

Amon 2008). It is possible that *S. cerevisiae* cells have evolved and retained so many cyclins (six of the B-type alone) simply for use in the complex meiotic program, while in mitosis these extra cyclins provide little advantage. It is also possible that the lower nutrient levels in meiotic cells compared to mitotic cells precludes expression of other B-type cyclins in S-phase and also slows down S-phase events.

Alternatively, it has been hypothesized that meiotic cells spend more time in S-phase than mitotic cells in order to set up later meiotic prophase events(Forsburg 2002). In support of this theory, it has been demonstrated that recombination initiation through formation of double-strand DNA breaks (DSBs) is tightly correlated to replication timing. A series of elegant experiments by Borde and colleagues show that DSBs form in a certain genome region approximately 2 hours after that region has undergone DNA replication. Local delays in replication result in proportional local delays in DSB formation. Thus, it has been suggested that a checkpoint response is set up during meiotic S-phase such that DSBs do not form before a region has undergone replication (Borde, Goldman et al. 2000). It is not entirely clear why such a checkpoint would be necessary, as meiotic chromosomes preferentially repair DSBs from their homolog rather than their sister chromatid, but it seems likely that chromosome structure is important for proper completion of complex prophase events such as recombination, and that S-phase events, particularly establishment of sister-chromatid cohesion, are important for setting up some elements of this structure. Additionally, replication would be significantly more

difficult for cells if a DNA region already had DSBs present as the replication fork moved through that particular region.

Figure 2

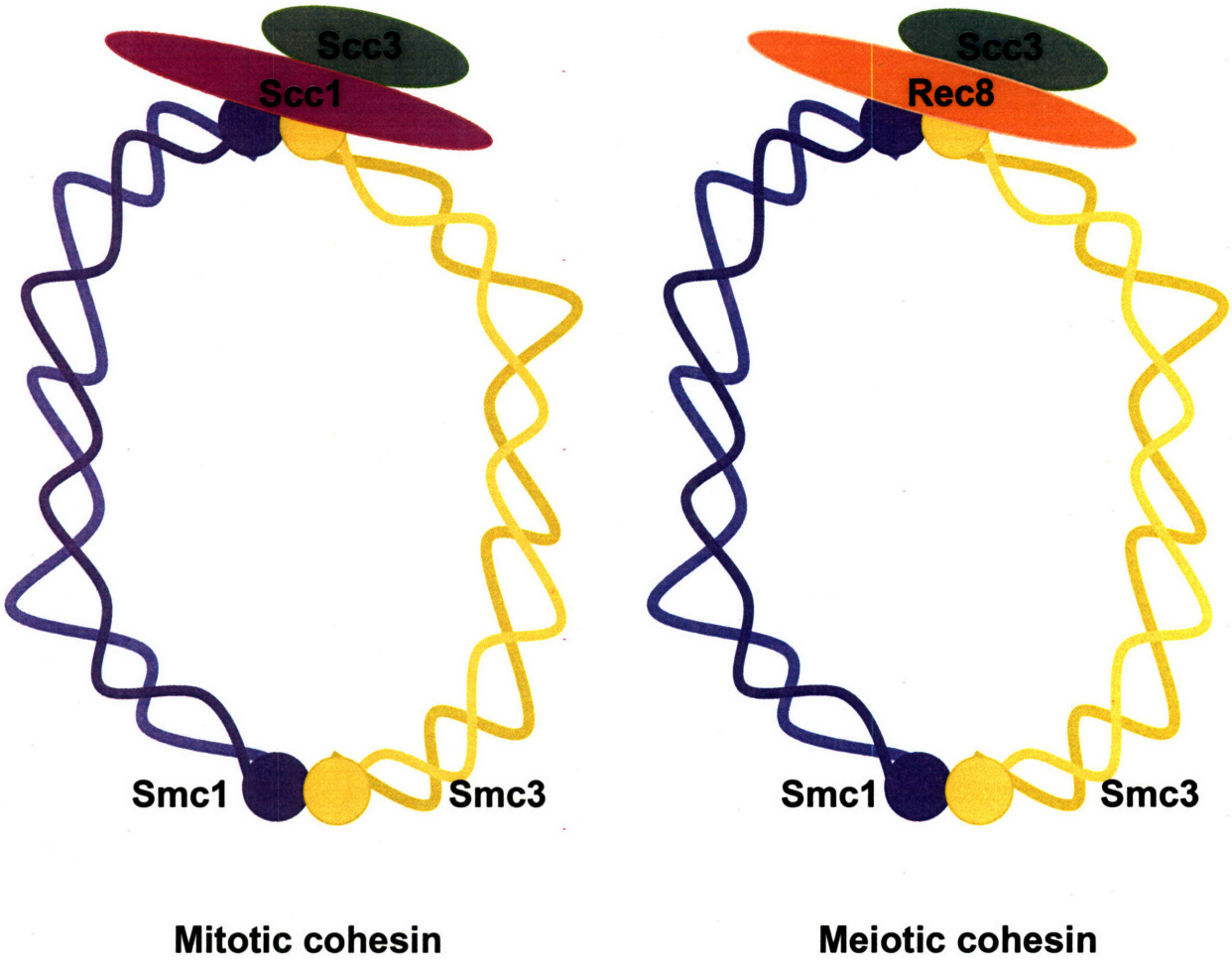

Figure 2: Mitotic versus meiotic cohesin
Cohesin is a ring-shaped complex consisting of four core proteins. Smc1, Smc3 and Scc3 are part of both the mitotic and meiotic cohesin complex, while Scc1 is replaced by Rec8 in meiosis. It is unclear whether the cohesin ring loops around both sisters together, or whether two cohesins, each surrounding a sister, dimerize to create cohesion. Cleavage of Scc1 in mitosis and Rec8 in meiosis releases sister chromatid cohesion.

Adapted from (Uhlmann 2003)

Meiotic prophase

The majority of early meiosis research has focused heavily on prophase chromosome structure. This is largely a result of the exquisite and well-conserved series of microscopically-visible changes that prophase chromosomes undergo, combined with the limited genetic, biochemical and molecular tools available to researchers until the last few decades. Chromosomes in early prophase are in a largely uncompacted stage, possibly as a result of chromatin disruption during DNA replication. As cells progress through prophase, chromosomes increase their compaction in cytologically distinct stages. Description of these stages- leptotene, zygotene, pachytene, diplotene, and diakenesis- served as the basis for much early understanding of meiotic prophase (Figure 3) (Zickler and Kleckner 1998). Indeed, with modern techniques, it can be shown that cytological prophase stages correlate closely with core prophase events, such as pairing, recombination and synaptonemal complex (SC) formation. SC formation, in particular has been well correlated with chromosome condensation (Figure 3) (Zickler and Kleckner 1999; Henderson and Keeney 2004; Storlazzi, Tesse et al. 2008). The formation of Axial Elements (AEs, also called Lateral Elements or LEs) that assemble along chromosomes as an early step in SC formation serve as a scaffold for the condensing meiotic DNA. AEs are composed of a number of proteins, including Rec8 and the early meiotic protein Hop1 (Homolog pairing 1). Transverse elements (TEs) then join the AEs of homologous chromosomes to form mature

SC. A major component of TEs is the coiled coil protein Zip1, named for its ability to "zip up" homologs during mid to late prophase. Zip1 is initially present in an extra-DAPI cluster called a Polycomplex (PC). Zip1 then associates in foci on chromosomes and eventually forms visible ribbons as it zips AEs together. The SC is thought to stabilize homologous chromosomes as they undergo the complex process of recombination. Following recombination, in late prophase, Zip1 ribbons disappear from chromosomes so that homologs can more efficiently segregate at anaphase I. The function of the SC is not well elucidated despite volumes of research on the topic. Interestingly, the SC structure is extremely well conserved between species, though there is minimal sequence conservation of SC proteins. The model most consistent with the current literature suggests that Zip1 helps stabilize condensing chromosomes and recombination intermediates (Page and Hawley 2004; Revenkova and Jessberger 2006). It is unclear, however, whether the dramatic changes seen in prophase chromosome structure are the cause of or rather just visual manifestations of core prophase events such as pairing and recombination, which, as will be discussed in some detail later, are essential to enable proper meiotic segregation.

Figure 3

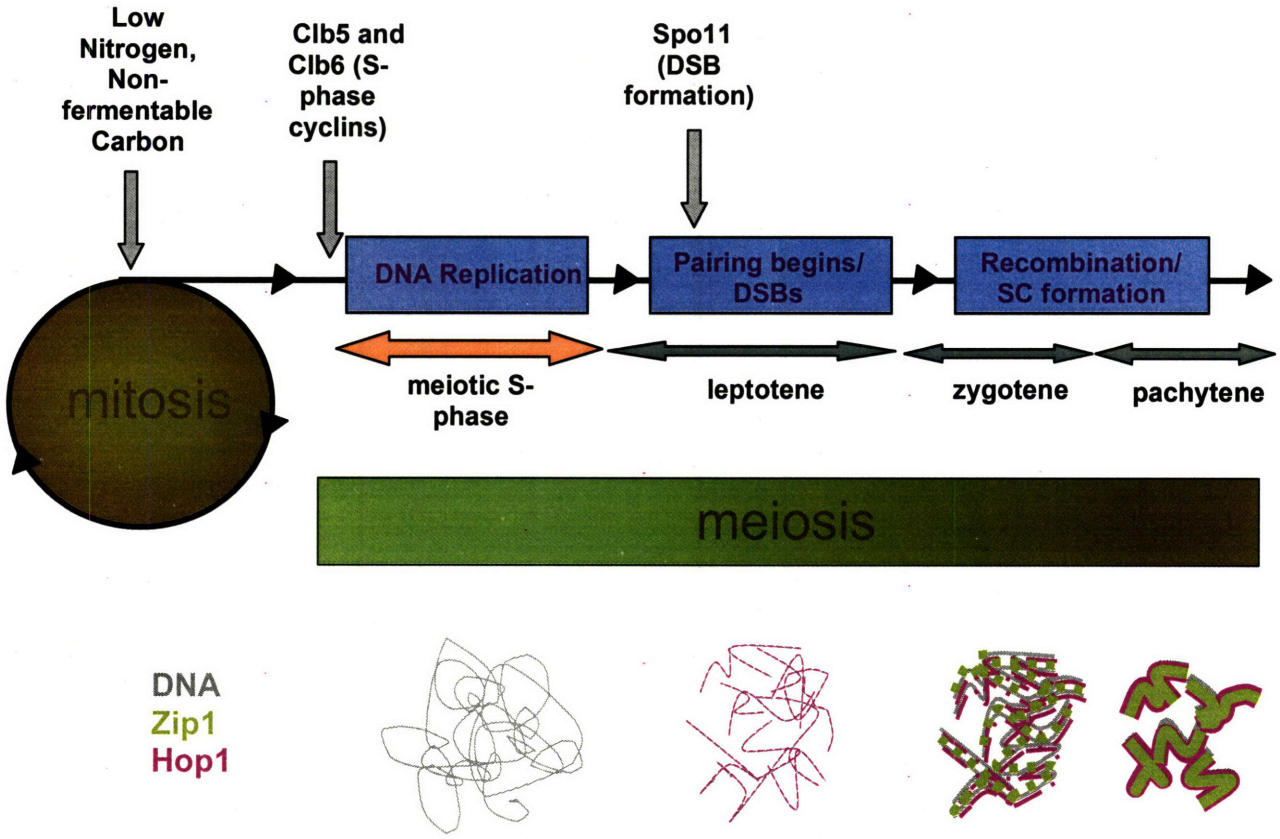

Figure 3: Meiotic entry, S-phase and prophase events
Upon Nitrogen starvation and the absence of a fermentable Carbon source, *S. cerevisiae* enter the meiotic program. Meiotic DNA replication utilizes B-type cyclins Clb5 and Clb6 to initiate DNA replication. Following S phase, meiotic cells enter prophase. Prophase includes number of cytologically defined stages including leptotene, zygotene and pachytene. Diplotene and diakineses follow pachytene, but are not included in this diagram. The meiotic events occuring during each stage are noted in the blue boxes above the meiotic stage names. At the bottom of the figure is a schematic of chromosome structure and SC asssembly at the different stages of prophase. Lateral elements (LEs), including Hop1 assemble onto chromosomes first to form axes. These LEs are connected by the coiled-coil protein Zip1, which stabilizes both homolog axes by "zipping" them together.

Figure 4

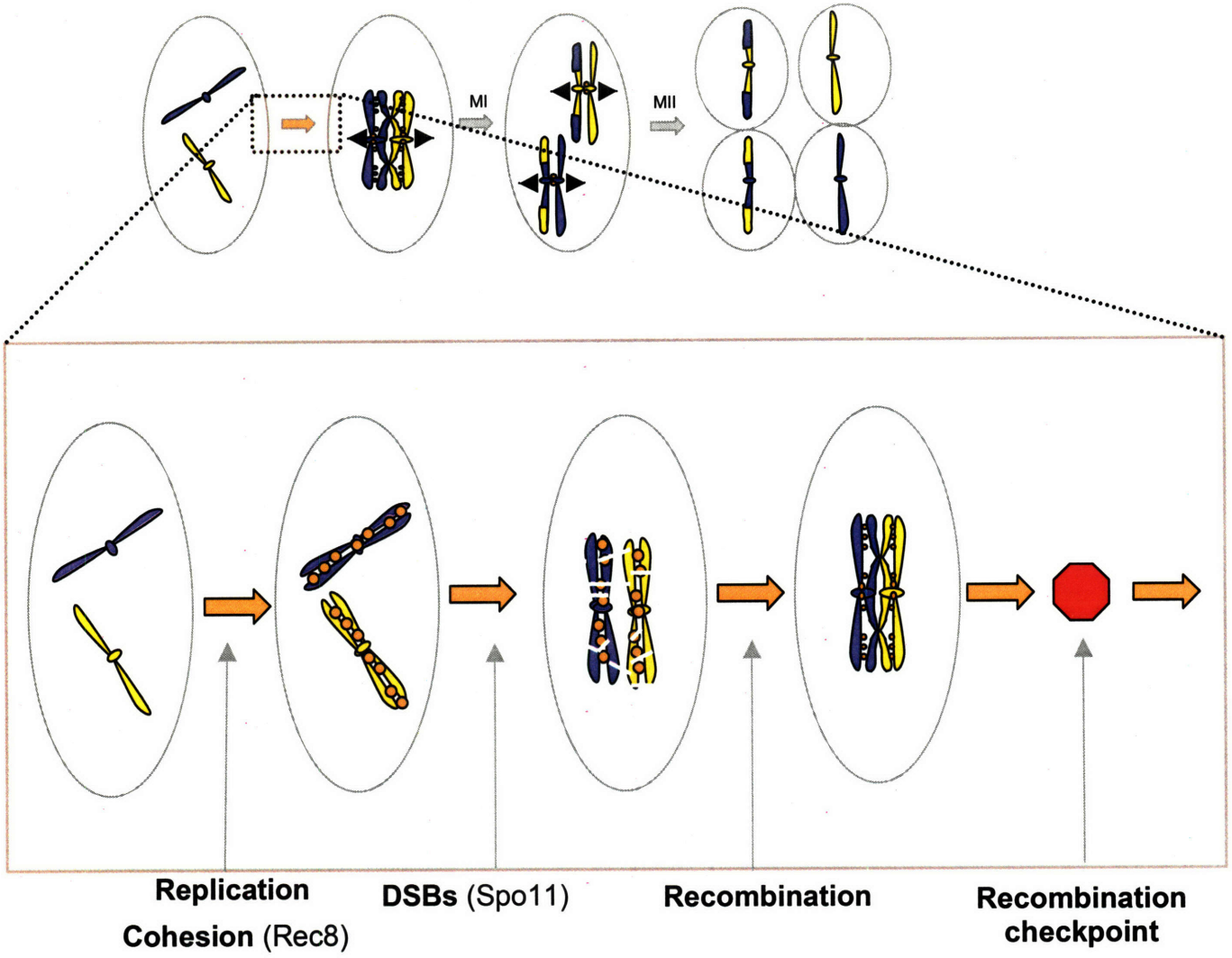

Figure 4: Prophase events
Another schematic of prophase events is shown above, highlighting the importance of the Recombination checkpoint in regulating passage out of meiotic prophase and into segregation phases.

Late prophase checkpoint control

Following a number of complex prophase events, homologous chromosomes are linked at the DNA level as a result of recombination, as well as through cohesin linking sister chromatids (Figure 4). Successful completion of this structure appears to be the major goal of meiotic prophase, after which cells are prepared to enter the meiotic divisions. Prophase exit, much like meiotic entry, is primarily regulated at the transcriptional level, with the transcription factor Ndt80 (Non-diTyrosine 80, note that diTyrosine is a component of mature spore walls) serving as the central regulator. Ndt80 activates expression of the so-called middle meiotic genes, which include factors important for chromosome segregation such as Clb1, Clb3 and Clb4 and higher levels of Ndt80 itself (Benjamin, Zhang et al. 2003). In addition to being regulated transcriptionally, phosphorylation of Ndt80 and stability of an inhibitory partner protein, Sum1 (Suppressor of *mar1-1*, an allele of *SIR2*), are controlled by a degenerate network known as the pachytene or recombination checkpoint. This checkpoint also controls CDK activity through activation of the CDK inhibitor Swe1 (*Saccharomyces* Wee1). The presence of recombination or SC intermediates, such as single-stranded DNA, act as signals that are transduced to result in lower levels of Ndt80 phosphorylation and increased stability of Sum1 and Swe1. The end result of incomplete recombination or SC formation is the inhibition of Ndt80 and failure of cells to express middle meiotic genes. Cells thus remain in the pachytene stage of late prophase until inhibitory signals

cease to exist or until cells manage to adapt to the checkpoint and bypass its inhibitory effects. One factor important for adaptation is the proline isomerase Fpr3 (FK506-Sensitive Proline Rotamase), which appears to act through inhibition of checkpoint factors following exposure of cells to persistent recombination intermediates (Xu, Ajimura et al. 1995; Pierce, Benjamin et al. 2003; Hochwagen, Tham et al. 2005; Hochwagen and Amon 2006).

Meiosis I chromosome segregation

Pachytene is the point of maximal chromosome condensation and homolog interaction. As cells progress out of pachytene upon satisfaction of the recombination checkpoint, the final step of recombination repair is completed and the SC is disassembled (Zickler and Kleckner 1999; Page and Hawley 2004). Atttached homologs, called bivalents, are now ready to align at the center of the nucleus for Meiosis I segregation. Homologous kinetechores are each attached to a microtubule from an opposing spindle pole body (SPB) through a "search and capture" mechanism similar to that used in mitosis. We will discuss later how Meiosis I kinetechore-microtubule attachment is unique, with the primary difference being the coorientation of sister kinetechores, meaning that sister kinetechores do not attach to microtubules emanating from opposing spindle pole bodies as is the case for mitosis and Meiosis II, but to microtubules emanating from the same spindle pole. Once the two homologs of each bivalent

are successfully attached to opposing SPBs, cells are ready to undergo the metaphase I to anaphase I transition (Marston and Amon 2004). Achievement of correct attachment for each bivalent is a difficult process, however, and is thus monitored by a surveillance mechanism known as the spindle assembly checkpoint. The meiotic spindle assembly checkpoint appears to function in a manner similar to its mitotic version. The most downstream effect of this checkpoint is through control of cohesin cleavage. Cells that are not prepared to undergo the metaphase I to anaphase I transition do not activate the anaphase promoting complex, also called the cyclosome (APC/C). The APC is a ubiquitin ligase complex that mediates degradation of Securin (Pds1 in *S. cerevisiae*). Securin is the inhibitor of the protease Separase (Esp1 in *S.cerevisiae*), which is responsible for cleaving Rec8 in meiosis and Scc1 in mitosis (Figure 5). Rec8 cleavage releases the cohesin complex from chromosomes and allows separation of sister chromatids. Until Separase is activated, cohesin holds bivalents together, counteracting spindle forces. Satisfaction of the spindle checkpoint at Meiosis I causes specific cleavage of cohesin complexes located along chromosome arms. This cleavage allows newly-recombined homologs to move to opposite ends of the nucleus in a reductional division at anaphase I, while remaining centromere-proximal cohesin keeps sisters from separating in Meiosis I (Shonn, McCarroll et al. 2000; Craig and Choo 2005). The basis for this differential cohesin cleavage will be discussed in detail in upcoming sections.

After homologs segregate reductionally at anaphase I, the spindle disassembles and cells enter a brief prophase II prior to assembly of the metaphase II spindle. In mitotic divisions, a segregation phase must be followed by a round of DNA replication before chromosomes can segregate again. This is not the case in meiosis. The mechanisms by which meiotic cells avoid an intervening DNA replication stage between Meiosis I and Meiosis II is not clear, but evidence points to an intermediate level of CDK activity between the meiotic segregation stages, such that CDK activity is too high to allow reassembly of the pre-RC, but low enough that spindle disassembly can occur. This hypothesis, though supported by some work in *Xenopus laevis* extracts, has yet to be vigorously tested *in vivo* in any organism (Nasheuer, Smith et al. 2002; Marston and Amon 2004).

Meiosis II chromsome segregation

At metaphase II, chromosomes again align at the nuclear center, stretched between two SPBs by opposing kinetechore-microtubule attachments. The major difference between the situation in Meiosis I, however, is that now individual homologs align with sister chromatids attached to opposite SPBs in what is termed "sister chromatid biorientation". This type of attachment is also seen in mitosis at the metaphase to anaphase transition (Marston and Amon 2004).

As we saw in Meiosis I, Meiosis II segregation is controlled by the spindle assembly checkpoint, whose action has been investigated thoroughly in mitosis. This checkpoint senses unoccupied kinetechores or lack of tension between each kinetechore and its attached SPB. When such "stop" signals are no longer present, the APC is again activated, allowing degradation of Securin, activation of Separase, and cleavage of the remaining Rec8 (Figure 5). This results in equational chromosome segregation, such that sister chromatids end up at opposite poles, and a tetranucleate structure is visible, with each nuclear lobe holding half the genetic content of the original meiotic cell. Nuclei separate as spore walls are assembled by a number of factors activated in a late meiotic transcriptional program. Complete sporulation results in tetrads, structures in which four spores, each with 1N DNA content, are packaged together. These spores can be released from their surrounding membrane and each can be propagated as a haploid, or two spores of opposite mating type may fuse to form another diploid that can propogate mitotically or undergo another round of meiosis (Marston and Amon 2004).

Figure 5

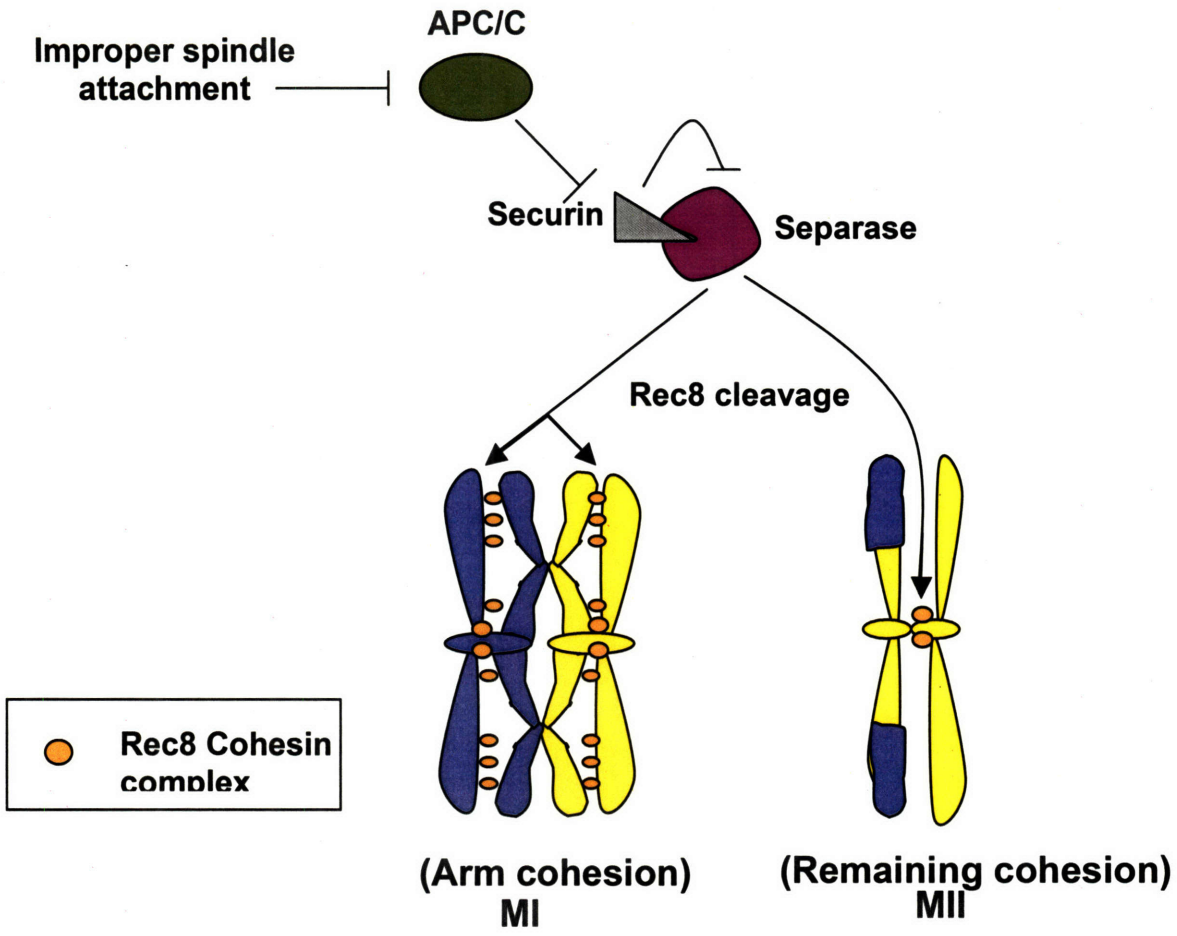

Figure 5: Meiotic spindle assembly checkpoint
The spindle assembly checkpoint acts at both the metaphase I to anaphase I transition and the metaphase II to anaphase II transition to ensure that chroosomes are not segregated until they are correctly attached to the MI or MII spindle. Most of the details have been studied in mitosis, but appear to hold true in meiosis as well. Presence of an unattached kinetchore or lack of tension at the metaphase spindle causes inhibition of the APC/C. This level of control prevents degradation of Securin, the inhibitory partner of Separase. Once chromosomes are properly attached to the metaphase I or metaphase II spindle, the APC/C is activated, Securin is degraded by the proteasome and Separase is active to cleave Rec8 and release cohesin from chromosome arms at Meiosis I and centromeres at Meiosis II.

Meiotic specializations

In the preceding walk through meiosis, I focused on what was happening to chromosomes, but did not discuss how the chromosomes were sorted in the manner described. If we think of meiosis as an extended, modified mitosis-like process, then we can identify meiotic specializations that allow a more complex chromosome dance than that seen in mitosis. The three major specializations responsible are homolog association and attachment, sister chromatid coorientation, and stepwise loss of cohesion (Lee and Amon 2001; Marston and Amon 2004). I will now discuss the importance of each of these processes and mechanisms involved as understood thus far.

Mitosis is essentially a cycle of duplication and sorting. Cells double their genetic content and then must make sure that this content is divided in such a way that each resultant cell gets exactly one copy of each homolog. This is achieved through attachment of newly formed sister chromatids, central positioning of attached sisters, and a spindle that pulls one sister of each homolog to a given pole. If we think of mitosis as a repeating "copy, attach, position, pull" cycle, the last three steps comprise the sorting mechanism. This is more accurately represented by "copy, $attach_{sisters}$, $position_{sisters}$, $pull_{sisters}$". The order here is important. Sisters cannot be positioned on the spindle until they are created and attached, and cannot be pulled apart until they are positioned to create tension to do the pulling.

Meiosis, where the resultant cells need exactly one copy of each homolog pair, can then be similarly described as such: "copy, $attach_{sisters}$, $attach_{homologs}$, $position_{homologs}$, $pull_{homologs}$, $position_{sisters}$, $pull_{sisters}$". With this notation, it is clear that meiosis has three basic steps that are unique and therefore require unique mechanisms to achieve. The "$attach_{homologs}$" step is achieved through pairing and recombination, the "$position_{homologs}$" step is achieved through sister chromatid coorientation, and the "$pull_{homologs}$" step occurs properly as a result of stepwise loss of cohesion. Again, order is important here. Homologs must be attached in prophase before they can be positioned and pulled in Meiosis I. I will start by discussing this first unique meiotic step.

Figure 6

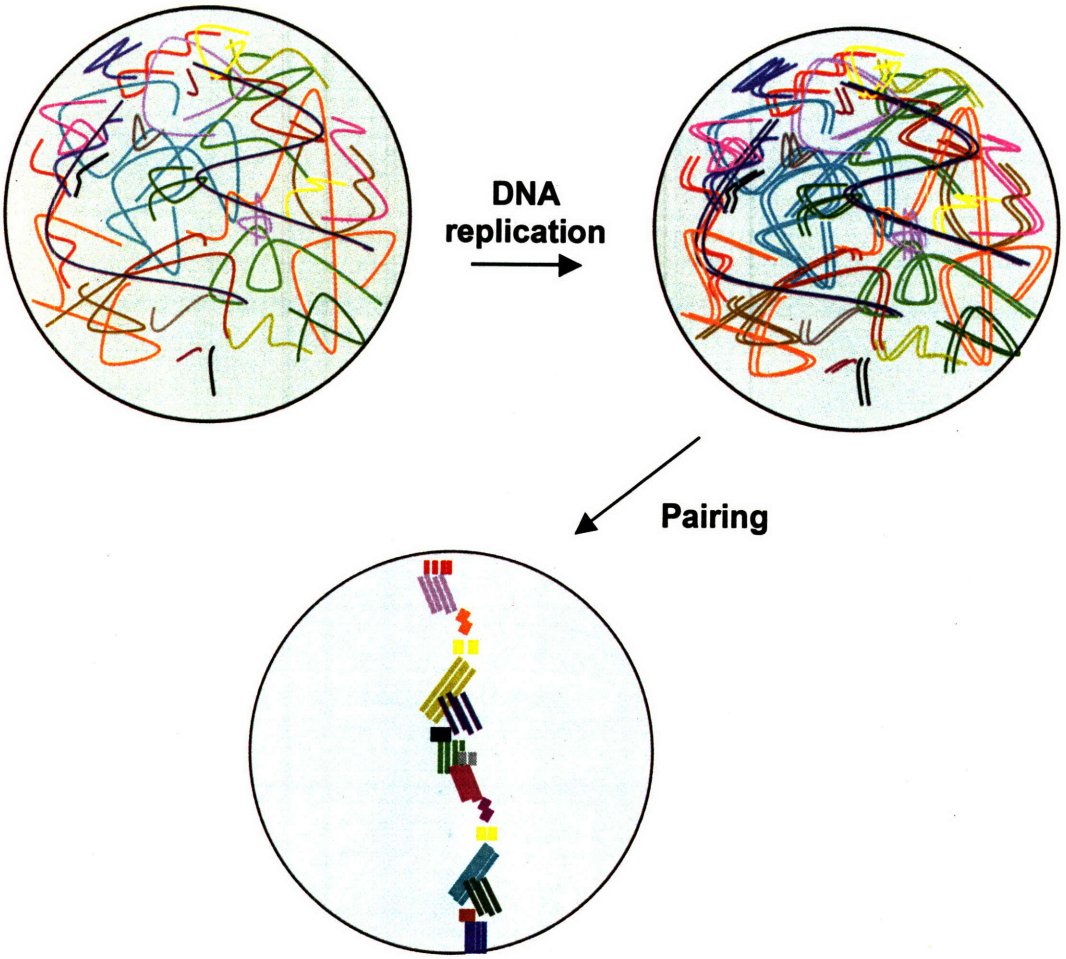

Figure 6: The pairing problem
In this shematic, we see 16 pairs of scattered homologs as is the case in *S. cerevisiae* prior to DNA replication. Following DNA replication, pairing is initiated by unknown mechanisms. Along with chromosome condensation and linking of homologs through recombination, pairing is essential to allow alignment of chromosomes at the metaphase I plate and proper Meiosis I chromosome segregation.

Meiotic chromosome pairing

Attachment of homologs is necessary to provide a counter-force to the Meiosis I spindle force on homolog pairs. Although I introduce this as merely a complementary process to sister attachment, it is much more difficult to accomplish. Attachment of sisters through sister chromatid cohesion is mechanistically linked to the creation of sisters by DNA replication. As homolog pairs are not created together, however, a similar mechanism is not possible. Therefore, cells complete a remarkably elegant series of events throughout meiotic prophase in order to achieve homolog linkage. Homolog pairs, with one "mom homolog" and one "dad homolog" for each chromosome of the genome, are initially distributed in the nucleus in a relatively random fashion. Prior to attachment, therefore, these homologs must be aligned in a process known as "chromosome pairing" (Figure 6). Pairing is one of the great accomplishments of biology and yet very poorly understood on a mechanistic level. Sometime between the completion of DNA replication and linkage of homologs, in a process that occurs with reproducible timing in all meiotic organisms, paired homologs emerge from the relatively disorganized mass of DNA present in the early meiotic nucleus (McKee 2004). This task is particularly astounding in complex organisms, such as humans, with enormous genomes and large tracts of repetitive regions. Nevertheless, cells of all organisms can correctly determine

which chromosomes are homologous and position these chromosomes next to one another.

How do they do it? Unfortunately, pairing mechanism is the biggest remaining meiotic mystery. The little that we understand about pairing has emerged recently and is woefully incomplete. A major reason for the lack of progress in meiotic pairing research is likely due to temporal and apparently mechanistic linkage between pairing and recombination. Recombination, the process by which homologs are physically attached and by which genetic diversity is generated, cannot progress until homologs are proximal. The first step of recombination, DSB formation, is also necessary for pairing to occur (Zickler and Kleckner 1998; Whitby 2005; Keeney and Neale 2006). Therefore it seems that pairing and recombination are partially interdependent, making them difficult to mechanistically differentiate.

Recombination has been successfully studied on a mechanistic level, likely due to the presence of stable intermediates and DNA-DNA interactions that result in often unique DNA products (Whitby 2005). Pairing interactions may not involve DNA-DNA interactions, and certainly do not alone result in unique DNA products. Therefore mechanism must be examined live or in a cytological population study with frequent timepoints. Both of these types of experiments can be performed now, but were not accessible until recently, whereas the studies of DNA structure and DNA sequence in meiotic products that have served as the basis for recombination research have been possible for decades.

One major area of progress in pairing research lies in a type of segregation that is independent of recombination. This is termed "distributive segregation" and appears to be present in many organisms, and is even the norm in a few cases. This phenomenon in yeast was first conclusively shown by Dawson and colleagues through clever experiments using homeologous chromosomes. This group constructed diploid *S. cerevisiae* strains with only a single copy of chromosome 5. In place of the missing homolog, Dawson and colleagues substituted the homeologous chromosome from the closely related *S. carlsbergensis*. These two yeast strains are too highly divergent to undergo recombination, yet surprisingly, *S. cerevisiae* chromosome 5 segregated to the opposite pole from *S. carlsbergensis* chromosome 5 over 90% of the time (Maxfield Boumil, Kemp et al. 2003). This result is not what one would expect if, as discussed above, homololgous chromosomes must be attached in a bivalent structure to segregate to opposite poles in Meiosis I. This phenomenon of recombination-independent Meiosis I segregation appears to represent a cellular backup mechanism. Distributive segregation allows even homologs that have failed to recombine properly a chance to segregate normally. It is additionally possible that distributive segregation represents an ancestral meiotic mechanism that was replaced in most instances by the more efficient recombination-based homolog segregation mechanism seen widely today.

The mechanism responsible for distributive segregation is likely based on a phenomenon described recently by Roeder and colleagues. This group found

that in early prophase, localization of the centromere-assciated SIC (synaptonemal initiation complex) reveals 16 discrete foci. This pattern of localization is unexpected as diploid yeast contain 32 homologs in 16 homolog pairs. As homologs are not yet paired in early prophase, it is strange that only 16 centromere foci are visible. Roeder and colleagues went on to show that each focus represents two centromeres and that these couplings are dynamic and largely non-homologous (Tsubouchi and Roeder 2005). Thus it appears that in early prophase, before pairing is underway, cells are testing partners by coming together at centromeres, then reiteratively switching partners. It is likely that in Dawson's homeologous chromosome experiments, the divergent chromosomes ended up coupled to each other when the other correct pairs had aligned, thus allowing the positioning of homeologous chromosomes opposite each other in Meiosis I, and resultant proper segregation.

The centromere coupling mechanism in *S. cerevisiae* is probably an early step in the complete pairing mechanism. In *Drosophila melanogaster*, however, a similar mechanism appears to be solely responsible for pairing of homologs in males and pairing of chromosome IV in all flies. Male *D. melanogaster* do not undergo meiotic recombination. Additionally, chromosome IV, the smallest of *D. melanogaster* chromosomes, does not undergo meiotic recombination in either sex. Nevertheless, *D. melanogaster* properly segregate their chromosomes at meiosis I with an equivalent degree of accuracy seen in more conventional meioses. This occurrence appears to be the result of tight association of

Drosophila chromosomes at distinct heterochromatic regions (Hiraoka, Dernburg et al. 1993; Fung, Marshall et al. 1998). These "pairing regions" appear to mediate homolog recognition and are responsible for proper meiosis I segregation. *S. cerevisiae* do not have classical heterochromatin. Centromeres, however, show some similar characteristics to heterochromatin of other organisms. Thus it is possible that early meiotic centromere coupling in budding yeast is mechanistically related to heterochromatin-mediated pairing in flies.

Further support for the role of chromatin structure in pairing comes from studies in wheat. Wheat, as is true of many well-studied plant models, is polyploid. Hexaploid wheat consists of three distinct, but closely related genomes. Polyploidy presents an extra layer of difficulty for cells hoping to pair homologous chromosomes. The *Ph1* wheat locus represents the first pairing mutant identified in any organism. This locus has been shown to be necessary to favor pairing of homologs over homeologs. Recent molecular characterization of *Ph1* shows it to be important for regulating chromatin structure during pairing, drawing interesting parallels to *Drosophila* pairing and *S. cerevisiae* centromere coupling (Griffiths, Sharp et al. 2006).

While chromatin status and heterochromatic regions are likely to be important for pairing, it is almost certain that other mechanisms also contribute. This is especially likely when one considers both ends of the spectrum with regard to chromatin complexity. Budding yeast lie at one extreme, with much smaller chromatin variations than more complex organisms. They do not contain

DNA methylation, an important component of heterochromatin structure, and have relatively simple centromeres and telomeres. Nevertheless, budding yeast are able to pair chromosomes effectively. At the end of the spectrum are humans and plants. The human genome is rife with heterochromatin, consisting of massive centromeric regions and huge areas of repetitive DNA. Even so, the human chromosomes are paired efficiently and accurately during meiosis. Many plant species show even higher levels of heterochromatin and more repetitive DNA than the human genome. The lily, for example, has a genome 40 times the size of humans, with 99% consisting of transposable elements . Additionally, while the *Ph1* locus is important to prevent homeologous pairing in wheat, it is not needed for homologous or homeologous chromosomes to align. Thus chromatin status probably plays a role in initial chromosome sorting, but is likely not responsible for the sequence-specific mechanisms that achieve normal pairing in most organisms.

Meiotic Recombination

While very little is known of how homologs pair, a wealth of literature exists on the mechanism of homolog attachment through recombination. Early in prophase, meiotic cells initiate a large number of breaks throughout their genome. A subset of these breaks, which total 200 to 300, will serve as substrates for crossover recombination. The remaining breaks will have to be

repaired through a mechanism that does result in linkages between homologs or crossover products. DSBs are initiated by the topoisomerase Spo11 (Sporulation factor 11) with assistance of a large complex of supporting proteins. Absence of any one of the over a dozen proteins in this DSB initiation complex will result in an inability to create breaks. In general, DSBs are distributed randomly throughout the genome. There are "hotspots" that experience a higher break frequency than average and "coldspots" that experience a lower break frequency than average, but the variation is relatively mild. Hotspot regions generally lie in intergenic promoter regions and mid-arm along chromosomes, wheras the major coldspot exists near the rDNA region on chromosome 12 (Keeney 2001; Martini and Keeney 2002; Keeney and Neale 2006; Blitzblau, Bell et al. 2007; Buhler, Borde et al. 2007).

Once DSBs are initiated by Spo11, DNA ends are resected in order to leave single-stranded 3' overhangs. It is not clear how resection occurs, but it appears that the MRX complex (consisting of Mre11, Rad50 and Xrs1) is involved. This complex is also known to be important for DNA damage repair in mitosis, as is true of a number of meiotic recombination factors. Meiotic recombination can thus be thought of as a complex DNA repair mechanism with several competing pathways. Newly resected 3' overhangs are coated by RPA (Replication Protein A), which along with Rad51 (Radiation sensitive factor 51), Dmc1 (Disrupted meiotic cDNA 1) and other factors mediates invasion of dsDNA by 3' overhang. Invasion occurs preferentially on the chromosome homologous

to the broken ends rather than the sister chromatid. This is the opposite of the situation seen in mitotic DNA repair and is likely due to involvement of meiosis-specific repair factors, such as Dmc1. Stable strand invasion results in replication from the free 3' invading end using the homolog as a template. This causes greater stabilization of the annealed intermediate and fills in some of the gap created by DSB formation and resection. The steps that follow this initial strand invasion have only recently been clarified (Whitby 2005).

The basic DSB model for recombination outlined by Szostak (Figure 7) has been widely regarded for decades as the definitive model of meiotic recombination. This model proposes that following DSB formation, resection, and strand invasion, the second ssDNA 3' end is "captured" by annealing to the closely positioned homologous single-stranded homologous sequence exposed by the movement of the replication fork from the first 3' end (also called branch migration). Both ends continue to synthesize DNA to fill their gaps, until the four free ends became repaired through ligation, creating the famous "double Holliday Junction" (dHJ), which must then be cut and repaired again to separate the four tangled DNA strands. Szostak proposed that dHJs could be cut in two ways, with one resulting in flanking DNA sequences in their original conformation (non-crossovers) and the other resulting in flanking sequences from different original homologs now joined in the same DNA strand (crossovers) (Whitby 2005).

Despite the elegance of the later stages of this model, recent work indicates that it is not complete. One requirement of the Szostak model is that an increase in non-crossovers would result in a decrease in crossovers and *visa versa*. Recently, however, mutants were identified that showed specific decreases in crossover formation, but no corresponding change in non-crossovers. These crossover-specific factors, called Zmms (named after founding members Zip1, Zip2, Zip3, Mer3, and Msh5), interestingly encompass members of the aforementioned synaptonemal initiation complex that is apparently important for early pairing, providing another link between chromosome pairing and recombination (Allers and Lichten 2001; Borner, Kleckner et al. 2004; Lynn, Soucek et al. 2007). New models based on this and other data support a more complex model than Szostak envisioned. This model (Figure 8) includes three possible destinies for a DSB. The break can proceed by a pathway that looks very much like the Szostak model, except where a dHJ can only be resolved one way, into a crossover product. The second pathway proposes capture of the second 3' end following replication from the first 3' end and branch migration, but no new replication from captured end. This mechanism results in two single HJ (sHJ), which can be cut and repaired to produce exclusively crossover products. The resolvase responsible for cutting sHJs in the second pathway has been identified as Mus81 (MMS and UV Sensitive factor 81). No resolvase has yet been identified to cut dHJs in the first pathway, though this is an extremely active area of research. The third and final pathway that a DSB can follow begins like the first dHJ route, but after strand

invasion and some replication of the 3' overhang with the homologous template, the two homologs will dissociate. The originally unbroken homolog will require no repair while the non-invading 3' overhang will anneal to the newly replicated segment of the invading 3' overhang to create a gapped duplex that simply requires further replication and ligation. This third pathway results exclusively in non-crossover products (Whitby 2005).

Despite the apparent complexity of this new model, it has several simple and important implications. Firstly, the model suggests that the decision of a DSB to become a crossover or non-crossover product is made early in prophase, not at the point of dHJ resolution, as was previously thought. The basis for this designation has long been of interest given its relationship to a process known as "crossover interference". Crossover products result in a physical structure at the site of exchange known as a chiasma. Chiasmata are cytologically visible in most organisms and early observation revealed that each pair of homologs generally shows one chiasma per chromosome arm regardless of chromosome size. Additionally, chiasmata are almost never observed near centromeres or telomeres, despite the generally random nature of DSB formation. It seemed unlikely based on these observations, that DSBs were randomly designated to a crossover or non-crossover path. Instead, it seemed that approximately one DSB per chromosome must become a crossover and that the remaining DSBs are funneled into non-crossover fates. The early timing of this designation suggested by the modified DSB recombination model has led

researchers to reevaluate possible mechanisms for crossover interference. For example, it was widely believed that mature SC mediated interference, but as SC is assembled after the designation appears to occur, this is no longer a likely explanation. A current interference model, proposed by Kleckner, hypothesizes that a DSB that goes to the primary Zmm-dependent crossover pathway in budding yeast causes a release of chromosome axis stress, pushing nearby DSBs to resolve as non-crossovers (Allers and Lichten 2001; Kleckner 2006).

Another important result of the modified DSB recombination model is the ability to explain inter-organism recombination variations. Many organisms, such as budding yeast and humans show crossover interference. Fission yeast, however, do not show interference. It is now thought that the Zmm pathway experiences interference, while the Mus81-dependent sHJ pathway does not. It is believed that organisms with no or little crossover interference create crossovers primarily through the sHJ pathway, while organisms with interference use primarily the Zmm-dependent crossover pathway. This discovery has helped to tie together meiotic research from a variety or organisms (Whitby 2005).

Why do meiotic cells make so many DSBs? In *S. cerevisiae*, only a third of DSBs become chiasmata, so why do cells risk so much DNA damage and take so much energy to repair breaks that do not assist in chromosome segregation? Non-crossover products, while useless for chiasmata formation, do increase genetic diversity as a result of gap formation and repair from of a

non-isogenic homolog. The creation of genetic diversity is, of course, thought to be a major reason for the existence of meiosis so non-crossovers could exist as purely an evolutionary tool. It is also likely, however, that early steps in strand-invasion contribute to the pairing of homologs. In support of this possibility, Spo11 and Dmc1 are important for proper chromosome pairing (see Chapter 4). This area requires additional research and may shed significant light on the mystery of pairing.

Figure 7

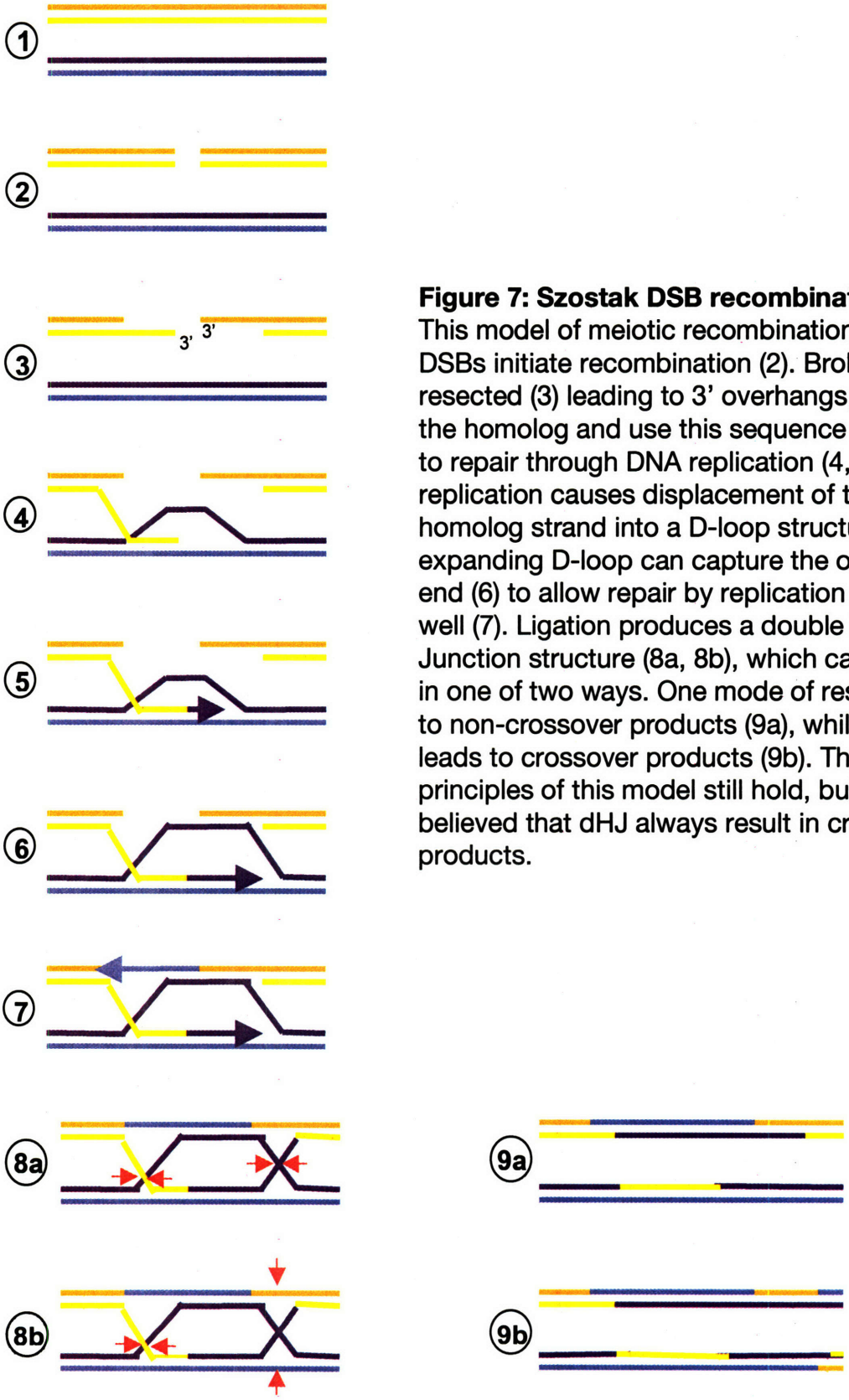

Figure 7: Szostak DSB recombination model
This model of meiotic recombination proposes that DSBs initiate recombination (2). Broken ends are resected (3) leading to 3' overhangs, which invade the homolog and use this sequence as a template to repair through DNA replication (4, 5). Continuing replication causes displacement of the opposite homolog strand into a D-loop structure. This expanding D-loop can capture the other broken 3' end (6) to allow repair by replication of this end as well (7). Ligation produces a double Holliday Junction structure (8a, 8b), which can be resolved in one of two ways. One mode of resolution, leads to non-crossover products (9a), while the other leads to crossover products (9b). The basic principles of this model still hold, but it is now believed that dHJ always result in crossover products.

Adapted from (Whitby 2005)

Figure 8

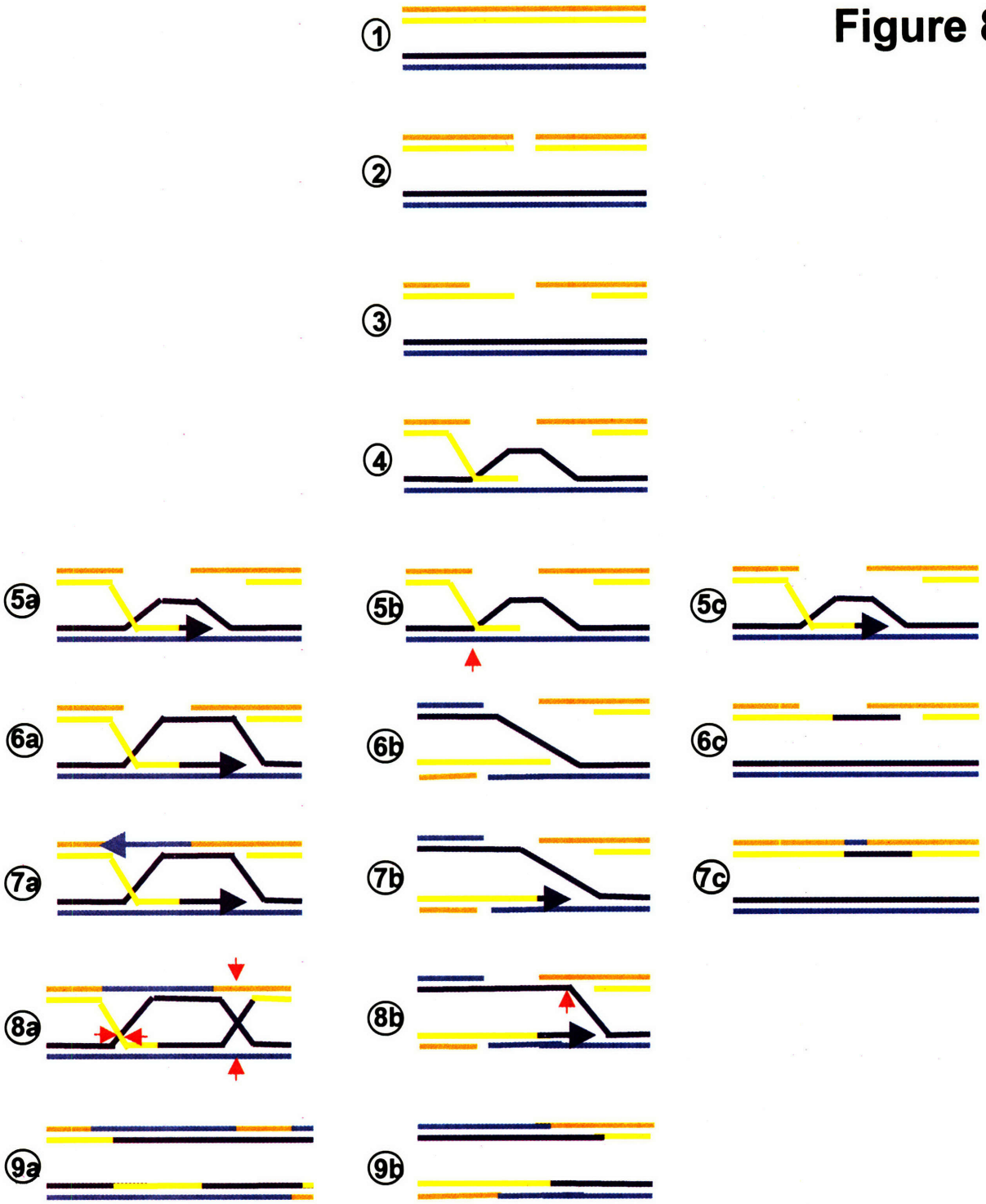

Figure 8: Current DSB model for recombination pathways
See text for an explanation of the three modes of DSB repair thought to function during meiosis. Note that the a and b pathways produce crossover products, while the c pathway produces noncrossover products. *S. cerevisiae* generate crossovers primarily through the interference-generating pathway a, while *S. pombe* rely almost exclusively on pathway b, which does not show crossover interference. The majority of DSBs in most organisms are repaired through pathway c.

Adapted from (Whitby 2005)

Sister kinetechore coorientation

Proper pairing and recombination result in bivalents that are capable of opposing spindle tension at Meiosis I through generation of chiasmata. Chiasmata alone, however, do not allow homologs to segregate at the metaphase I to anaphase I transition. For each homolog to segregate apart, its sister kinetechores must also be coordinated to move together to the same pole. If sister kinetechores attached to opposite SPBs in Meiosis I, as they do in mitosis and Meiosis II, tension would be generated at metaphase I, but chromosomes would not be able to move apart (Figure 9). All four sisters would remain in the center of the nucleus, with centromeric cohesion opposing spindle forces, a situation that does not occur in a normal meiosis. How then is this sister chromatid coorientation achieved?

A major breakthrough in the understanding of coorientation came with the identification of three proteins: Mam1 (Monopolar Attachment during Meiosis 1), Lrs4 (Loss of rDNA Silencing 4), and Csm1 (Chromosome Segregation in Meiosis 1) that associate into the so-called "monopolin complex" and are responsible for proper meiotic chromosome segregation (Toth, Rabitsch et al. 2000; Rabitsch, Petronczki et al. 2003; Marston and Amon 2004). Monopolins associate with kinetechores in Meiosis I, but not Meiosis II, and their localization appears to depend on the Polo kinase, Cdc5 (Lee and Amon 2003). Proper

maintanance of monopolins at kinetechores through Meiosis I depends on the meiosis-specific factor Spo13 (Katis, Matos et al. 2004; Lee, Kiburz et al. 2004). Work by Monje-Casas, Prabhu and colleagues has shown high Cdc5 and Mam1 expression to be sufficient for sister kinetechore coorientation in mitosis, where such orientation normally does not occur. Additionally this group found that Mam1 physically holds sister centromeres together in a cohesin-independent fashion (Monje-Casas, Prabhu et al. 2007). Electron microscopy indicates that only one microtubule mediates attachment of each homolog to the Meiosis I spindle (Winey, Morgan et al. 2005), but it is not clear whether two sister kinetechores are fused to create a single functional kinetechore or whether the kinetechore of one sister is blocked from association with microtubules. The mechanism of action of monopolins is also unclear, although it has been shown to depend on the Casein Kinase Hrr25 (Homologous Recombinational Repair factor 25). Association of Hrr25 with Mam1, as well as its kinase activity, is necessary for its role in coorientation (Petronczki, Matos et al. 2006). The involvement of Hrr25 in coorientation of sister kinetechores is particularly interesting as Casein Kinases appear to play a similar role in other organisms, including *S. pombe*. Interestingly, in *S. pombe*, sister kinetechore coorientation appears to be linked to cohesion regulation, as Rec8 plays an important role in both processes (Watanabe 2006).

Figure 9

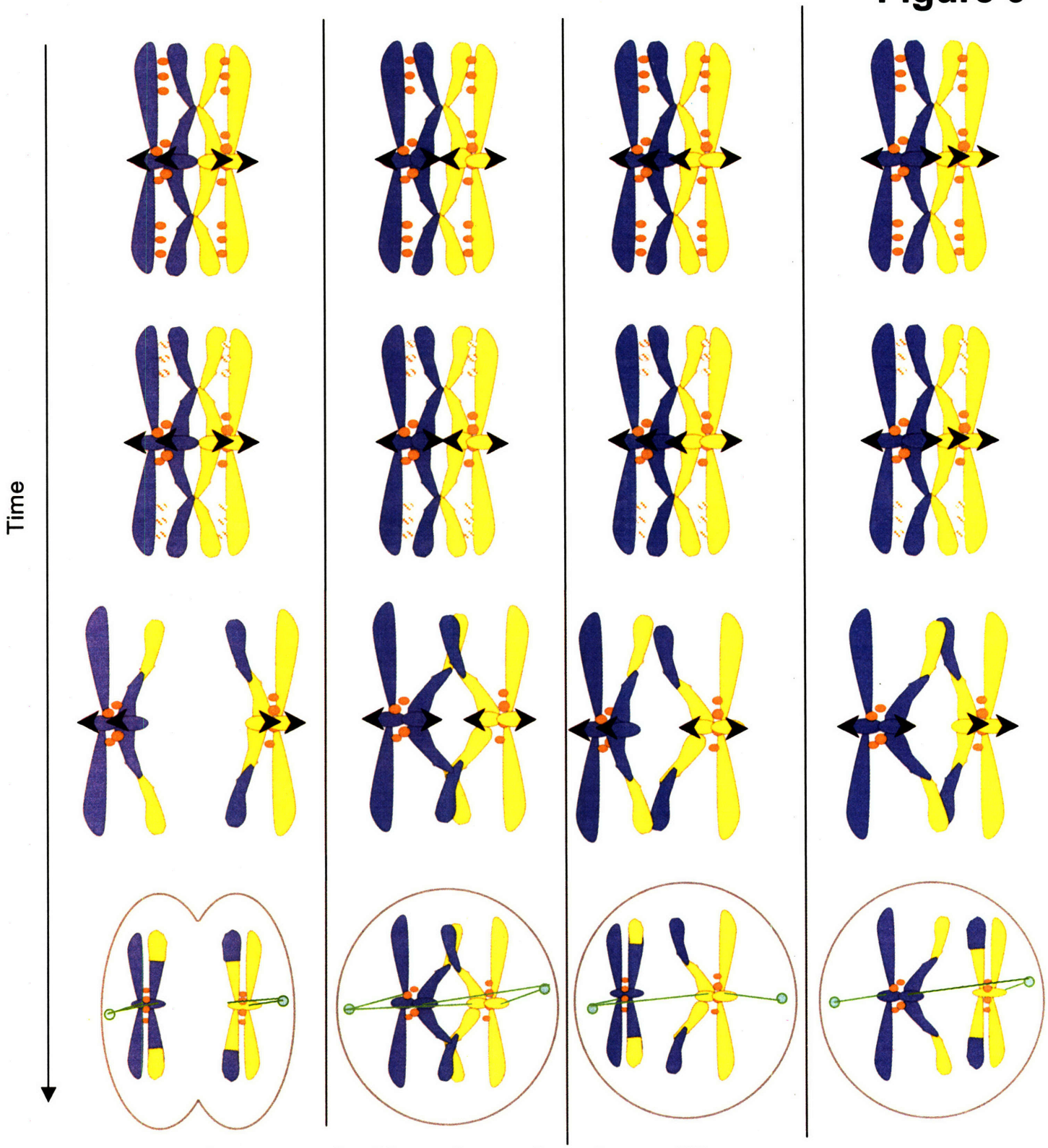

Figure 9: Tension-generating kinetechore orientations at MI
Meiotic cells require a mechanism to coorient sister chromatids prior to Meiosis I chromosome segregation. Shown above in columns are the four possible ways that independent sister kinetechores could attach to the metaphase I spindle to generate tension. Note that only the left-most situation, where sister kinetechores are cooriented, allows Meiosis I chromosome segregation. All other possibilities result in one or both homologs remaining suspended at the metaphase I plate. Note that progression from prophase I to anaphase I proceeds downward from the top of the page for each possible attachment scheme. Arrowheads indicate direction of kinetechore orientation.

Step-wise loss of cohesion

The final meiotic specialization that allows reductional Meiosis I segregation is the step-wise loss of the cohesin complex. It has been stated in previous sections that arm cohesins are cleaved at anaphase I, and centromere-proximal cohesins are cleaved at anaphase II (Figures 10, 11) (Lee and Amon 2001; Marston and Amon 2004). How does the cell differentially regulate these two cohesin populations? The cohesin complex contains the same core proteins at chromosome arms and centromeres and in both cohesin populations, Rec8 is cleaved by Separase. Nevertheless, approximately 50 kilobases of Rec8 around each centromere are protected from cleavage at anaphase I (Kiburz, Reynolds et al. 2005).

Several factors have been identified as important for step-wise loss of cohesion. Spo13, mentioned above as important for sister coorientation, is also involved in protection of centromeric Rec8 during Meiosis I, as *spo13Δ* cells show increased sister separation at Meiosis I (Lee, Amon et al. 2002; Shonn, McCarroll et al. 2002). A factor first identified in *D. melanogaster*, called *MEI-S332*, has recently been identified in other organisms as well (Kerrebrock, Moore et al. 1995; Katis, Galova et al. 2004; Kitajima, Kawashima et al. 2004; Marston, Tham et al. 2004; Rabitsch, Gregan et al. 2004; Hamant, Golubovskaya et al. 2005; Riedel, Katis et al. 2006; Tang, Shu et al. 2006). Sgo1

(Shugoshin, meaning "guardian spirit" in Japanese) is essential for maintanance of centromeric Rec8 beyond anaphase I and is functionally widely conserved (Kitajima, Kawashima et al. 2004). Moreover, Sgo1 associates precisely with the 50 kilobase protected region of Rec8 near centromeres and appears to act partially through recruitment of PP2A phosphatase to centromere-proximal cohesin (Katis et al. 2006; Tang, Shu et al. 2006; (Kiburz, Reynolds et al. 2005)). This finding is intriguing in light of evidence that Rec8 is highly phosphorylated and that such phosphorylation may promote its cleavage. Depletion of Cdc5 results in hypo-phosphorylated Rec8 and a delay in Rec8 cleavage (Lee and Amon 2003). It is attractive to hypothesize that Sgo1 acts through dephosphorylation of centromeric Rec8, thus inhibiting cleavage specifically in this region. The actual situation is likely more complex than this simple model suggests and will be discussed in depth in Chapter II (Figure 12).

Conclusions on the role of specialized meiotic mechanisms

Meiotic reductional segregation is a challenge for cells set up to divide mitotically. Cells have met this challenge, however, through a remarkable set of adaptations. The ability to link homologs and thus create tension at metaphase I, the ability to coorient sister kinetechores, forcing sisters to segregate together at anaphase I, and the ability to remove cohesins in stages to provide and release tension between homologs at Meiosis I and sisters at Meiosis II, are all

necessary for the completion of a reductional and then equational round of segregation. These two rounds of segregation allow creation of haploid gametes through meiosis (Lee and Amon 2001). All three of these specializations are present in some form in every meiotic organism. There are a number of differences in how meiosis is achieved throughout nature, however. I have thus far focused on meiosis in *S. cerevisiae*, with only brief commentary on the situation in other organisms. I will now discuss some important differences in meiosis in organisms more complex than budding yeast.

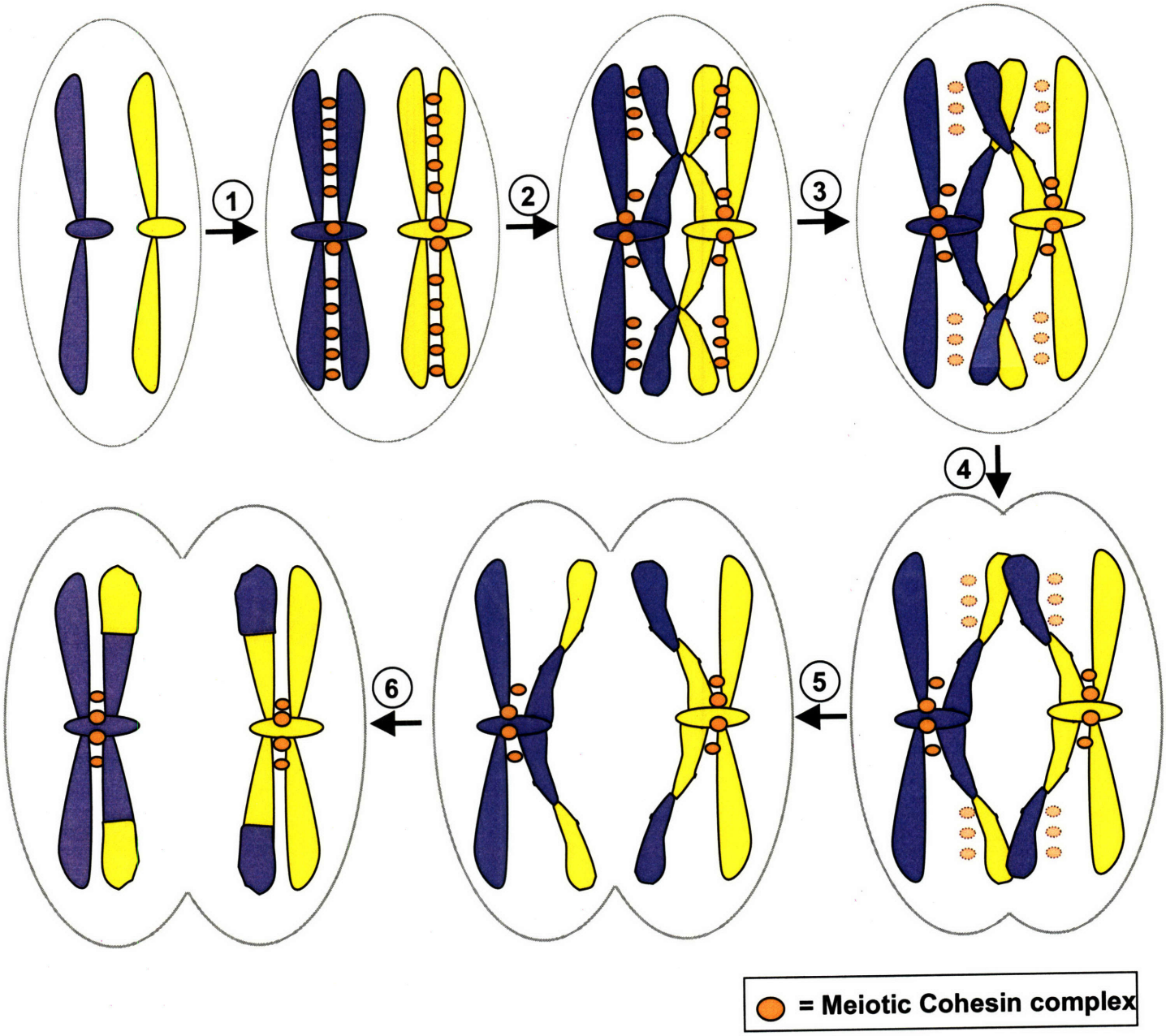

Figure 10: Arm cohesin loss at MI
Chromosomes entering meiosis undergo DNA replication, during which Rec8-containing cohesin is laid down along the length of chromosomes (1). During prophase, homologs undergo recombination, linking homolog pairs into bivalents by chiasmata (2). As chromosomes undergo the metaphase I to anaphase I transition (3), loss of cohesin through proteolytic cleavage by Separase of Rec8 that is distal to chiasmata allows release of homogs from the bivalent structure, and segregation to opposite spindle poles (4, 5, 6). Note that centromere-proximal cohesin is still necessary to hold sister chromatids together. Also note that for simplicity, only a single homolog pair is represented here.

Figure 11

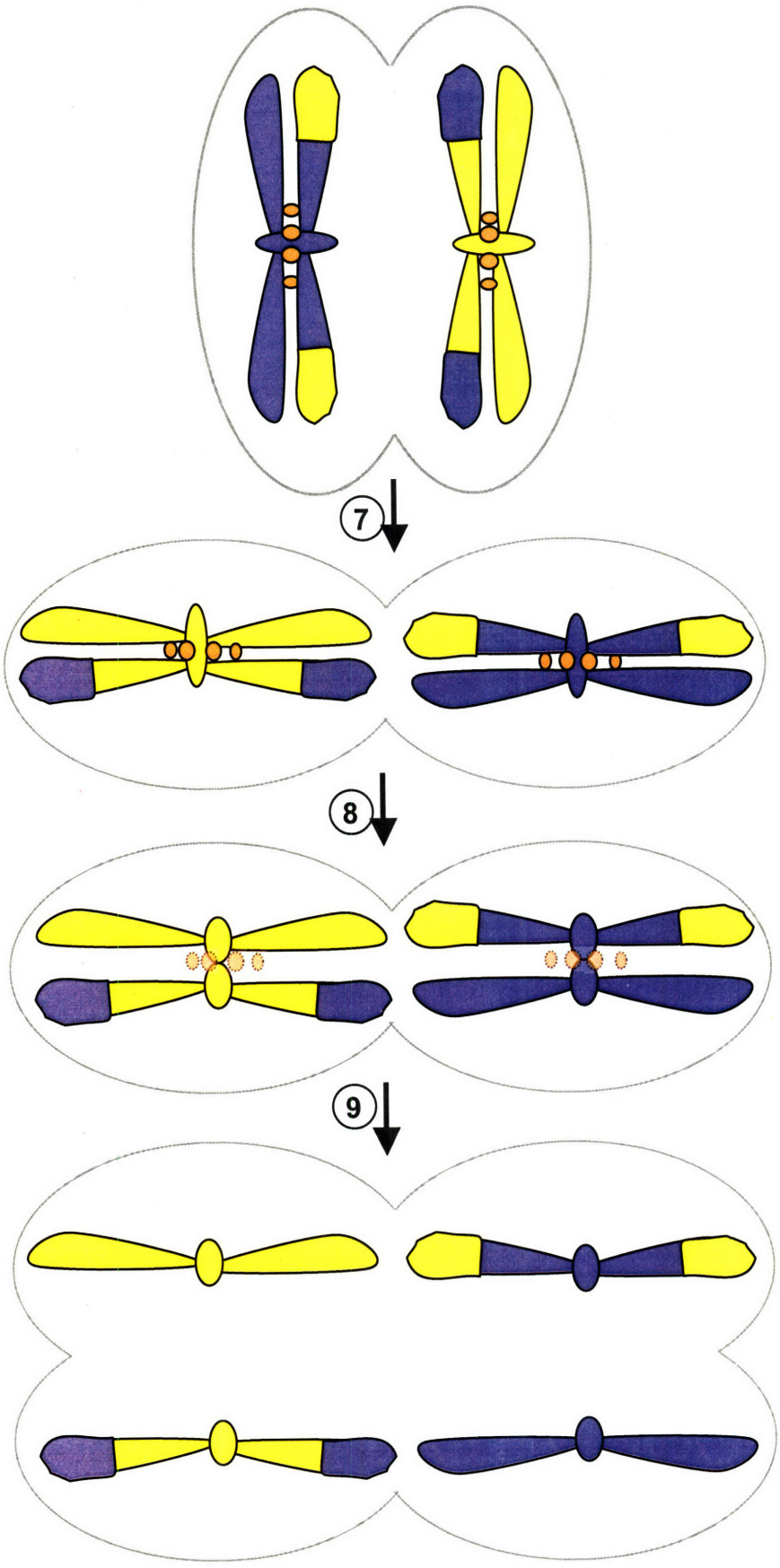

Figure 11: Centromere-proximal cohesin loss at MII
Following Meiosis I chromosome segregation, chromosomes align on the Meiosis II spindle, now with sister chromatids oriented to segregate apart (7). Loss of remaining cohesin (8) through proteolytic cleavage by Separase, allows sisters to segregate to opposite poles and the generation of balanced tetranucleates with half the genetic content of the starting meiotic cell. Note that only one homolog pair is shown here for simplicity

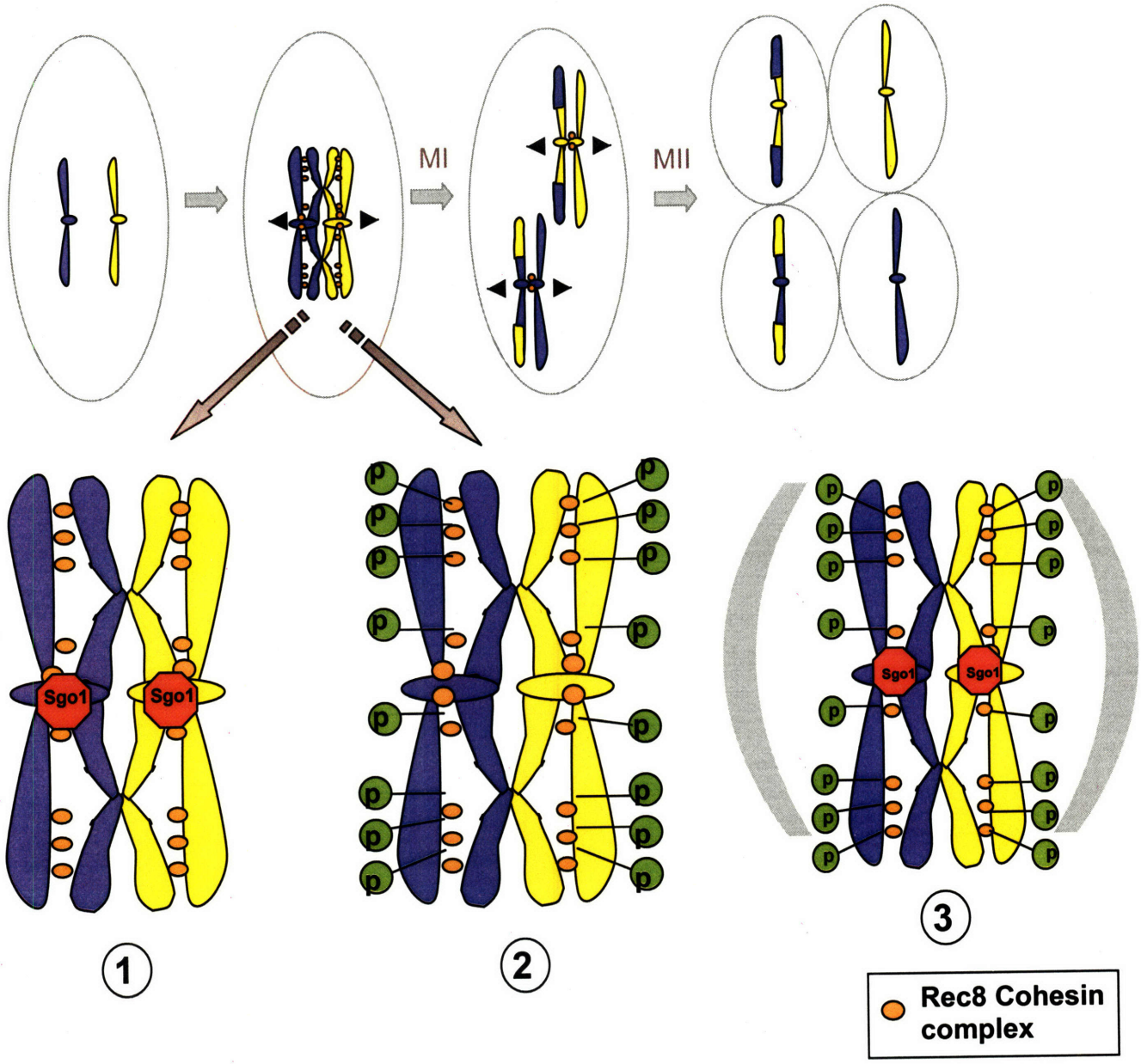

Figure 12: Mechanisms of step-wise cohesin removal
Step-wise removal of Rec8 as is seen in meiosis appears to be generated by two mechanisms. Mechanism 1 protects centromeric Rec8 from cleavage until Meiosis II. This appears to be the mode of action of Sgo1 as well as Spo13, to a lesser degree. Mechanism 2 promotes specific cleavage of arm cohesin. This mechanism could support data that Cdc5 depletion causes a delay in Rec8 cleavage and metaphase I arrest. It is most likely, based on all available data, that the actual regulation of Rec8 cleavage is more like mechanism 3 above, where both centromere protection of cohesin and arm promotion of cohesin cleavage contribute to its step-wise loss.

Meiosis in complex eukaryotes

Homolog linkage, sister kinetechore coorientation at Meiosis I, and step-wise loss of cohesion are all essential to proper meiotic chromosome segregation. These three meiotic specializations differ greatly, however, in the level of conservation of mechanisms underlying each process. Recombination mechanisms allowing homolog linkage are extremely well-conserved, with some variations in which crossover recombination pathway is utilized more between different organisms. Cellular regulation responsible for step-wise cohesion loss is also quite well-conserved, with Sgo1 playing a central role in many organisms examined to date.

Complex organisms often contain additional cohesion regulation through increased cohesin complex variants and additional steps of regulation to be discussed below, but the basic mechanism by which different cohesin pools are cleaved at Meiosis I versus Meiosis II appear to be similar to the situation in budding yeast. Sister kinetechore coorientation in Meiosis I appears to be the least mechanistically conserved of the three specializations that have been discussed here. Monopolins have not been identified yet in organisms other than yeast and may not exist. This difference may be based on the huge variability in centromere and kinetechore structure and size in different organisms. Probably as a result of larger centromeres, kinetechores, and

chromosomes, organisms that are more complex than budding yeast require many more microtubules to achieve chromosome segregation than the single microtubule that is apparently capable of mediating chromosome segregation in *S. cerevisiae*. These complex organisms thus likely regulate sister kinetechore coorientation in ways that are different than those used in budding yeast, where each kinetechore mediates attachment to a single microtubule in Meiosis I and Meiosis II.

It is not yet clear how yeast cells control sister kinetechore coorientation. This process is even less understood in more complex organisms. There are aspects of meiosis in complex eukaryotes, however, that are clearly regulated differently than is the case for budding yeast. Some of this variation appears to be based on size, as *S. cerevisiae* cells contain a relatively small genome, partitioned into small chromosomes. Human chromosomes range from 51 to 245 Megabases, while the largest budding yeast chromosome is only 1.5 Megabases in length. Large chromosomes require additional condensation to progress through meiosis without tangling DNA in the process. This additional condensation is probably the basis for an additional level of cohesin regulation in complex eukaryotes.

These organisms show not only the step-wise loss of cohesion, which we have just discussed, but also a large-scale removal of cohesion during prophase. This cohesin removal accounts for around 90% of the total meiotic cohesin removal and is independent of Rec8 cleavage, but dependent on Polo

kinase. It is likely that as complex eukaryotic chromosomes condense during meiosis, they must remove some of their cohesin packaging in order to achieve the extremely high levels of compaction seen in late prophase (Sumara, Vorlaufer et al. 2002; Weitzer and Uhlmann 2002). It is additionally possible that the majority of cohesin is removed in prophase to expedite the meiotic divisions. The large amount of cohesin used in early prophase to maintain large chromosomes in a decondensed structure, and possibly assist prophase progression, might be too much for Separase to cleave in an efficient fashion. A similar prophase cohesin removal has recently been described in yeast, as well, but appears to operate on a much smaller scale, with only a fraction of Rec8 removed prior to meiotic divisions (Yu and Koshland 2005).

Aside from chromosome size, yeast differ from complex eukaryotes in being single-celled. Multi-cellular organisms must coordinate meiosis with the development of the rest of the animal, and must also put greater care into gamete quality. A single yeast cell can result in production of millions of meiotic offspring in a short time frame. Animals, however, may produce only one or a few offspring in their lifetimes, so it is important for these offspring to be of high fitness. Additionally, the relatively large number of genes in complex eukaryotes create more opportunities for meiotic and mitotic mistakes. Complex eukaryotes counter these gamete quality concerns through variations in the checkpoints seen in budding yeast. Mammalian cells appear to have more checkpoints than *S. cerevisiae*, with additional control in late prophase. More importantly,

however, defective mammalian meiotic cells do not generally arrest for a period and then adapt to the defect and proceed, as is the case in budding yeast. A major output of mammalian meiotic checkpoints is apoptosis. Strangely, this apoptotic control appears more stringent in male mice than female mice. This results in females producing larger numbers of aneuploid gametes than males, though it is not clear if this same reasoning holds for humans (Morelli and Cohen 2005; Cohen, Pollack et al. 2006; Pacchierotti, Adler et al. 2007).

In humans, a larger contribution to aneuploid gametes in females appears to result from a developmental characteristic of oogenesis. Human females begin gametogenesis during early development. Oocytes are not used, however, until puberty. This means that many gametes in women remain arrested in the diplotene stage of late prophase for decades before ovulation and activation by sperm fusion. The rate of aneuploidy in oocytes increases dramatically with maternal age, leading many to speculate that the prophase arrest experienced by oocytes is only sustainable effectively for a limited time. This argument makes sense as chromosomes have already undergone recombination and are arrested with cohesin and chiasmata holding bivalents together. This arrest is after the mass removal of cohesin from chromosomes, so it is attractive to speculate that slow dissociation of the remaining cohesins from chromosome arms over time results in unstable bivalents and missegregation in aged oocytes. This model is consistent with the observation that most chromosome missegregation in older mothers occurs in Meiosis I and that missegregation

occurs preferentially between homologs with a more distal chiasma and thus less cohesion holding homologs together (Lenzi, Smith et al. 2005; Morelli and Cohen 2005; Cohen, Pollack et al. 2006; Pacchierotti, Adler et al. 2007).

Conclusion and perspectives

There has been tremendous progress in meiotic research over the last several years. We now understand much of the basis for the key processes of recombination, coorientation, and step-wise loss of cohesion. *S. cerevisiae* have served as an excellent model for understanding meiotic mechanism. Almost every major breakthrough in meiosis research has, at least in part, depended on the genetic and molecular tractability of budding yeast. These discoveries have helped form a framework from which to ask more complex questions about meiotic mechanism. How do chromosomes pair? How is cohesin regulation achieved in meiosis? How are prophase events coordinated? Questions such as these have been of great interest to me in my graduate research.

I will discuss my work towards answering such questions in later chapters. Namely, I have identified Rec8 phosphorylation sites and found that phosphorylation at these sites plays a role in promoting preferential cleavage of arm cohesin at Meiosis I. I have also investigated the role of Rec8 in prophase progression and found that phosphorylation of Rec8 is important for SC formation and that this role is separable from the role of Rec8 in sister chromatid

cohesion. I have additionally studied the properties of homolog pairing in prophase and have performed an initial characterization of this process.

Meiotic research holds great promise for understanding infertility and aneuploidy-based disease states. Aneuploidy results in spontaneous abortion in an estimated 35% of human embryos. Additionally, 0.3% of human newborns are aneuploid, mostly due to trisomy 21, better known as Down's syndrome (Hassold and Hunt 2001; Hunt and Hassold 2002; Hunt and Hassold 2008). Additionally, with age of pregnancy increasing in the U.S., infertility is becoming a major area of concern for many couples. It is of significant interest, then, to better understand the mechanisms by which chromosomes complete the complex dance underlying meiosis.

References:

Allers, T. and M. Lichten (2001). "Differential timing and control of noncrossover and crossover recombination during meiosis." Cell **106**(1): 47-57.

Benjamin, K. R., C. Zhang, et al. (2003). "Control of landmark events in meiosis by the CDK Cdc28 and the meiosis-specific kinase Ime2." Genes Dev **17**(12): 1524-39.

Blitzblau, H. G., G. W. Bell, et al. (2007). "Mapping of meiotic single-stranded DNA reveals double-stranded-break hotspots near centromeres and telomeres." Curr Biol **17**(23): 2003-12.

Borde, V., A. S. Goldman, et al. (2000). "Direct coupling between meiotic DNA replication and recombination initiation." Science **290**(5492): 806-9.

Borner, G. V., N. Kleckner, et al. (2004). "Crossover/noncrossover differentiation, synaptonemal complex formation, and regulatory surveillance at the leptotene/zygotene transition of meiosis." Cell **117**(1): 29-45.

Buhler, C., V. Borde, et al. (2007). "Mapping meiotic single-strand DNA reveals a new landscape of DNA double-strand breaks in Saccharomyces cerevisiae." PLoS Biol **5**(12): e324.

Carlile, T. M. and A. Amon (2008). "Meiosis I is established through division-specific translational control of a cyclin." Cell **133**(2): 280-91.

Cha, R. S., B. M. Weiner, et al. (2000). "Progression of meiotic DNA replication is modulated by interchromosomal interaction proteins, negatively by Spo11p and positively by Rec8p." Genes Dev **14**(4): 493-503.

Cohen, P. E., S. E. Pollack, et al. (2006). "Genetic analysis of chromosome pairing, recombination, and cell cycle control during first meiotic prophase in mammals." Endocr Rev **27**(4): 398-426.

Craig, J. M. and K. H. Choo (2005). "Kiss and break up--a safe passage to anaphase in mitosis and meiosis." Chromosoma **114**(4): 252-62.

Dirick, L., L. Goetsch, et al. (1998). "Regulation of meiotic S phase by Ime2 and a Clb5,6-associated kinase in Saccharomyces cerevisiae." Science **281**(5384): 1854-7.

Forsburg, S. L. (2002). "Only connect: linking meiotic DNA replication to chromosome dynamics." Mol Cell **9**(4): 703-11.

Fung, J. C., W. F. Marshall, et al. (1998). "Homologous chromosome pairing in Drosophila melanogaster proceeds through multiple independent initiations." J Cell Biol **141**(1): 5-20.

Griffiths, S., R. Sharp, et al. (2006). "Molecular characterization of Ph1 as a major chromosome pairing locus in polyploid wheat." Nature **439**(7077): 749-52.

Hamant, O., I. Golubovskaya, et al. (2005). "A REC8-dependent plant Shugoshin is required for maintenance of centromeric cohesion during meiosis and has no mitotic functions." Curr Biol **15**(10): 948-54.

Hassold, T. and P. Hunt (2001). "To err (meiotically) is human: the genesis of human aneuploidy." Nat Rev Genet **2**(4): 280-91.

Henderson, K. A. and S. Keeney (2004). "Tying synaptonemal complex initiation to the formation and programmed repair of DNA double-strand breaks." Proc Natl Acad Sci U S A **101**(13): 4519-24.

Hiraoka, Y., A. F. Dernburg, et al. (1993). "The onset of homologous chromosome pairing during Drosophila melanogaster embryogenesis." J Cell Biol **120**(3): 591-600.

Hochwagen, A. and A. Amon (2006). "Checking your breaks: surveillance mechanisms of meiotic recombination." Curr Biol **16**(6): R217-28.

Hochwagen, A., W. H. Tham, et al. (2005). "The FK506 binding protein Fpr3 counteracts protein phosphatase 1 to maintain meiotic recombination checkpoint activity." Cell **122**(6): 861-73.

Huang, C. E., M. Milutinovich, et al. (2005). "Rings, bracelet or snaps: fashionable alternatives for Smc complexes." Philos Trans R Soc Lond B Biol Sci **360**(1455): 537-42.

Hunt, P. A. and T. J. Hassold (2002). "Sex matters in meiosis." Science **296**(5576): 2181-3.

Hunt, P. A. and T. J. Hassold (2008). "Human female meiosis: what makes a good egg go bad?" Trends Genet **24**(2): 86-93.

Ivanov, D. and K. Nasmyth (2005). "A topological interaction between cohesin rings and a circular minichromosome." Cell **122**(6): 849-60.

Ivanov, D., A. Schleiffer, et al. (2002). "Eco1 is a novel acetyltransferase that can acetylate proteins involved in cohesion." Curr Biol **12**(4): 323-8.

Kassir, Y., N. Adir, et al. (2003). "Transcriptional regulation of meiosis in budding yeast." Int Rev Cytol **224**: 111-71.

Katis, V. L., M. Galova, et al. (2004). "Maintenance of cohesin at centromeres after meiosis I in budding yeast requires a kinetochore-associated protein related to MEI-S332." Curr Biol **14**(7): 560-72.

Katis, V. L., J. Matos, et al. (2004). "Spo13 facilitates monopolin recruitment to kinetochores and regulates maintenance of centromeric cohesion during yeast meiosis." Curr Biol **14**(24): 2183-96.

Keeney, S. (2001). "Mechanism and control of meiotic recombination initiation." Curr Top Dev Biol **52**: 1-53.

Keeney, S. and M. J. Neale (2006). "Initiation of meiotic recombination by formation of DNA double-strand breaks: mechanism and regulation." Biochem Soc Trans **34**(Pt 4): 523-5.

Kerrebrock, A. W., D. P. Moore, et al. (1995). "Mei-S332, a Drosophila protein required for sister-chromatid cohesion, can localize to meiotic centromere regions." Cell **83**(2): 247-56.

Kiburz, B. M., D. B. Reynolds, et al. (2005). "The core centromere and Sgo1 establish a 50-kb cohesin-protected domain around centromeres during meiosis I." Genes Dev **19**(24): 3017-30.

Kitajima, T. S., S. A. Kawashima, et al. (2004). "The conserved kinetochore protein shugoshin protects centromeric cohesion during meiosis." Nature **427**(6974): 510-7.

Kleckner, N. (2006). "Chiasma formation: chromatin/axis interplay and the role(s) of the synaptonemal complex." Chromosoma **115**(3): 175-94.

Lee, B. and A. Amon (2001). "Meiosis: how to create a specialized cell cycle." Curr Opin Cell Biol **13**(6): 770-7.

Lee, B. H. and A. Amon (2003). "Role of Polo-like kinase CDC5 in programming meiosis I chromosome segregation." Science **300**(5618): 482-6.

Lee, B. H., A. Amon, et al. (2002). "Spo13 regulates cohesin cleavage." Genes Dev **16**(13): 1672-81.

Lee, B. H., B. M. Kiburz, et al. (2004). "Spo13 maintains centromeric cohesion and kinetochore coorientation during meiosis I." Curr Biol **14**(24): 2168-82.

Lenzi, M. L., J. Smith, et al. (2005). "Extreme heterogeneity in the molecular events leading to the establishment of chiasmata during meiosis i in human oocytes." Am J Hum Genet **76**(1): 112-27.

Lynn, A., R. Soucek, et al. (2007). "ZMM proteins during meiosis: crossover artists at work." Chromosome Res **15**(5): 591-605.

Marston, A. L. and A. Amon (2004). "Meiosis: cell-cycle controls shuffle and deal." Nat Rev Mol Cell Biol **5**(12): 983-97.

Marston, A. L., W. H. Tham, et al. (2004). "A genome-wide screen identifies genes required for centromeric cohesion." Science **303**(5662): 1367-70.

Martini, E. and S. Keeney (2002). "Sex and the single (double-strand) break." Mol Cell **9**(4): 700-2.

Maxfield Boumil, R., B. Kemp, et al. (2003). "Meiotic segregation of a homeologous chromosome pair." Mol Genet Genomics **268**(6): 750-60.

McKee, B. D. (2004). "Homologous pairing and chromosome dynamics in meiosis and mitosis." Biochim Biophys Acta **1677**(1-3): 165-80.

Monje-Casas, F., V. R. Prabhu, et al. (2007). "Kinetochore orientation during meiosis is controlled by Aurora B and the monopolin complex." Cell **128**(3): 477-90.

Morelli, M. A. and P. E. Cohen (2005). "Not all germ cells are created equal: aspects of sexual dimorphism in mammalian meiosis." Reproduction **130**(6): 761-81.

Nasheuer, H. P., R. Smith, et al. (2002). "Initiation of eukaryotic DNA replication: regulation and mechanisms." Prog Nucleic Acid Res Mol Biol **72**: 41-94.

Nasmyth, K. (2005). "How might cohesin hold sister chromatids together?" Philos Trans R Soc Lond B Biol Sci **360**(1455): 483-96.

Nasmyth, K. and C. H. Haering (2005). "The structure and function of SMC and kleisin complexes." Annu Rev Biochem **74**: 595-648.

Pacchierotti, F., I. D. Adler, et al. (2007). "Gender effects on the incidence of aneuploidy in mammalian germ cells." Environ Res **104**(1): 46-69.

Page, S. L. and R. S. Hawley (2004). "The genetics and molecular biology of the synaptonemal complex." Annu Rev Cell Dev Biol **20**: 525-58.

Petronczki, M., J. Matos, et al. (2006). "Monopolar attachment of sister kinetochores at meiosis I requires casein kinase 1." Cell **126**(6): 1049-64.

Pierce, M., K. R. Benjamin, et al. (2003). "Sum1 and Ndt80 proteins compete for binding to middle sporulation element sequences that control meiotic gene expression." Mol Cell Biol **23**(14): 4814-25.

Rabitsch, K. P., J. Gregan, et al. (2004). "Two fission yeast homologs of Drosophila Mei-S332 are required for chromosome segregation during meiosis I and II." Curr Biol **14**(4): 287-301.

Rabitsch, K. P., M. Petronczki, et al. (2003). "Kinetochore recruitment of two nucleolar proteins is required for homolog segregation in meiosis I." Dev Cell **4**(4): 535-48.

Revenkova, E. and R. Jessberger (2006). "Shaping meiotic prophase chromosomes: cohesins and synaptonemal complex proteins." Chromosoma **115**(3): 235-40.

Riedel, C. G., V. L. Katis, et al. (2006). "Protein phosphatase 2A protects centromeric sister chromatid cohesion during meiosis I." Nature **441**(7089): 53-61.

Schwob, E. and K. Nasmyth (1993). "CLB5 and CLB6, a new pair of B cyclins involved in DNA replication in Saccharomyces cerevisiae." Genes Dev **7**(7A): 1160-75.

Shonn, M. A., R. McCarroll, et al. (2000). "Requirement of the spindle checkpoint for proper chromosome segregation in budding yeast meiosis." Science **289**(5477): 300-3.

Shonn, M. A., R. McCarroll, et al. (2002). "Spo13 protects meiotic cohesin at centromeres in meiosis I." Genes Dev **16**(13): 1659-71.

Skibbens, R. V., M. Maradeo, et al. (2007). "Fork it over: the cohesion establishment factor Ctf7p and DNA replication." J Cell Sci **120**(Pt 15): 2471-7.

Smith, K. N., A. Penkner, et al. (2001). "B-type cyclins CLB5 and CLB6 control the initiation of recombination and synaptonemal complex formation in yeast meiosis." Curr Biol **11**(2): 88-97.

Storlazzi, A., S. Tesse, et al. (2008). "Coupling meiotic chromosome axis integrity to recombination." Genes Dev **22**(6): 796-809.

Stuart, D. and C. Wittenberg (1998). "CLB5 and CLB6 are required for premeiotic DNA replication and activation of the meiotic S/M checkpoint." Genes Dev **12**(17): 2698-710.

Sumara, I., E. Vorlaufer, et al. (2002). "The dissociation of cohesin from chromosomes in prophase is regulated by Polo-like kinase." Mol Cell **9**(3): 515-25.

Tang, Z., H. Shu, et al. (2006). "PP2A is required for centromeric localization of Sgo1 and proper chromosome segregation." Dev Cell **10**(5): 575-85.

Toth, A., K. P. Rabitsch, et al. (2000). "Functional genomics identifies monopolin: a kinetochore protein required for segregation of homologs during meiosis i." Cell **103**(7): 1155-68.

Tsubouchi, T. and G. S. Roeder (2005). "A synaptonemal complex protein promotes homology-independent centromere coupling." Science **308**(5723): 870-3.

Uhlmann, F. (2003). "Chromosome cohesion and separation: from men and molecules." Curr Biol **13**(3): R104-14.

Watanabe, Y. (2006). "A one-sided view of kinetochore attachment in meiosis." Cell **126**(6): 1030-2.

Weitzer, S. and F. Uhlmann (2002). "Chromosome segregation: playing polo in prophase." Dev Cell **2**(4): 381-2.

Whitby, M. C. (2005). "Making crossovers during meiosis." Biochem Soc Trans **33**(Pt 6): 1451-5.

Winey, M., G. P. Morgan, et al. (2005). "Three-dimensional ultrastructure of Saccharomyces cerevisiae meiotic spindles." Mol Biol Cell **16**(3): 1178-88.

Xu, L., M. Ajimura, et al. (1995). "NDT80, a meiosis-specific gene required for exit from pachytene in Saccharomyces cerevisiae." Mol Cell Biol **15**(12): 6572-81.

Yu, H. G. and D. Koshland (2005). "Chromosome morphogenesis: condensin-dependent cohesin removal during meiosis." Cell **123**(3): 397-407.

Zickler, D. and N. Kleckner (1998). "The leptotene-zygotene transition of meiosis." Annu Rev Genet **32**: 619-97.

Zickler, D. and N. Kleckner (1999). "Meiotic chromosomes: integrating structure and function." Annu Rev Genet **33**: 603-754.

Chapter 2:

Rec8 Phosphorylation and Recombination Promote the Step-wise Loss of Cohesins in Meiosis

Reprinted from Nature Publishing Group:

Gloria A. Brar, Brendan M. Kiburz, Yi Zhang , Ji-Eun Kim, Forest White and Angelika Amon

Nature 441, 532-536

Abstract

Meiosis is a specialized cell division in which a single round of DNA replication is followed by two consecutive chromosome segregation phases. The step-wise loss of cohesins, protein complexes that hold sister chromatids together, is essential for the two chromosome segregation phases to occur (Marston and Amon 2004). Loss of cohesins from chromosome arms is essential for homologous chromosomes to segregate during meiosis I. Retention of cohesins around centromeres until meiosis II is required for the accurate segregation of sister chromatids during meiosis II. Here we show that phosphorylation of the cohesin subunit Rec8 contributes to cohesin removal from chromosomes. Cells carrying versions of Rec8 in which phosphorylation sites are mutated to residues that can no longer be phosphorylated are delayed in cohesin removal. Furthermore, Rec8 is phosphorylated on S521 on chromosome arms but not around centromeres during meiosis I, implicating phosphorylation of Rec8 in regulating the stepwise loss of cohesins from chromosomes. Finally, we show that meiotic recombination functions together with Rec8 phosphorylation and Sgo1 to bring about the stepwise loss of cohesins from chromosomes and thus the establishment of the meiotic chromosome segregation pattern.

Introduction

Gamete formation relies on meiosis, a specialized cell cycle. During the meiotic cell cycle, DNA replication is followed by two rounds of chromosome segregation, in which homologs segregate during the first division and sister chromatids are partitioned in the second. Critical to the faithful execution of this specialized chromosome segregation pattern is the way in which cohesin complexes, which hold sister chromatids together, are lost from chromosomes (Marston and Amon 2004). Unlike in mitosis during which cohesins are removed along the entire length of chromosomes at the metaphase – anaphase transition, cohesins are lost from meiotic chromosomes in a stepwise manner. Loss of cohesins from chromosome arms allows the segregation of homologous chromosomes during meiosis I because it causes the resolution of meiotic recombination events, which hold homologous chromosomes together prior to anaphase I (Buonomo, Rabitsch et al. 2003). Maintenance of cohesins around centromeres beyond anaphase I and cohesin removal at the metaphase II – anaphase II transition are essential for accurate segregation of sister chromatids during meiosis II. Several factors have been identified that are required for maintaining cohesins around centromeres during meiosis I: Mei-S332/Sgo1, which localizes to regions around centromeres (Kerrebrock, Moore et al. 1995; Tang, Bickel et al. 1998; Katis, Galova et al. 2004; Kitajima, Kawashima et al. 2004; Marston, Tham et al. 2004), the spindle checkpoint component Bub1(Kitajima, Kawashima et al. 2004; Tang, Sun et al. 2004; Kiburz, Reynolds et al. 2005; Kitajima, Hauf et al. 2005), the kinetochore proteins Iml3 and Chl4

(Marston, Tham et al. 2004), and the meiosis-specific protein Spo13 (Lee, Amon et al. 2002; Shonn, McCarroll et al. 2002; Katis, Matos et al. 2004). The mechanisms whereby these proteins prevent cohesin removal around centromeres during meiosis I are not understood.

Cohesins are removed from chromosomes by a protease known as Separase (Esp1 in yeast). After the ubiquitin-dependent destruction of its inhibitory subunit Securin (Pds1 in yeast) mediated by the Anaphase Promoting Complex/Cyclosome (APC/C), Separase cleaves a subunit of the cohesin complex, Scc1/Mcd1 during mitosis or the meiosis-specific variant Rec8 during meiosis, allowing for anaphase chromosome movement to occur (Nasmyth and Haering 2005). In meiosis, it has recently been shown that the polo kinase Cdc5 contributes to cohesin removal that is cleavage-independent and occurs during prophase (Yu and Koshland 2005). The protein kinase also plays a role in promoting cleavage by Separase during mitosis as well as meiosis (Alexandru, Uhlmann et al. 2001) (Lee and Amon 2003) (Clyne, Katis et al. 2003). Furthermore, during meiosis, phopshorylation of the cohesin subunit Rec8 is significantly decreased in the absence of Cdc5 (Lee and Amon 2003), raising the possibility that Rec8 phosphorylation is important for the protein's cleavage and thus anaphase I onset.

Results

Mapping Rec8 phosphorylation sites

To determine the importance of Rec8 phosphorylation in cohesin cleavage we mapped the phosphorylation sites of Rec8. We isolated endogenous Rec8 from cells arrested in metaphase I either by depletion of the APC/C activator Cdc20 (Lee and Amon ; Lee and Amon 2003) or by expression of a non-degradable version of Pds1 from the meiosis-specific *DMC1* promoter (*pDMC1-PDS1dBΔ,* see Materials and Methods). In both arrests, Rec8 is highly phosphorylated (data not shown). We also isolated Rec8 from cells arrested in metaphase I due to the depletion of Cdc5 to be able to identify the phosphorylation sites whose phosphorylation depended on Cdc5. Rec8 isolated from the three arrests was resolved by SDS-PAGE gel and subjected to in-gel digest with either trypsin or chymotrypsin followed by LC-MS/MS to identify phosphorylation sites (an example MS/MS spectrum is shown in Figure 1). The procedure was performed several times until subsequent analyses did not yield additional phosphorylation sites. This analysis covered 66 percent of Rec8 obtained from Pds1dBΔ expressing cells, 77 percent of Rec8 obtained from Cdc20-depleted cells, and 65 percent of Rec8 obtained from Cdc5-depleted cells (Figure 2A-C). The overall coverage of Rec8 from arrests in which Rec8 is phosphorylated was 85 percent. Selected regions (Figure 2A - C) were not amenable to gel-digest LC-MS/MS analysis, most likely due to incompatibility with reverse-phase liquid

chromatography (peptides which were too hydrophilic or too hydrophobic) or poor peptide fragmentation resulting in low-quality MS/MS spectra.

Figure 1: Example of a MS/MS spectrum.
MS/MS spectrum resulting from isolation and fragmentation of the quadruply-charged precursor ion of the doubly phosphorylated peptide KYKGLpTpTVWLLSALGNSIVK on a quadruple time-of-flight mass spectrometer. Sequence coverage generated by singly-charged y-type fragment ions enables confident identification of the peptide.

Figure 1

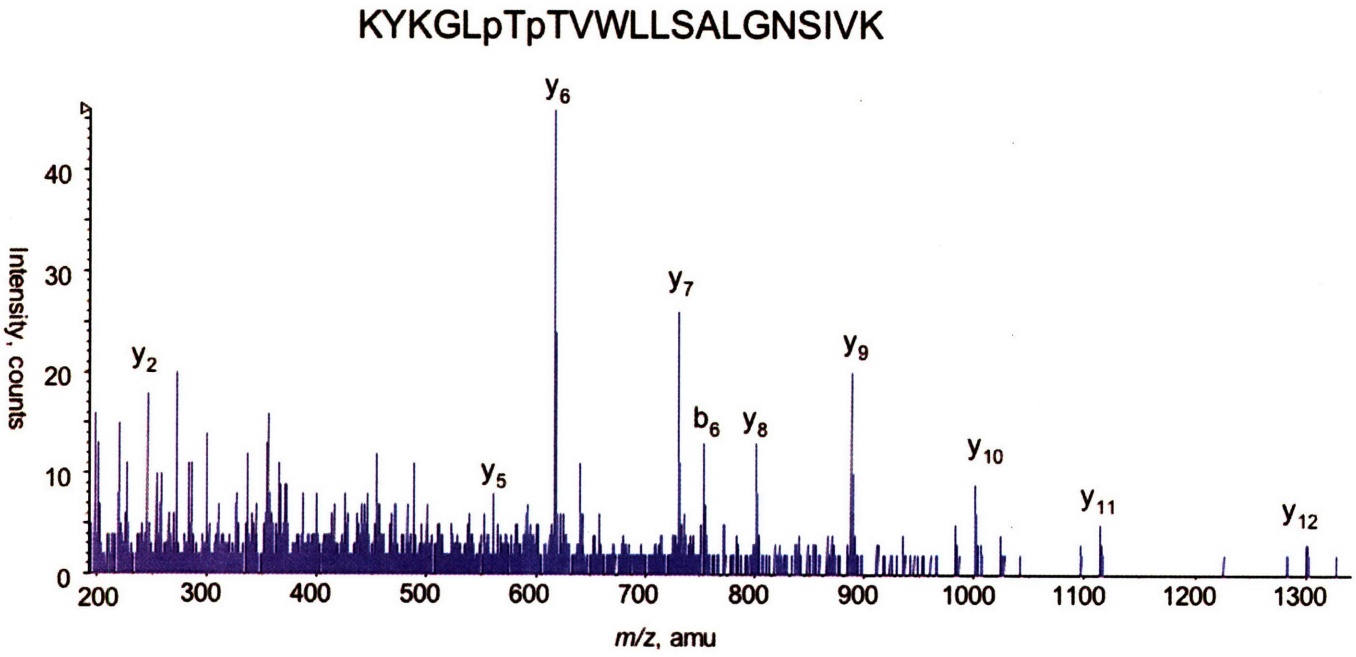
KYKGLpTpTVWLLSALGNSIVK
Intensity, counts
m/z, amu
y6
y7
y2
y9
b6
y8
y5
y10
y11
y12
0
10
20
30
40
200
300
400
500
600
700
800
900
1000
1100
1200
1300

Figure 2: Coverage of the Rec8 in the various cells cycle arrest.
(A – C) Rec8 protein sequence with sequences covered in the mass-spectrometry analyses shown in red. (A) shows the coverage of Rec8 in Cdc20-depleted cells (A5441), (B) shows coverage in cells expressing Pds1dbΔ (A10925) and (C) shows coverage in Cdc5-depleted cells (A9858). For each condition, gel digestion and MS analyses was performed with both chymotrypsin and trypsin in separate analyses. The coverage map is a summation of the peptides from both types of enzymatic digestion. Peptides identified by LC-MS/MS analysis, MASCOT database search, and manual sequence confirmation are indicated in bold red, phosphorylation sites are indicated by blue italics. In almost all cases, sufficient fragmentation information was available to unambiguously assign specific sites of phosphorylation. Sites, which could not be unambiguously localized have been indicated by lower case.

(D) Migration of Rec8 mutants in SDS Page: cells were harvested and lysed for Western blot analysis from wild type (A1972), *pCLB2-CDC5* (A6143), *rec8-17A* (A14750) and *rec8-29A* (A14872) cells, resolved by SDS PAGE and visualized using an anti-HA antibody.

Figure 2

a

pCLB2-CDC20

MAPLSLNFKD DKKYKGLTTV WLLSALGNSI VKESNNYYSN KSNSTGNISS
STVKKKDIVN ISIPKTCDEI QNFENDFSLR YISNLLYGVT ICYNKKTEYV
LNDLNHLLVQ LQKNDVYAFK AKNKSTRING LNSNNSIIGN KNNNYTWEEC
VFFDDDPLYD ITKVPALEFL NTTLQDNVSF IEEAKSIRRQ DYINELSNSN
RFELHGDMTN SDAQSNLGSN VRNSFPLDEI PVDVDFNLDL DDIVsHQGtP
LGSHSSSQKD GNDFKFNYQG DELVLNFEND NENNsNGGED tsVENEGPVA
NLKDYELGLE AQASEEENDL QQKVNTRMQR GHRADVGGQF SKVQFDAKTS
YPNEVLKFNH GNYSHLMEKN RIRKLTGQNF LTSNISSLVR SCGEEEFSST
NWLSIFNDFS NIKTSEWDLN SQGFSSVERG RKRAHSLVST QSSNSTRSHE
YGRKSFRNNK NDNYSSDMEN DNLLLNLEQI NEDLEDGHYI EENSQGNILD
FNLNLPPSSF GRSHTRNSTR SSGFNEDIVG ALRRRVGPSE QNFAEEDDSS
NSCFSEGSQQ NLQQEKTNFQ DVILDYQTKK FYDYIKERSI VVGRTTRSNP
PFKRKMLLVD IIPSRMGEAQ TGANFDDVER GVSRQIAASA FLSLLNLATK
GMVKLNEYPV ADAVTKDLKL RREDEIIVYA

b

pDMC1-PDS1dbΔ

MAPLSLNFKD DKKYKGLTTV WLLSALGNSI VKESNNYYSN KSNSTGNISS
STVKKKDIVN ISIPKTCDEI QNFENDFSLR YISNLLYGVT ICYNKKTEYV
LNDLNHLLVQ LQKNDVYAFK AKNKSTRING LNSNNSIIGN KNNNYTWEEC
VFFDDDPLYD ITKVPALEFL NttLQDNVSF IEEAKSIRRQ DYINELSNSN
RFELHGDMTN SDAQSNLGSN VRNSFPLDEI PVDVDFNLDL DDIVSHQGTP
LGSHSSSQKD GNDFKFNYQG DELVLNFEND NENNSNGGED TSVENEGPVA
NLKDYELGLE AQASEEENDL QQKVNTRMQR GHRADVGGQF SKVQFDAKTS
YPNEVLKFNH GNYSHLMEKN RIRKLTGQNF LTSNISSLVR SCGEEEFSST
NWLSIFNDFS NIKTSEWDLN SQGFSSVERG RKRAHSLVST QSSNSTRSHE
YGRKSFRNNK NDNYSSDMEN DNLLLNLEQI NEDLEDGHYI EENSQGNILD
FNLNLPPSSF GRSHTRNSTR SSGFNEDIVG ALRRRVGPSE QNFAEEDDSS
NSCFSEGSQQ NLQQEKTNFQ DVILDYQTKK FYDYIKERSI VVGRTTRSNP
PFKRKMLLVD IIPSRMGEAQ TGANFDDVER GVSRQIAASA FLSLLNLATK
GMVKLNEYPV ADAVTKDLKL RREDEIIVYA

c

pCLB2-CDC5

MAPLSLNFKD DKKYKGLTTV WLLSALGNSI VKESNNYYSN KSNSTGNISS
STVKKKDIVN ISIPKTCDEI QNFENDFSLR YISNLLYGVT ICYNKKTEYV
LNDLNHLLVQ LQKNDVYAFK AKNKSTRING LNSNNSIIGN KNNNYTWEEC
VFFDDDPLYD ITKVPALEFL NTTLQDNVSF IEEAKSIRRQ DYINELSNSN
RFELHGDMTN SDAQSNLGSN VRNSFPLDEI PVDVDFNLDL DDIVSHQGTP
LGSHSSSQKD GNDFKFNYQG DELVLNFEND NENNSNGGED TSVENEGPVA
NLKDYELGLE AQASEEENDL QQKVNTRMQR GHRADVGGQF SKVQFDAKTS
YPNEVLKFNH GNYSHLMEKN RIRKLTGQNF LTSNISSLVR SCGEEEFSST
NWLSIFNDFS NIKTSEWDLN SQGFSSVERG RKRAHSLVST QSSNSTRSHE
YGRKSFRNNK NDNYSSDMEN DNLLLNLEQI NEDLEDGHYI EENSQGNILD
FNLNLPPSSF GRSHTRNSTR SSGFNEDIVG ALRRRVGPSE QNFAEEDDSS
NSCFSEGSQQ NLQQEKTNFQ DVILDYQTKK FYDYIKERSI VVGRTTRSNP
PFKRKMLLVD IIPSRMGEAQ TGANFDDVER GVSRQIAASA FLSLLNLATK

d

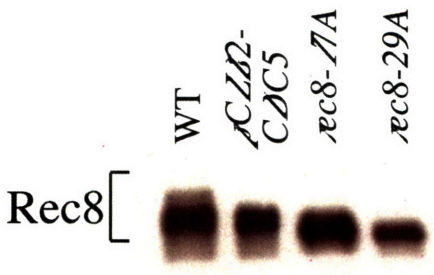

Our mass spectrometry analyses identified a total of 24 phosphorylation sites. Mutation of these sites to alanines led to progressive loss of Rec8 phosphorylation as judged by the loss of slower migrating forms of Rec8 on SDS -PAGE (Figure 2D), which have been shown to be due to phosphorylation (Lee and Amon 2003). The identity of these phosphorylation sites is shown in Table 2. Seven sites (Y14, T18, T19, S314, S494, S521, S522) were found to be phosphorylated in Cdc5-depleted cells and either in Cdc20-depleted cells or Pds1dBΔ-expressing cells. Six other sites were found to be phosphorylated in either Cdc20-depleted cells or Pds1dBΔ expressing cells, but the sites were not covered in the mass-spectrometry analysis of Rec8 obtained from Cdc5-depleted cells. Eleven sites (S136, T173, S179, S197, S199, S215, S386, S387, S410, S465, S466) were phosphorylated in Rec8 obtained either from Cdc20-depleted cells, Pds1dBΔ-expressing cells, or both, but not from Cdc5-depleted cells. This indicates that phosphorylation of these 11 sites is Cdc5-dependent and raises the possibility that these sites are phosphorylated by Cdc5 *in vivo*. 10 of the 11 sites phosphorylated in a Cdc5-dependent manner were serines (Table 2). All 11 sites contain at least one asparagine (one site contained a glutamine) in the –3 to –1 region. In all instances, the aspargine is preceded byeither a serine, aspartic acid or glutamic acids within three amino acids. Furthermore, a polar amino acid is found at position +4 in all sites. Thus, Cdc5-dependent phosphorylation sites are defined by the motif S/E/D – X_{0-2} – N(Q) – X_{0-2} – Sp (Tp)

$-X_3-\pi$, where π represents a polar amino acid (Table 1). We also noticed other features that, though not present in all sites, appear enriched in the area surrounding the Cdc5-dependent phosphorylation sites. First, an aliphatic amino acid is frequently present in the +1 to +3 region, which has previously been found to be a feature of sites phopshorylated by Cdc5 *in vitro* (Hu and Elledge 2002; Shou, Azzam et al. 2002). Also the asparagine is often preceded by a leucine (or isoleucine) within three amino acids. With this description of Cdc5-dependent phosphorylation sites in hand it will perhaps be possible to identify Cdc5 target sites using computational approaches.

Table 1
CDC5-dependent phosphorylation sites

-10	-9	-8	-7	-6	-5	-4	-3	-2	-1		1	2	3	4	5	6	7	8	9	10
T	R	I	N	G	L	N	S	N	N	S136	I	I	G	N	K	N	N	N	Y	T
K	V	P	A	L	E	F	L	N	T	T173	L	Q	D	N	V	S	F	I	E	E
F	L	N	T	T	L	Q	D	N	V	S179	F	I	E	E	A	K	S	I	R	R
I	R	R	Q	D	Y	I	N	E	L	S197	N	S	N	R	F	E	L	H	G	D
R	Q	D	Y	N	N	E	L	S	N	S199	N	R	F	E	L	H	G	D	M	T
H	G	D	M	N	N	S	D	A	Q	S215	N	L	G	S	N	V	R	N	S	F
T	G	Q	N	F	L	T	S	N	I	S386	S	L	V	R	S	C	G	E	E	E
G	Q	N	F	L	T	S	N	I	S	S387	L	V	R	S	C	G	E	E	E	F
T	N	W	L	S	I	F	N	D	F	S410	N	I	K	T	S	E	W	D	L	N
S	F	R	N	N	K	N	D	N	Y	S465	S	D	M	E	N	D	N	L	L	L
F	R	N	N	K	N	D	N	Y	S	S466	D	M	E	N	D	N	L	L	L	N

Consensus that fits 11/11 sites: S/E/D - X_{0-2} - N(Q) - X_{0-2} - Sp(Tp) - X_3 - π

Amino acids with similar biochemical properties were grouped together:
N/Q: purple
E/D: green
S/T surrounding the phosphorylated residue: yellow
L/I/V: blue
π: polar amino acids

Table 2: Cdc5 independent phosphorylation sites:

Residue	*pCLB2-CDC20* arrest	*pDMC1-PDS1dbΔ* arrest	*pCLB2-CDC5* arrest	*rec8-6A*	*rec8-11A*	*rec8-psa*	*rec8-17A*	*rec8-21A*	*rec8-24A*	*rec8-29A*
Y14	N	NC	Y						x	x
T18	N	N	Y					x	x	x
T19	N	N	Y					x	x	x
S314	Y	Y	Y		x		x	x	x	x
S494	Y	NC	Y					x	x	x
S521	Y	Y	Y	x	x		x	x	x	x
S522	Y	Y	Y		x		x	x	x	x

Cdc5 dependent phosphorylation sites:

Residue	*pCLB2-CDC20* arrest	*pDMC1-PDS1dbΔ* arrest	*pCLB2-CDC5* arrest	*rec8-6A*	*rec8-11A*	*rec8-psa*	*rec8-17A*	*rec8-21A*	*rec8-24A*	*rec8-29A*
S136	N	Y	N		x	x	x	x	x	x
T173	Y	N	N	x	x	x	x	x	x	x
S179	Y	Y	N			x	x	x	x	x
S197	Y	Y	N	x	x	x	x	x	x	x
S199	N	Y	N		x	x	x	x	x	x
S215	N	Y	N			x	x	x	x	x
S386	Y	Y	N	x	x	x	x	x	x	x
S387	Y	Y	N	x	x	x	x	x	x	x
S410	N	Y	N			x	x	x	x	x
S465	Y	NC	N			x	x	x	x	x
S466	Y	NC	N			x	x	x	x	x

Key
N: Not identified as phosphorylated

Y: Identified as phosphorylated
NC: Not covered
x: Denotes sites mutated in various mutants

Phosphorylations sites not covered in the *pCLB2-CDC5* arrest that fit the Cdc5 consensus:

Residue	*pCLB2-CDC20* arrest	*pDMC1-PDS1dbΔ* arrest	*pCLB2-CDC5* arrest	*rec8-6A*	*rec8-11A*	*rec8-psa*	*rec8-17A*	*rec8-21A*	*rec8-24A*	*rec8-29A*
T249	Y	NC	NC		x		x	x	x	x
S285	Y	N	NC				x	x	x	x
S421	NC	Y	NC					x	x	x

Phosphorylations sites not covered in the *pCLB2-CDC5* arrest that do not fit the Cdc5 consensus:

Residue	*pCLB2-CDC20* arrest	*pDMC1-PDS1dbΔ* arrest	*pCLB2-CDC5* arrest	*rec8-6A*	*rec8-11A*	*rec8-psa*	*rec8-17A*	*rec8-21A*	*rec8-24A*	*rec8-29A*
S245	Y	NC	NC	x	x		x	x	x	x
T291**	Y	N	NC							
S292	Y	N	NC						x	x

Putative Cdc5 phosphorylation sites in regions of Rec8 not covered by any mass-spectrometry analysis:***

Residue	*pCLB2-CDC20* arrest	*pDMC1-PDS1dbΔ* arrest	*pCLB2-CDC5* arrest	*rec8-6A*	*rec8-11A*	*rec8-psa*	*rec8-17A*	*rec8-21A*	*rec8-24A*	*rec8-29A*
S125	NC	NC	NC							x
T126	NC	NC	NC							x
S224	NC	NC	NC							x
S404	NC	NC*	NC*							x
S425	NC	NC*	NC							x
S552	NC	NC	NC						x	x

Covered in late round while manuscript in preparation. Only non-phosphorylated peptide identified.
Identified in late round while manuscript in preparation.
**Selected based on general similarity to Cdc5-dependent sites identified in early mass spectrometry rounds.

Investigating the functional significance of Rec8 phosphorylation

A defect in cohesin removal is expected to interfere with entry into anaphase I (Buonomo, Clyne et al. 2000). To determine the importance of Rec8 phosphorylation in cohesin removal we mutated the phosphorylated sites within Rec8 to amino acids that can no longer be phosphorylated. Mutation of individual phosphorylation sites to alanine did not affect sporulation efficiency (data not shown). Thus, owing to the large number of phosphorylation sites within Rec8 we mutated several phosphorylation sites simultaneously and examined the phenotypes of a select number of *REC8* mutants. The order in which phosphorylation sites were mutated was determined by the order in which the sites were identified in the mass-spectrometry analyses. Figure 3A shows two examples of such an analysis. Cells carrying a version of *REC8* that had six (*rec8-6A,* Figure 3) or 11 sites (*rec8-11A,* Figure 3) mutated to alanine did not exhibit a metaphase I delay but experienced a delay in prophase I (2 hours in this experiment). Deletion of *REC8* causes cell cycle arrest in prophase I due to an inability to repair meiotic double strand breaks (Klein, Mahr et al. 1999). Although spore viability was not significantly reduced in the mutants (Figure 3A), the 2 hour prophase delay exhibited by the *rec8-6A* and *rec8-11A* mutants points towards these *rec8* alleles not being fully functional. This result additionally raises the possibility that phosphorylation of Rec8 is important for the protein's prophase functions.

Next we examined the consequences of mutating the 11 residues, whose phosphorylation was shown to depend on Cdc5 to alanine by our mass-

spectrometry analysis (*rec8-psa*). Cells expressing this allele neither exhibited a prophase I delay nor a delay in metaphase I (Figure 3B) indicating that our mass-spectrometry analysis did not identify all Cdc5-dependent phosphorylation sites. This was not surprising given that the coverage in the Cdc5-depletion arrest was only 65%. We therefore, in addition to the known Cdc5-dependent sites (S136, T173, S179, S197, S199, S215, S386, S387, S410, S465, S466), mutated sites found to be phosphorylated in the *pCLB2-CDC20* and/or *pCLB2-PDS1dBΔ* arrests but were not covered in the Cdc5-depletion arrest (S245, T249, S285) as well as three Cdc5-independent sites (S314, S521, S522) to alanine (*rec8-17A*, Figure 3). Cells expressing this *REC8* mutant exhibited a 1 hour prophase I delay. In addition, this mutant showed a metaphase I delay (Figure 4A). Although the delay was not as dramatic as that observed in cells expressing a non-cleavable version of Rec8 (compare Figure 4A and Figure 5A), this result indicates that expression of this mutant version of *REC8* interferes with the onset of anaphase I. Entry into anaphase II was only slightly if at all delayed in the *rec8-17A* mutant (Figure 5B) suggesting that Rec8 phosphorylation is less important for this cell cycle transition. We also examined mutants in which all phosphorylated serines and threonines, except two recently identified sites (T291, S292), were mutated to alanine (*rec8-21A*; Figure 3) and mutants that had additional putative Cdc5 phosphorylation sites mutated to alanine that were not covered in any of the mass-spectrometry analyses (*rec8-24A, rec8-29A*; Figure 3). Cells expressing Rec8-21A, Rec8-24A or Rec8-29A appeared to be delayed in metaphase I though the extent of the delay was

difficult to assess owing to the severe prophase I delay exhibited by the mutants (Figure 3C). We conclude that mutating Rec8's phosphorylation sites leads to impairment in Rec8's prophase function and interferes with anaphase I entry. Because the anaphase I entry delay was the least obscured by the prophase delay in the *rec8-17A* mutant and because the mutant was likely to have most Cdc5-dependent phosphorylation sites mutated to alanine, we analyzed this mutant in more detail.

Figure 3: Mutation of the phosphorylation sites in Rec8 to alanine interferes with progression through meiosis I.
Wild-type cells (A1972, A1656; closed diamonds) and cells expressing various *REC8* mutants (A: *rec8-6A* [A15042] open circles; *rec8-11A* [A15044] closed circles; B: *rec8-psa* [A15364] closed triangles; C: *rec8-21A* [A14352] open squares; *rec8-24A* [A14091] closed squares; *rec8-29A* [A14342] open diamonds) were sporulated. Time points were taken at the indicated times to determine the percentage of cells in prophase (left panel), of metaphase I cells (middle panel) and of the sum of bi- and tetra-nucleate cells (right panel). The number in brackets located next to the legend indicates the percentage of viable spores derived from previous analysis for the given strains (n=176).

Figure 3

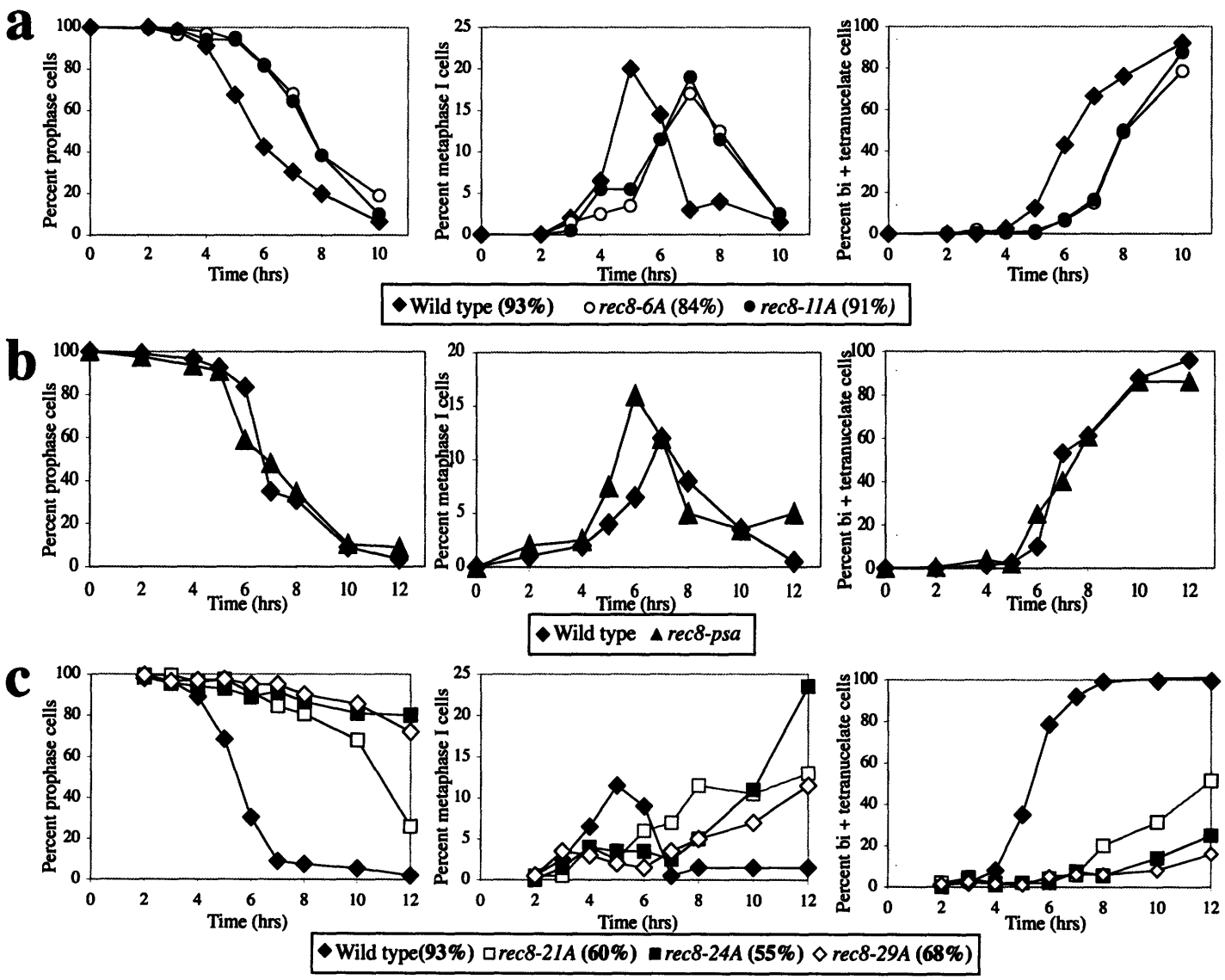
a
Percent prophase cells
Time (hrs)
Percent metaphase I cells
Time (hrs)
Percent bi + tetranucelate cells
Time (hrs)
◆Wild type (93%) ○rec8-6A (84%) ●rec8-11A (91%)
b
Percent prophase cells
Time (hrs)
Percent metaphase I cells
Time (hrs)
Percent bi + tetranucelate cells
Time (hrs)
◆Wild type ▲rec8-psa
c
Percent prophase cells
Time (hrs)
Percent metaphase I cells
Time (hrs)
Percent bi + tetranucelate cells
Time (hrs)
◆Wild type(93%) □rec8-21A (60%) ■rec8-24A (55%) ◇rec8-29A (68%)

Figure 5: Mutations in the phosphorylation or cleavage sites of Rec8 interferes with chromosome segregation.
(A) Wild type (A1972, closed diamonds) and cells expressing a non-cleavable version of *REC8* (*REC8-NC,* A13539, open triangles) were induced to sporulate. At the indicated time the percentage of cells in prophase I (left panel), in metaphase I (middle panel) and the sum of bi- and tetra-nucleate cells (right panel) was determined.

(B) Wild type (A15086, closed diamonds) and *rec8-17A* mutant (A14750, closed triangles) cells were induced to sporulate and the percentage of metaphase II cells was determined at the indicated time.

Figure 5

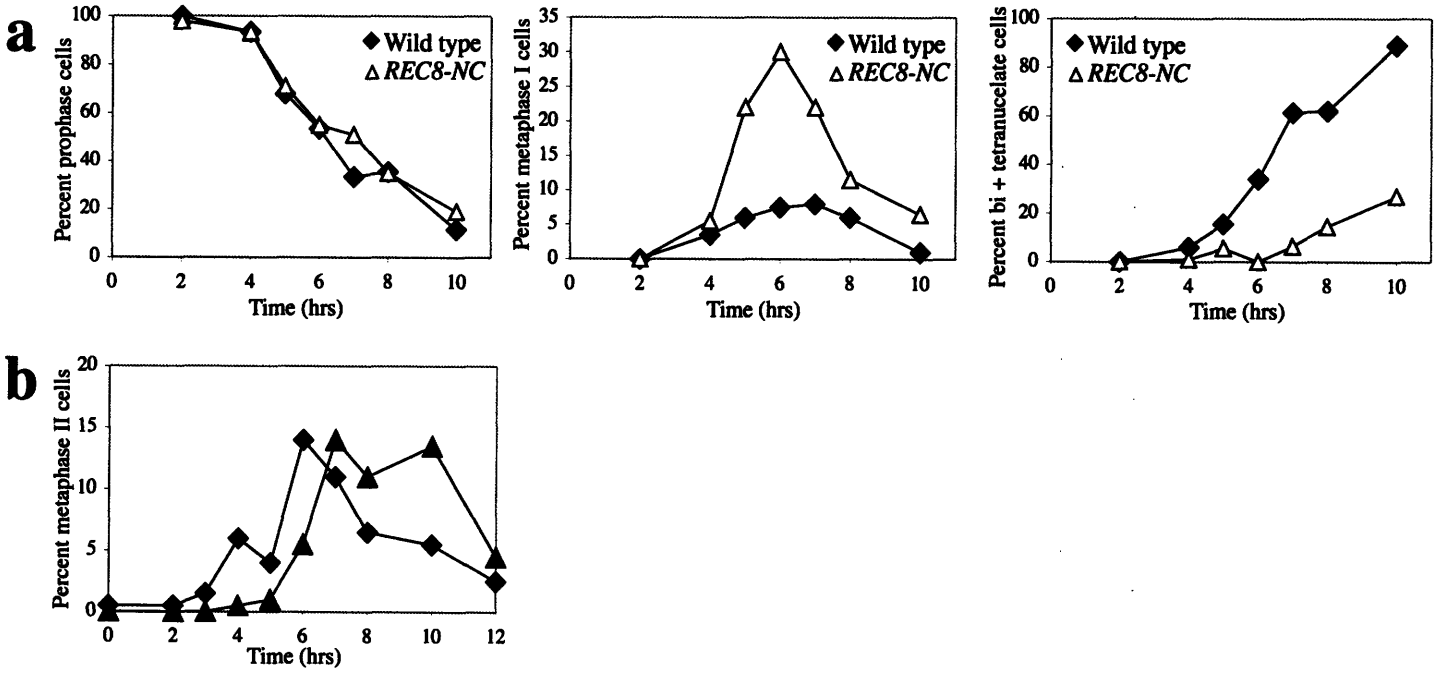
a
Percent prophase cells
Wild type
REC8-NC
Time (hrs)
Percent metaphase I cells
Wild type
REC8-NC
Time (hrs)
Percent bi + tetranucelate cells
Wild type
REC8-NC
Time (hrs)
b
Percent metaphase II cells
Time (hrs)

Investigating the role of Rec8 phosphorylation in anaphase I entry

To determine why *rec8-17A* mutants were delayed in anaphase I entry we first examined whether the delay was due to stabilization of Pds1. Analysis of Pds1 by indirect *in situ* immunofluorescence revealed that *rec8-17A* cultures contained a significant fraction of metaphase I cells lacking Pds1 (Figure 4C, Figure 6A). This was not only apparent when Pds1 was analyzed in metaphase I cells but also when all pre-anaphase I cells were examined (Figure 6B). A population of pre-anaphase I cells lacking Pds1 staining persisted up to 7 hours after entry into the meiotic cell cycle in *rec8-17A* mutant cells. We conclude that the metaphase I delay observed in the *rec8-17A* mutant is at least in part due to events occurring after the degradation of Pds1.

To determine the effects of Rec8 phosphorylation on cohesin cleavage we examined the accumulation of the C-terminal Rec8 cleavage product by Western blot analysis. In wild-type cells, the C-terminal Rec8 cleavage product accumulated 4 hours after transfer of cells into sporulation-inducing conditions (Figure 4B). As expected the *rec8-psa* mutant did not exhibit a Rec8 cleavage delay (Figure 7). In the *rec8-17A* mutant, the protein assembled onto chromosomes normally as judged by Rec8 localization on chromosomes spreads and by chromatin immunopreciptitation (ChIP) analysis (Figure 4D, E) but cleavage did not occur until 7 hours in *rec8-17A* mutants (Figure 4A, B). This delay was only in part due to defects in prophase I. The prophase I delay observed in the *rec8-17A* mutant was 90 minutes, whereas Rec8 cleavage was

delayed by 3 hours (Figure 4A, B). Our results indicate that cleavage of the rec8-17A mutant protein is delayed not only due to the delays in prophase I but also due to direct interference with events occurring after the degradation of Pds1. We conclude that phosphorylation of Rec8 is important for its timely cleavage.

Figure 4: Rec8 cleavage is delayed in *rec8-17A* cells.
(A, B) Wild type (A14655; diamonds) and *rec8-17A* mutant (A14746, triangles) cells both carrying a *REC8-HA* fusion were induced to sporulate. Cells also lacked the ubiquitn ligase *UBR1* to facilitate detection of the Rec8 cleavage product. At the indicated times the percentage of metaphase I cells (B, left panel), of prophase (B, solid symbols) and the sum of bi- and tetra-nucleate cells (B, open symbols) was determined. Rec8-3HA and Pgk1 were analyzed by Western blotting (A). Pgk1 was used as a loading control in Western blots.
(C) Wild type (A14923) and *rec8-17A* mutant (A14861) cells both carrying a *PDS1-13MYC* fusion were induced to sporulate. At the indicated times meiotic progression was scored and Pds1 status was noted for all metaphase I cells.
(D) The localization of Rec8 is shown on chromosome spreads of wild-type cells and *rec8-17A* mutants. Rec8 is shown in red, DNA in blue in the merge.

(E) Wild type *REC8-3HA* (A1972) and *rec8-17A-3HA* (A13559) were induced to sporulate along with a wild type strain lacking the tagged *REC8* allele (A4962). Samples were taken for chromatin immunoprecipitation after 4 hours. PCR analysis of immunoprecipitated samples (anti-HA), mock-treated samples (MOCK), and input DNA (1:250) are shown along with a schematic diagram indicating locations of chromosomes III primer sets. Cen3 corresponds to the core centromere, Carc1 and C191.5 correspond to cohesin-rich regions in the pericentromere and arm, respectively, and C281 corresponds to an arm sequence with which cohesin associates poorly.

Figure 4

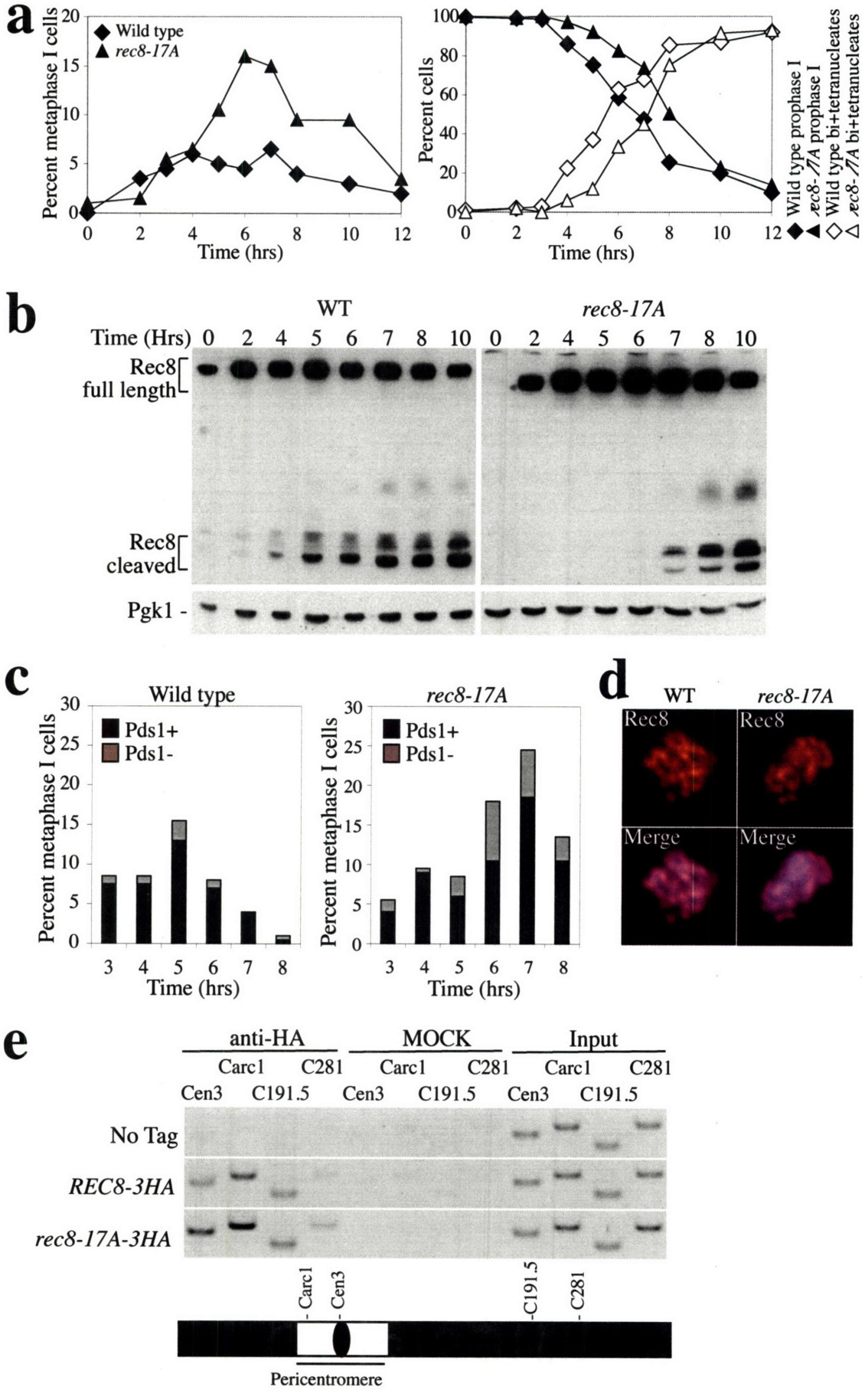
a
Percent metaphase I cells
Wild type
rec8-17A
Time (hrs)
Percent cells
Wild type prophase I
rec8-17A prophase I
Wild type bi+tetranucleates
rec8-17A bi+tetranucleates
b
WT
rec8-17A
Time (Hrs) 0 2 4 5 6 7 8 10 0 2 4 5 6 7 8 10
Rec8 full length
Rec8 cleaved
Pgk1 -
c
Wild type
rec8-17A
Pds1+
Pds1-
Percent metaphase I cells
Time (hrs)
d
WT
rec8-17A
Rec8
Merge
e
anti-HA
MOCK
Input
Carc1
C281
Cen3
C191.5
No Tag
REC8-3HA
rec8-17A-3HA
Pericentromere

Figure 6: Metaphase I cells lacking Pds1 accumulate in *rec8-17A* mutants.
(A) Examples of metaphase I cells that contain Pds1 in the nucleus and metaphase I cells that lack Pds1. Pds1 is shown in red, microtubules in green and DNA is shown in blue.

(B) Wild type (A14723) and *rec8-17A* mutant (A14861) cells both carrying a *PDS1-13MYC* fusion were induced to sporulate. At the indicated times the percentage of mononucleate cells lacking Pds1 (open diamonds), of mononucleate cells that contain Pds1 (closed squares) were counted. In a separate counts the percentage of metaphase I cells (closed diamonds) and the percentage of the sum of bi- and tetranucleate was determined.

Figure 6

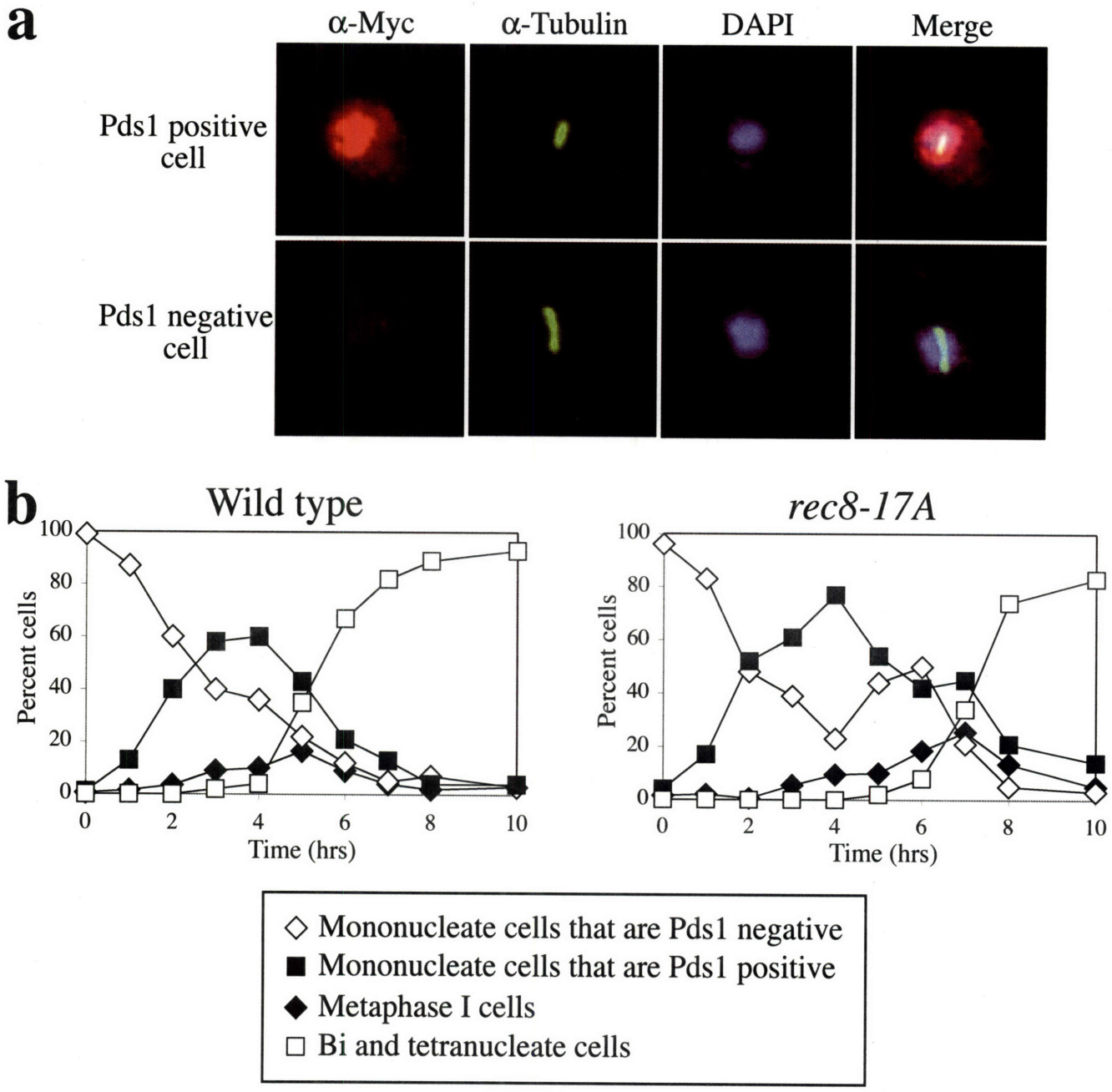
a
α-Myc
α-Tubulin
DAPI
Merge
Pds1 positive cell
Pds1 negative cell
b
Wild type
rec8-17A
Percent cells
Time (hrs)
0
20
40
60
80
100
0
2
4
6
8
10
◇ Mononucleate cells that are Pds1 negative
■ Mononucleate cells that are Pds1 positive
◆ Metaphase I cells
□ Bi and tetranucleate cells

Figure 7: Rec8 cleavage in the *rec8-psa* mutant
Wild type (A14655) and *rec8-psa* (A15364) mutant cells both carrying a *REC8-HA* fusion and a deletion in *UBR1* were induced to sporulate. At the indicated times, samples were taken for Western blot analysis and to determine meiotic progression. Note progression through meiosis for this experiment is shown in Figure 3B.

Figure 7

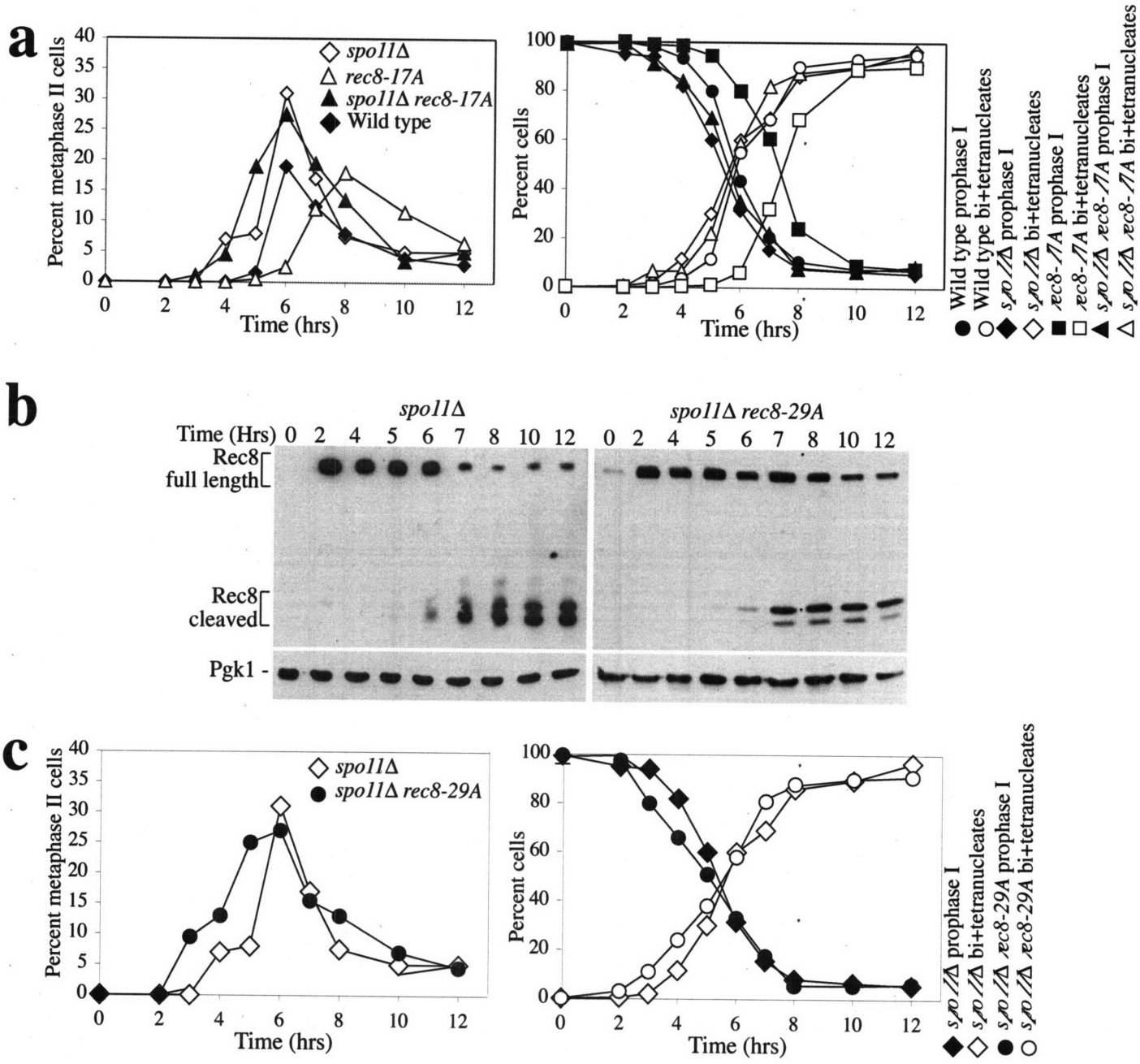
a
Percent metaphase II cells
spo11Δ
rec8-17A
spo11Δ rec8-17A
Wild type
Time (hrs)
Percent cells
Time (hrs)
Wild type prophase I
Wild type bi+tetranucleates
spo11Δ prophase I
spo11Δ bi+tetranucleates
rec8-17A prophase I
rec8-17A bi+tetranucleates
spo11Δ rec8-17A prophase I
spo11Δ rec8-17A bi+tetranucleates
b
spo11Δ
spo11Δ rec8-29A
Time (Hrs) 0 2 4 5 6 7 8 10 12 0 2 4 5 6 7 8 10 12
Rec8 full length
Rec8 cleaved
Pgk1
c
Percent metaphase II cells
spo11Δ
spo11Δ rec8-29A
Time (hrs)
Percent cells
Time (hrs)
spo11Δ prophase I
spo11Δ bi+tetranucleates
spo11Δ rec8-29A prophase I
spo11Δ rec8-29A bi+tetranucleates

Examining the impact of recombination on cohesin cleavage

We also examined the effects of eliminating meiotic recombination on *rec8-17A* mutants. To prevent meiotic recombination we deleted *SPO11*, a gene required to form the recombination-initiating double strand breaks (Bergerat, de Massy et al. 1997; Keeney, Giroux et al. 1997). Surprisingly, deletion of *SPO11* abolished the delay in Rec8 observed in the *rec8-17A* mutant (Figure 8A). Furthermore, cell cycle delays imposed by the rec8-17A mutant were also eliminated (Figure 8B). Similar results were obtained when a catalytic dead version of *SPO11 (spoII-Y135F)* mutant was employed ((Keeney, Giroux et al. 1997), Figure 9) indicating that Spo11's recombination function rather than its role in premeiotic DNA replication was responsible for this suppression. The fact that deletion of *SPO11* allowed Rec8-17A-expressing cells to progress through meiosis I without a delay was expected because abolishing recombination eliminates the need for arm cohesion removal for progression through meiosis I. However, interference with cohesin cleavage is expected to cause a delay in metaphase II in the absence of recombination (Buonomo, Clyne et al. 2000), which was not the case in the *rec8-17A spo11Δ* mutant (Figure 8B). Similar results were obtained in *rec8-29A spo11Δ* mutants (Figure 8A, B). These results indicate that in the absence of recombination Rec8 phosphorylation is not as important for cohesin removal as it is when recombination occurs.

Figure 8: Elimination of recombination abolishes the Rec8 cleavage delay in *rec8-17* and *rec8-29A* mutants due to retention of arm cohesion past meiosis I in a *MAD2*-dependent mannner.
(A, B) *spo11Δ* (A14755; diamonds), *spo11Δ rec8-17A* (A14847, triangles) and *spo11Δ rec8-29A* (A14872, circles) mutant cells both carrying a *REC8-HA* fusion and a deletion in *UBR1* were induced to sporulate. At the indicated times the percentage of metaphase II cells (B, left panel), of mononucleate (B, solid symbols) and the sum of bi- and tetra-nucleate cells (B, open symbols) was determined. Rec8-3HA and Pgk1 were analyzed by Western blotting (A).

(C, D) *spo11Δ* (A9498, closed circles), *spo11Δ pCLB2-SGO1*(A14938, squares) and *pCLB2-SGO1*(A11251, open circles) cells carrying *CEN5-GFP* dots were induced to sporulate. (C) At 12 hours samples were taken to determine GFP dot segregation in tetrads. 100 cells were counted per strain per time point. (D) At the indicated times samples were taken to determine the percentage of metaphase II cells.

(E) *spo11Δ* (A9498), *spo11Δ pCLB2-SGO1*(A14938), *pCLB2-SGO1*(A11251), *spo11Δ pCLB2-SGO1 mad2Δ* (A15345) and *pCLB2-SGO1 mad2Δ* (A15344) cells carrying *CEN5-GFP* dots were induced to sporulate. At 12 hours samples were taken to determine GFP dot segregation in tetrads. Note that it has previously been established that *mad2Δ* mutants to not show chromsome segregation defects or kinetechore attachment defects in meiosis II (Shonn, Murray et al.).

Figure 8

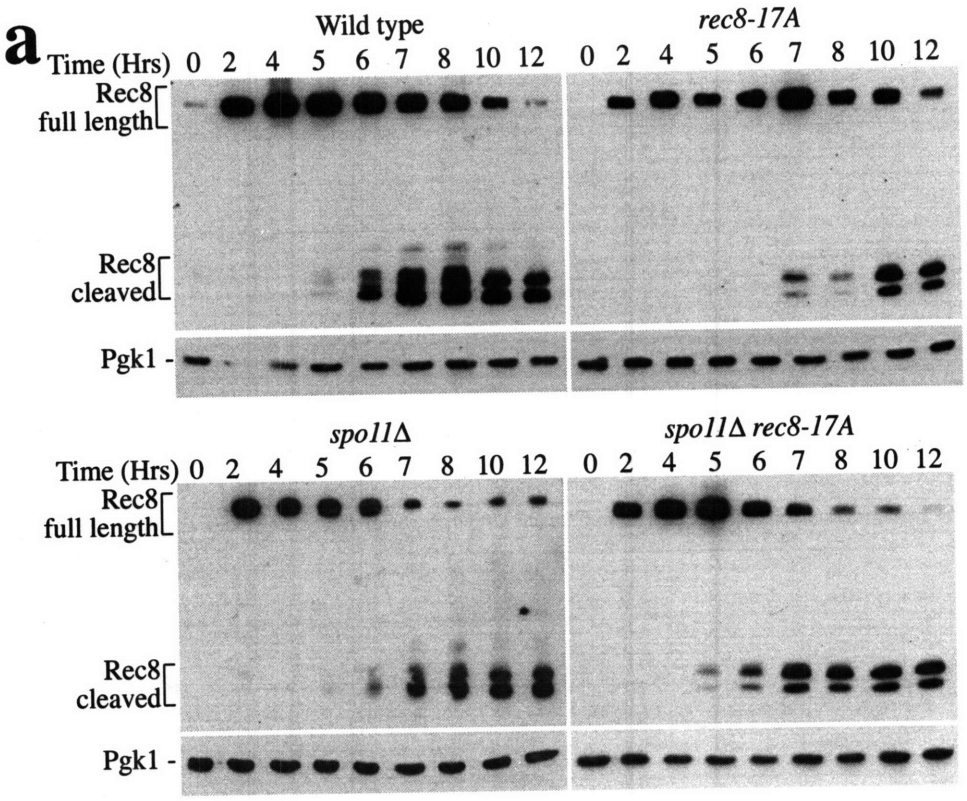
a
Wild type
rec8-17A
Time (Hrs) 0 2 4 5 6 7 8 10 12
Rec8 full length
Rec8 cleaved
Pgk1
spo11Δ
spo11Δ rec8-17A
b
Percent tetranucelate cells
spo11Δ
pCLB2-SGO1
pCLB2-SGO1 spo11Δ
pCLB2-SGO1 spo11Δ mad2Δ
pCLB2-SGO1 mad2Δ
spo11Δ mad2Δ
mad2Δ
c
spo11Δ pCLB2-SGO1
spo11Δ
pCLB2-SGO1
Percent metaphase II cells
Time (hrs)

Figure 9: Rec8-17A cleavage in cells expressing a catalytically dead version of *SPO11*.
spo11Δ rec8-17A (A14847, triangles) and *spo11-Y135F rec8-17A* (A15363, circles) mutant cells both carrying a *REC8-HA* fusion and a deletion in *UBR1* were induced to sporulate. At the indicated times samples were taken for Western blot analysis (A) and to determine the percentage of prophase cells and the sum of bi- and tetra-nucleate cells (B).

Figure 9

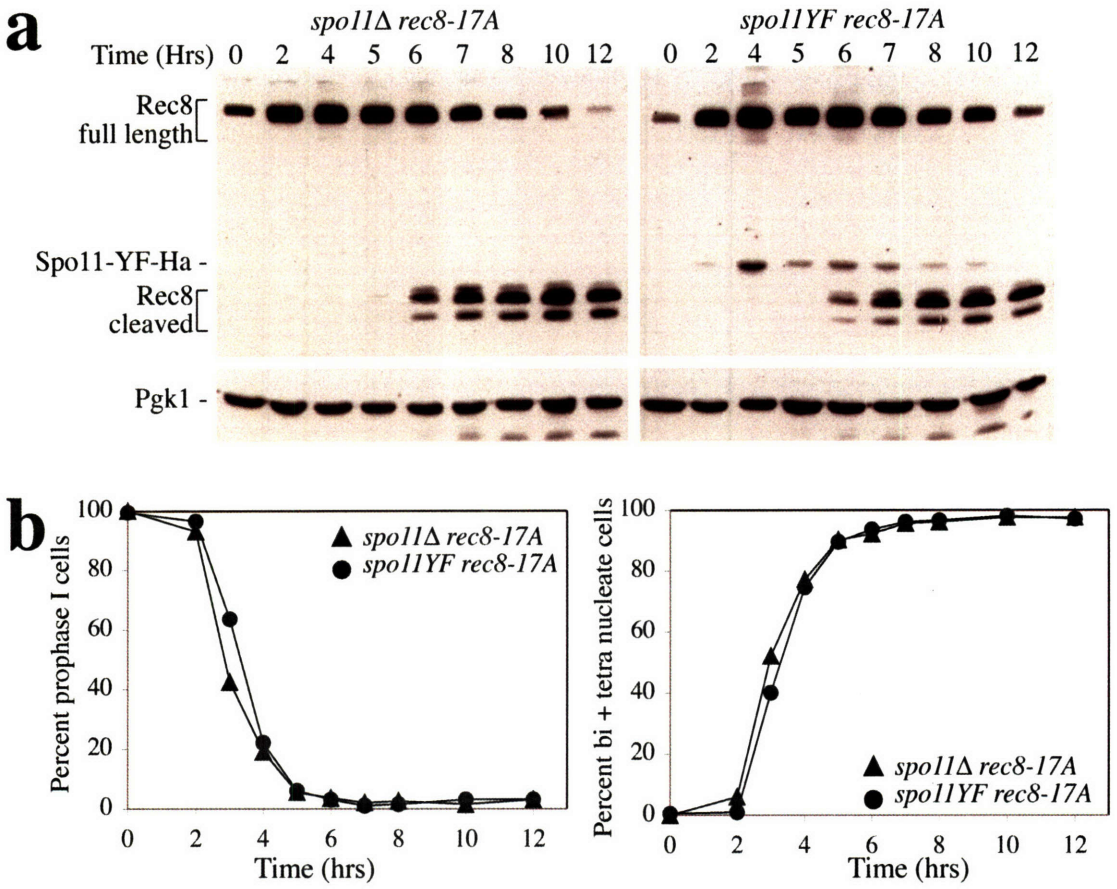
a
spo11Δ rec8-17A
spo11YF rec8-17A
Time (Hrs) 0 2 4 5 6 7 8 10 12
0 2 4 5 6 7 8 10 12
Rec8 full length
Spo11-YF-Ha -
Rec8 cleaved
Pgk1 -
b
Percent prophase I cells
spo11Δ rec8-17A
spo11YF rec8-17A
Time (hrs)
Percent bi + tetra nucleate cells
spo11Δ rec8-17A
spo11YF rec8-17A
Time (hrs)

Why does elimination of recombination suppress the cleavage defect observed in *rec8-17A* mutants? In *spo11Δ* and *rec8-17A spo11Δ* mutants loss of cohesins from chromosome arms and from centromeric regions occurs almost simultaneously as evidenced by the absence of binucleate *spo11Δ* or *rec8-17A spo11Δ* or *rec8-29A spo11Δ* cells with cohesins concentrated around centromeres (Figure 10A, C). In fact, the fraction of cells with only centromeric cohesins is the same in *spo11Δ* mutants as in *spo11Δ sgo1Δ* double mutants (Figure 10C). This finding raises the possibility that in the *spo11Δ* mutant the bulk of cohesin removal occurs during meiosis II. As during this division phosphorylation appears less important for Rec8 cleavage (Figure 5B), the *rec8-17A* mutant may no longer interfere with Rec8 cleavage. To test this hypothesis we examined the effects deleting *SPO11* in Sgo1-depleted cells (Sgo1 was depleted during meiosis by replacing the *SGO1* promoter with the *CLB2* promoter, which is repressed during meiosis [*pCLB2-SGO1* (Lee, Kiburz et al. 2004). In Sgo1-depleted cells, the second meiotic division is random due to the absence of any cohesion between sister chromatids. This phenotype can be observed when cells carry a tandem array of tet operator sequences near the centromere on one of the two homologs and also express a tet repressor GFP fusion that binds to these repeats (heterozygous *CEN5* GFP dots; (Toth, Rabitsch et al. 2000)). 50 percent of tetrads will contain a GFP dot in only one of the four spores and 50% of tetrads with contain a GFP signal in two of the four

spores (Figure 8C, Figure 10D). Remarkably, *spo11Δ pCLB2-SGO1* mutants segregate sister chromatids correctly in almost 90% of cells (Figure 8C). Furthermore, deletion of *SPO11* restored metaphase II to Sgo1-depleted cells (Figure 8D, Figure 10E). Similar results were obtained with other recombination mutants that abolished chiasma formation. Inactivation of Spo11's catalytic function (*spo11-YF* mutant, (Keeney, Giroux et al. 1997)) and inhibition of strand resection (*rad50S* mutant, (Alani, Padmore et al. 1990)) also suppressed the meiosis II mis-segregation that occurs in the absence of Sgo1 (Figure 11). This observation together with the finding that chromosomes segregation was again random in *spo11Δ pCLB2-SGO1 mad2Δ* triple mutants (Figure 8E) provided insight into why cohesin removal did not occur during meiosis I in the absence of recombination: In the absence of linkages between homologs, chromosomes fail to attach properly to the meiosis I spindle. This leads to the activation of the spindle assembly checkpoint, which in turn prevents the removal of cohesins from chromosomes. Cells nevertheless undergo anaphase I as chromosomes lack the necessary linkages to prevent meiosis I spindle elongation (Shonn, McCarroll et al. 2000; Shonn, Murray et al. 2003) and cells progress into meiosis II. This results in metaphase II chromosomes with cohesins on chromosome arms. These observations, together with the finding that Rec8 phosphorylation is not important for Rec8 cleavage during meiosis II explains why elimination of recombination abolishes the Rec8 cleavage delay in the *rec8-17A* mutant and point to an essential role for recombination in establishing the step-wise loss of cohesins from chromosomes.

Figure 10: Deletion of *SPO11* rescues the Rec8 cleavage delay in *rec8-17A* and *rec8-29A* mutants.
(A, B) *spo11Δ* (A14755; open diamonds), *spo11Δ rec8-17A* (A14847, closed triangles) and *spo11Δ rec8-29A* (A14872, closed circles) mutant cells both carrying a *REC8-HA* fusion and a deletion in *UBR1* were induced to sporulate. At the indicated times the percentage of metaphase II cells (A, right panel), of prophase cells (B, left panel) and of sporulated cells (B, right panel) was determined. The left panel in (A) shows the percentage of cells that exhibit strong Rec8 staining all over spread chromosomes ("full rec8", solid bar), that exhibit weak Rec8 staining all over chromosomes ("partial Rec8", grey bars) and Rec8 only at centromeres ("centromeric Rec8", white bars). 180 cells were counted per strain from a 6-hour time point

(C, D) Wild type (A2704, circles), *spo11Δ*, open squares and *spo11Δ pCLB-SGO1* (A15023, closed squares)cells carrying a *REC8-HA* fusion were induced to sporulate. Samples were taken at the indicated time points to determine Rec8 localization by immunofluorescence on chromosome spreads (C) and percent of bi and tetra nucleate cells (D). 100 mononucleate and binucleate cells were counted per strain per timepoint. Note that these samples were taken from the time course shown in Figure 12C and D.

(E) Strains and experimental conditions are described in Figure 8C, D. *spo11Δ* (A9498, closed circles), *spo11Δ pCLB2-SGO1*(A14938, closed squares) and *pCLB2-SGO1*(A11251, open circles) cells carrying *CEN5-GFP* dots were induced to sporulate. Samples were taken at the indicated time points to determine the percentage of bi- and tetranucleate cells.

Figure 10

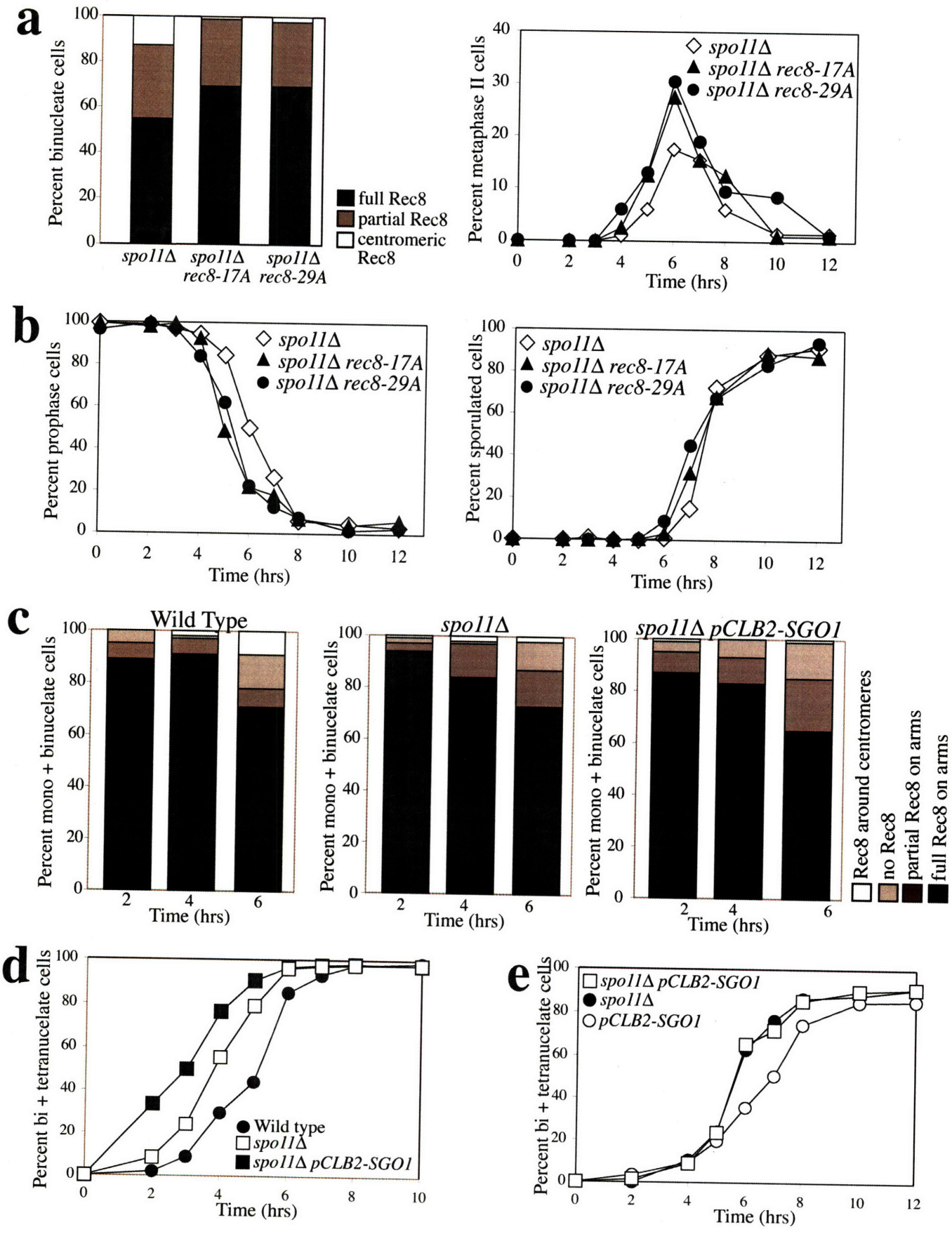
a
Percent binucleate cells
full Rec8
partial Rec8
centromeric Rec8
spo11Δ
spo11Δ rec8-17A
spo11Δ rec8-29A
Percent metaphase II cells
Time (hrs)
b
Percent prophase cells
Percent sporulated cells
c
Wild Type
Percent mono + binucelate cells
Rec8 around centromeres
no Rec8
partial Rec8 on arms
full Rec8 on arms
d
Percent bi + tetranucelate cells
Wild type
e
spo11Δ pCLB2-SGO1
pCLB2-SGO1

Figure 11: Depletion of Sgo1 in *spo11-Y135F* and *rad50S* mutants allows proper meiosis II chromosome segregation in Sgo1-depleted cells. *pCLB2-SGO1*(A11251), *rad50S* (A15347), *rad50S pCLB2-SGO1* (A15366), *spo11-Y135F* (A15349) and *spo11-Y135F pCLB2-SGO1* (A15351) cells carrying *CEN5-GFP* dots were induced to sporulate. At 12 hours samples were taken to determine GFP dot segregation in tetrads. Note that *pCLB2-SGO1* (A11251) control strain is the same as shown in Figure 8E.

Figure 11

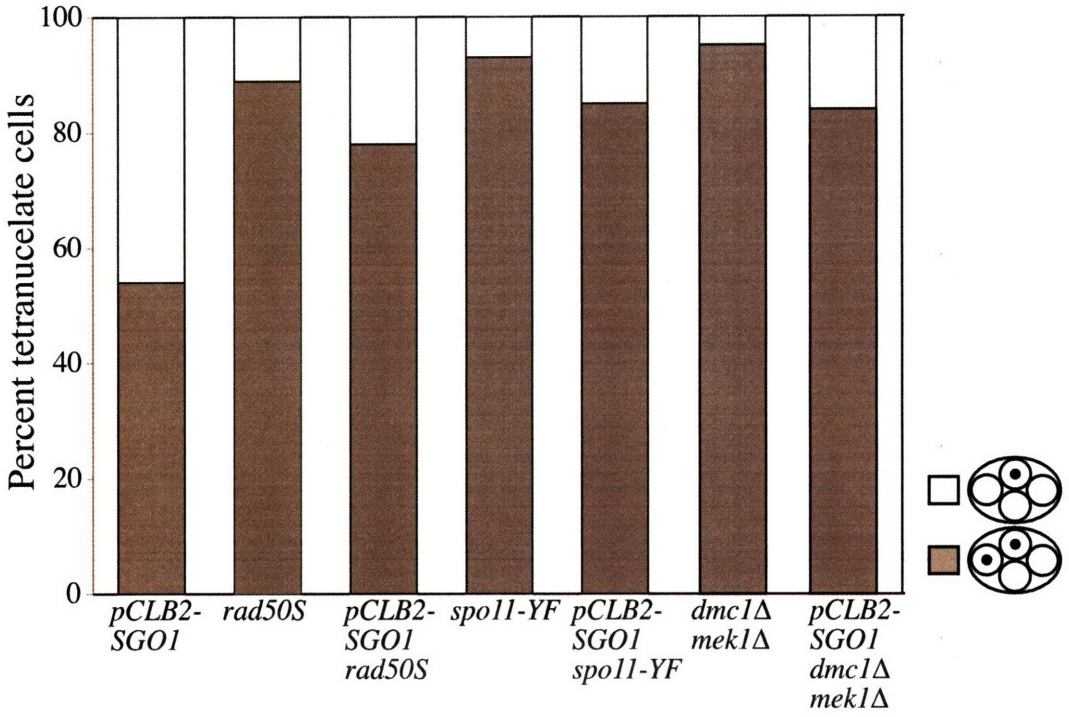
Percent tetranucelate cells
100
80
60
40
20
0
pCLB2-SGO1
rad50S
pCLB2-SGO1 rad50S
spo11-YF
pCLB2-SGO1 spo11-YF
dmc1Δ mek1Δ
pCLB2-SGO1 dmc1Δ mek1Δ

Assessing the relationship between Sgo1 and Rec8 phosphorylation

Proteins required to protect cohesins around centromeres from removal during meiosis I could function by preventing Rec8 phosphorylation. Indeed two recent studies show that Sgo1 recruits the protein phosphatase PP2A to chromosomes (Riedel 2008; Kitajima 2008). If Sgo1 solely functioned to prevent centromeric cohesin removal by preventing the phosphorylation of Rec8, inactivation of *SGO1* should not affect the phenotype exhibited by *rec8-17A* expressing cells. Surprisingly, depletion of Sgo1 in Rec8-17A-expressing cells led to Rec8 cleavage, almost to the extent seen in wild-type cells and an elimination of the metaphase I delay (Figure 12B, C, Figure 13A). This result suggests that *SGO1* affects cohesin cleavage by means other than or in addition to preventing Rec8 phosphorylation. An alternative, though less likely, explanation for the wild-type pattern of Rec8 cleavage and meiotic progression in the *rec8-17A pCLB2-SGO1* mutant is that our mass-spectrometry analysis missed key phosphorylation sites, whose phosphorylation allow for highly efficient cleavage of the Rec8-17A mutant protein only in the absence of *SGO1*. To distinguish between these possibilities we examined Rec8 cleavage in cells depleted for Cdc5. Cdc5 was depleted from meiotic cells by placing the gene under the *CLB2* promoter (*pCLB2-CDC5*(Lee and Amon 2003)). Cells also lacked *SPO11* to avoid delays in Rec8 cleavage due to Cdc5's role in meiotic recombination (Clyne, Katis et al. 2003). Rec8 cleavage was greatly delayed in *spo11Δ pCLB2-CDC5* cells (Figure 12C). Depletion of Sgo1 allowed Rec8 cleavage to occur

more efficiently (Figure 12C). Furthermore, Rec8 was completely lost from chromosomes in 30% of *pCLB2-CDC5 pCLB2-SGO1* cells compared to in only 9%, of *pCLB2-CDC5* cells 6 hours after transfer of cells into sporulation-inducing conditions (Figure 14). Cells also underwent anaphase I spindle elongation (Figure 12D, Figure 13B). To examine whether the observed spindle elongation reflected chromosome segregation we examined the segregation of *CEN5* GFP dots. In metaphase I-arrested *spo11Δ pCLB2-CDC5* mutants, two juxtaposed GFP dots are visible because sister kinetochores attach to opposite poles rather than the same pole in meiosis I and the tension exerted by the spindle leads to separation of CEN5 GFP dots (Clyne, Katis et al. 2003; Lee and Amon 2003). In 50 percent of *spo11Δ pCLB2-CDC5 pCLB2-SGO1,* as well as *pCLB2-CDC5 pCLB2-SGO1* cells, the GFP dots were separated by at least 2 μm and often more (Figure 12E, Figure 13D) and anaphase I spindle elongation occurred (Figure 13C). These results indicate that *SGO1* affects cohesin cleavage by means other than or in addition to preventing Rec8 phosphorylation.

Figure 12: Depletion of Sgo1 partially alleviates the need for Rec8 phosphorylation and Cdc5 in Rec8 cleavage and anaphase I entry.
(A, B) Wild type (A15086, closed diamonds), *rec8-17A* (A14750, closed triangles), *pCLB2-SGO1* (A15085, open diamonds) and *rec8-17A pCLB2-SGO1* (A15084, open triangles) were induced to sporulate. At the indicated times samples were taken to determine the percentage of metaphase I cells (B, top panel) and prophase I cells (A, bottom panel) and Rec8 protein by Western blot analysis (B). Note that in this experiment the *rec8-17A* mutant did not exhibit a prophase delay.

(C, D) *spo11Δ* (A15022, open diamonds), *spo11Δ pCLB2-CDC5* (A15025, closed diamonds), and *spo11Δ pCLB2-CDC5 pCLB2-SGO1* (A15000, closed circles) cells were induced to sporulate. At the indicated times samples were taken to determine the percentage of anaphase I cells (D) and Rec8 protein levels by Western blot analysis (C).

(E) *spo11Δ pCLB2-CDC5* (A14657, closed diamonds), *pCLB2-CDC5 pCLB2-SGO1* (A14870, closed triangles), and *spo11Δ pCLB2-CDC5 pCLB2-SGO1* (A14776, closed circles) cells all carrying *CEN5-GFP* dots were induced to sporulate. At the indicated times samples were taken to determine the percentage of cells with GFP dots separated by at least 2 μm. 200 cells were counted per strain per time point.

Figure 12

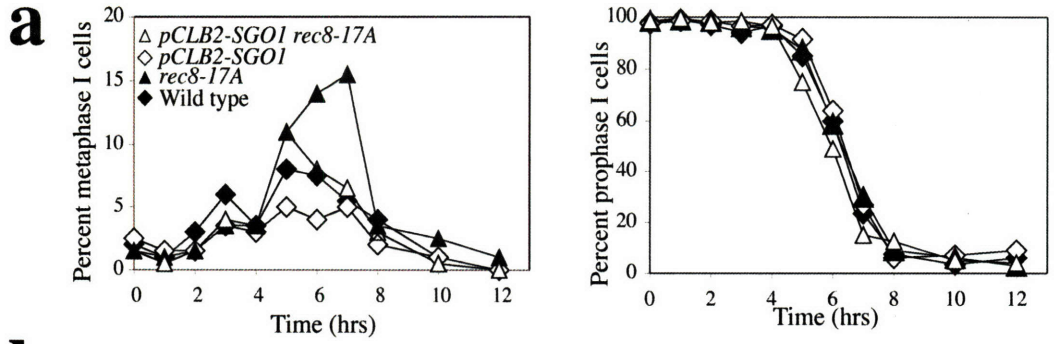
a
Percent metaphase I cells
Time (hrs)
△ pCLB2-SGO1 rec8-17A
◇ pCLB2-SGO1
▲ rec8-17A
◆ Wild type
Percent prophase I cells
Time (hrs)

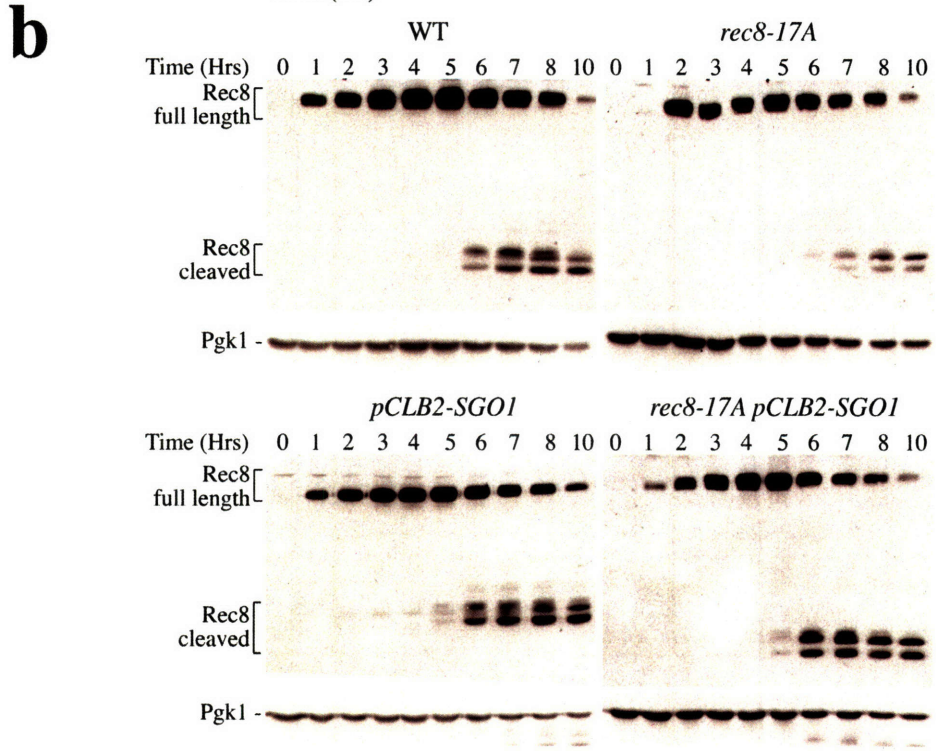
b
WT
rec8-17A
Time (Hrs) 0 1 2 3 4 5 6 7 8 10
Rec8 full length
Rec8 cleaved
Pgk1
pCLB2-SGO1
rec8-17A pCLB2-SGO1

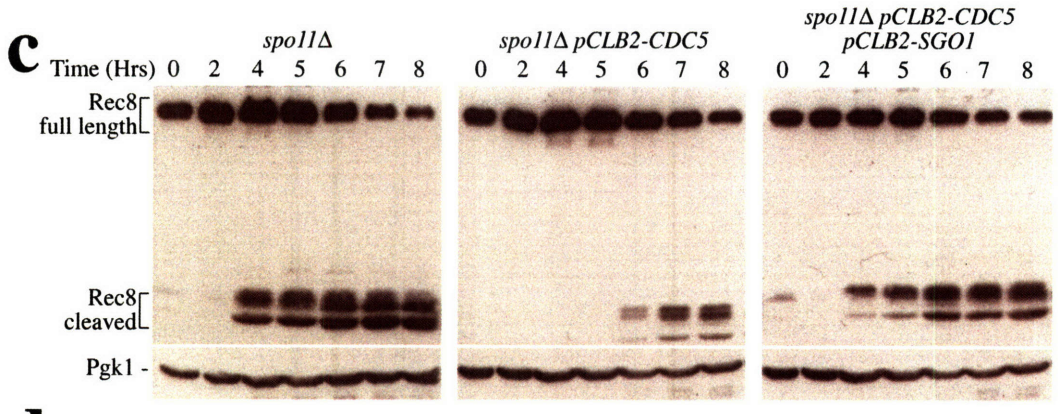
c
spo11Δ
spo11Δ pCLB2-CDC5
spo11Δ pCLB2-CDC5 pCLB2-SGO1
Time (Hrs) 0 2 4 5 6 7 8
Rec8 full length
Rec8 cleaved
Pgk1

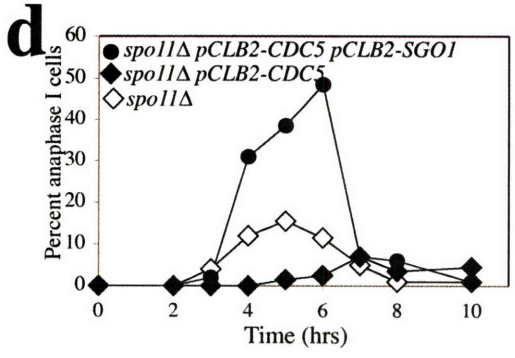
d
Percent anaphase I cells
Time (hrs)
spo11Δ pCLB2-CDC5 pCLB2-SGO1
spo11Δ pCLB2-CDC5
spo11Δ

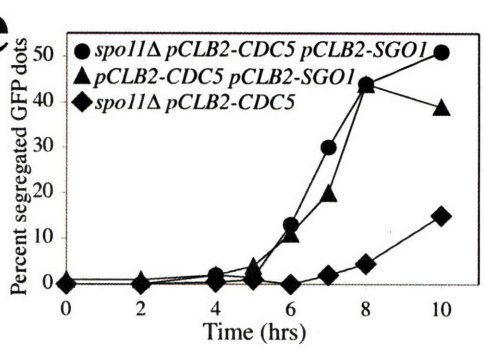
e
Percent segregated GFP dots
Time (hrs)
spo11Δ pCLB2-CDC5 pCLB2-SGO1
pCLB2-CDC5 pCLB2-SGO1
spo11Δ pCLB2-CDC5

Figure 13: Depletion of Sgo1 partially alleviates the need for Rec8 phosphorylation and Cdc5 in Rec8 cleavage and anaphase I entry.
(A) Wild type (A15086, closed diamonds), *rec8-17A* (A14750, closed triangles), *pCLB2-SGO1* (A15085, open diamonds) and *rec8-17A pCLB2-SGO1* (A15084, open triangles) were induced to sporulate. At the indicated times samples were taken to determine the percentage of metaphase II cells (left panel) and the sum of bi- and tetranucleate cells (right panel).

(B) *spo11Δ* (A15022, open diamonds), *spo11Δ pCLB2-CDC5* (A15025, closed diamonds), and *spo11Δ pCLB2-CDC5 pCLB2-SGO1* (A15000, closed circles) cells were induced to sporulate. At the indicated times samples were taken to determine the percentage of prophase cells (left panel) and the sum of bi- and tetranucleate cells (right panel).

(C) *spo11Δ pCLB2-CDC5* (A14657, closed diamonds), *pCLB2-CDC5 pCLB2-SGO1* (A14870, closed triangles), and *spo11Δ pCLB2-CDC5 pCLB2-SGO1* (A14776, closed circles) cells all carrying *CEN5-GFP* dots were induced to sporulate. At the indicated times samples were taken to determine the percentage of anaphase I cells (left panel) and the sum of bi- and tetranucleate cells (right panel).

(D) Examples of separated GFP dot in *spo11Δ pCLB2-CDC5 pCLB2-SGO1* (A14776) cells. GFP dots are shown in green, DNA in blue.

Figure 13

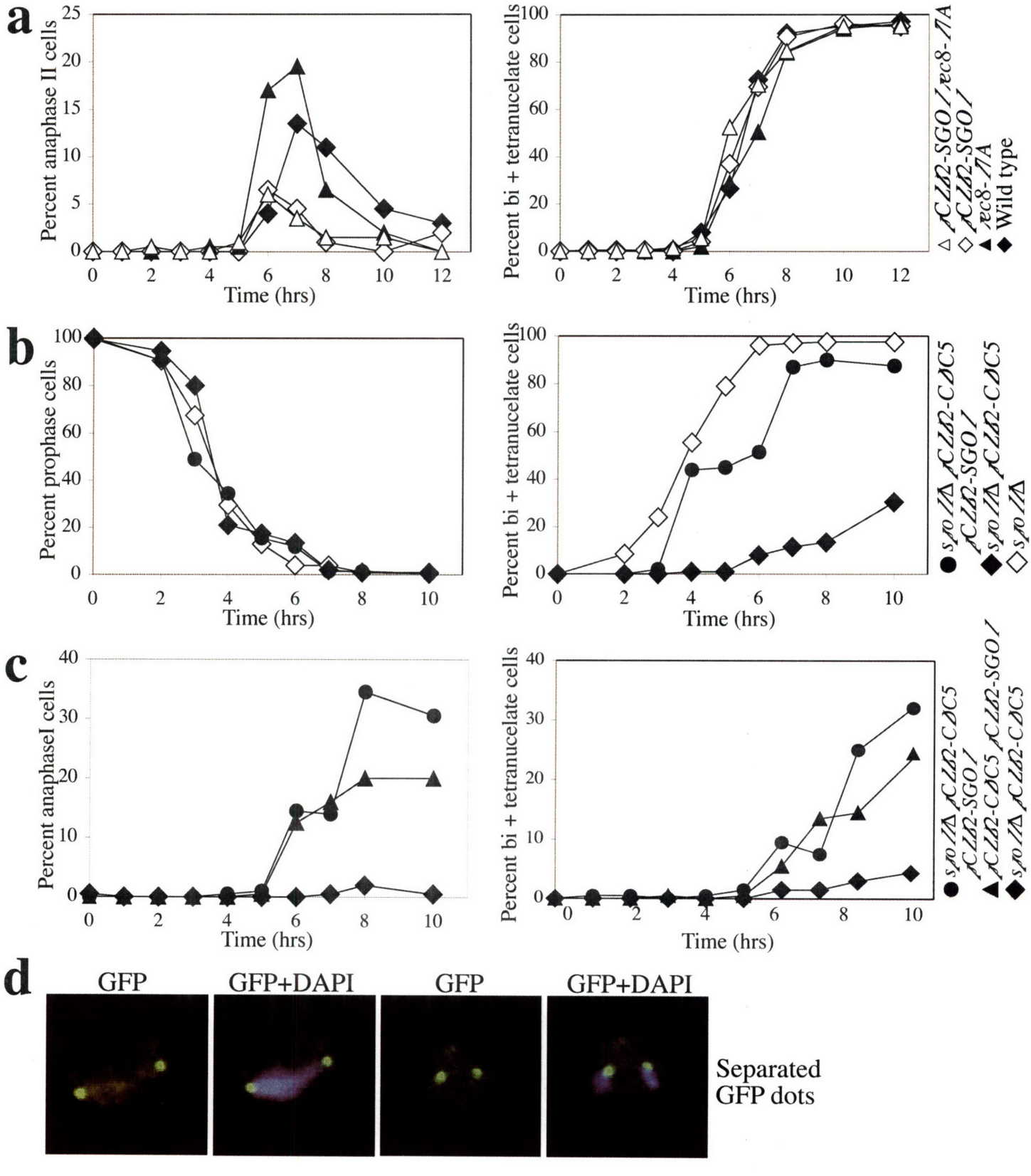
a
Percent anaphase II cells
Time (hrs)
Percent bi + tetranucelate cells
Time (hrs)
△ rec8-HA
◇ rec8-HA
▲ Wild type
◆ Wild type
b
Percent prophase cells
Time (hrs)
Percent bi + tetranucelate cells
Time (hrs)
● spo11Δ rec8-cdc5
rec8-SGO1
◆ spo11Δ rec8-cdc5
◇ spo11Δ
c
Percent anaphaseI cells
Time (hrs)
Percent bi + tetranucelate cells
Time (hrs)
● spo11Δ rec8-cdc5
rec8-SGO1
▲ rec8-cdc5 rec8-SGO1
◆ spo11Δ rec8-cdc5
d
GFP
GFP+DAPI
GFP
GFP+DAPI
Separated
GFP dots

Figure 14: Depletion of Sgo1 allows Rec8 removal from chromosomes in Cdc5-depleted cells.
The cells analyzed in this figure were obtained from the time course shown in Figure 12C and D.
(A) *spo11Δ pCLB2-CDC5* and *spo11Δ pCLB2-CDC5 pCLB2-SGO1* cells were induced to sporulate. At the indicated times samples were taken and the percentage of cells with Rec8 present at wild-type levels on all chromosomes (black), with some Rec8 present on chromosomes (grey) or no Rec8 (white) on chromosomes was determine on chromosome spreads.

(B) Examples of the categories of Rec8 staining on chromosomes. "Full" represents wild-type levels of association of Rec8 with chromosomes. "Parital" represents a small, but detectable amount of Rec8 on chromosomes and "none" indicates no Rec8 staining on chromosomes. Rec8 is shown in red, DNA in blue. We frequently observe large amounts of Rec8 concentrated between two DNA masses (an example is shown in the right panel of "partial" category) in *spo11Δ PCLB2-CDC5 pCLB2-SGO1* cells. The identity of the region where Rec8 remains associated with chromosomes in these cells is not known, but may, based on their position between DAPI masses, represent telomeres.

Figure 14

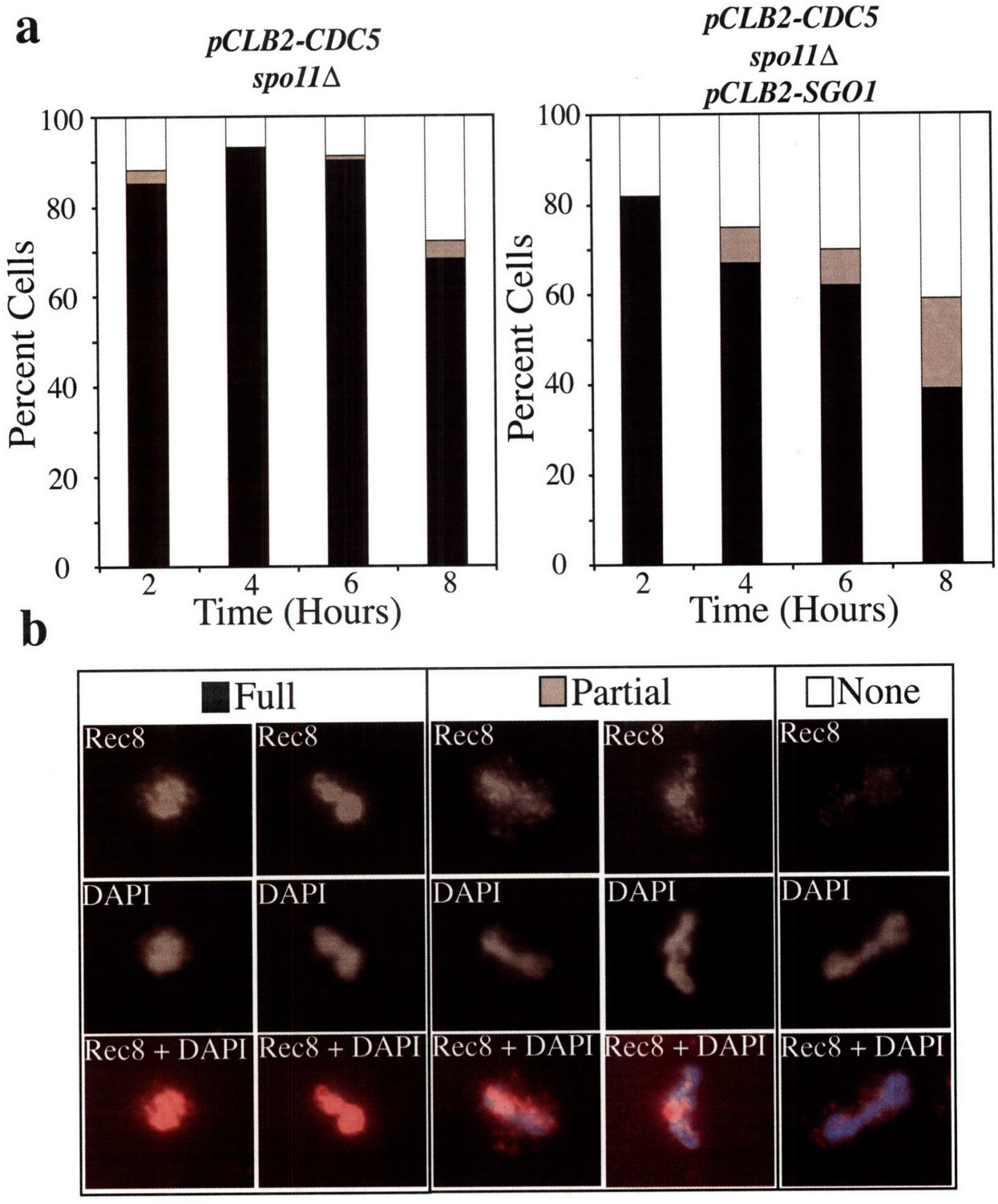
a
pCLB2-CDC5
spo11Δ
pCLB2-CDC5
spo11Δ
pCLB2-SGO1
Percent Cells
Time (Hours)
0
20
40
60
80
100
2
4
6
8
b
Full
Partial
None
Rec8
DAPI
Rec8 + DAPI

Analysis of phospho-Rec8 chromosome localization

Our data indicate that phosphorylation of Rec8 is important for the efficient cleavage of Rec8. Next we wished to determine whether Rec8 phosphorylation contributes to establishing the stepwise nature of this process. To this end we raised two antibodies, one that specifically recognizes phosphorylated serine 136 and one that recognizes phospho serine 521 (Materials and Methods; Figure 15A, Figure 16A). As predicted by the mass-spectrometry analysis phosphorylation of S136 is Cdc5-dependent, phosphorylation of S521 is Cdc5-independent (Figure 15A, B; Figure 16B; Figure 8). The anti-phospho S136 antibody only recognized Rec8 on Western blots (Figure 15A, B, data not shown). The anti phospho S521 antibody recognized phospho-S521 on Western blots and chromosome spreads (Figure 15A - C) but failed to efficiently precipitate Rec8 in chromatin immunoprecipiation assays (data not shown).

To determine whether Rec8 phosphorylation on S521 mirrored the differential loss of arm and centromeric cohesins during meiosis I in that phosphorylation occurred on chromosome arms prior to anaphase I but was excluded from centromeric regions, we compared the distribution of a Rec8-Myc fusion (total Rec8) with that of Rec8 recognized by the anti phospho S521 antibody. To identify centromeric regions, cells also contained a tagged version of the kinetochore protein Ndc10. The Rec8-Myc signal appeared continuous and was found in long stretches on chromosome spreads, presumably representing chromosome axes. In contrast, the anti phospho S521 signal

appeared fragmented (Figure 15D) and frequently did not overlap with the Ndc10-Ha foci. Whereas the anti-Myc signal overlapped with an average of 9 (SD=1.8) out of an average of 15 Ndc10-Ha foci (SD=1.8) per cell (n=12), the anti phospho S521 signal only co localized with an average of 4 (SD=1.2) out of 16 Ndc10 foci (SD=0.74) per cell (n=12; Figure 15E). Furthermore, the anti phospho S521 signal was absent from chromosome spreads of binucleate (anaphase I – metaphase II) cells (Figure 15D), when only centromeric cohesins are left on chromosomes. Thus it appears that S521 phosphorylation is reduced or perhaps even excluded from centromeric regions in pre-anaphase cells, but present on chromosome arms. We do not know whether Rec8 is phosphorylated prior to its removal in metaphase II. We have not detected an anti phospho S521 signal in any binucleate cells. This result suggests that Rec8 phosphorylation on S521 is not a prerequisite for Rec8 removal during meiosis II, which would be consistent with the observation that the *rec8-17A* mutant does not exhibit a delay in metaphase II.

Figure 16: Rec8 phosphorylation on S136 and S521 is regulated during meiosis.

(A) The cells analyzed in this figure were obtained from the time course shown in Figure 15A. Wild type (A1972, open symbols) and *rec8-17A* mutant (A13559, closed symbols) cells were induced to sporulate and the percentage of metaphase I cells (right panel) and the percentage of mononucleate and the sum of bi and tetranucleate cells was determined at the indicated time.

(B) The cells analyzed in this figure were obtained from the time course shown in Figure 15A. *pCLB2-CDC20* (A5441, diamonds) and *pCLB2-CDC5* (A9858, circles) cells were induced to sporulate and the percentage of prophase and metaphase I cells (right panel) was determined at the indicated time.

Figure 16

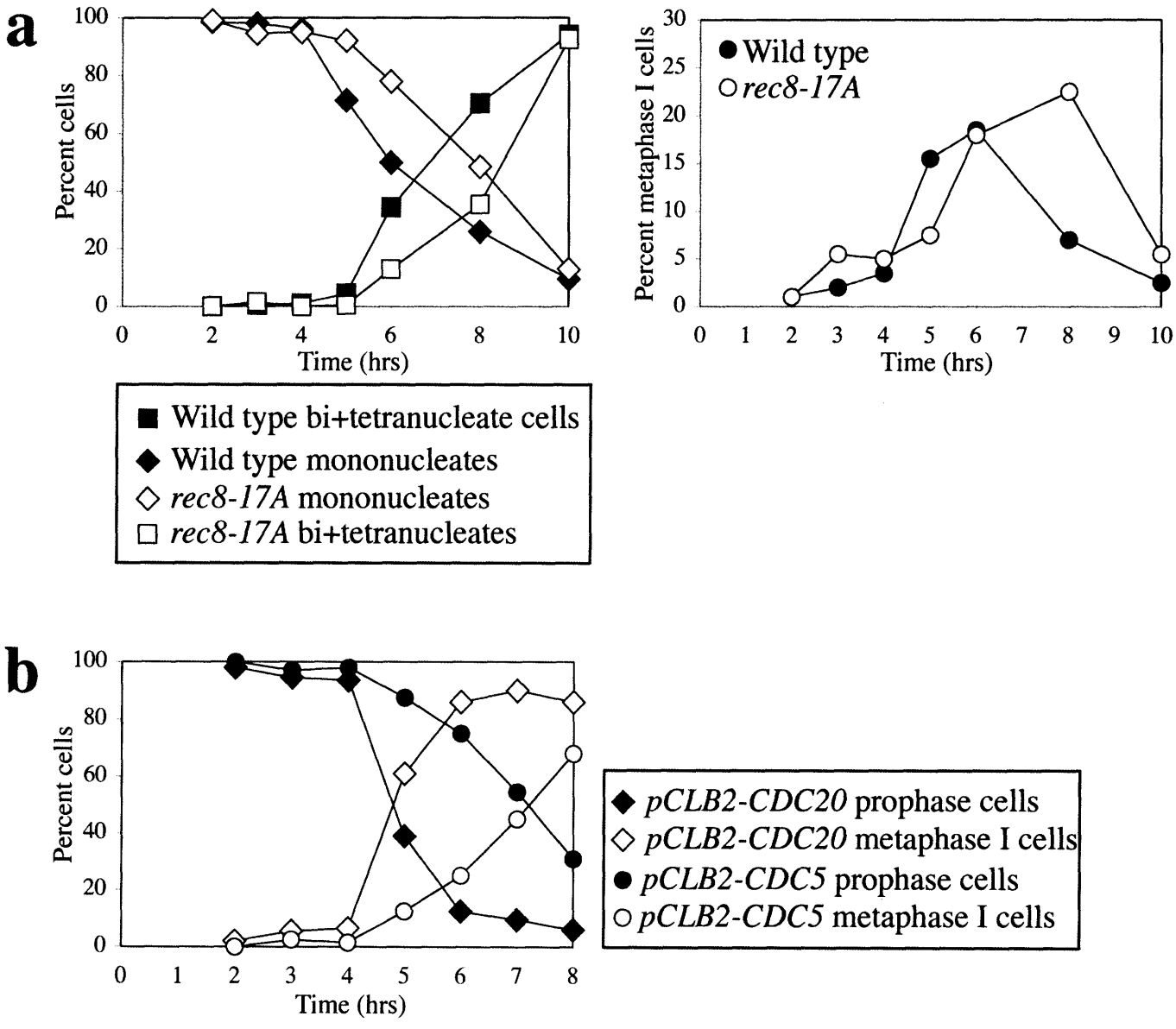
a
Percent cells
Time (hrs)
Wild type bi+tetranucleate cells
Wild type mononucleates
rec8-17A mononucleates
rec8-17A bi+tetranucleates
Percent metaphase I cells
Wild type
rec8-17A
b
pCLB2-CDC20 prophase cells
pCLB2-CDC20 metaphase I cells
pCLB2-CDC5 prophase cells
pCLB2-CDC5 metaphase I cells

Figure 15: Serine 521 phosphorylation is reduced around centromeres during meiosis I.
(A) Wild type (A1972) cells and *rec8-17A* mutants (A13559) were induced to sporulate. At the indicated times Rec8-HA was immunoprecipitated and separated on SDS PAGE (Materials and Methods). Blots were then probed with either anti HA-antibodies or anti phospho S136 (α-pS136) or anti phospho S521 α-pS521) antibodies.

(B) *pCLB2-CDC20* (A5441) and *pCLB2-CDC5* (A9858) cells were induced to sporulate. At the indicated times Rec8-Myc was immunoprecipitated and separated on SDS PAGE. Blots were then probed with either anti Myc-antibodies or anti phospho S136 (α-pS136) or anti phospho S521 (α-pS521) antibodies.

(C) Wild type (A14655) cells and *rec8-17A* mutants (A14746) were induced to sporulate. After 4 hours cells were harvested and α-pS521 staining was analyzed chromosome spreads. α-pS521 staining is shown in green and DNA in blue.

(D, E) Wild-type cells carrying a *REC8-MYC* fusion and a *NDC10-HA* fusion (A3640) were spread and the distribution of Rec8 was determined either using an α-Myc or an α-pS521 antibodies. Examples of prophase and binucleate cells are shown. Rec8 is shown in green, Ndc10 in red and DNA in blue. (E) shows the number of Ndc10 foci overlapping with the α-Myc and α-pS521 staining. All Ndc10 foci were scored for 12 cells per condition.

Figure 15

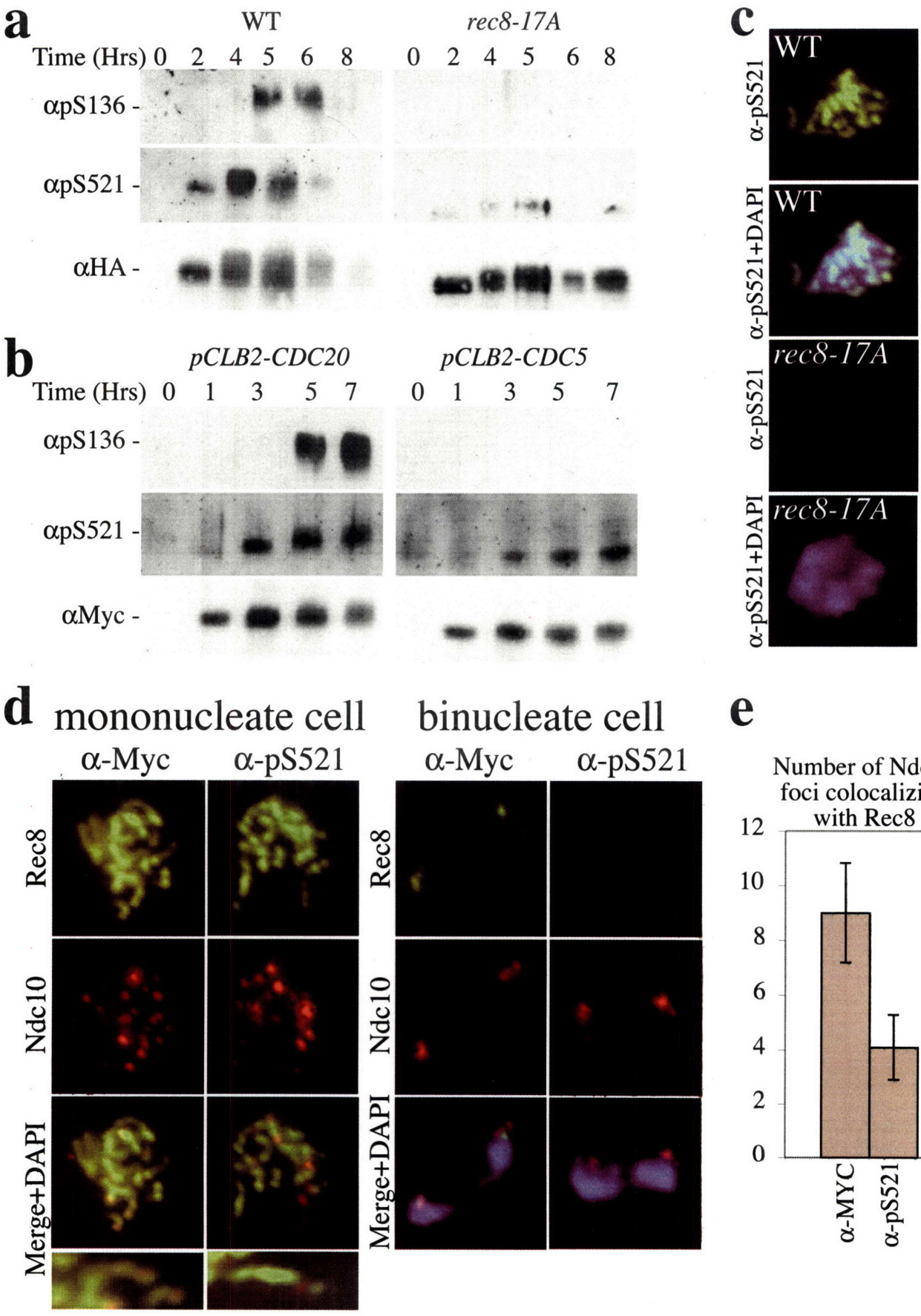
a
WT
rec8-17A
Time (Hrs) 0 2 4 5 6 8
0 2 4 5 6 8
αpS136 -
αpS521 -
αHA -
b
pCLB2-CDC20
pCLB2-CDC5
Time (Hrs) 0 1 3 5 7
0 1 3 5 7
αpS136 -
αpS521 -
αMyc -
c
WT
α-pS521
WT
α-pS521+DAPI
rec8-17A
α-pS521
rec8-17A
α-pS521+DAPI
d
mononucleate cell
binucleate cell
α-Myc
α-pS521
α-Myc
α-pS521
Rec8
Ndc10
Merge+DAPI
Rec8
Ndc10
Merge+DAPI
e
Number of Ndc10 foci colocalizing with Rec8
12
10
8
6
4
2
0
α-MYC
α-pS521

Discussion

How are Sgo1 and Rec8 phosphorylation related?

Work by the Nasmyth and Watanabe groups indicates that Sgo1 recruits PP2A to centromeric regions and this event is important for the step-wise loss of cohesion from chromosomes (Nasmyth ; Watanabe).To determine whether factors involved in bringing about the step-wise loss of cohesion participate in establishing the pattern of S521 phosphorylation on chromosomes we examined the phosphorylation status of S521 in prophase spreads of *BUB1* deleted or Sgo1-depleted cells. Inactivation of neither gene lead to increased detection of a phospho S521 signal around centromeres on chromosome spreads (data not shown). This finding indicates that Sgo1and Bub1 either only regulate the phosphorylation state of a subset of Rec8 phosphorylation sites or that they affect cohesins at centromeric regions through means other than preventing Rec8 phosphorylation. Several lines of evidence are consistent with the latter idea. Inactivation of Sgo1 not only allowed efficient Rec8 cleavage and anaphase I spindle elongation in the *rec8-17A* mutant but also in Cdc5-depleted cells. It is possible that in the absence of Sgo1, low levels of Cdc5 and other protein kinases are now capable of bringing about cohesin removal. We consider this possibility unlikely because both, sister chromatid separation and spindle elongation occur with remarkable efficiency. We favor the idea that Sgo1 affects the phosphorylation state of other cohesin subunits around centromeres and/or affects Separase activity. The fact that depletion of Sgo1 allowed complete cohesin removal in 30 percent of Cdc5-depleted cells furthermore

raises the interesting possibility that Sgo1 not only regulates cohesins around centromeres but also in a more global manner.

Bulk Rec8 phosphorylation promotes anaphase I entry

We have investigated how Rec8 phosphorylation affects cohesin removal and meiotic chromosome segregation. This study not only produced the first *in vivo*-derived consensus sequence for targets of Polo kinases but also provided insights into how cohesin removal is regulated in meiosis. The finding that single phosphorylation site mutants as well as mutants containing only a small number (up to 11) of phosphorylation sites mutated to alanine did not interfere with the metaphase – anaphase transition suggests that it is overall phosphorylation rather than phosphorylation of a specific site that is important for Rec8 cleavage. Only when we mutated all Cdc5 phosphorylation sites identified in the mass spectrometry analysis as well as potential Cdc5 phosphorylation sites (*rec8-17A* mutant) did we begin to see a delay in Rec8 cleavage and anaphase I onset. The delay in Rec8 cleavage we observed in the *rec8-17A* mutant was significantly shorter than that observed in cells depleted for Cdc5. We believe one or several of the following reasons to be responsible for this difference. Cells depleted for Cdc5 exhibit a defect in Pds1 degradation, which delays Rec8 cleavage (Clyne, Katis et al. 2003). Second, additional Cdc5 phosphorylation sites may exist that have not been identified by our mass-spectrometry analysis. Finally, Cdc5 may have targets other than Rec8, whose phosphorylation is important for Rec8 cleavage. Analysis of the *rec8-17A* mutants nevertheless

implicates phosphorylation of Rec8 in cohesin removal. This finding together with the observation that Rec8 phosphorylation is regulated in that phosphorylation of at least S521 is reduced or absent around centromeres during meiosis I, indicates that Rec8 phosphorylation contributes to the step-wise loss of cohesins from chromosomes.

Recombination promotes step-wise loss of cohesion

Our results also revealed a previously unrecognized role for recombination in establishing the step-wise loss of cohesion. Recombination establishes linkages between homologs, which is essential for silencing of the spindle checkpoint and thus the timely removal of cohesins from chromosome arms. In the absence of recombination linkages between homologs are not forged and the spindle assembly checkpoint is not silenced. As a result meiosis I cohesin removal is disrupted. As meiotic progression continues due to meiotic cell cycle events being uncoupled (Marston, Lee et al. 2003), meiosis II chromosomes are generated with cohesins on chromosome arms. Thus recombination not only ensures the correct attachment of bivalents to the meiosis I spindle but, together with Rec8 phosphorylation and Sgo1, establishes the stepwise loss of cohesion, another key aspect or meiotic chromosome segergation.

Materials and Methods

Strains and Plasmids:

The strains used in this study are all derivatives of SK1. The *pCLB2-CDC20* and *pCLB2-CDC5* fusions and *ubr1Δ::KanMX4* are described in (Lee and Amon 2003). The The *pCLB2-SGO1* fusion is described in(Marston, Tham et al. 2004). The *pDMC1-PDS1dbΔ* construct was generated by cloning the *DMC1* promoter upstream of *PDS1* lacking the destruction box (*PDS1dbΔ;* (Cohen-Fix, Peters et al. 1996; Shonn, McCarroll et al. 2000). The construct was integrated at the *DMC1* locus. *REC8-3HA*, GFP dots and *spo11::URA3* were described in (Klein, Mahr et al. 1999). Pds1-18Myc and *rec8Δ::KanMX4* were described in (Toth, Rabitsch et al. 2000).

pA498 was generated by cloning Rec8-3HA into Yiplac128.

Sporulation conditions:

Cells were grown to saturation in YPD (YEP + 2% glucose) for 24 hours, diluted into YPA (YEP + 2% KAc) at OD_{600} = 0.3 and grown overnight. Cells were then washed with water and resuspended in SPO medium (0.3% KAc [pH = 7.0]) at OD_{600} = 1.9 at 30°C to induce sporulation.

Rec8 Phospho-site mutants:

Plasmids based on *pA498* were mutated with Stratagene Quikchange kit and then integrated at the *REC8* locus into *rec8Δ* strain A3498. Single-copy insertion

was verified by Southern blot analysis. All mutants contained a triple HA tag at the C-terminus.

Western blot analysis:

Cells were harvested, incubated in 5% trichloroacetic acid (TCA) and lysed as described in (Moll, Tebb et al. 1991). Immunoblots were performed as described in (Cohen-Fix, Peters et al. 1996). Rec8-9Myc was detected using a mouse anti-Myc antibody (Covance) at a 1:1000 dilution. Pgk1 was detected using a mouse anti-PGK1 antibody (Molecular Probes) at a 1:5000 dilution. Rec8-HA was detected using a mouse anti-HA antibody (HA.11, Covance) at a 1:1000 dilution. Vph1 was detected using a mouse antibody (Molecular Probes) at a 1:2000 dilution. The secondary antibody used was a goat anti-mouse antibody conjugated to horseradish peroxidase (HRP; Jackson Immunoresearch) at a 1:2000 dilution.

Phospho-antibody Western blots:

Blots were blocked for 4 hr. at room temperature in 3.5% BSA in TBST, then incubated with 1:500 rabbit phospho-antibody in 1%BSA, TBST and incubated overnight at 4°C. Blots wre washed five times with TBST and incubated with goat anti-rabbit antibody conjugated to horseradish peroxidase (HRP; Jackson Immunoresearch) at a 1:5000 dilution. Antibodies were custom-made by Abgent Technologies against phospho-S521 and phospho-S136 Rec8 peptides using peptide HTRNSTR(pS)SGFNEDIC and NGLNSNN(pS)IIGNKNNC, respecitvely.

Chromatin Immunoprecipitation:

ChIP was performed as described in (Kiburz, Reynolds et al. 2005). Primer sequences are available upon request.

Mass Spectrometry:

Rec8-Myc was Immunoprecipitated, run on a 6% Acrylamide gel and stained with Colloidal blue staining kit (Invitrogen). Protein bands from each condition were subjected to in-gel digestion using trypsin (Promega) (375 ng/band in 30 μL of 100 mM ammonium acetate) or chymotrypsin (Roche) (600 ng/band in 30 μL of 100 mM ammonium acetate). Extracted peptides were dried to 1-2 μL and reconstituted in 0.1% acetic acid prior to loading on an Fe^{3+}-charged IMAC column. IMAC enrichment of phosphorylated peptides and LC-MS/MS analysis on a QSTAR XL quadrupole time-of-flight mass spectrometer (Applied Biosystems) was performed as described previously(Zhang, Wolf-Yadlin et al. 2005).

Immunoprecipitation:

Cells were harvested, incubated in 5% TCA, washed with acetone and dried overnight. Pellets were then lysed in 50mMTris-Hcl pH7.5, 1mM EDTA, 15mM PNP, 60mM Bgpp, 50mM DTT, 0.1mM NaVa, 1x complete protease inhibitors solution (Roche) and glass beads in Biopulverizer (FastPrep). Samples were then

boiled with 1% SDS, diluted 9-fold in NP40 buffer (150mM NaCl, 1%NP40 by mass, 50mM Tris-HCl pH 7.5). Extracts were incubated for 1-2 hours at 4 degrees with 1:150 9E10 mouse anti-Myc antibody (Covance) or 1:150 HA.11 mouse anti-HA antibody (Covance). Extracts were then incubated overnight at 4 degrees with 60 μl-120 μl Protein G Sepharose beads (Pierce) per 2mL-15mL IP. IPs were washed 2x with NP40 buffer, 1x NP40 buffer + 1% Bme, 2x NP40 buffer + 1% Bme + 2M Urea, 1x 10mM Tris-HCl pH7.5. Beads were resuspended in 3x SDS Sample buffer and boiled.

Immunolocalization analysis on chromosome spreads:

Chromosomes were spread as described in (Nairz and Klein 1997). Rec8-Myc was detected using rabbit anti-Myc antibodies (Gramsch) at a 1:150 dilution and anti-rabbit FITC antibodies (Jackson Immunoresearch) at a 1:300 dilution. Ndc10-6HA was detected using a mouse anti-HA antibody (Babco) at a 1:200 dilution and an anti-mouse Cy3 antibody at a 1:300 dilution. Rec8-HA was detected using mouse anti-HA antibodies (Covance) at 1:500 and anti-mouse Cy3 antibody at 1:200. Phospho-S521 Rec8 was detected using custom antibody rb7064 at 1:250 and anti-rabbit FITC antibody at 1:250.

Whole cell immunofluorescence:

Indirect *in situ* immunofluorescence was carried out as described in (Visintin, Craig et al. 1998). Rat anti-tubulin antibodies (Oxford Biotechnology) and anti-rat FITC antibodies (Jackson Immunoresearch) were used at a 1:100 dilution.

Pds1-Myc was detected using a mouse anti-HA antibody (Covance) at a 1:250 dilution and an anti-mouse Cy3 secondary antibody (Jackson Immunoresearch) at a 1:1000 dilution. Unless otherwise indicated, for all experiments 200 cells were counted per strain per time-point.

We define metaphase I cells as cells with an undivided nucleus and a meiotic spindle spanning the nucleus. We chose these two criteria and did not include the state of Pds1 staining because cells could be arrested/present in metaphase I because they have not yet degraded Pds1 (as is the case in checkpoint arrested cells) or because they are defective in Rec8 cleavage after Pds1 has been degraded (as is seen as in the *rec8-17A* mutant.

References:

Alani, E., R. Padmore, et al. (1990). "Analysis of wild-type and rad50 mutants of yeast suggests an intimate relationship between meiotic chromosome synapsis and recombination." Cell **61**(3): 419-36.

Alexandru, G., F. Uhlmann, et al. (2001). "Phosphorylation of the cohesin subunit Scc1 by Polo/Cdc5 kinase regulates sister chromatid separation in yeast." Cell **105**(4): 459-72.

Bergerat, A., B. de Massy, et al. (1997). "An atypical topoisomerase II from Archaea with implications for meiotic recombination." Nature **386**(6623): 414-7.

Buonomo, S. B., R. K. Clyne, et al. (2000). "Disjunction of homologous chromosomes in meiosis I depends on proteolytic cleavage of the meiotic cohesin Rec8 by separin." Cell **103**(3): 387-98.

Buonomo, S. B., K. P. Rabitsch, et al. (2003). "Division of the Nucleolus and Its Release of CDC14 during Anaphase of Meiosis I Depends on Separase, SPO12, and SLK19." Dev Cell **4**(5): 727-39.

Clyne, R. K., V. L. Katis, et al. (2003). "Polo-like kinase Cdc5 promotes chiasmata formation and cosegregation of sister centromeres at meiosis I." Nat Cell Biol **5**(5): 480-5.

Cohen-Fix, O., J. M. Peters, et al. (1996). "Anaphase initiation in Saccharomyces cerevisiae is controlled by the APC-dependent degradation of the anaphase inhibitor Pds1p." Genes Dev **10**(24): 3081-93.

Hu, F. and S. J. Elledge (2002). "Bub2 is a cell cycle regulated phospho-protein controlled by multiple checkpoints." Cell Cycle **1**(5): 351-5.

Katis, V. L., M. Galova, et al. (2004). "Maintenance of cohesin at centromeres after meiosis I in budding yeast requires a kinetochore-associated protein related to MEI-S332." Curr Biol **14**(7): 560-72.

Katis, V. L., J. Matos, et al. (2004). "Spo13 facilitates monopolin recruitment to kinetochores and regulates maintenance of centromeric cohesion during yeast meiosis." Curr Biol **14**(24): 2183-96.

Keeney, S., C. N. Giroux, et al. (1997). "Meiosis-specific DNA double-strand breaks are catalyzed by Spo11, a member of a widely conserved protein family." Cell **88**(3): 375-84.

Kerrebrock, A. W., D. P. Moore, et al. (1995). "Mei-S332, a Drosophila protein required for sister-chromatid cohesion, can localize to meiotic centromere regions." Cell **83**(2): 247-56.

Kiburz, B. M., D. B. Reynolds, et al. (2005). "The core centromere and Sgo1 establish a 50-kb cohesin-protected domain around centromeres during meiosis I." Genes Dev **19**(24): 3017-30.

Kitajima, T. S., S. Hauf, et al. (2005). "Human Bub1 defines the persistent cohesion site along the mitotic chromosome by affecting Shugoshin localization." Curr Biol **15**(4): 353-9.

Kitajima, T. S., S. A. Kawashima, et al. (2004). "The conserved kinetochore protein shugoshin protects centromeric cohesion during meiosis." Nature **427**(6974): 510-7.

Klein, F., P. Mahr, et al. (1999). "A central role for cohesins in sister chromatid cohesion, formation of axial elements, and recombination during yeast meiosis." Cell **98**(1): 91-103.

Lee and Amon, d. n. s.

Lee, B. H. and A. Amon (2003). "Role of Polo-like kinase CDC5 in programming meiosis I chromosome segregation." Science **300**(5618): 482-6.

Lee, B. H., A. Amon, et al. (2002). "Spo13 regulates cohesin cleavage." Genes Dev **16**(13): 1672-81.

Lee, B. H., B. M. Kiburz, et al. (2004). "Spo13 maintains centromeric cohesion and kinetochore coorientation during meiosis I." Curr Biol **14**(24): 2168-82.

Marston, A. L. and A. Amon (2004). "Meiosis: cell-cycle controls shuffle and deal." Nat Rev Mol Cell Biol **5**(12): 983-97.

Marston, A. L., B. H. Lee, et al. (2003). "The Cdc14 Phosphatase and the FEAR Network Control Meiotic Spindle Disassembly and Chromosome Segregation." Dev Cell **4**(5): 711-26.

Marston, A. L., W. H. Tham, et al. (2004). "A genome-wide screen identifies genes required for centromeric cohesion." Science **303**(5662): 1367-70.

Moll, T., G. Tebb, et al. (1991). "The role of phosphorylation and the CDC28 protein kinase in cell cycle-regulated nuclear import of the S. cerevisiae transcription factor SWI5." Cell **66**(4): 743-58.

Nairz, K. and F. Klein (1997). "mre11S--a yeast mutation that blocks double-strand-break processing and permits nonhomologous synapsis in meiosis." Genes Dev **11**(17): 2272-90.

Nasmyth, K. personal communication.

Nasmyth, K. and C. H. Haering (2005). "The structure and function of SMC and kleisin complexes." Annu Rev Biochem **74**: 595-648.

Shonn, M. A., R. McCarroll, et al. (2000). "Requirement of the spindle checkpoint for proper chromosome segregation in budding yeast meiosis." Science **289**(5477): 300-3.

Shonn, M. A., R. McCarroll, et al. (2002). "Spo13 protects meiotic cohesin at centromeres in meiosis I." Genes Dev **16**(13): 1659-71.

Shonn, M. A., A. L. Murray, et al. (2003). "Spindle checkpoint component Mad2 contributes to biorientation of homologous chromosomes." Curr Biol **13**(22): 1979-84.

Shou, W., R. Azzam, et al. (2002). "Cdc5 influences phosphorylation of Net1 and disassembly of the RENT complex." BMC Mol Biol **3**: 3.

Tang, T. T., S. E. Bickel, et al. (1998). "Maintenance of sister-chromatid cohesion at the centromere by the Drosophila MEI-S332 protein." Genes Dev **12**(24): 3843-56.

Tang, Z., Y. Sun, et al. (2004). "Human Bub1 protects centromeric sister-chromatid cohesion through Shugoshin during mitosis." Proc Natl Acad Sci U S A **101**(52): 18012-7.

Toth, A., K. P. Rabitsch, et al. (2000). "Functional genomics identifies monopolin: a kinetochore protein required for segregation of homologs during meiosis i." Cell **103**(7): 1155-68.

Visintin, R., K. Craig, et al. (1998). "The phosphatase Cdc14 triggers mitotic exit by reversal of Cdk-dependent phosphorylation." Mol Cell **2**(6): 709-18.

Watanabe, Y. personal communication.

Yu, H. G. and D. Koshland (2005). "Chromosome morphogenesis: condensin-dependent cohesin removal during meiosis." Cell **123**(3): 397-407.

Zhang, Y., A. Wolf-Yadlin, et al. (2005). "Time-resolved mass spectrometry of tyrosine phosphorylation sites in the epidermal growth factor receptor signaling network reveals dynamic modules." Mol Cell Proteomics **4**(9): 1240-50.

Chapter 3:

Rec8 Promotes Synaptonemal Complex Formation and Meiotic Prophase Progression

Gloria A. Brar, Angelika Amon

Abstract:

In meiosis, chromosomes undergo two rounds of chromosome segregation. The differences in Meiosis I and Meiosis II segregation are based on a number of meiotic specializations, including differential regulation of the meiotic cohesin Rec8 (Lee and Amon 2001). I find that Rec8 is additionally important to proper formation of the Synaptonemal Complex (SC) and prophase progression. I show that cohesion itself is not required for the prophase function of Rec8, but that this role is regulated through Rec8 phosphorylation. I additionally show that post-replicatively associated Rec8 is capable of supporting SC formation. I conclude that Rec8 performs roles important to multiple meiotic stages, thus ensuring order and directionality of the meiotic program.

Introduction:

Meiosis is the well-conserved process by which diploid cells produce haploid products; these products include eggs and sperm in multicellular organisms and spores in the budding yeast *Saccharomyces cerevisiae*. This process is essentially a modified mitotic cell cycle, with the most notable modification being the presence of two chromosome segregation phases following only a single DNA replication phase. The second segregation phase (MII), termed an equational segregation, involves newly replicated sister chromatids segregating from each other and is also the type of segregation that occurs in mitosis. In contrast, the first segregation phase (MI), called a reductional segregation, requires that homologous chromosomes segregate apart. For this to occur, these homologs must first be aligned and then linked through recombination (Lee and Amon 2001; Marston and Amon 2004). The process of recombination is complex and partially dependent on stabilization of paired homologs by a proteinaceous structure called the Synaptonemal Complex (SC) (Storlazzi, Tesse et al. 2008).

In mitosis and meiosis, sister chromatids are held together by the cohesin complex. This mitotic complex consists of four core proteins: Scc3, Smc1, Smc3 and Scc1. The meiotic complex also contains the same basic proteins, with the exception that Scc1 replaced by the meiosis-specific cohesin, Rec8. The cohesin complex is loaded onto chromosomes during DNA replication, such that newly formed sister chromatids are immediately tethered to existing

chromosomes (Forsburg 2002; Uhlmann 2003). At the end of meiotic prophase, homologs are linked through DNA attachments as a result of recombination, as well as cohesin linkages between sister chromatids. For this structure to specifically release homologs for MI chromosome segregation, cohesions must be removed along chromosome arms. Cohesins are maintained at centromeres, as this allows sister chromatids to continue to associate until the metaphase II to anaphase II transition. At this point, remaining cohesin is removed, allowing the formation of four balanced gametes (Lee and Amon 2001; Marston and Amon 2004).

The process by which cohesin is removed at the metaphase to anaphase transitions is well studied. Satisfaction of the spindle checkpoint, through proper chromosome attachment to the meiotic spindle causes activation of the Separase protease through degradation of its partner inhibior, Securin, by the APC/C (Anaphase promoting complex/Cyclosome). Active Separase cleaves Rec8, causing removal of cohesin from chromosomes. This process appears to occur through a largely identical mechanism in Meiosis I and Meiosis II. Centromeric Rec8, however, is protected from cleavage at the metaphase I to anaphase I transition by mechanisms that include association of centromeric Rec8 with the protector protein Shugoshin (Sgo1) and preferential phosphorylation of arm cohesions (Shonn, McCarroll et al. 2000; Uhlmann 2003; Katis, Matos et al. 2004; Kitajima, Kawashima et al. 2004; Marston, Tham et al. 2004; Rabitsch, Gregan et al. 2004; Brar, Kiburz et al. 2006).

Though Rec8 has primarily been studied for its cohesin role at both meiotic metaphase to anaphase transitions, it has been observed that cells deleted for *REC*8 show a large defect in exit from prophase, long before cells initiate the first chromosome segregation phase (Klein, Mahr et al. 1999). This defect is dependent on the creation of DSBs by Spo11, supporting a possible role for Rec8 in recombination. It is unclear, however, whether this role is simply a manifestation of the inability to hold and release sister chromatids (the Rec8 cohesin function) or an alternative function of Rec8. We show that Rec8 performs two independent functions in meiosis. Rec8 is important for proper assembly of the synaptonemal complex, and thus prophase progression, as well as its more defined role in holding sister chromatids together from the time they are replicated until the metaphase to anaphase transitions.

Results:

The role of Rec8 in SC formation

Because of its role as a core component of the meiotic cohesin complex, Rec8 plays a vital role in holding chromosomes together to ensure proper meiotic chromosome segregation. This cohesive role of Rec8 provides tension between attached homologs in metaphase I and sister chromatids in metaphase II that counteracts spindle tension and allows proper positioning of chromosomes and correct segregation at anaphase I and II (Marston and Amon 2004). It is not surprising, therefore, that *rec8Δ* cells show significant meiotic defects and low spore viability (Klein, Mahr et al. 1999). It is surprising, however, that *rec8Δ* cells are substantially defective in prophase progression, as there is no established reason that prophase cells should require sister chromatid cohesion. We sought to determine how Rec8 might be involved in prophase events by examining various cohesin-related mutants including mutations that prevented formation of sister chromatids, mutations in cohesin components besides Rec8 and mutations in factors known to be involved in cohesin function. Based on the significant conservation of meiotic processes among organisms and the genetic tractability of budding yeast, we chose to conduct our studies of Rec8 function in *Saccharomyces cerevisiae.*

To begin our investigation of the role of Rec8 in prophase, we first observed the formation of the SC, as assembly of this complex serves as a major cytological marker for prophase progression (Revenkova and Jessberger

2006). Following meiotic DNA replication, chromosomes initiate recombination through DSBs and chromosomes (Zickler and Kleckner 1998; Keeney and Neale 2006) begin to condense. A driving force behind this condensation appears to be Lateral Elements (LEs, also called Axial Elements or AEs) that assemble along chromosomes and serve as a scaffold for the progressing meiotic DNA. LEs are composed of a number of proteins, including Rec8 and the early meiotic protein Hop1. Mature SC is then formed by the joining of the LEs of homologous chromosomes through transverse elements (TEs). A major component of TEs is the coiled coil protein Zip1 (Zickler and Kleckner 1998; Page and Hawley 2004).

We scored meiotic chromosome spreads with samples taken as cells progressed through meiosis. Mononucleate cells were scored based on the pattern of Zip1 staining, into four categories: none/PC, minimal, partial, and full (Figure 1A). In wild-type cells, Zip1 is initially present in an extra-DAPI cluster called a Polycomplex (PC). Zip1 then associates in foci on chromosomes and eventually forms visible ribbons as it zips LEs together. Following recombination, in late prophase, Zip1 ribbons disappear from chromosomes so that homologs can more efficiently segregate at anaphase I (Figure 1B, 1C; (Page and Hawley 2004).

In *spo11Δ* cells, very little SC was ever assembled, even by 8 hours when 86% of cells had progressed past prophase (Figure 1C, Figure 2A). As previously observed (Klein, Mahr et al. 1999), we found that Zip1 assembly in cells deleted for *REC8* was nearly as poor as that seen in *spo11* cells, with a peak of assembled Zip1 of only 24% compared to 75% in wild-type cells (Figure

1C). Based on these data, we conclude that either Rec8 or the presence of a nearby sister chromatid appears to be essential for proper SC assembly.

To determine which of these cases is correct, we examined Zip1 assembly in a strain depleted meiotically for pre-RC component Cdc6 (*cdc6-mn)*. This strain does not undergo meiotic DNA replication, but otherwise progresses through meiosis relatively normally (Hochwagen, Tham et al. 2005). We found that *cdc6-mn* cells assemble Zip1 in a pattern nearly identical to wild-type cells (Figure 1C). These data indicate that the presence of a sister chromatid is dispensible for proper SC formation. Additionally, cohesin-functional Rec8 has been thought to depend on DNA replication (Forsburg 2002; Uhlmann 2003). Our data indicate that Rec8 plays an important role in prophase progression and that prophase-functional Rec8 is independent of DNA replication. We wondered if the reason for the differential Zip1 assembly in *rec8Δ* cells and *cdc6-mn* cells was due to interference of SC assembly by free sister chromatids present in *rec8* delete cells, but not those cells lacking Cdc6. To address this concern, we looked at *cdc6-mn rec8Δ* double mutant cells. We found that in these cells SC was assembled as poorly as in cells deleted for *REC8* (Figures 1C), indicating that the severe Zip1 assembly defect in *rec8Δ* cells reflects a direct or indirect role for Rec8 protein in SC assembly, rather than simply a need for properly tethered sister chromatids as the SC is formed.

We next examined Zip1 in a strain deleted for S-phase cyclins, *CLB5* and *CLB6.* This strain does not undergo meiotic DNA replication or DSB formation

(Smith, Penkner et al. 2001) and these cells showed poor SC assembly, similar to that seen in *rec8Δ* or *spo11Δ* cells (Figure 1C). These data support the importance of DSBs for SC formation and also indicate that this role is sister chromatid-independent.

The data thus far suggested the importance of the cohesin Rec8 in SC assembly, but not cohesion between sister chromatids. We wished to determine whether another cohesin could substitute for Rec8 in this role, so we examined cells in which Rec8's mitotic counterpart, Scc1, is expressed in place of Rec8 in meiosis (*pREC8-SCC1)*. These cells were unable to assemble Zip1 (Figure 1D), despite the ability of Scc1 to substitute for Rec8 in its Meiosis I cohesin role (Lee and Amon 2003). These data support the possibility that the cohesive and prophase roles of Rec8 are separable. We next examined cells expressing only an uncleavable version of Rec8 (*rec8-N*) (Buonomo, Clyne et al. 2000) and found that these cells were able to assemble Zip1 properly (Figure 1D), indicating that Rec8 cleavage, though essential for Meiosis I and Meiosis II chromosome segregation, does not contribute to Rec8's role in promoting prophase events.

Since Rec8's cohesin role and prophase role appeared to have differing requirements, we wished to determine whether Rec8's contribution to SC assembly required other cohesin-related proteins. This has been suggested to be the case, as fellow cohesin complex member Smc3 appears to associate along with Rec8 in AEs (Klein, Mahr et al. 1999). In support of this model, we found that cells meiotically-depleted for cohesin complex member Scc3 showed severe defects in Zip1 assembly (Figure 1E), suggesting that Rec8's prophase

function, like its later cohesin functions, is in the context of the cohesin complex. In further support of this model, cells depleted for Eco1, an acetyl-transferase required to load the cohesin complex onto chromosomes (Ivanov, Schleiffer et al. 2002), also show a defect in Zip1 assembly (Figure 1E). This defect is less than that seen in *rec8Δ* cells or Smc3-depleted cells, but this could be due to an incomplete depletion of Eco1, judged by ability of cells to form a stable metaphase I conformation (data not shown) indicating some level of functional cohesion. Note that this is not the case in either *rec8Δ* cells or cells depleted for Smc3 (data not shown).

Figure 1: Rec8 and the cohesin complex is required for Zip1 assembly, but Rec8 cleavage and presence of a sister chromatid is not
(A) Examples of meiotic cells that are harvested with Zip1 staining assayed on chromosome spreads. Cells carry a Rec8-3HA construct. α-Zip1 is shown in green, α-HA is shown in red, and DNA staining is shown in blue.

(B) Wild-type (A7097) cells were induced to sporulate. At the indicated times, cells were harvested and chromosome spreads were assayed for Zip1 staining according to the categores shown in (A). 100 mononucleate cells were counted per strain per timepoint. Note that this data is also shown in (C).

(C) Wild-type (A7097, closed squares), *spo11Δ* (A8477, closed triangles), *rec8Δ* A16664, closed circles), *pSCC1-CDC6* (A15880, open squares), *pSCC1-CDC6 rec8Δ* (A17021, open triangles), and *clb5Δ clb6Δ* (A16113, open circles) were induced to sporulate. At the indicated times, cells were harvested and chromosome spreads were assayed for Zip1 staining. Note that cells were scored as having SC if they showed partial or full SC according to the categories shown in (A). 100 mononucleate cells were counted per strain per timepoint. Note that meiotic progression of these strains is presented in Figure 2A.

(D) *REC8-3HA* (A13946, closed squares), *pREC8-SCC1-3HA* (A16132, closed triangles), and *REC8-N* (A13539, closed circles) were induced to sporulate. At the indicated times, cells were harvested and chromosome spreads were assayed for Zip1 staining. Note that cells were scored as having SC if they showed partial or full SC according to the categories shown in (A). 100 mononucleate cells were counted per strain per timepoint. Note that meiotic progression of these strains is presented in Figure 2B.

(E) Wild-type (A1972, closed squares), *pCLB2-SCC3* (A20163, closed triangles), and *pCLB2-ECO1* (A20081, closed circles) were induced to sporulate. At the indicated times, cells were harvested and chromosome spreads were assayed for Zip1 staining. Note that cells were scored as having SC if they showed partial or full SC according to the categories shown in (A). 100 mononucleate cells were counted per strain per timepoint. Note that meiotic progression of these strains is presented in Figure 2C.

Figure 1

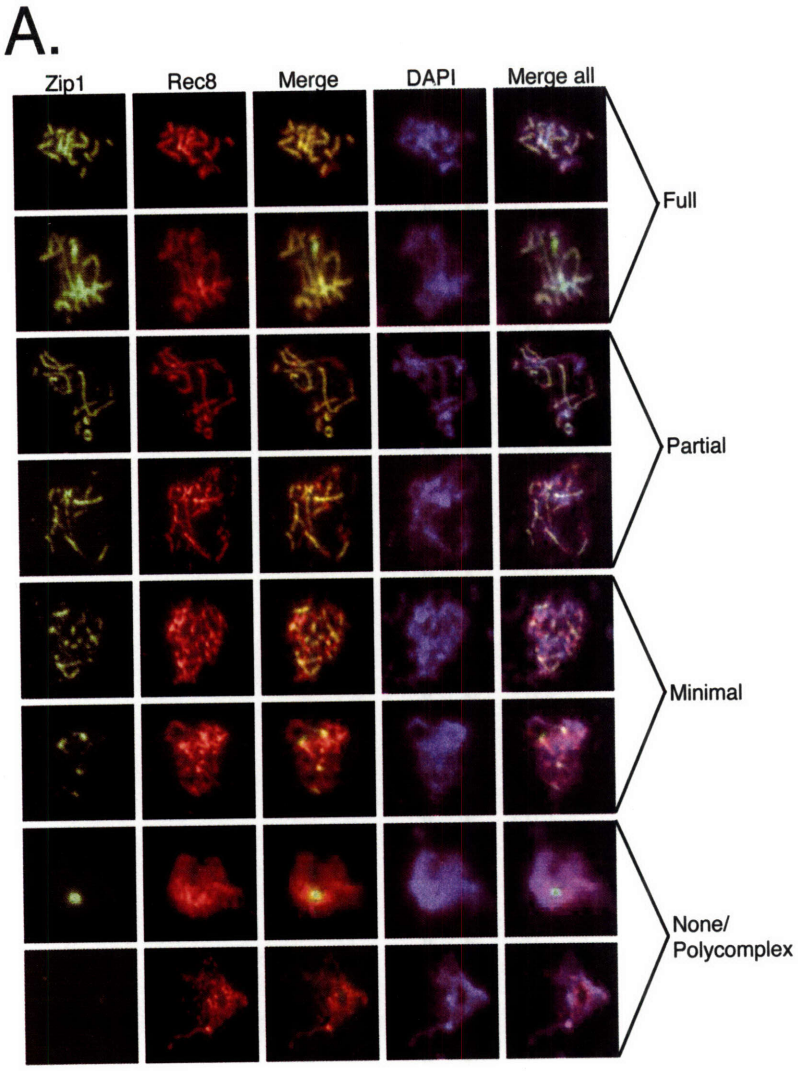
A.
Zip1
Rec8
Merge
DAPI
Merge all
Full
Partial
Minimal
None/
Polycomplex

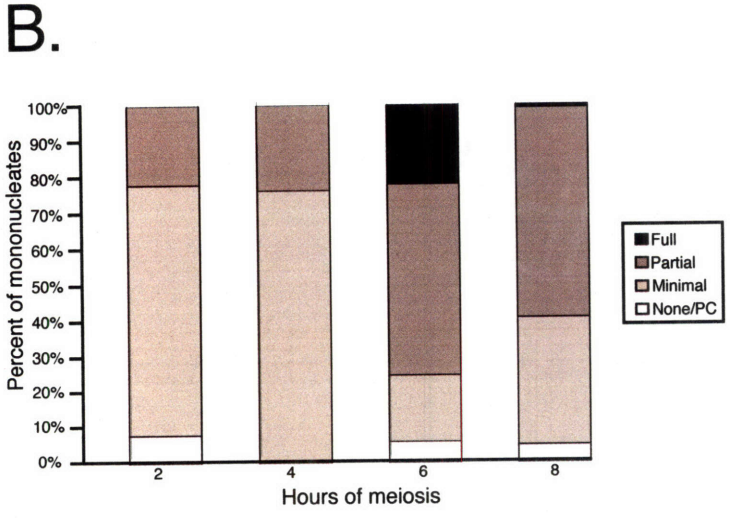
B.
Percent of mononucleates
100%
90%
80%
70%
60%
50%
40%
30%
20%
10%
0%
2
4
6
8
Hours of meiosis
Full
Partial
Minimal
None/PC

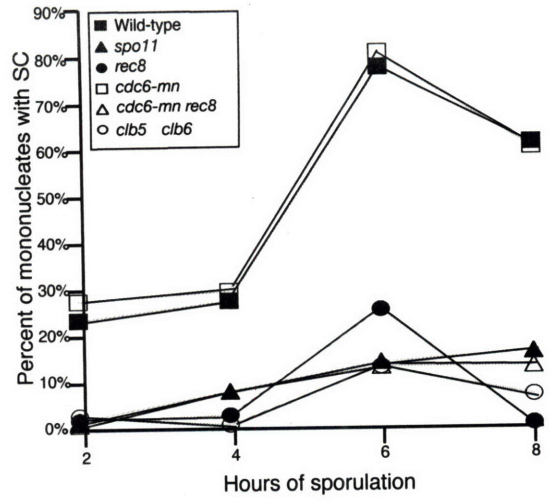
C.
Percent of mononucleates with SC
90%
80%
70%
60%
50%
40%
30%
20%
10%
0%
Wild-type
spo11
rec8
cdc6-mn
cdc6-mn rec8
clb5 clb6
2
4
6
8
Hours of sporulation

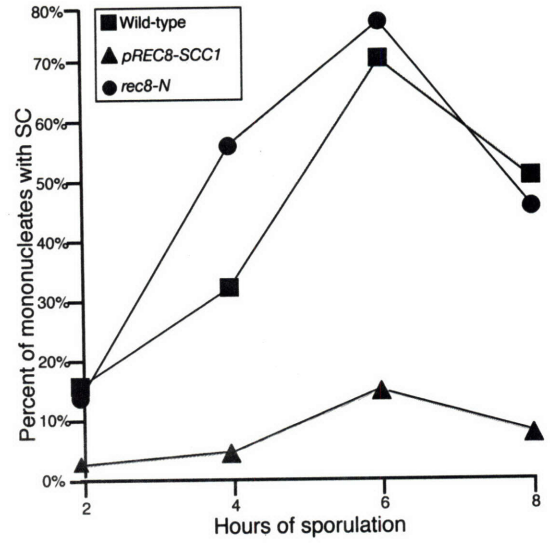
D.
Percent of mononucleates with SC
80%
70%
60%
50%
40%
30%
20%
10%
0%
Wild-type
pREC8-SCC1
rec8-N
2
4
6
8
Hours of sporulation

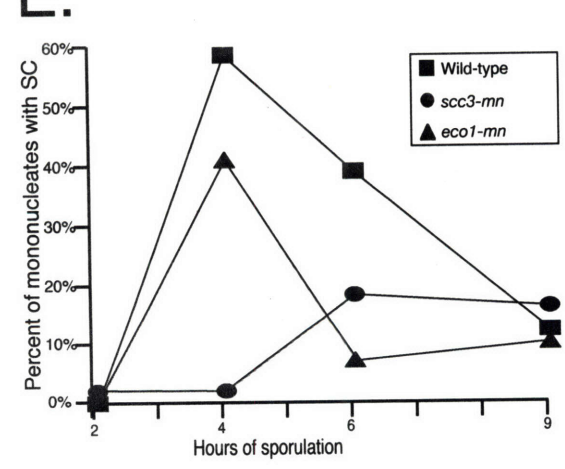
E.
Percent of mononucleates with SC
60%
50%
40%
30%
20%
10%
0%
Wild-type
scc3-mn
eco1-mn
2
4
6
9
Hours of sporulation

Figure 2: Meiotic progression of strains in Figure 1
(A) Wild-type (A7097, closed squares), *spo11Δ* (A8477, closed triangles), *rec8Δ* A16664, closed circles), *pSCC1-CDC6* (A15880, open squares), *pSCC1-CDC6 rec8Δ* (A17021, open triangles), and *clb5Δ clb6Δ* (A16113, open circles) were induced to sporulate. At the indicated times, samples were taken and subjected to α-tubulin IF to determine the percentage of cells with unassembled spindles. 200 cells were counted per strain per timepoint.

(B) *REC8-3HA* (A13946, closed squares), *pREC8-SCC1-3HA* (A16132, closed triangles), and *REC8-N* (A13539, closed circles) were induced to sporulate. At the indicated times, samples were taken and subjected to α-tubulin IF to determine the percentage of cells with unassembled spindles. 200 cells were counted per strain per timepoint.

(C) Wild-type (A1972, closed squares), *pCLB2-SCC3* (A20163, closed triangles), and *pCLB2-ECO1* (A20081, closed circles) were induced to sporulate. At the indicated times, samples were taken and subjected to α-tubulin IF to determine the percentage of cells with unassembled spindles. 200 cells were counted per strain per timepoint.

Figure 2

A.

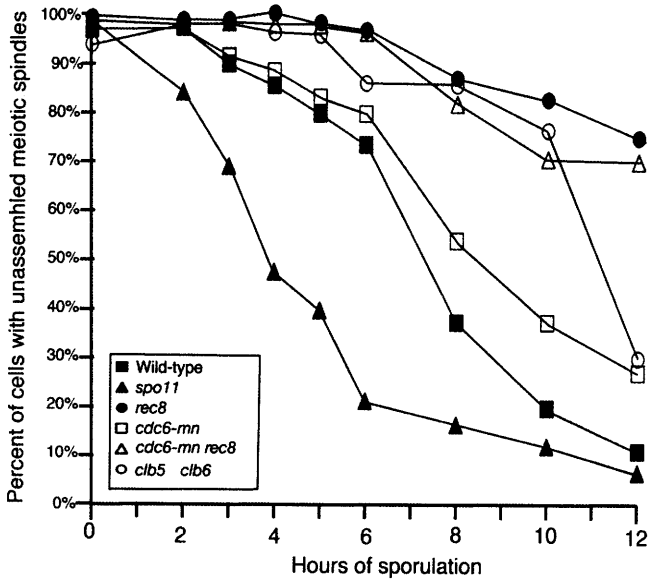
Percent of cells with unassemhled meiotic spindles
100%
90%
80%
70%
60%
50%
40%
30%
20%
10%
0%
0
2
4
6
8
10
12
Hours of sporulation
Wild-type
spo11
rec8
cdc6-mn
cdc6-mn rec8
clb5 clb6

B.

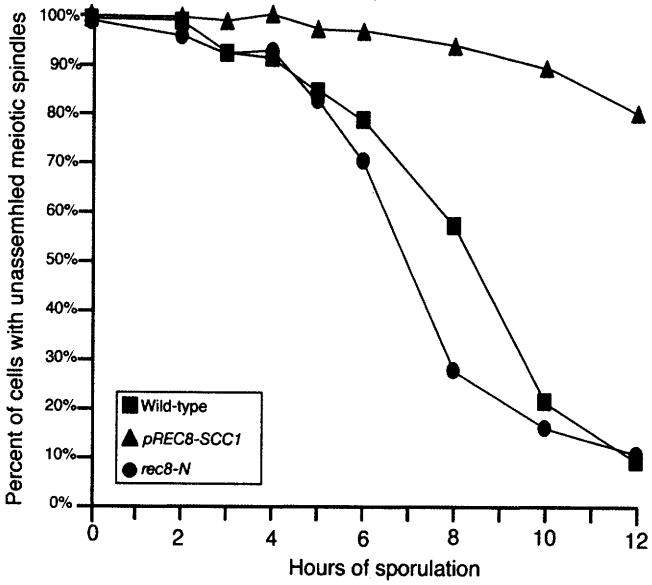
Percent of cells with unassemhled meiotic spindles
100%
90%
80%
70%
60%
50%
40%
30%
20%
10%
0%
0
2
4
6
8
10
12
Hours of sporulation
Wild-type
pREC8-SCC1
rec8-N

C.

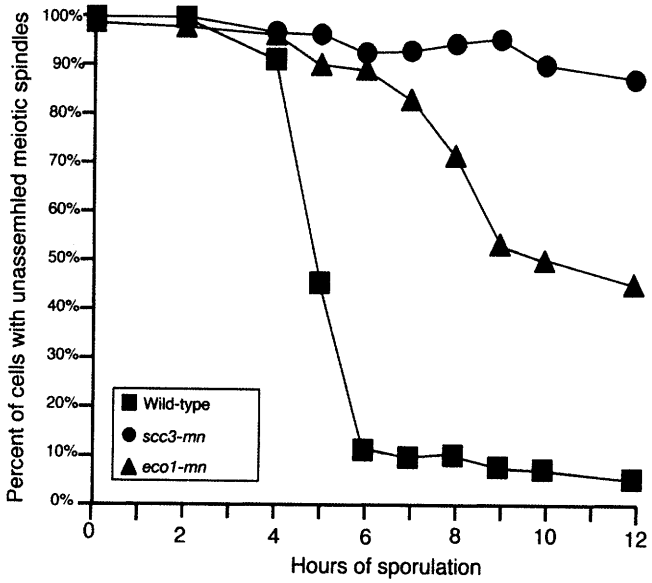
Percent of cells with unassemhled meiotic spindles
100%
90%
80%
70%
60%
50%
40%
30%
20%
10%
0%
0
2
4
6
8
10
12
Hours of sporulation
Wild-type
scc3-mn
eco1-mn

Our analysis thus far indicated a role for Rec8 in prophase distinct from its well-defined role as a cohesin in Meiosis I and II. We wished to examine additional Rec8 mutants to better understand how Rec8 might be contributing to progression of prophase events. We previously generated a number of Rec8 mutants based on identified phospho-sites. We mutated various combinations of phosphorylation sites to a non-phosphorylatable residue (Alanine) to examine the importance of these sites to Rec8 cleavage and noted that 17 phospho-sites had to be mutated at once for cells to delay Rec8 cleavage and accumulate in Metaphase I. We also noted that this *rec8-17A* mutant showed a delay in prophase exit that was dependent on Spo11 and that smaller mutants (*rec8-6A, rec8-11A)* showed a similar prophase delay, but no metaphase I accumulation. A *rec8-29A* mutant showed a severe prophase delay that made it difficult to assess metaphase I to anaphase I progression(Brar, Kiburz et al. 2006). These mutants all expressed normal levels of Rec8 and mutant protein associated with chromosomes normally as judged by immunofluorescence of chromosome spreads (Brar, Kiburz et al. 2006).

We decided to look more closely at these Rec8 mutants with a focus on their effects on prophase events. We found that Zip1 assembly was severely defective in *rec8-6A, rec8-17A* and *rec8-29A* cells as judged by the ability of cells to form partial or full Zip1 ribbons (Figure 3B). When we judged cells only by ability to assemble full Zip1, we found an even more dramatic defect, with no full SC observed in any of the three Rec8 phospho-mutants (Figure 3E).

Figure 3: Rec8 phosphorylation contributes to SC assembly in a Cdc5-independent manner

(A) Wild-type (A1972, closed squares), *rec8Δ* (A3528, closed triangles), *rec8-29A* (A14385, closed circles), *rec8-17A* (A13535, open squares), *rec8-6A* (A15042, open triangles), and *pCLB2-CDC5* (A5844, open circles) cells were induced to sporulate. At the indicated times, samples were taken and subjected to α-tubulin Immunofluorescence (IF) to determine the percentage of cells with unassembled spindles. 200 cells were counted per strain per timepoint.

(B) Wild-type (A1972, closed squares), *rec8Δ* (A3528, closed triangles), *rec8-29A* (A14385, closed circles), *rec8-17A* (A13535, open squares), *rec8-6A* (A15042, open triangles), and *pCLB2-CDC5* (A5844, open circles) cells were induced to sporulate. At the indicated times, cells were harvested and chromosome spreads were assayed for Zip1 staining. Note that cells were scored as having SC if they showed partial or full SC according to the categories shown in Figure 1A. 100 mononucleate cells were counted per strain per timepoint.

(C) Wild-type (A14655, closed squares) and *rec8-psa* (A15364, closed triangles) were induced to sporulate. At the indicated times, samples were taken and subjected to α-tubulin IF to determine the percentage of cells with unassembled spindles. 200 cells were counted per strain per timepoint.

(D) Wild-type (A14655, closed squares) and *rec8-psa* (A15364, closed triangles) were induced to sporulate. At the indicated times, cells were harvested and chromosome spreads were assayed for Zip1 staining. Note that cells were scored as having SC if they showed partial or full SC according to the categories shown in Figure 1A. 100 mononucleate cells were counted per strain per timepoint.

(E) Wild-type (A1972, closed squares), *rec8Δ* (A3528, closed triangles), *rec8-29A* (A14385, closed circles), *rec8-17A* (A13535, open squares), *rec8-6A* (A15042, open triangles), and *pCLB2-CDC5* (A5844, open circles) cells were induced to sporulate. At the indicated times, cells were harvested and chromosome spreads were assayed for Zip1 staining. Note that cells were scored for full SC according to the categories shown in Figure 1A. 100 mononucleate cells were counted per strain per timepoint. Note that this is the same data plotted in (B), with only full SC charted here.

(F) Wild-type (A14655, closed squares) and *rec8-psa* (A15364, closed triangles) were induced to sporulate.At the indicated times, cells were harvested and chromosome spreads were assayed for Zip1 staining. Note that cells were scored for full SC according to the categories shown in Figure 1A. 100 mononucleate cells were counted per strain per timepoint. Note that this is the same data plotted in (D), with only full SC charted here.

Figure 3

A.

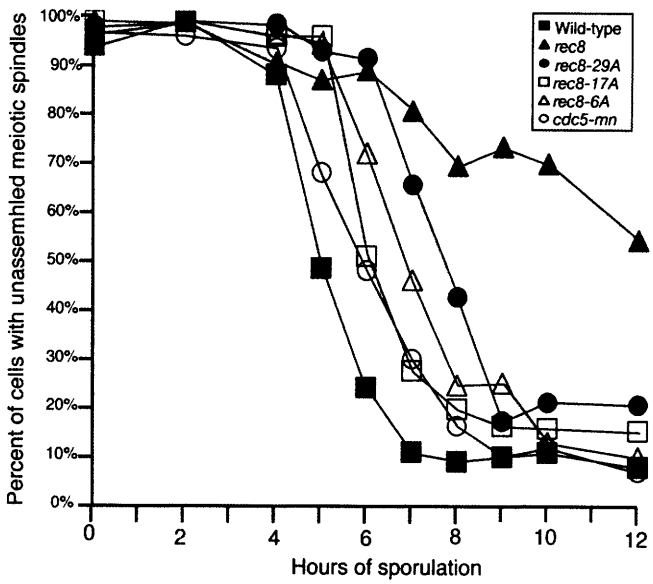

C.

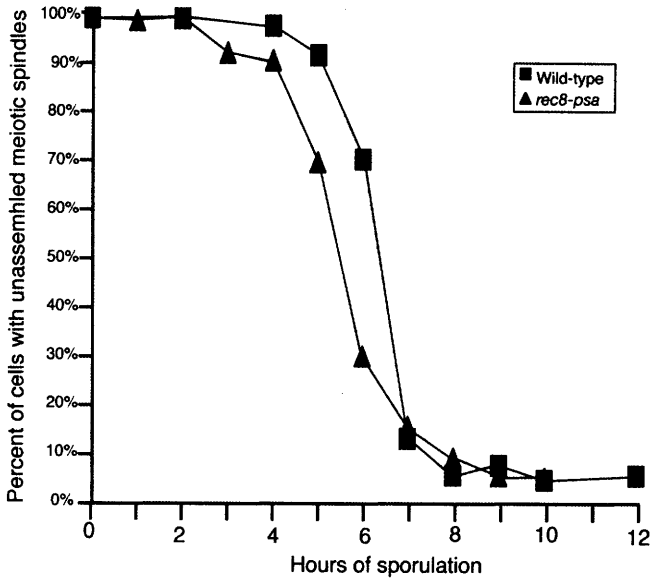

B.

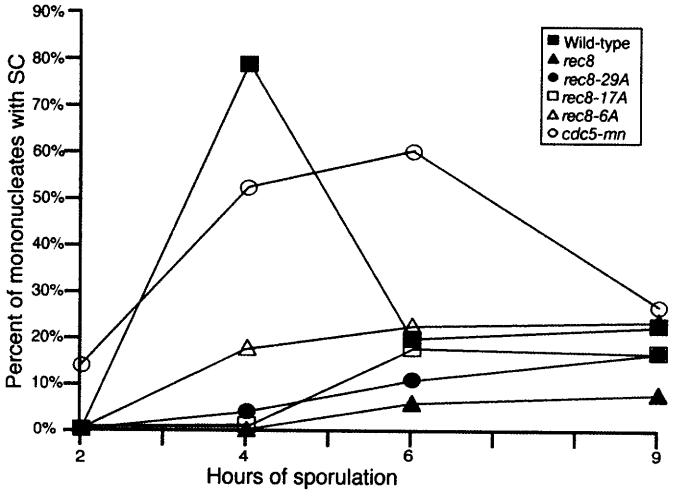

D.

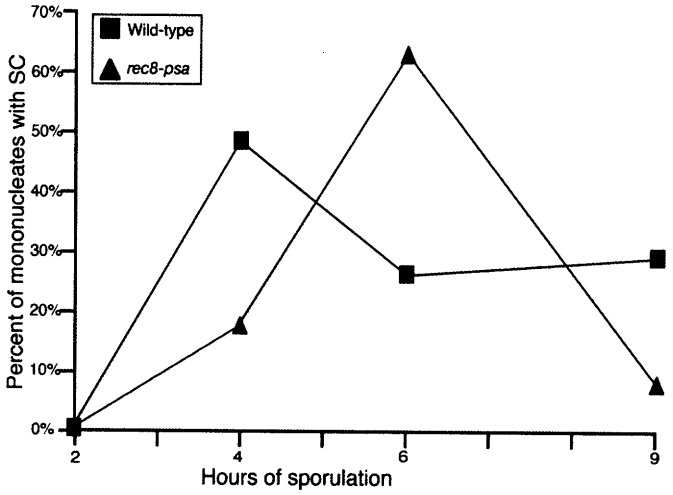

E.

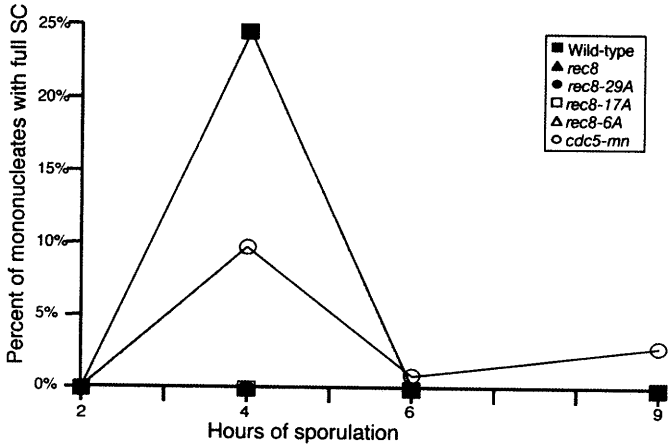

F.

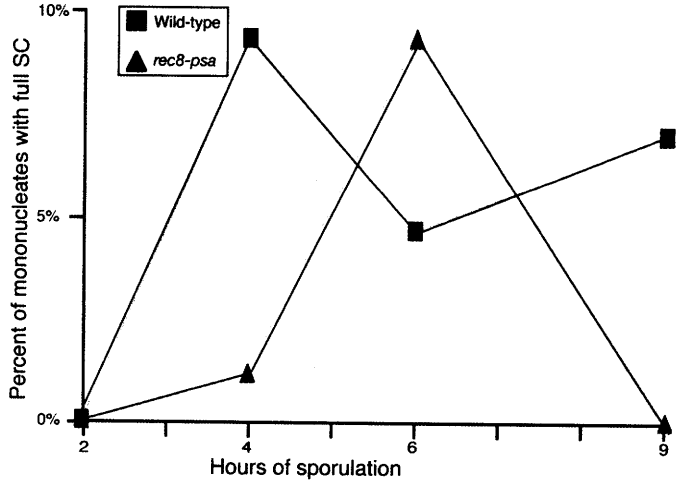

We also examined LE formation in *rec8-6A* and *rec8-17A* mutants (Figure 4). When Hop1 staining was scored in a manner similar to the Zip1 assay previously described, we saw no defect in LE assembly in *rec8-6A* or *rec8-17A* cells, in contrast to *rec8Δ* cells, which assemble no substantial LEs as Rec8 is an important structural component of these elements (Figure 4A, 4C). We thus conclude that Rec8 phosphorylation appears to play a role in SC formation subsequent to LE assembly.

Figure 4: Lateral Element assembly is not defective in *rec8-6A* or *rec8-17A* cells, though Transverse Element assembly is defective.
(A) Examples of meiotic cells that are harvested with Hop1 staining assayed on chromosome spreads. Cells carry a Rec8-3HA construct. α-Hop1 is shown in green, α-HA is shown in red, and DNA staining is shown in blue.

(B) Wild-type (A7097, closed squares), *rec8-6A* (A15042, closed triangles), *rec8-17A* (A13535, closed circles), and *rec8Δ* (A16664, open squares) cells were induced to sporulate. At the indicated times, samples were taken and subjected to α-tubulin IF to determine the percentage of cells with unassembled spindles. 200 cells were counted per strain per timepoint. Note that these data are from the same experiment presented in Figure 1, so Wild-type and *rec8Δ* controls are identical to those shown in Figure 1C.

(C) Wild-type (A7097, closed squares), *rec8-6A* (A15042, closed triangles), *rec8-17A* (A13535, closed circles), and *rec8Δ* (A16664, open squares) cells were induced to sporulate. At the indicated times, cells were harvested and chromosome spreads were assayed for Hop1 staining. Note that cells were scored as having LEs if they showed partial or full Hop1 staining according to the categories shown in Figure 4A. 100 mononucleate cells were counted per strain per timepoint. Note that these data are from the same experiment presented in Figure 1.

(D) Wild-type (A7097, closed squares), *rec8-6A* (A15042, closed triangles), *rec8-17A* (A13535, closed circles), and *rec8Δ* (A16664, open squares) cells were induced to sporulate. At the indicated times, cells were harvested and chromosome spreads were assayed for Zip1 staining. Note that cells were scored as having SC if they showed partial or full SC according to the categories shown in Figure 1A. 100 mononucleate cells were counted per strain per timepoint. Note that these data are from the same experiment presented in Figure 1.

(E) Wild-type (A7097, closed squares), *rec8-6A* (A15042, closed triangles), *rec8-17A* (A13535, closed circles), and *rec8Δ* (A16664, open squares) cells were induced to sporulate. At the indicated times, cells were harvested and chromosome spreads were assayed for Zip1 staining. Note that cells were scored for full SC according to the categories shown in Figure 1A. 100 mononucleate cells were counted per strain per timepoint. Note that this is the same data plotted in (D), with only full SC charted here. Also note that these data are from the same experiment presented in Figure 1.

Figure 4

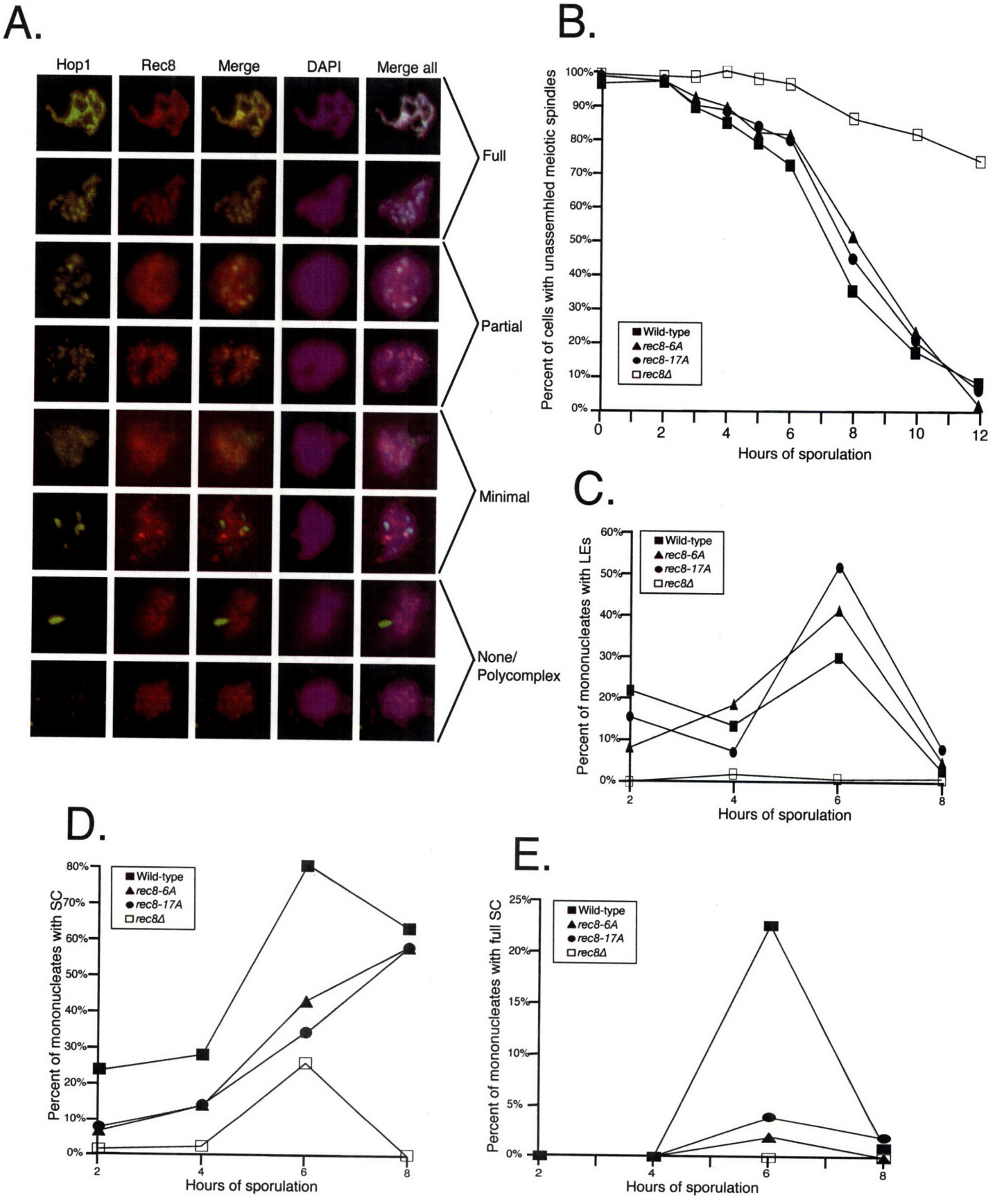
A.
Hop1
Rec8
Merge
DAPI
Merge all
Full
Partial
Minimal
None/
Polycomplex
B.
Percent of cells with unassemhled meiotic spindles
100%
90%
80%
70%
60%
50%
40%
30%
20%
10%
0%
0
2
4
6
8
10
12
Hours of sporulation
Wild-type
rec8-6A
rec8-17A
rec8Δ
C.
Percent of mononucleates with LEs
60%
50%
40%
30%
20%
10%
0%
2
4
6
8
Hours of sporulation
Wild-type
rec8-6A
rec8-17A
rec8Δ
D.
Percent of mononucleates with SC
80%
70%
60%
50%
40%
30%
20%
10%
0%
2
4
6
8
Hours of sporulation
Wild-type
rec8-6A
rec8-17A
rec8Δ
E.
Percent of mononucleates with full SC
25%
20%
15%
10%
5%
0%
2
4
6
8
Hours of sporulation
Wild-type
rec8-6A
rec8-17A
rec8Δ

Rec8 phosphorylation and SC assembly

Through previous work, we showed that Rec8 is phosphorylated by the Polo kinase Cdc5, as well as other unidentified kinases (Clyne, Katis et al. 2003; Lee and Amon 2003; Brar, Kiburz et al. 2006). Cdc5 depleted cells have been shown to exhibit a delay in exit from prophase (Clyne, Katis et al. 2003; Lee and Amon 2003), so we wished to determine whether Cdc5 phosphorylation contributed to the prophase defect seen in our phospho-mutants. Surprisingly, this was not the case. When we examined a mutant with all 11 identified Cdc5-dependent sites on Rec8 mutated to alanine (*rec8-psa;* (Clyne, Katis et al. 2003; Lee and Amon 2003; Brar, Kiburz et al. 2006), we found no delay in prophase exit (Figure 3C). We also found that these cells were capable of assembling Zip1 to wild-type levels and could assemble full SC (Figures 3D, 3F). Strangely, these cells actually appeared to have a defect in disassembly of the SC that we cannot explain at this time (Figures 3D, 3F). It was possible that our inability to see significant SC assembly defects based on Cdc5 phosphorylation of Rec8 was simply due to sites that we missed in our initial phospho-mapping. To address this concern, we examined SC formation in cells depleted for Cdc5. These cells showed a mild delay in exit from prophase, but this did not appear to be due to a defect in SC assembly, as cells depleted for Cdc5 were able to assemble SC to normal levels (Figure 3A, 3B). Interestingly, like *rec8-psa* mutants, cells depleted for Cdc5 also show persistent SC, indicative of a possible role for Cdc5 phosphorlyation of Rec8 in SC disassembly. We therefore conclude that

although Rec8 phosphorylation appears to play a role in assembly of SC, Cdc5-dependent phosphorylation does not play a major role in this function.

We have attempted to identify the kinase responsible for the prophase delay in these Rec8 phospho-mutants and have been thus far unsuccessful. Thus far, we have excluded Cdc5, Cdc28, Ime2, Ipl1, Mek1, Cdc15, Cdc7, Mec1 and Rad53 through either meiotic depletion or treatment of cells with specific kinase inhibitors (data not shown), though we cannot exclude combinations of the above kinases at this time. Indeed, while investigating a role for Rec8 in prophase, we examined a number of different phospho-site mutants. We were unable to identify any mutants with individual or fewer than 6 sites mutated *(rec8-6A)* that showed a consistent prophase defect (data not shown), thus we focused our attention on the mutants discussed here.

Given the large number of phospho-sites present on Rec8, it is possible that multiple kinases act in concert to promote prophase progression. It is also possible, however, that the prophase defects that we observe in specific Rec8 phospho-mutants are due to structural changes in the protein and not actually phosphorylation events on the residues mutated. To address this issue, we generated phospho-mimetic mutants. When all six alanines in the *rec8-6A* are instead mutated to glutamates or aspartates (*rec8-6E, rec8-6D)*, we see no Rec8 association on chromosomes (data not shown), indicating that these mutations result in an unstable protein. The sole phospho-mimetic mutation that we were able to generate that results in stable protein mutates Serine 521 to Aspartate (*rec8-S521D).* Mutant cells with this residue mutated to an alanine (*rec8-S521A)*

to render Rec8 non-phosphorylatable show a variable defect in SC formation. These cells show a consistent defect when compared to wild-type cells, but the degree of defect is highly variable (data not shown). Phospho-mimetics for this site show a rescue of the prophase delay in *rec8-S521A* cells (Figure 5A). *rec8-S521D* cells also show a full rescue of the SC assembly defect seen in *rec8-S521A* cells (Figure 5B). These data support the role of phosphorylation in SC assembly, though we believe that the variable defect seen in *rec8-S521A* cells supports a model in which normally multiple Rec8 phosphorylation sites, possibly phosphorylated by multiple kinases, act together responsible for supporting Rec8's prophase function.

Figure 5: A phosphomimetic Rec8 mutant can rescue the SC and prophase defect in a phosphomutant.
(A) Wild-type (A20066, squares), *rec8-S521A* (A17011, triangles), and *rec8-S521D* (A20076, circles) cells were induced to sporulate. At the indicated times, samples were taken and subjected to α-tubulin IF to determine the percentage of cells with unassembled spindles. 200 cells were counted per strain per timepoint.

(B) Wild-type (A20066, squares), *rec8-S521A* (A17011, triangles), and *rec8-S521D* (A20076, circles) cells were induced to sporulate. At the indicated times, cells were harvested and chromosome spreads were assayed for Zip1 staining. Note that cells were scored as having SC if they showed partial or full SC according to the categories shown in Figure 1A. 100 mononucleate cells were counted per strain per timepoint.

Figure 5

A.

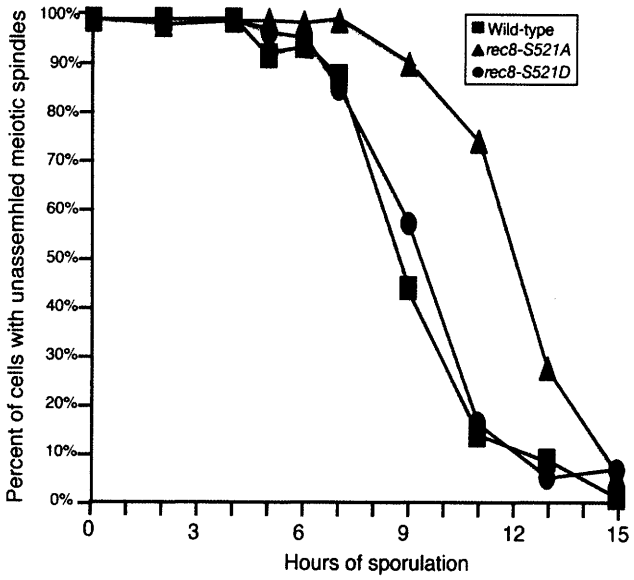
Percent of cells with unassemhled meiotic spindles
100%
90%
80%
70%
60%
50%
40%
30%
20%
10%
0%
0
3
6
9
12
15
Hours of sporulation
Wild-type
rec8-S521A
rec8-S521D

B.

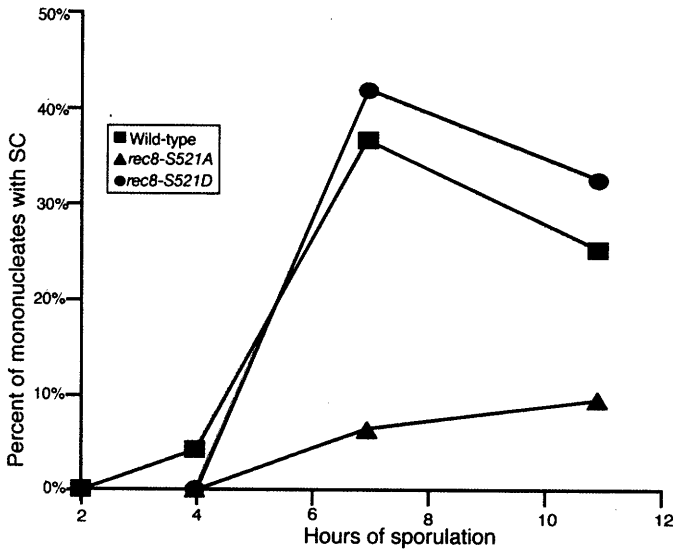
Percent of mononucleates with SC
50%
40%
30%
20%
10%
0%
2
4
6
8
10
12
Hours of sporulation
Wild-type
rec8-S521A
rec8-S521D

The role of Rec8 in recombination progression

Proper progression through prophase largely depends on proper completion of recombination (Hochwagen and Amon 2006). The importance of SC assembly to prophase progression is still not entirely clear. Certain SC mutants show defects in progression through prophase, but it has been speculated that the SC exists to stabilize recombination intermediates, so it has been difficult to functionally dissect SC assembly from recombination in their roles in prophase progression. Having determined that Rec8 plays a role in SC assembly, we next sought to examine whether Rec8 might also play a role in recombination. To this end, we performed Southern blots designed to follow recombination status of the *HIS4/LEU2* locus (Hunter and Kleckner 2001). As previously described, we found that cells deleted for *REC8* showed normal appearance of DSBs, but a delay in the appearance of mature recombination products compared to wild-type cells (Figure 6A, C, E, Figure 7; (Klein, Mahr et al. 1999). The replacement of *REC8* by *SCC1* was unable to rescue this recombination defect (Figure 6A, C, E, Figure 7). As we have previously described, *cdc6-mn* cells show relatively normal recombination progression with respect to DSBs and mature recombination products (Figure 6A, C, E, Figure 7; (Hochwagen, Tham et al. 2005). Although *rec8-6A* cells show no detectable defect in DSB formation or mature recombination product formation, *rec8-29A* cells make DSBs at normal levels and with normal timing, but show a defect comparable to *rec8Δ* in the appearance of mature recombination products (Figure 6A, C, E, Figure 7).

Figure 6: *rec8-6A* cells show a primary defect in SC formation, while *rec8-29A* cells have a recombination defect as well
(A) Wild-type (A1556), *rec8Δ* (A18933), *pSCC1-CDC6* (A10912), *pREC8-SCC1* (A16132), *rec8-29A* (A16997), and *rec8-6A* (A18936) cells were induced to sporulate. At the indicated times, cells were harvested and assayed by Southern blot for DSBs and recombination products at *HIS4/LEU2*. Meiotic progression for strains in this experiment is presented in Figure 7.

(B) Wild-type (A1972, closed squares), *mek1Δ* (A20156, closed triangles), *rec8-6A* (A15042, closed circles), *rec8-6A mek1Δ* (A20154, open squares), *rec8-29A* (A14385, open triangles), and *rec8-29A mek1Δ* (A20157, open circles) cells were induced to sporulate. At the indicated times, samples were taken and subjected to α-tubulin IF to determine the percentage of cells with unassembled spindles. 200 cells were counted per strain per timepoint. Note that these data are from the same experiment as (D)

(C) Blots from (A) were subjected to densitometric analysis to quantitate the intensity of the bands representing DSBs. Values were normalized to the adjacent lane region for each strain and each timepoint.

(D) Wild-type (A1972, closed squares), *pch2Δ* (A21053, closed triangles), *rec8-6A* (A15042, closed circles), *rec8-6A pch2Δ* (A20151, open squares), *rec8-29A* (A14385, open triangles), and *rec8-29A pch2Δ* (A20164, open circles) cells were induced to sporulate. At the indicated times, samples were taken and subjected to α-tubulin IF to determine the percentage of cells with unassembled spindles. 200 cells were counted per strain per timepoint. Note that these data are from the same experiment as (B)

(E) Blots from (A) were subjected to densitometric analysis to quantitate the intensity of the bands representing the upper recombinant band. Values were normalized to the "Mom" parental band for each strain and each timepoint.

Figure 6

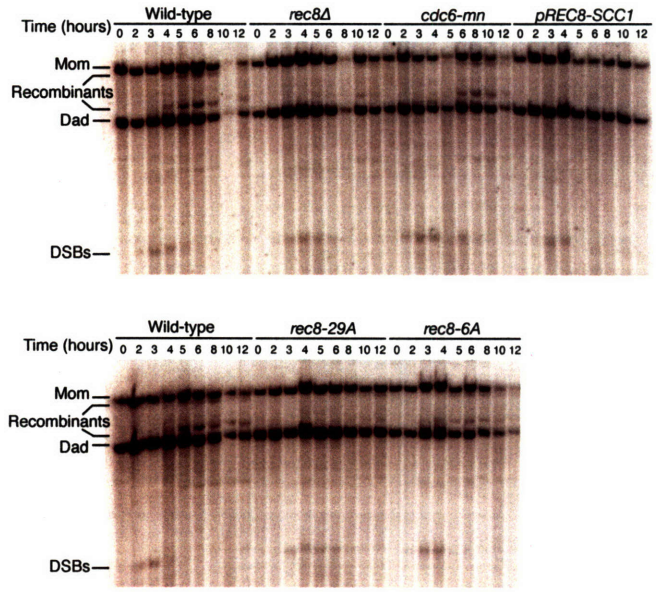
A.
Wild-type
rec8Δ
cdc6-mn
pREC8-SCC1
Time (hours) 0 2 3 4 5 6 8 10 12
Mom
Recombinants
Dad
DSBs
Wild-type
rec8-29A
rec8-6A
Time (hours) 0 2 3 4 5 6 8 10 12
Mom
Recombinants
Dad
DSBs

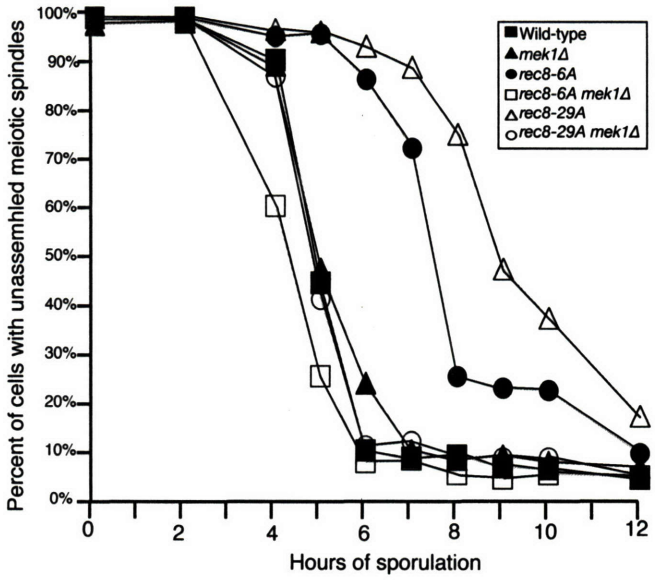
B.
Wild-type
mek1Δ
rec8-6A
rec8-6A mek1Δ
rec8-29A
rec8-29A mek1Δ
Percent of cells with unassemhled meiotic spindles
100%
90%
80%
70%
60%
50%
40%
30%
20%
10%
0%
0
2
4
6
8
10
12
Hours of sporulation

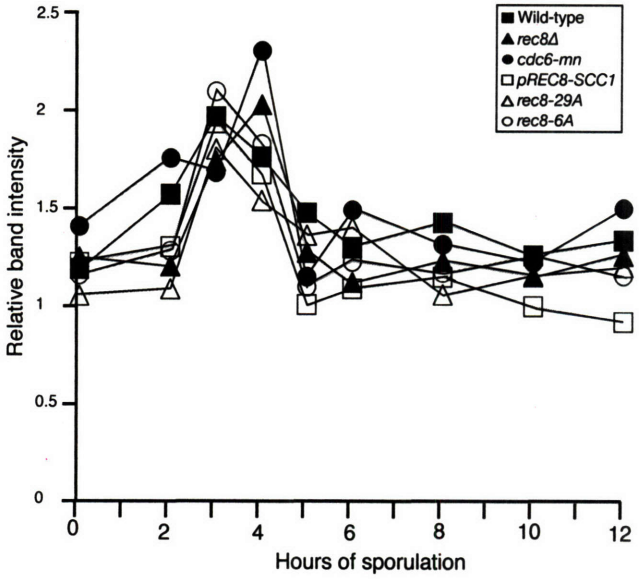
C.
Wild-type
rec8Δ
cdc6-mn
pREC8-SCC1
rec8-29A
rec8-6A
Relative band intensity
2.5
2
1.5
1
0.5
0
0
2
4
6
8
10
12
Hours of sporulation

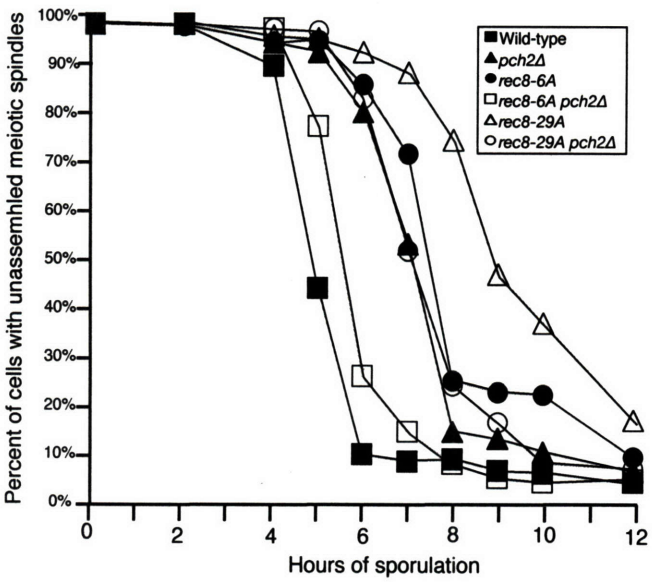
D.
Wild-type
pch2Δ
rec8-6A
rec8-6A pch2Δ
rec8-29A
rec8-29A pch2Δ
Percent of cells with unassemhled meiotic spindles
100%
90%
80%
70%
60%
50%
40%
30%
20%
10%
0%
0
2
4
6
8
10
12
Hours of sporulation

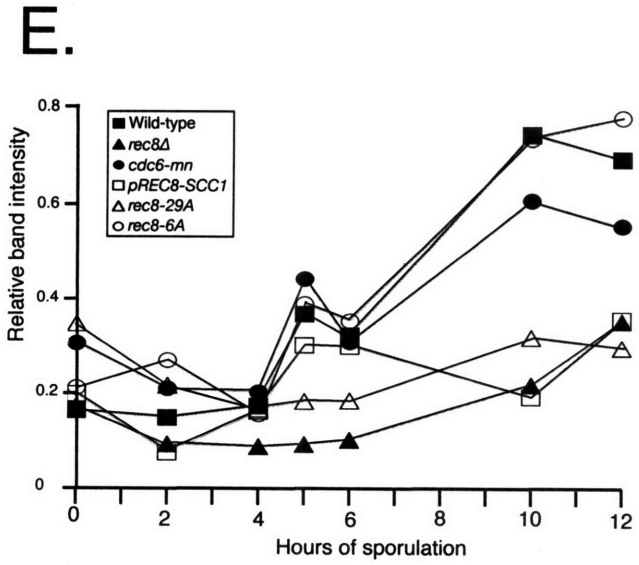
E.
Wild-type
rec8Δ
cdc6-mn
pREC8-SCC1
rec8-29A
rec8-6A
Relative band intensity
0.8
0.6
0.4
0.2
0
0
2
4
6
8
10
12
Hours of sporulation

Figure 7: Meiotic progression of strains in Figure 6A
Wild-type (A1556), *rec8Δ* (A18933), *pSCC1-CDC6* (A10912), *pREC8-SCC1* (A16132), *rec8-29A* (A16997), and *rec8-6A* (A18936) cells were induced to sporulate. At the indicated times, samples were taken and subjected to α-tubulin IF to determine the percentage of cells with unassembled spindles. 200 cells were counted per strain per timepoint.

Figure 7

A.

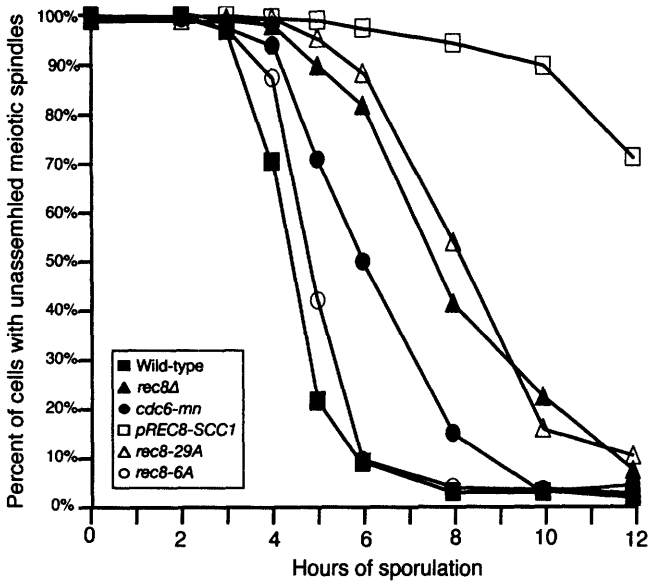
Percent of cells with unassemhled meiotic spindles
100%
90%
80%
70%
60%
50%
40%
30%
20%
10%
0%
0
2
4
6
8
10
12
Hours of sporulation
Wild-type
rec8Δ
cdc6-mn
pREC8-SCC1
rec8-29A
rec8-6A

These data represent a qualitative difference between *rec8-6A* and *rec8-29A* cells. It appears that Rec8-6A is capable of supporting normal recombination, while Rec8-29A is not. Neither protein is capable of supporting normal SC formation. To probe this relationship further, we looked at these two mutants in two different recombination checkpoint-defective backgrounds. The recombination checkpoint is a surveillance pathway at the end of the pachytene stage of prophase that involves a rather complex and redundant set of proteins. This checkpoint is dependent on DSB formation by Spo11 and is thought to sense the presence of incomplete recombination products or improper SC (Hochwagen and Amon 2006). Mek1 is a key kinase in this checkpoint. When we deleted *MEK1* in *rec8-6A* and *rec8-29A* cells, we found a rescue of the prophase delays in both Rec8 mutants (Figure 6B).

Pch2 is a nucleolar protein, thought to be primarily responsible for pachytene delays in response to SC defects, but its deletion is unable to rescue delays due to recombination-based defects (San-Segundo and Roeder 1999; Hochwagen and Amon 2006; Mitra and Roeder 2007). When *PCH2* is deleted in *rec8-6A* and *rec8-29A* cells, there is a rescue of the prophase delay in *rec8-6A* cells, but only a partial rescue of the prophase exit delay seen in *rec8-29A* cells (Figure 6D). This result is consistent with our observation that *rec8-29A* mutants show recombination deficiencies in addition to SC formation defects, while the prophase delay in *rec8-6A* cells is primarily due to problems assembling proper SC. This finding is consistent with the observation that *rec8-6A* cells show a

relatively high spore viability of 84%, compared to 68% in *rec8-29A* cells (Brar, Kiburz et al. 2006). *rec8Δ* cells produce essentially no viable spores, but this is likely due primarily to the lack of functional cohesion in these mutants resulting in random chromosome segregation, rather than the relatively smaller role of Rec8 in recombination progression.

Promotion of SC assembly by an artificially-induced Rec8 pool

Our data strongly suggest a prophase function for Rec8 distinct from its well-characterized role in chromosome cohesion. Most notably, Rec8's role in prophase progression is independent of DNA replication, though cohesins are loaded onto sister chromatids during S phase. We wished to determine if Rec8 could associate with chromosomes and support SC assembly if supplied to cells following DNA replication. We reasoned that mitotic cohesin can be loaded onto chromosomes in a DSB-dependent, but replication-independent manner, so perhaps this was also the case in meiosis (Strom, Lindroos et al. 2004; Unal, Arbel-Eden et al. 2004). We constructed cells with β-estradiol (βE)-inducible Rec8 in a *spo11Δ* background. Such cells were induced to enter meiosis in the absence of βE and allowed to complete DNA replication. We then induced *REC8* expression, initiated DSBs with 20 Krad γ-irradiation (γIR), and assayed after several hours for Zip1 assembly (Figure 8A). When cells were exposed to neither βE nor γIR, no Zip1 ribbons were seen (Figure 8B, left-hand column). The same is the case for cells irradiated, but not treated with βE, indicating again that in

the absence of Rec8, cells do not efficiently assemble SC (Figure 8B, second colum from the left). When we induced Rec8 in cells in the absence of DSBs, we were able to observe a low level of Zip1 assembly (Figure 8B, third column from the left). In contrast, when we exposed cells to both βE and γIR, 35% of cells were able to assemble SC (Figure 8B, right-most column). Immunofluorescence of cells in which βE was added revealed that, as expected, Rec8 expression was induced in these cells and associated with chromosomes (Figure 8F). This was not true of cells in which βE was not added. Similarly, Rad51 foci, indicative of DSBs in the process of repair (Whitby 2005), were present in irradiated cells but not in non-irradiated cells (Figure 8F). We additionally performed this experiment with an inducible, non-cleavable form of Rec8 (Rec8-N) as the only Rec8 source and found that this version was also able to support some SC assembly in a DSB-dependent manner (Figure 8E). These data indicate that functional Rec8 can be post-replicatively "activated" without cleavage.

Our experiments show that post-replicatively induced Rec8 can support SC assembly in the presence of DSBs, but the quality and levels of SC achieved were not as high as we had expected if post-replicative Rec8 was fully functional for Zip1 assembly. We reasoned that it was possible that most cells were not given wild-type conditions to complete SC assembly. The population was likely asynchronous at the point at which Rec8 was induced and DSBs were formed, and some cells may have been past the stage at which they are able to assemble SC before entering the meiotic divisions. To address this concern, we performed a similar experiment as described above, but with cells

deleted for the transcription factor *NDT80*. Ndt80 is required for progression from prophase into the meiotic divisions as the most downstream component of the recombination checkpoint (Hochwagen and Amon 2006). The cells in this experiment are blocked in late prophase at a stage when SC assembly, once achieved, should be maintained. Under these conditions, βE-treated, γ-irradiated cells assemble superior levels and quality of SC compared to non-arrested conditions. 49% of these cells assemble Zip1 on chromosomes, as opposed to only 10% in irradiated cells without Rec8 and 7% in non-irradiated cells with Rec8 induced (Figure 8C). We found that these SC tracts were dependent on the presence of stable Rec8, as isogenic cells that instead express a βE-inducible unstable Rec8 version that is rapidly degraded, achieve SC assembly at much lower levels than those with wild-type Rec8 induced (Figure 8D). Even in this case, however, some SC (15%) can be formed, and this level is dependent again on both Rec8 expression and DSBs (Figure 8D).

Figure 8: Post-replicative Rec8 is sufficient for SC assembly in the presence of DSBs

(A) This is a schematic of the experimental scheme used in parts (B) - (E). *rec8::pGAL1-REC8-3HA spo11Δ GAL4-ER* cells are induced to sporulate, allowed 4.5 hours to complete DNA replication, then treated with 1μM β-Estradiol. Cells are allowed to sporulate for 1.5 hours, then γ-irradiated with 20KRad to induce DSBs. Cells continue sporulation until 9 hours, when they are harvested and assayed for α-Zip1 and α-HA staining. A sample is also taken at 6.5 hours to assay for DSBs by α-Rad51 staining.

(B) Cells of the genotype described in (A) were induced to sporulate and treated as described in (A). At 9 hours, cells with the indicated treatments were harvested and chromosome spreads were assayed for Zip1 staining into the categories shown in Figure 1A. 100 mononucleate cells were counted per strain per timepoint.

(C) *rec8::pGAL1-REC8-3HA spo11Δ GAL4-ER ndt80Δ* cells were induced to sporulate and treated as described in (A). At 9 hours, cells with the indicated treatments were harvested and chromosome spreads were assayed for Zip1 staining into the categories shown in Figure 1A. 100 mononucleate cells were counted per strain per timepoint.

(D) *rec8::pGAL1-REC8-3HA-degron spo11Δ GAL4-ER* cells were induced to sporulate and treated as described in (A). At 9 hours, cells with the indicated treatments were harvested and chromosome spreads were assayed for Zip1 staining into the categories shown in Figure 1A. 100 mononucleate cells were counted per strain per timepoint.

(E) *rec8::pGAL1-REC8-N-3HA spo11Δ GAL4-ER* cells were induced to sporulate and treated as described in (A). At 9 hours, cells with the indicated treatments were harvested and chromosome spreads were assayed for Zip1 staining into the categories shown in Figure 1A. 100 mononucleate cells were counted per strain per timepoint.

(F) These are examples of Rec8 and Rad51 staining in cells treated as described in (A). At 6.5 hours, cells were harvested and chromosome spreads were stained for Rec8, Rad51 and DNA. α-HA is shown in green, α-Rad51 is shown in red, and DNA is shown in blue.

Figure 8

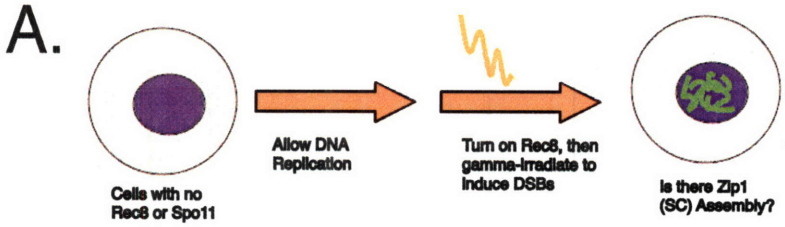
A.
Cells with no Rec8 or Spo11
Allow DNA Replication
Turn on Rec8, then gamma-irradiate to induce DSBs
Is there Zip1 (SC) Assembly?

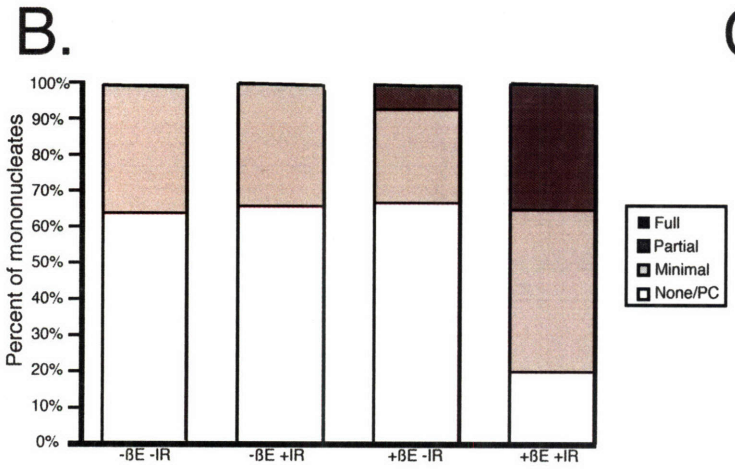
B.
Percent of mononucleates
100%
90%
80%
70%
60%
50%
40%
30%
20%
10%
0%
-βE -IR
-βE +IR
+βE -IR
+βE +IR
Full
Partial
Minimal
None/PC

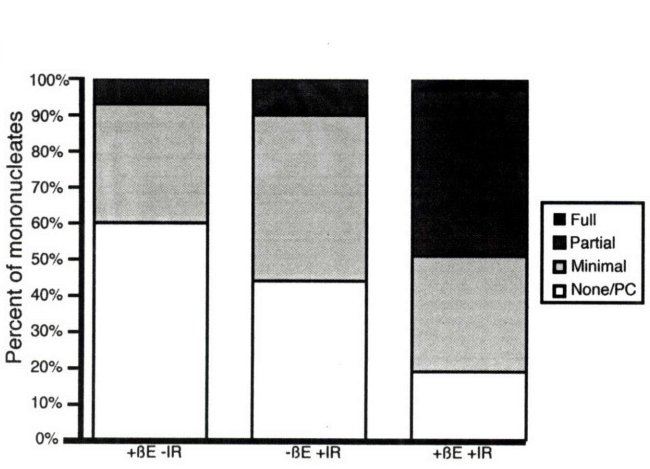
C.
Percent of mononucleates
100%
90%
80%
70%
60%
50%
40%
30%
20%
10%
0%
+βE -IR
-βE +IR
+βE +IR
Full
Partial
Minimal
None/PC

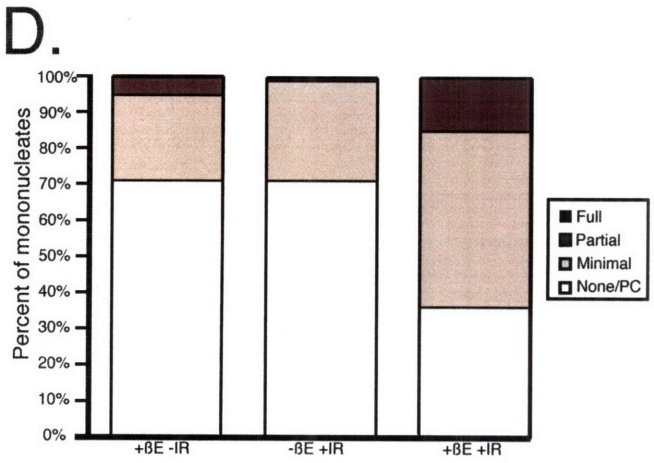
D.
Percent of mononucleates
100%
90%
80%
70%
60%
50%
40%
30%
20%
10%
0%
+βE -IR
-βE +IR
+βE +IR
Full
Partial
Minimal
None/PC

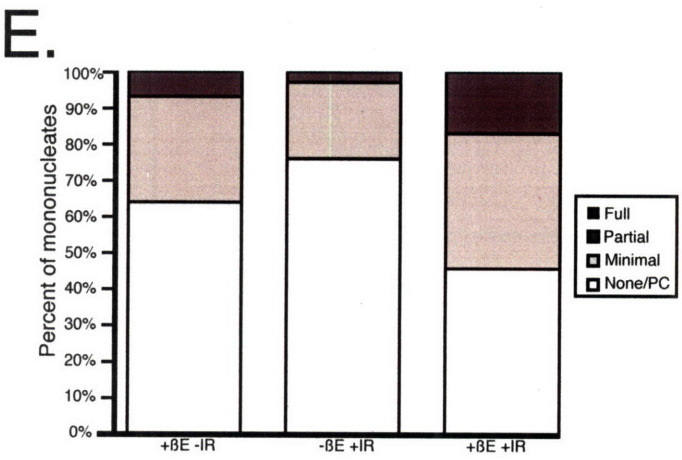
E.
Percent of mononucleates
100%
90%
80%
70%
60%
50%
40%
30%
20%
10%
0%
+βE -IR
-βE +IR
+βE +IR
Full
Partial
Minimal
None/PC

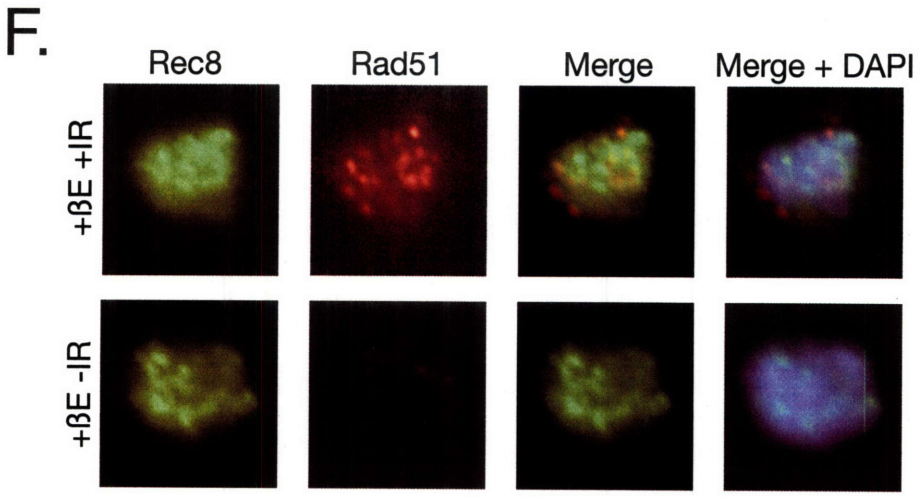
F.
Rec8
Rad51
Merge
Merge + DAPI
+βE +IR
+βE -IR

Discusssion:

Rec8 promotes SC assembly in a manner independent of DNA replication

We have investigated the role that the meiotic cohesin Rec8 plays in prophase. We have found that Rec8 promotes synaptonemal complex (SC) formation in a manner that is independent of DNA replication. This is a surprising result, as DNA replication has been shown to be required for generating cohesive function of the cohesin complex (Forsburg 2002; Uhlmann 2003). It is also surprising that a complex structure such as the SC can assemble normally in the absence of sister chromatids. We and others find that the ability to properly assemble an SC is dependent specifically on Rec8 (Klein, Mahr et al. 1999), as its mitotic counterpart Scc1 cannot support SC assembly when expressed in meiosis. We also find that Rec8 promotes SC assembly in a manner that is independent of its cleavage, as an uncleavable version of Rec8 can fully support SC assembly. Despite these notable different requirements for Rec8's cohesive and SC functions, we find that the fellow cohesin complex member, Scc3, is also needed for SC assembly, suggesting strongly that Rec8 acts as part of the cohesin complex for both functions identified.

Rec8 phosphorylation contributes to SC assembly

We further investigated the role of Rec8 phosphorylation in prophase Rec8 function. The phospho-mutant allele, *rec8-6A* shows separate effects on Rec8's

functions. *rec8-6A* cells are capable of holding sister chromatids together, as evidenced by the normal metaphase I in these cells, but the cells are delayed in exit from prophase and show a correlative defect in Zip1 assembly compared to wild-type cells. We find that *rec8-6A* cells do not exhibit a recombination defect, though it is possible that such a defect exists, but is below the threshold of detection of our assay. However, the fact that deletion of the "SC checkpoint" component *PCH2* rescues the prophase delay seen in *rec8-6A* cells, argues that the defect in prophase progression in these cells may, in fact, be due entirely to the importance of Rec8 to SC assembly.

Examination of *rec8-29A* similarly shows an SC assembly defect, but also a defect in recombination progression similar to that seen in *rec8Δ* cells, despite the previously-demonstrated presence of apparently stable, chromatin-associated Rec8-29A protein (Brar, Kiburz et al. 2006). These data presents the possibility that Rec8 and its phosphorylation is directly important for recombination, SC, *and* its cohesive function (discussed in Brar 2006). Another possibility, and the one that we favor, is that Rec8 phosphorylation is primarily important for SC assembly in prophase, and that sufficiently large defects in SC structure result in recombination defects. Thus, we suggest that the recombination defect seen in *rec8-29A* cells is an indirect consequence of the importance of SC for proper recombination.

In either case, the Rec8 phosphosite-mutants that we investigated are defective in SC assembly and prophase progression. We show that this phosphorylation is not dependent on Cdc5, despite other important roles for

Cdc5 in prophase. Our attempts to identify the responsible kinase have been unsuccessful thus far. Given the number of *in vivo* phosphosites present on Rec8 and the fact that many site mutants present a prophase progression defect (data not shown), we suspect that multiple kinases may be involved in activating Rec8 for its role in prophase progression.

We recognize that it is possible that Rec8's role in SC assembly is simply extremely sensitive to protein structure and that our Rec8 phosphosite-mutants show prophase defects simply as a result of altered structure. This concern is difficult to address, as no structure has been solved for Rec8. We believe that this is not the case, however, for several reasons. First, we present the *rec8-S521D* phospho-mimetic Rec8 mutant that rescues the prophase exit delay seen in *rec8-S521A* mutants and also rescues the SC defect in this mutant. Further, we find that Rec8 protein mutated on 11 Cdc5-dependent sites (*rec8-psa)* does not exhibit a prophase progression delay or an inability to assemble normal SC. These are the sites of phosphorylation that we know to be dispensible for SC structure, based on the fact that cells depleted for Cdc5 still support normal Zip1 assembly. It seems unlikely that so many other Rec8 site mutants show defects, while this rather large mutant does not if SC assembly depends simply on precise Rec8 structure (data not shown). Finally, the fact that Zip1 assembly is normal in mutants lacking a sister chromatid suggests that SC organization is not inherently dependent on precise chromosome structure and that specific cues, such as phosphorylation, may drive its assembly rather than gross chromosome conformational status.

Rec8 as a regulator of meiotic order and directionality

Why would meiotic cells utilize one protein for several disparate functions? We show that Rec8 is imperative for progression of meiotic cells out of prophase due to its function in SC assembly. Rec8 has been studied primarily for its cohesin function. In conjunction with the cohesin complex, Rec8 holds recombined homologs together at metaphase I until satisfaction of the spindle checkpoint activates specific cleavage of Rec8 along chromosome arms and reductional segregation. Centromeric Rec8 is protected from cleavage, through mechanisms that involve the protein Shugoshin (Sgo1) and Rec8 phosphorylation status. Then, at the metaphase II to anaphase II transition, remaining Rec8 is cleaved and sister chromatids segregate at metaphase II (Marston and Amon 2004).

Rec8 thus provides three independent functions identified thus far. We argue that this is an efficient way for cells to ensure directionality. Rec8 is present as cells replicate to hold together newly formed sister chromatids. Then, once sisters are attached, Rec8 assists in SC formation and prophase progression. This link helps ensure that, under normal conditions, only cells that have replicated can go on to the complicated series of prophase events that result in linked homologs. The presence of Rec8 allows cells to progress to meiotic divisions, at which point arm Rec8 is removed to allow the first meiotic division to occur properly. Rec8 holds sisters together until anaphase II, thus

assuring proper equational segregation at this division. We are unaware of any other structural meiotic protein that is involved in regulating so many meiotic steps. By requiring Rec8 for prophase progression, divisions can only occur in cells with properly attached chromosomes. Further, the cell seems to use Rec8 for multiple functions through regulation at the level of phosphorylation by multiple kinases. It appears from our studies that Rec8 phosphorylation regulates prophase function and the ability to segregate homologs at meiosis I, while keeping sisters attached until meiosis II. Interestingly, Rec8 has also been shown to be important for timely completion of S-phase, though this role has not been well-studied (Cha, Weiner et al. 2000).

REC8 is highly functionally conserved in most meiotic unicellular and multicellular animals, including humans. In mammalian cells, the vast majority of Rec8 cohesin complexes are removed from chromosomes in a cleavage-independent manner prior to the first meiotic division (Sumara, Vorlaufer et al. 2002). It is thought that this eases the burden on Separase, such that meiotic divisions can occur relatively rapidly once initiated. It is unclear, however, why cells would waste so much energy to incorporate extra Rec8 onto chromosome just to remove it shortly afterwards. Mutations in mammalian *REC8* have also been shown to result in prophase defects, indicating likely similar Rec8 prophase function as we observe in budding yeast (Xu, Beasley et al. 2005). Perhaps the extra Rec8 in prophase that is removed independent of its cleavage is used to assist in SC assembly and prophase progression. Once cells have properly assembled SC, this extra population of Rec8 can be removed to allow

more synchronous metaphase to anaphase transitions during the meiotic divisions.

Our findings indicate that the prophase function of Rec8 is significantly more sensitive to perturbation that Rec8's later cohesin roles. For example, *rec8-29A* associates with chromosomes in patterns and at levels that are comparable to wild-type cells, and sister chromatids do not separate prematurely (data not shown), but these cells are exceedingly slow at completing prophase. This observation, that cells require greater Rec8 "function" in prophase than during the divisions, is consistent with a speculative model in which cells could require greater Rec8 levels in mammalian prophase than for subsequent divisions. Weighing against this hypothesis, however, is our observation that yeast cells with only a single copy of *REC8* progress through prophase normally (data not shown). An alternative hypothesis is that the large number of DSBs initiated in prophase requires large amounts of Rec8 to stabilize nearby DNA structure. This is consistent with the observation that mitotic cells recruit cohesins to newly formed DSBs, as well as to other sites in the genome, in response to DSB initiation (Strom, Lindroos et al. 2004; Unal, Arbel-Eden et al. 2004; Unal, Heidinger-Pauli et al. 2007).

The phenomenon of prophase removal of Rec8 has also been recently observed in budding yeast, although to a much lesser extent than that seen in mammalian cells. As mammalian chromosomes are larger than those in yeast, and undergo much greater compaction during prophase, it is possible that extra

Rec8 simply helps these cells hold their broken, uncompacted chromosomes together in early prophase and that this role is unnecessary in yeast.

It is interesting to consider the significance of meiotic prophase in human female gametogenesis. In humans, oocytes are arrested in prophase for decades. This correlates with a female-specific increase in aneuploid and inviable gametes produced with age (Hassold and Hunt 2001; Hunt and Hassold 2002; Hunt and Hassold 2008). It is interesting to consider, then, the importance of stable chromosome structure and cohesion in arrested oocytes. It is likely that greater understanding of Rec8, which functions in both prophase chromosome structure and cohesion, is highly relevant to better understanding of the timely issue of human fertility.

We have shown that the cohesin Rec8 and its phosphorylation are important for meiotic prophase progression. Rec8 allows proper assembly of Zip1 to form transverse elements, completing SC formation. We find that the role of Rec8 in SC formation is independent of DNA replication and Rec8 cleavage, and that we can generate a pool of Rec8 that is prophase-functional in a DSB-dependent manner.

Materials and Methods:

Strains and plasmids: All strains described are of the SK1 background of *Saccharomyces cerevisiae.* Deletions have all been performed by one-step gene replacement as described in (Longtine, McKenzie et al. 1998). Meiotic depletions are achieved by one-step promoter replacement as described in (Lee and Amon 2003; Hochwagen, Tham et al. 2005). Rec-N is described in (Buonomo, Clyne et al. 2000). Unstable Rec8 was constructed using plasmid AA624, by fusing Rec8 with UBI4 with the first ubiquitin separated by a Proline to prevent cotranslational cleavage. Estrogen-inducible Rec8 was constructed as used in (Carlile and Amon 2008). Rec8 phosphomutants are described in (Brar, Kiburz et al. 2006), except *rec8-S521A* and *rec8-S521D,* which were constructed with site-directed mutagenesis using Stratagene Quikchange kit and plasmid AA498.

Synchronous meiosis: Cells were grown to saturation in YPD (YEP + 2% glucose) for 24 hours, diluted into YPA (YEP + 2% KAc) at OD_{600} = 0.3 and grown overnight. Cells were then washed with water and resuspended in SPO medium (0.3% KAc [pH = 7.0]) at OD_{600} = 1.9 at 30°C to induce sporulation.

Irradiation: Irradiation was performed using 1 minute exposures on a Gammacell 220E Cesium irradiator to yield 20 Krad.

Southern blot analysis: Southern blot analysis was conducted as described by (Hunter and Kleckner 2001). Blots were quantified using ImageQuant software (Amersham Biosciences).

Meiotic spreads and immunofluorescence: Chromosome spreads and immunofluorescence were performed as described in (Marston, Lee et al. 2003) Rad51 was visualized with the (y-180) rabbit IgG (Santa Cruz) at 1:200 dilution. Zip1 was visualized with a rabbit antibody that was a generous gift of S. Roeder and F. Klein at 1:200 dilution. Hop1 was visualized with a rabbit antibody that was a generous gift of S. Roeder at 1:200 dilution. Rec8-HA was visualized with an HA.11 (16B12) mouse antibody (Covance) at 1:200 dilution.

References:

Brar, G. A., B. M. Kiburz, et al. (2006). "Rec8 phosphorylation and recombination promote the step-wise loss of cohesins in meiosis." Nature **441**(7092): 532-6.

Buonomo, S. B., R. K. Clyne, et al. (2000). "Disjunction of homologous chromosomes in meiosis I depends on proteolytic cleavage of the meiotic cohesin Rec8 by separin." Cell **103**(3): 387-98.

Carlile, T. M. and A. Amon (2008). "Meiosis I is established through division-specific translational control of a cyclin." Cell **133**(2): 280-91.

Cha, R. S., B. M. Weiner, et al. (2000). "Progression of meiotic DNA replication is modulated by interchromosomal interaction proteins, negatively by Spo11p and positively by Rec8p." Genes Dev **14**(4): 493-503.

Clyne, R. K., V. L. Katis, et al. (2003). "Polo-like kinase Cdc5 promotes chiasmata formation and cosegregation of sister centromeres at meiosis I." Nat Cell Biol **5**(5): 480-5.

Forsburg, S. L. (2002). "Only connect: linking meiotic DNA replication to chromosome dynamics." Mol Cell **9**(4): 703-11.

Hassold, T. and P. Hunt (2001). "To err (meiotically) is human: the genesis of human aneuploidy." Nat Rev Genet **2**(4): 280-91.

Hochwagen, A. and A. Amon (2006). "Checking your breaks: surveillance mechanisms of meiotic recombination." Curr Biol **16**(6): R217-28.

Hochwagen, A., W. H. Tham, et al. (2005). "The FK506 binding protein Fpr3 counteracts protein phosphatase 1 to maintain meiotic recombination checkpoint activity." Cell **122**(6): 861-73.

Hunt, P. A. and T. J. Hassold (2002). "Sex matters in meiosis." Science **296**(5576): 2181-3.

Hunt, P. A. and T. J. Hassold (2008). "Human female meiosis: what makes a good egg go bad?" Trends Genet **24**(2): 86-93.

Hunter, N. and N. Kleckner (2001). "The single-end invasion: an asymmetric intermediate at the double-strand break to double-holliday junction transition of meiotic recombination." Cell **106**(1): 59-70.

Ivanov, D., A. Schleiffer, et al. (2002). "Eco1 is a novel acetyltransferase that can acetylate proteins involved in cohesion." Curr Biol **12**(4): 323-8.

Katis, V. L., J. Matos, et al. (2004). "Spo13 facilitates monopolin recruitment to kinetochores and regulates maintenance of centromeric cohesion during yeast meiosis." Curr Biol **14**(24): 2183-96.

Keeney, S. and M. J. Neale (2006). "Initiation of meiotic recombination by formation of DNA double-strand breaks: mechanism and regulation." Biochem Soc Trans **34**(Pt 4): 523-5.

Kitajima, T. S., S. A. Kawashima, et al. (2004). "The conserved kinetochore protein shugoshin protects centromeric cohesion during meiosis." Nature **427**(6974): 510-7.

Klein, F., P. Mahr, et al. (1999). "A central role for cohesins in sister chromatid cohesion, formation of axial elements, and recombination during yeast meiosis." Cell **98**(1): 91-103.

Lee, B. and A. Amon (2001). "Meiosis: how to create a specialized cell cycle." Curr Opin Cell Biol **13**(6): 770-7.

Lee, B. H. and A. Amon (2003). "Role of Polo-like kinase CDC5 in programming meiosis I chromosome segregation." Science **300**(5618): 482-6.

Longtine, M. S., A. McKenzie, 3rd, et al. (1998). "Additional modules for versatile and economical PCR-based gene deletion and modification in Saccharomyces cerevisiae." Yeast **14**(10): 953-61.

Marston, A. L. and A. Amon (2004). "Meiosis: cell-cycle controls shuffle and deal." Nat Rev Mol Cell Biol **5**(12): 983-97.

Marston, A. L., B. H. Lee, et al. (2003). "The Cdc14 phosphatase and the FEAR network control meiotic spindle disassembly and chromosome segregation." Dev Cell **4**(5): 711-26.

Marston, A. L., W. H. Tham, et al. (2004). "A genome-wide screen identifies genes required for centromeric cohesion." Science **303**(5662): 1367-70.

Mitra, N. and G. S. Roeder (2007). "A novel nonnull ZIP1 allele triggers meiotic arrest with synapsed chromosomes in Saccharomyces cerevisiae." Genetics **176**(2): 773-87.

Page, S. L. and R. S. Hawley (2004). "The genetics and molecular biology of the synaptonemal complex." Annu Rev Cell Dev Biol **20**: 525-58.

Rabitsch, K. P., J. Gregan, et al. (2004). "Two fission yeast homologs of Drosophila Mei-S332 are required for chromosome segregation during meiosis I and II." Curr Biol **14**(4): 287-301.

Revenkova, E. and R. Jessberger (2006). "Shaping meiotic prophase chromosomes: cohesins and synaptonemal complex proteins." Chromosoma **115**(3): 235-40.

San-Segundo, P. A. and G. S. Roeder (1999). "Pch2 links chromatin silencing to meiotic checkpoint control." Cell **97**(3): 313-24.

Shonn, M. A., R. McCarroll, et al. (2000). "Requirement of the spindle checkpoint for proper chromosome segregation in budding yeast meiosis." Science **289**(5477): 300-3.

Smith, K. N., A. Penkner, et al. (2001). "B-type cyclins CLB5 and CLB6 control the initiation of recombination and synaptonemal complex formation in yeast meiosis." Curr Biol **11**(2): 88-97.

Storlazzi, A., S. Tesse, et al. (2008). "Coupling meiotic chromosome axis integrity to recombination." Genes Dev **22**(6): 796-809.

Strom, L., H. B. Lindroos, et al. (2004). "Postreplicative recruitment of cohesin to double-strand breaks is required for DNA repair." Mol Cell **16**(6): 1003-15.

Sumara, I., E. Vorlaufer, et al. (2002). "The dissociation of cohesin from chromosomes in prophase is regulated by Polo-like kinase." Mol Cell **9**(3): 515-25.

Uhlmann, F. (2003). "Chromosome cohesion and separation: from men and molecules." Curr Biol **13**(3): R104-14.

Unal, E., A. Arbel-Eden, et al. (2004). "DNA damage response pathway uses histone modification to assemble a double-strand break-specific cohesin domain." Mol Cell **16**(6): 991-1002.

Unal, E., J. M. Heidinger-Pauli, et al. (2007). "DNA double-strand breaks trigger genome-wide sister-chromatid cohesion through Eco1 (Ctf7)." Science **317**(5835): 245-8.

Whitby, M. C. (2005). "Making crossovers during meiosis." Biochem Soc Trans **33**(Pt 6): 1451-5.

Xu, H., M. D. Beasley, et al. (2005). "Absence of mouse REC8 cohesin promotes synapsis of sister chromatids in meiosis." Dev Cell **8**(6): 949-61.

Zickler, D. and N. Kleckner (1998). "The leptotene-zygotene transition of meiosis." Annu Rev Genet **32**: 619-97.

Chapter 4:

Examination of the Mechanism of Meiotic Pairing

Gloria A. Brar, Andreas Hochwagen, Angelika Amon

Abstract

The defining feature of meiosis is the creation of haploid gametes from a diploid precursor cell. Achievement of this cellular goal requires a series of events including segregation of homologs in a reductional division at Meiosis I and the absence of a second DNA replication phase between Meiosis I and Meiosis II (Marston and Amon 2004). Reductional segregation is unique to meiosis and depends on the alignment of homologs in prophase through a poorly-understood process called pairing. This chapter aims to increase understanding of pairing mechanism through the examination of its relationship to other meiotic processes and basic observation of chromosome pairing in live cells. Early pairing stages depend on ATP and actin filaments, but not the cytological structure known as the bouquet. Pairing is influenced by SC components including Hop1, Zip1 and the meiotic cohesin Rec8, but does not depend on DNA replication or the presence of a sister chromatid. Pairing depends heavily on the presence of DSBs, though requires only a fraction of the normal number of DSBs generated in early prophase. These studies help clarify the principles behind meiotic pairing and provide a framework for delving into the details of pairing mechanism.

Introduction

The importance of pairing to meiotic segregation

The meiotic cell cycle is a specialized set of nuclear divisions in which one DNA replication phase is followed by two chromosome segregation phases. The second meiotic division is similar to mitosis in that sister chromatids are segregated apart. In contrast, during the first meiotic division homologous chromosomes (homologs) segregate away from each other. This unique feature of the meiotic cell cycle is conserved among eukaryotes and requires several specializations including the pairing of homologous chromosomes in preparation for recombination. Chiasmata, the physical manifestations of crossover recombination, along with distal sister chromatid cohesion, provide the tension necessary to align homologs at the metaphase I spindle and allow their segregation to opposite poles at anaphase I. The proper completion of meiosis I is necessary for balanced gamete formation (Lee and Amon 2001; Marston and Amon 2004).

Pairing refers to the alignment of homologous chromosomes (Roeder 1995; Yamamoto and Hiraoka 2001; McKee 2004). This phenomenon is distinct from the phenomenon of synapsis, which generally follows meiotic homologous pairing and describes the zipping together of chromosomes by a tripartite proteinaceous structure called the synaptonemal complex (SC). Although synapsis is generally homologous, it is not restricted to homologs, and in certain mutant backgrounds may be entirely non-homologous (Zickler and Kleckner

1998). Both pairing and synapsis occur during the meiotic cell cycle, but pairing is by definition homologous and thus plays a more essential role in proper meiosis I homolog segregation.

Early meiotic events

Budding yeast cells can be induced to enter the meiotic cell cycle from vegetative G1 phase by exposure to low nitrogen and carbon levels (Marston and Amon 2004). A number of factors including S-phase cyclins Clb5 and Clb6, along with the pre-Replicative Complex (pre-RC), act to initiate pre-meiotic DNA replication (Forsburg 2002). Replication is followed shortly by the initiation of early meiotic prophase events including homolog pairing and DNA double-strand break (DSB) formation. DSBs are catalyzed by the topoisomerase Spo11 as the first step of homologous recombination (Keeney and Neale 2006). Recombination and SC formation follow shortly and are generally complete by the end of the pachytene stage of mid-prophase. At this point, a recombination checkpoint, mediated through the transcription factor Ndt80, monitors the presence of recombination intermediates. If none are present, Ndt80 is free to activate transcription of genes required for progression into the meiotic divisions (Hochwagen and Amon 2006).

Normal pairing behavior and introduction of a standard pairing assay

Homologous chromosomes begin the meiotic cell cycle at an intermediate level of pairing that is thought to be based on the arrangement of chromosomes in

the somatic nucleus. Pairing then decreases during meiotic DNA replication, is regained shortly afterwards in the leptotene stage of prophase (see Chapter 1, Figure 3 for a summary of prophase stages) and peaks at pachytene (Weiner and Kleckner 1994; McKee 2004). The process of homolog pairing is not well-understood, largely due to technical constraints of experimental approaches available until recently.

To study pairing, I am using an *in vivo* GFP-tagging system in the budding yeast *S. cerevisiae* (Figure 1). In this assay, a Tet operator (TetO) array with approximately 250 TetO repeats is inserted at homologous sites in a diploid cell. In this same cell, a Tet repressor (TetR)-green fluorescent protein (GFP) fusion is expressed. *In vivo,* the TetR-GFP fusion protein binds the TetO arrays and the two tagged sites are visible by microscopy as green dots (Straight, Belmont et al. 1996; Michaelis, Ciosk et al. 1997). If the tagged chromosomes are closely juxtaposed, only one dot will be discernable due to the proximity of the two GFP signals. In contrast, if the homologs are not closely juxtaposed, two distinct GFP dots will be distinguishable. By assessing the ratio of one versus two dots visible at a particular time, one can determine the level of pairing at that time point.

As a control for non-specific clustering of arrays, a strain with TetO arrays at non-homologous chromosomal sites is also used in these experiments. The traditional pairing assay involves cell lysis and surface spreading of nuclei followed by fluorescence in situ hybridization (FISH) (Weiner and Kleckner 1994). While FISH allows easy examination of a number of different chromosomal sites,

spreads can disrupt loose chromosomal associations. Additionally, unlike the GFP dot system, FISH does not allow for real-time evaluation of pairing dynamics. For these reasons, the GFP dot assay may be a better system by which to analyze pairing. This assay has caveats as well, however, including its dependence on the resolution of light microscopy and some inherent instability of the tandem TetO arrays.

The locations of the GFP dots used in this chapter are shown in Figure 2. I have utilized strains with Tet Operator arrays at five different homologous sites, including: the *LEU2* locus (22 Kb from the centromere of Chromosome 3, or *CEN3*), the *LYS2* locus (232 KB from *CEN2*), the *URA3* locus (36 Kb from *CEN5*), *CEN5,* and 30 Kb from the telomere of Chromosome 5, or *TEL5*. This set of strains allows for the comparison and contrast between different types of chromosomal loci to better understand the rules that underly homolog pairing. When not specifically discussed, experiments are performed with *LYS2*-integrated Tet Operator arrays mid-arm on Chromosome 2, as this is likely the site most representative of the genome as the whole.

Using these strains, I have determined that DSBs are essential for proper pairing, that Synaptonemal Complex and cohesin components contribute to proper pairing, and that actin filaments promote pairing. I have found that DNA replication and telomere clustering are not important for proper pairing to occur. I have also found some variations in pairing behavior based on chromosomal location, although most chromosomal sites appear to pair with similar dynamics and dependencies.

Figure 1: An assay to monitor pairing in live cells

This figure represents the pairing assay used in this chapter. Homologous chromosomal loci are tagged with tandem Tet Operator (TetO) sequences. These cells also carry a fusion of Green Fluorescent Protein (GFP) and the Tet Repressor (TetR). These constructs result in a green dot visible under fluorescent microscopy at the site of TetO insertion. When homologous chromosomes are paired, GFP dots are too close to distinguish by light microscopy and appear as a single GFP dot. When homologs are unpaired, two GFP dots are visible by fluorescent microscopy. The standard pairing assay utilized here requires scoring 100 cells per strain per timepoint for the presence of one versus two GFP dots. Examples of cells with one versus two GFP dots are shown at the right of the figure. Only one pair of homologs (represented by black lines within the cell) is shown here for simplicity. GFP dots are represented by a green square on the black line. Frequently strains described in this chapter are deleted for *NDT80,* the transcription factor responsible for progression out of prophase. This deletion arrests cells at the pachytene stage of prophase, at the point of maximal pairing to increase synchrony and ease comparison of various strains.

Figure 1

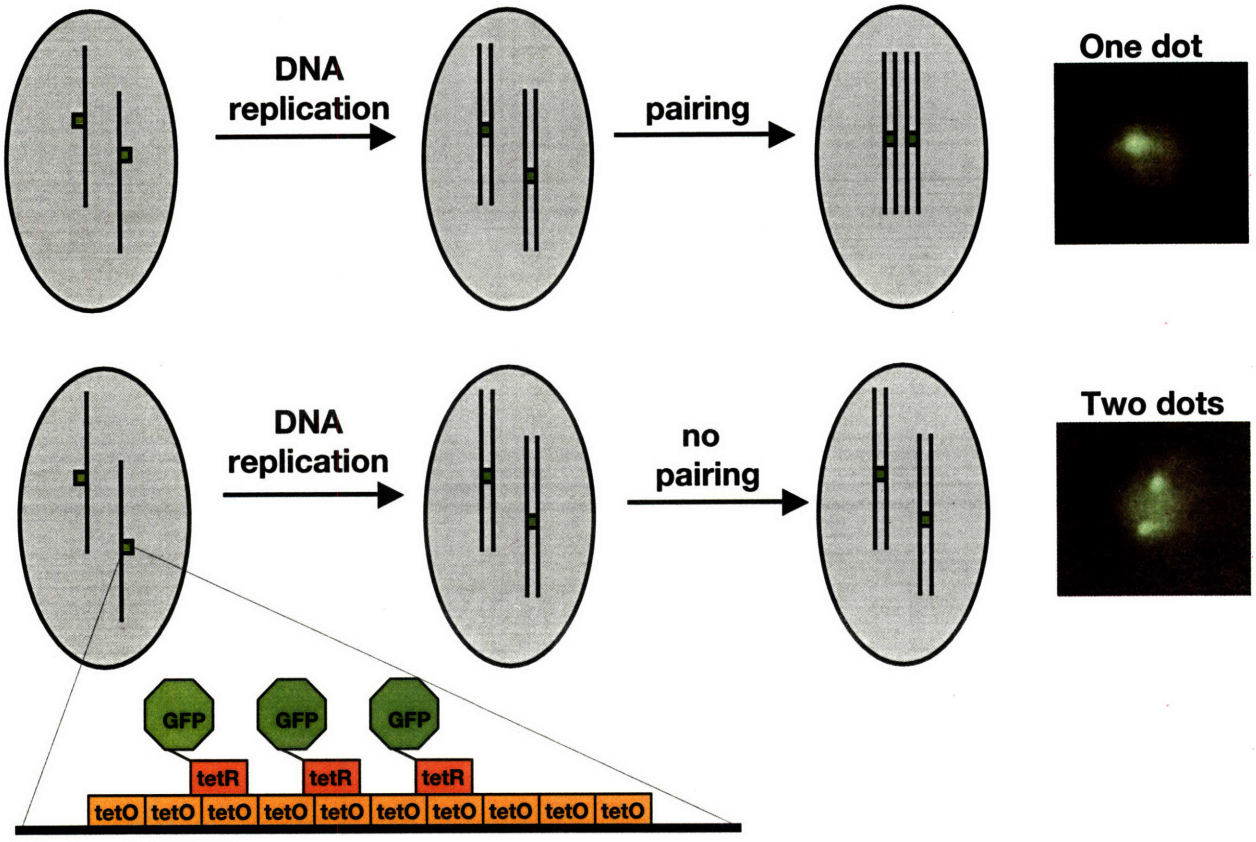
DNA
replication
pairing
One dot
DNA
replication
no
pairing
Two dots
GFP
GFP
GFP
tetR
tetR
tetR
tetO
tetO
tetO
tetO
tetO
tetO
tetO
tetO
tetO
tetO

Figure 2: Loci assayed for pairing in this study
This figure is a schematic of the yeast genome, with the five loci assayed for pairing in these studies denoted by green stars. The 16 yeast chromosomes are represented by horizontal blue lines with circles marking their centromeres. Chromosome 1 appears at the top of the figure, and the others are in numerical order, with 16 at the bottom of the figure. For these studies, tandem TetO arrays are inserted at the following sites:

-*LYS2,* mid-arm on chromosome 2
-*LEU2,* 22 Kb from the centromere of chromosome 3
-*URA3,* 36 Kb from the centromere of chromosome 5
-*CEN5,* adjacent to the centromere of chromosome 5
-*TEL5,* adjacent to the telomere of chromosome 5

Figure 2

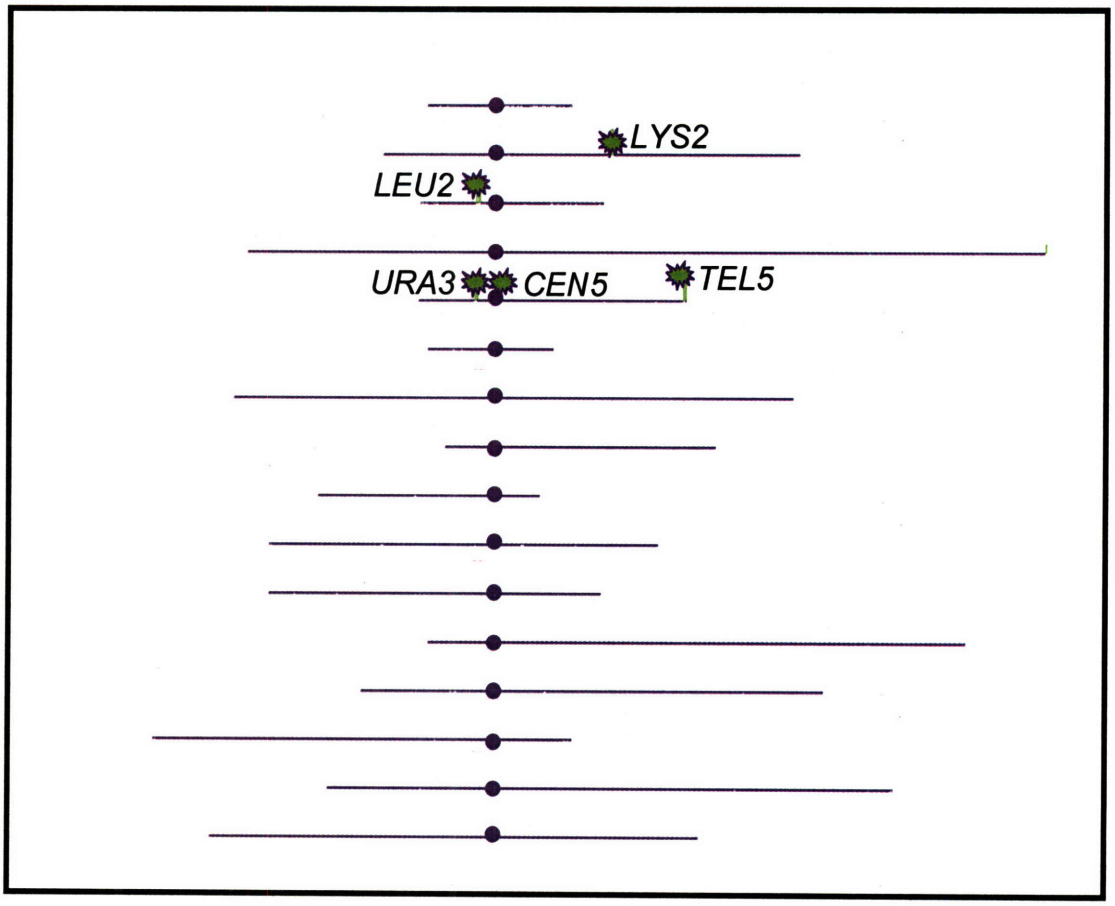

Results

Pairing at various chromosomal loci

Early meiotic cells display some residual somatic pairing which decreases coincident with DNA replication. By population analysis, pairing increases as cells progress through prophase, reaching a maximum as cells reach the pachytene stage in late prophase. As meiosis displays inherent asynchrony by population analysis, however, it can be difficult to compare pairing dynamics between experiments and different mutant backgrounds. To more accurately determine the ability of a given population of cells to pair, I thus examined pairing at five loci using the strains deleted for *NDT80* to arrest cells in pachytene, the stage of maximal homolog pairing. These data are shown in Figure 3. The pattern is essentially as described above at each locus, with chromosomes showing a high level of somatic clustering, then dispersal and reassociation specifically of homologous sites as cells progress into prophase. Non-homologous GFP dot controls show somatic clustering as cells enter meiosis, but progressive disassociation of GFP dots as cells meiose. Figure 3A compares strains with various centromere proximal GFP dots. The timing of pairing appears roughly similar in the three strains, but the *LEU2* locus undergoes significantly less dispersal of homologous sites early in meiosis. It is not clear why this is the case. It is interesting to note, however, that the *LEU2* locus is the site of one of the most active DSB hotspots in the *S. cerevisiae* genome (Storlazzi, Xu et al. 1995; Blitzblau, Bell et al. 2007). It is possible that

this distinction somehow alters the pairing dynamics at this site. Figure 3B shows three different loci on Chromosome 5. Again, all three sites show similar patterns of pairing, indicating no gross pairing difference between centromeres, telomeres and centromere-proximal arm loci. This is, however, a population assay, so it is possible that one site consistently pairs before another, but that chromosomal "zipping" occurs too quickly to distinguish with this experiment setup.

Figure 3: Pairing progression at various chromosomal loci

(A) Wild-type cells deleted for *NDT80* were induced to sporulate. The three blue lines represent tandem TetO arrays inserted at three different loci, *URA3* (dark blue circles), *TEL5* (bright blue circles) and *CEN5* (light blue circles). Note that all three strains are marked on chromosome 5. At the indicated times, samples were taken and assayed for pairing. 100 cells were counted per strain per timepoint. Non-homologous array strains are shown by open circles as a control for array clustering.

(B) Wild-type cells deleted for *NDT80* were induced to sporulate. The three blue lines represent tandem TetO arrays inserted at three different loci, *URA3* (dark blue circles), *LEU2* (darkest blue circles) and *CEN5* (light blue circles). Note that all three strains are marked at centromere-proximal sites. At the indicated times, samples were taken and assayed for pairing. 100 cells were counted per strain per timepoint. Non-homologous array strains are shown by open circles as a control for array clustering. Note that (A) and (B) are data from the same experiment.

Figure 3

A.

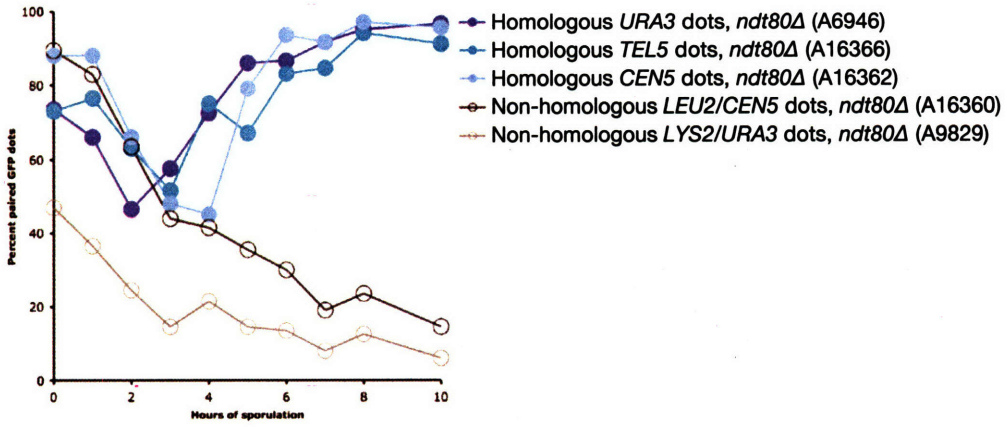
Percent paired GFP dots
Hours of sporulation
Homologous URA3 dots, ndt80Δ (A6946)
Homologous TEL5 dots, ndt80Δ (A16366)
Homologous CEN5 dots, ndt80Δ (A16362)
Non-homologous LEU2/CEN5 dots, ndt80Δ (A16360)
Non-homologous LYS2/URA3 dots, ndt80Δ (A9829)

B.

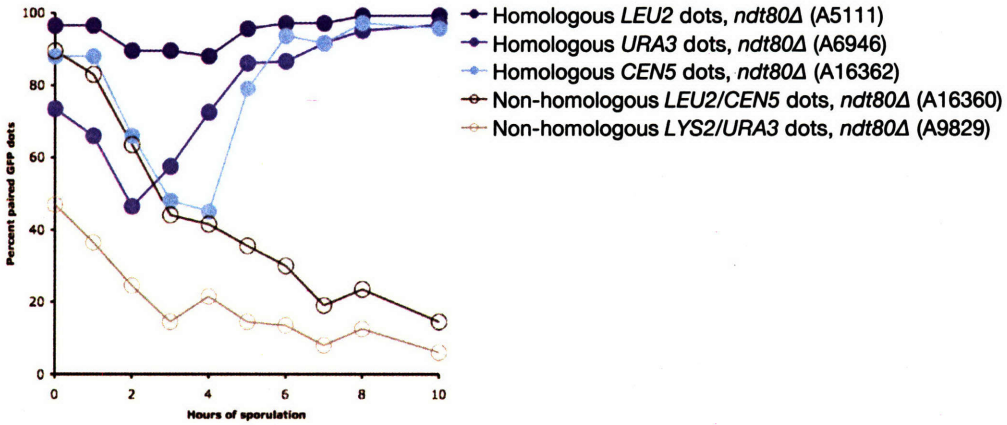
Percent paired GFP dots
Hours of sporulation
Homologous LEU2 dots, ndt80Δ (A5111)
Homologous URA3 dots, ndt80Δ (A6946)
Homologous CEN5 dots, ndt80Δ (A16362)
Non-homologous LEU2/CEN5 dots, ndt80Δ (A16360)
Non-homologous LYS2/URA3 dots, ndt80Δ (A9829)

The role of ATP in pairing

To begin to dissect the pairing mechanism, I wished to determine which basic cellular and meiotic processes might contribute to homolog pairing. I first examined the effects of ATP and cytoskeletal elements on pairing using the standard live-cell GFP dot assay discussed above. To deplete cellular ATP stores, I treated *LYS2* GFP dot-marked cells with two concentrations of the oxidative phosphorylation decoupler dinitrophenol (DNP) (Figure 4A). Untreated cells show the standard pattern of homologous pairing, while treatment of cells with 100μM DNP at 1 hour in sporulation medium led to a delay of 1 hour in pairing. Treatment at 1 hour in sporulation medium with 1mM DNP caused an even greater delay in chromosome pairing. Treatment with 1mM DNP at 4.5 hours in sporulation medium, however, led to little defect in pairing, indicating that initial pairing stages are more sensitive to cellular ATP status.

The role of actin filaments in pairing

It is not clear why ATP might be important for normal pairing, though it seems reasonable that cytoskeletal dynamics could be needed for the dramatic chromosome movements required to sort chromosomes into bivalent pairs. This movement is most dramatic in *Schizosaccharomyces Pombe*, where the prophase nucleus displays "horsetail" movement, with chromosomes anchored together at their telomeres and swept repeatedly across the nuclear length (Chikashige, Tsutsumi et al. 2006). This movement is dependent on cytoskeletal

components and has been shown to promote homolog pairing in fission yeast. Similarly, in budding yeast, microtubules have been shown to be important for pairing as treatment with the microtubule-destabilizing drug benomyl results in a defect in meiotic pairing. Benomyl treatment also caused gross changes in gene expression in meiotic cells, however, making it difficult to determine how directly microtubules are involved in pairing mechanism (Hochwagen, Wrobel et al. 2005). I wished to determine whether actin might contribute to pairing. Towards this end, I treated cells with the inhibitor of actin polymerization, Latrunculin A (Figure 4B, 4C). Pairing in *ndt80Δ* cells marked with GFP dots at the *LYS2* locus shows a significant dependence on actin filaments, with cells treated at 1 hour in sporulation medium with 200μM Latrunculin A show an inability to achieve wild-type levels of pairing seen in vehicle-treated control cells, even by 10 hours in sporulation medium (Figure 4B). Interestingly, actin filament formation appears to be important for early stages of pairing only, as cells treated with Latrunculin A at 4 hours, at a point where most cells are generally in mid-prophase, show no defect in pairing. Additionally, cells treated with Latrunculin A at 8 hours are able to maintain pairing normally, indicating that actin filaments are not required for pairing maintenance. The effects of Latrunculin A were also examined at the centromere-proximal *LEU2* locus with similar results (Figure 4C). Again, cells treated with 200μM Latrunculin A at 1 hour show a severe pairing defect, while cells treated at 4 or 8 hours do not show any significant defect in homolog pairing.

Figure 4: ATP and actin filaments promote pairing
(A) Wild-type cells deleted for *NDT80* and marked with homologous tandem TetO arrays at *LYS2* were induced to sporulate. Cells were treated, as described in the legend, with either vehicle control at 1 hour into (black circles), 100μM dinitrophenol (DNP) at 1 hour (dark gray circles), 1mM DNP at 1 hour (light gray circles), or 1mM DNP at 4.5 hours (green circles). At the indicated times, samples were taken and assayed for pairing. 100 cells were counted per treatment per timepoint.

(B) Wild-type cells deleted for *NDT80* and marked with homologous tandem TetO arrays at *LYS2* were induced to sporulate. Cells were treated, as described in the legend, with either vehicle control at 1 hour (black circles), 200μM latrunculin A (latA) at 1 hour (gray circles), 200μM latA at 4 hours (pink circles) or 200μM latA at 8 hours (red circles). At the indicated times, samples were taken and assayed for pairing. 100 cells were counted per treatment per timepoint.

(C) Wild-type cells deleted for *NDT80* and marked with homologous tandem TetO arrays at *LEU2* were induced to sporulate. Cells were treated, as described in the legend, with either vehicle control at 1 hour (black circles), 200μM latrunculin A (latA) at 1 hour (gray circles), 200μM latA at 4 hours (pink circles) or 200μM latA at 8 hours (red circles). At the indicated times, samples were taken and assayed for pairing. 100 cells were counted per treatment per timepoint.

Figure 4

A.

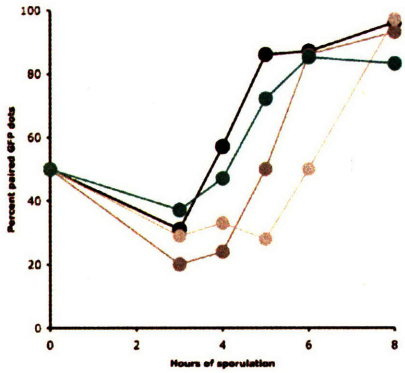

- Homologous *LYS2* dots, *ndt80Δ* (A9828) + 1 hr. vehicle control
- Homologous *LYS2* dots, *ndt80Δ* (A9828) + 1 hr. 100μM DNP
- Homologous *LYS2* dots, *ndt80Δ* (A9828) + 1 hr. 1mM DNP
- Homologous *LYS2* dots, *ndt80Δ* (A9828) + 4.5 hr. 1mM DNP

B.

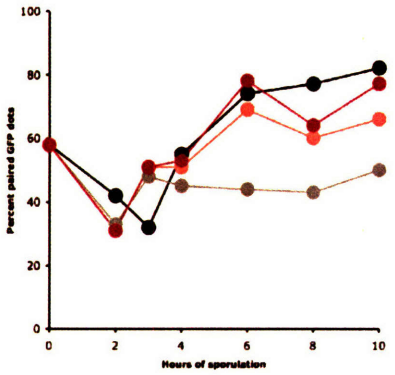

- Homologous *LYS2* dots, *ndt80Δ* (A16144) + 1 hr. vehicle control
- Homologous *LYS2* dots, *ndt80Δ* (A16144) + 1 hr. 200μM latA
- Homologous *LYS2* dots, *ndt80Δ* (A16144) + 4 hr. 200μM latA
- Homologous *LYS2* dots, *ndt80Δ* (A16144) + 8 hr. 200μM latA

C.

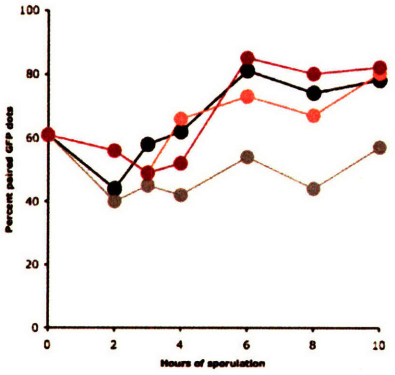

- Homologous *LEU2* dots, *ndt80Δ* (A16428) + 1 hr. vehicle control
- Homologous *LEU2* dots, *ndt80Δ* (A16428) + 1 hr. 200μM latA
- Homologous *LEU2* dots, *ndt80Δ* (A16428) + 4 hr. 200μM latA
- Homologous *LEU2* dots, *ndt80Δ* (A16428) + 8 hr. 200μM latA

Live analysis of pairing dynamics

The apparent roles of ATP, actin and microtubules in pairing suggest the possibility of pairing regulation at the level of chromosome movement. Therefore, I have undertaken some preliminary work on the dynamics of pairing using live cell time-lapse microscopy. I have determined that a given pair of homologous chromosomal loci show rapid and indirect motion with respect to each other during the process of pairing. Successful "locking in" of a pairing interaction is generally preceded by several transient interactions between the sites over a period of 1-2 hours. In agreement with population timecourse assays, no apparent difference in gross pairing movement patterns has been seen between arm, telomere, or centromeric loci. An example of some frames from these movies is shown in Figure 5. Live cell time-lapse microscopy will likely be a powerful tool to dissect pairing movement, but these studies will need to be expanded and combined with mathematical analysis.

Figure 5: Homologous loci exhibit dynamic behavior in the process of pairing. Homologous chromosomes are marked by Tet Operator array inserted at both *LYS2* loci. Cells are imaged by fluorescent time-lapse photography. Distances between GFP dots were determined using Openlab software and are charted above still images from a sample time-lapse movie.

Figure 5

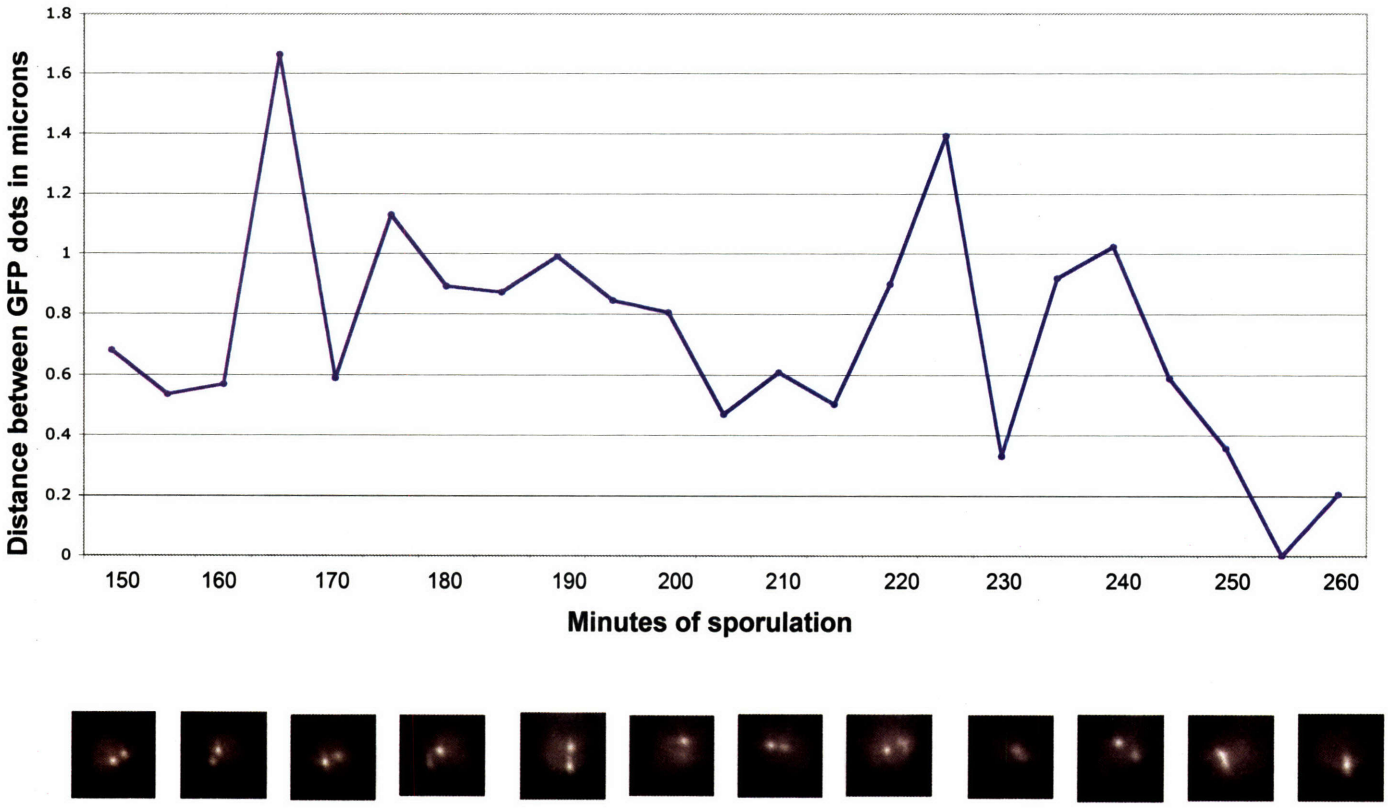
Distance between GFP dots in microns
1.8
1.6
1.4
1.2
1
0.8
0.6
0.4
0.2
0
150
160
170
180
190
200
210
220
230
240
250
260
Minutes of sporulation

Pairing and the bouquet

In somatic cells and early meiotic cells, chromosomes are tethered to the nuclear envelope through their telomeres. These telomeres are clustered together to form a mop-like structure called a "bouquet". The bouquet is a feature of early meiotic cells in many diverse organisms, though its function is not clear (Zickler and Kleckner 1998; Trelles-Sticken, Loidl et al. 1999; Jin, Fuchs et al. 2000). It has been suggested that the bouquet contributes to pairing by setting up a primary level of chromosome organization such that homology searches can occur in two dimensions rather than the three dimensions required for completely randomly positioned chromosomes. I examined the possibility that bouquet formation contributes to homolog pairing by examining homologous *LYS2* GFP dot association in strains deleted for *NDJ1* (Non-disjunction factor 1), a factor shown to be necessary for telomere clustering at the bouquet stage (Rockmill and Roeder 1998; Trelles-Sticken, Dresser et al. 2000). *ndj1Δ LYS2* GFP dot cells show only a mild delay in homolg pairing when compared to wild-type cells. *ndj1Δ* cells with GFP dots at *URA3* (Figure 6B) show a larger pairing defect than those with *LYS2* GFP dots (Figure 6A), but chromosomes are still capable of pairing even in the absence of *NDJ1*, indicating that bouquet formation is not necessary for homolog pairing to occur.

Figure 6: Telomere clustering through bouquet formation does not significantly contribute to pairing
(A) Wild-type (solid blue squares) or *ndj1Δ* (solid red squares) cells carrying homologous tandem TetO arrays at *LYS2* were induced to sporulate. At the indicated times, samples were taken and assayed for pairing. 100 cells were counted per strain per timepoint. Non-homologous array strains are shown by open squares as a control for array clustering.

(B) Wild-type (solid blue squares) or *ndj1Δ* (solid orange squares) cells carrying homologous tandem TetO arrays at *URA3* were induced to sporulate. At the indicated times, samples were taken and assayed for pairing. 100 cells were counted per strain per timepoint. Non-homologous array strains are shown by open squares as a control for array clustering.

Figure 6

A.

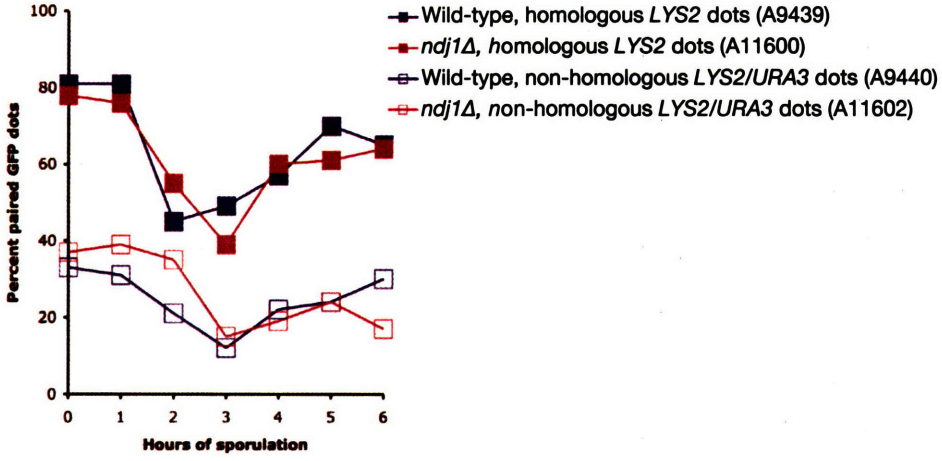
Percent paired GFP dots
Hours of sporulation
Wild-type, homologous LYS2 dots (A9439)
ndj1Δ, homologous LYS2 dots (A11600)
Wild-type, non-homologous LYS2/URA3 dots (A9440)
ndj1Δ, non-homologous LYS2/URA3 dots (A11602)

B.

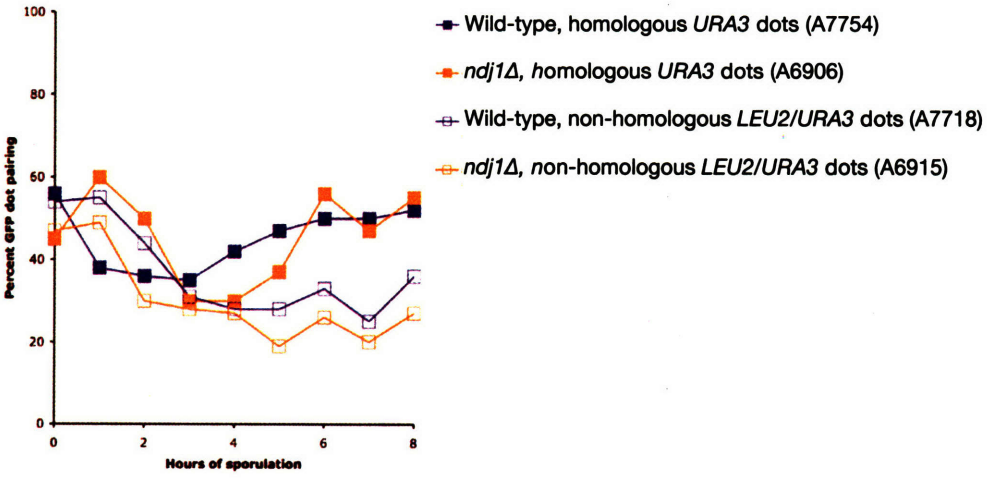
Percent GFP dot pairing
Hours of sporulation
Wild-type, homologous URA3 dots (A7754)
ndj1Δ, homologous URA3 dots (A6906)
Wild-type, non-homologous LEU2/URA3 dots (A7718)
ndj1Δ, non-homologous LEU2/URA3 dots (A6915)

The influence of DSBs on pairing

One process that has been implicated in chromosome pairing is DSB formation, the first step of recombination (Keeney and Neale 2006). It has been suggested that the single-stranded DNA that results from resection of DSBs reiteratively invades dsDNA in a search for homology and that this process is important for pairing (McKee 2004). To assess the importance of DSB formation in pairing, I utilized strains deleted for *SPO11*. Spo11 catalyzes DSBs through a topoisomerase-like mechanism requiring Tyrosine 135 (Diaz, Alcid et al. 2002). To determine the importance of Spo11 protein and its catalytic ativity to pairing, I examined GFP dot association in *spo11Δ* cells as well as *spo11-Y135F* cells, in which Spo11's catalytic Tyrosine is mutated to Phenylalanine, thus rendering it catalytically dead (Figure 7A).

Both *spo11Δ and spo11-Y135F* mutants show severe and equivalent pairing defects at the *LYS2* locus as well as the *URA3* locus in *ndt80Δ* cells, indicating that DSBs are essential to proper homolog pairing. Homologous GFP dot association at late timepoints in *spo11* mutants was not as low as non-homologous GFP dot association, however, suggesting that some basal level of pairing may be independent of DSBs. When *spo11Δ* cells were also deleted for *NDJ1*, they showed no significant further decrease in pairing, although as *spo11* cells are already so severly pairing defective, the assay may not be sensitive enough to detect further defect (Figure 8).

As DSBs appeared to be essential for proper pairing, I wished to further probe the relationship between these two processes. For this purpose, I utilized a series of *spo11* alleles generated by Scott Keeney's lab that are defective in DSB formation (Henderson and Keeney 2004). When examining pairing at the *LYS2* locus in *ndt80Δ* cells, I observed a binary effect on pairing with the series of *spo11* hypomorphs (Figure 7B). In *spo11* cells with approximately 20% or more of the normal level of DSBs, as measured by Southern blot at the *LEU2* locus (Henderson and Keeney 2004), pairing appeared to occur at wild-type levels (Figure 7B). In *spo11* cells with around 20% or fewer of the normal level of DSBs, pairing was severely defective. This effect was less bimodal at *LEU2*, with the same general trend as observed at the *LYS2* locus (Figure 7C). Cells appear to require approximately 40-50 DSBs (20% the normal 200-300 initiated per meiosis (Hochwagen and Amon 2006)) to support normal pairing. Fewer DSBs result in little or no pairing.

Given the significant importance of DSBs to pairing, I wished to determine whether later recombination mutants showed similar defects. Examination of cells deleted for meiotic strand invasion factor *DMC1* revealed a severe defect in homolog pairing in *ndt80Δ* cells with *LEU2* GFP dots (Figure 9A) and *LYS2* GFP dots (Figure 9B), indicating a general importance for strand invasion in the homology search.

Figure 7: DSB formation is required for pairing, but a fraction of wild-type DSBs are sufficient for pairing

(A) All strains shown are deleted for *NDT80*. Wild-type cells with homologous tandem TetO arrays at *LYS2* (solid dark blue circles), wild-type cells with homologous tandem TetO arrays at *URA3* (solid light blue circles), *spo11Δ* cells with homologous tandem TetO arrays at *LYS2* (solid light green circles), *spo11Δ* cells with homologous tandem TetO arrays at *URA3* (solid yellow circles), *spo11-Y135F* cells with homologous tandem TetO arrays at *LYS2* (solid dark green circles), *spo11-Y135F* cells with homologous tandem TetO arrays at *URA3* (solid orange circles), and wild-type cells with non-homologous tandem TetO arrays were induced to sporulate. At the indicated times, samples were taken and assayed for pairing. 200 cells were counted per strain per timepoint.

(B) All strains shown are deleted for *NDT80*. Wild-type cells with homologous tandem TetO arrays at *LYS2* (solid blue circles) and various *spo11* hypomorphic alleles (red, orange and yellow circles) were induced to sporulate. At the indicated times, samples were taken and assayed for pairing. 100 cells were counted per strain per timepoint. Note that each *spo11* allele is described in the figure key, with the percentage of wild-type DSBs noted in bold. Red lines represent strains that make the most DSBs, while yellow represent strains that make the least.

(C) All strains shown are deleted for *NDT80*. Wild-type cells with homologous tandem TetO arrays at *LEU2* (solid blue squares) and various *spo11* hypomorphic alleles (red, orange and yellow squares) were induced to sporulate. At the indicated times, samples were taken and assayed for pairing. 100 cells were counted per strain per timepoint. Note that each *spo11* allele is described in the figure key, with the percentage of wild-type DSBs noted in bold. Red lines represent strains that make the most DSBs, while yellow represent strains that make the least.

Figure 7

A.

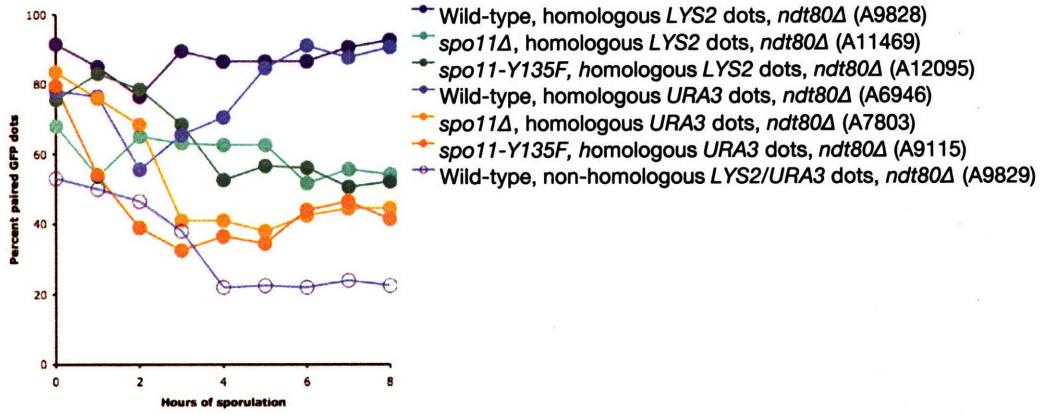
Percent paired GFP dots
Hours of sporulation
Wild-type, homologous LYS2 dots, ndt80Δ (A9828)
spo11Δ, homologous LYS2 dots, ndt80Δ (A11469)
spo11-Y135F, homologous LYS2 dots, ndt80Δ (A12095)
Wild-type, homologous URA3 dots, ndt80Δ (A6946)
spo11Δ, homologous URA3 dots, ndt80Δ (A7803)
spo11-Y135F, homologous URA3 dots, ndt80Δ (A9115)
Wild-type, non-homologous LYS2/URA3 dots, ndt80Δ (A9829)

B.

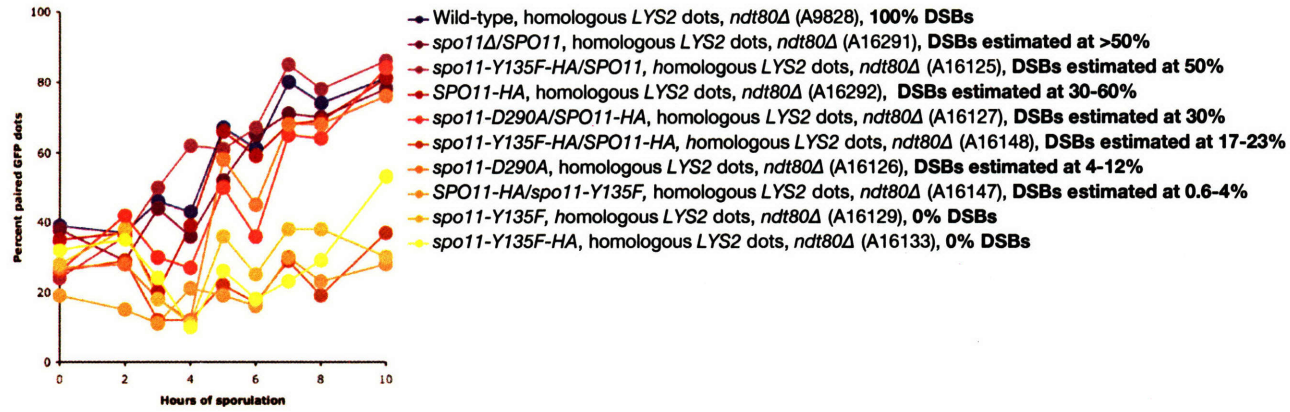
Percent paired GFP dots
Hours of sporulation
Wild-type, homologous LYS2 dots, ndt80Δ (A9828), 100% DSBs
spo11Δ/SPO11, homologous LYS2 dots, ndt80Δ (A16291), DSBs estimated at >50%
spo11-Y135F-HA/SPO11, homologous LYS2 dots, ndt80Δ (A16125), DSBs estimated at 50%
SPO11-HA, homologous LYS2 dots, ndt80Δ (A16292), DSBs estimated at 30-60%
spo11-D290A/SPO11-HA, homologous LYS2 dots, ndt80Δ (A16127), DSBs estimated at 30%
spo11-Y135F-HA/SPO11-HA, homologous LYS2 dots, ndt80Δ (A16148), DSBs estimated at 17-23%
spo11-D290A, homologous LYS2 dots, ndt80Δ (A16126), DSBs estimated at 4-12%
SPO11-HA/spo11-Y135F, homologous LYS2 dots, ndt80Δ (A16147), DSBs estimated at 0.6-4%
spo11-Y135F, homologous LYS2 dots, ndt80Δ (A16129), 0% DSBs
spo11-Y135F-HA, homologous LYS2 dots, ndt80Δ (A16133), 0% DSBs

C.

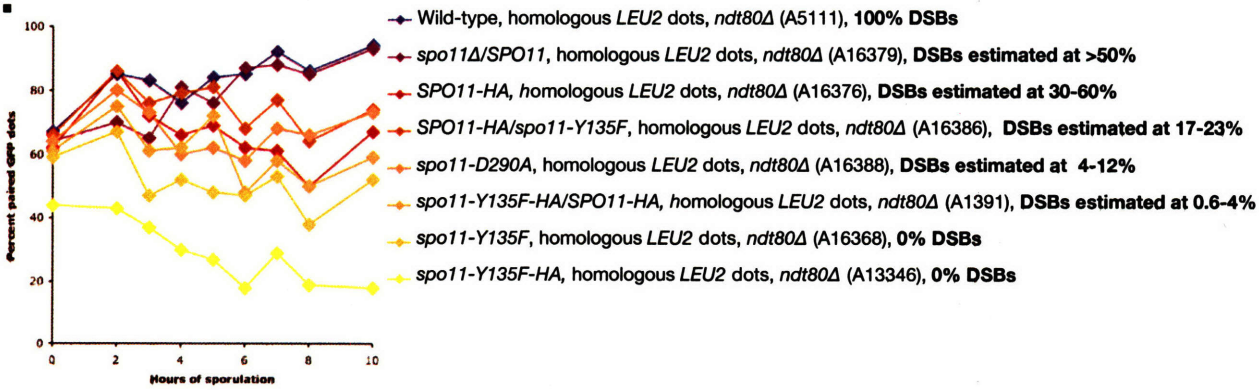
Percent paired GFP dots
Hours of sporulation
Wild-type, homologous LEU2 dots, ndt80Δ (A5111), 100% DSBs
spo11Δ/SPO11, homologous LEU2 dots, ndt80Δ (A16379), DSBs estimated at >50%
SPO11-HA, homologous LEU2 dots, ndt80Δ (A16376), DSBs estimated at 30-60%
SPO11-HA/spo11-Y135F, homologous LEU2 dots, ndt80Δ (A16386), DSBs estimated at 17-23%
spo11-D290A, homologous LEU2 dots, ndt80Δ (A16388), DSBs estimated at 4-12%
spo11-Y135F-HA/SPO11-HA, homologous LEU2 dots, ndt80Δ (A1391), DSBs estimated at 0.6-4%
spo11-Y135F, homologous LEU2 dots, ndt80Δ (A16368), 0% DSBs
spo11-Y135F-HA, homologous LEU2 dots, ndt80Δ (A13346), 0% DSBs

Figure 8: DSB and bouquet double mutants do not pair
All strains shown are deleted for *NDT80* and carry homologous tandem TetO arrays at *URA3*. Wild-type (solid black circles), *ndj1Δ* (solid red circles), *spo11Δ* (solid blue circles) and *ndj1Δ spo11Δ* (solid purple circles) were induced to sporulate. At the indicated times, samples were taken and assayed for pairing. 100 cells were counted per strain per timepoint. Wild-type cells with non-homologous tandem TetO arrays were induced to sporulate in parallel and are shown as open black circles.

Figure 8

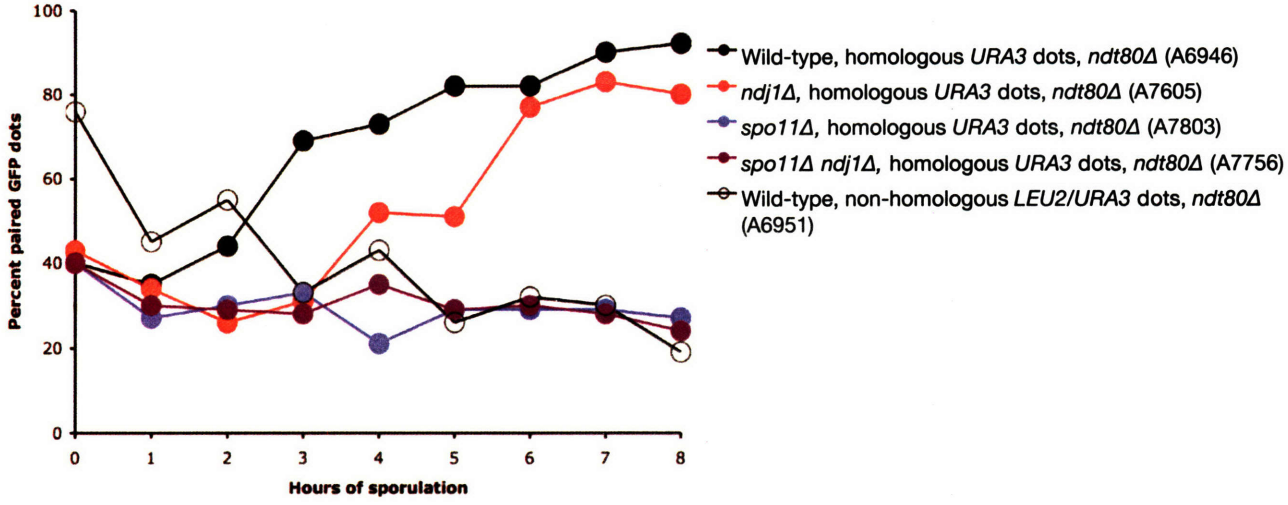
Percent paired GFP dots
100
80
60
40
20
0
0
1
2
3
4
5
6
7
8
Hours of sporulation
Wild-type, homologous URA3 dots, ndt80Δ (A6946)
ndj1Δ, homologous URA3 dots, ndt80Δ (A7605)
spo11Δ, homologous URA3 dots, ndt80Δ (A7803)
spo11Δ ndj1Δ, homologous URA3 dots, ndt80Δ (A7756)
Wild-type, non-homologous LEU2/URA3 dots, ndt80Δ (A6951)

Figure 9: Dmc1 is required for proper pairing
(A) All strains shown are deleted for *NDT80.* Wild-type cells carrying homologous tandem TetO arrays at *LEU2* (solid black circles), *dmc1Δ* cells carrying homologous tandem TetO arrays at *LEU2* (green circles) and wild-type cells carrying non-homologous tandem TetO arrays (open black circles) were induced to sporulate. At the indicated times, samples were taken and assayed for pairing. 100 cells were counted per strain per timepoint.

(B) All strains shown are deleted for *NDT80.* Wild-type cells carrying homologous tandem TetO arrays at *LYS2* (solid black squares), *dmc1Δ rad51Δ* cells carrying homologous tandem TetO arrays at *LYS2* (yellow squares) and wild-type cells carrying non-homologous tandem TetO arrays (open black squares) were induced to sporulate. At the indicated times, samples were taken and assayed for pairing. 100 cells were counted per strain per timepoint. Note that Rad51 and Dmc1 are partially redundant in their strand invasion role.

Figure 9

A.

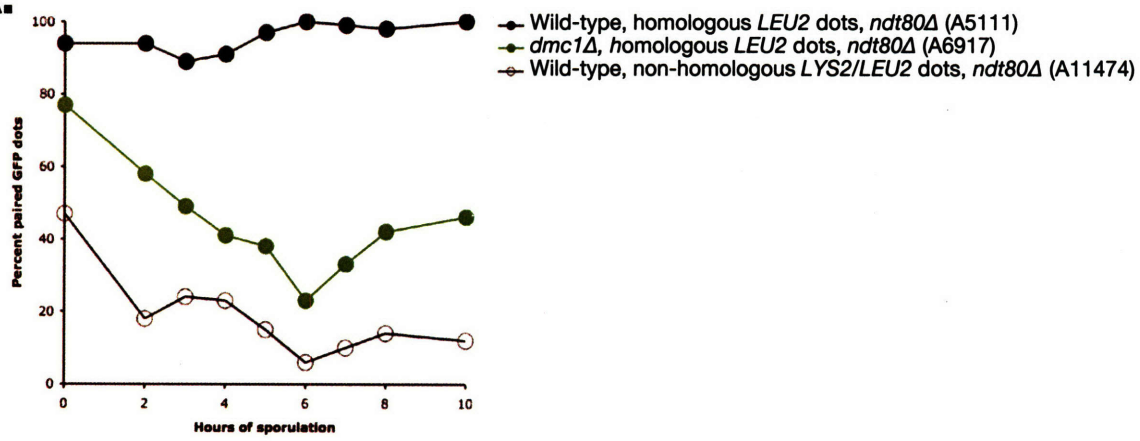
Percent paired GFP dots
Hours of sporulation
Wild-type, homologous LEU2 dots, ndt80Δ (A5111)
dmc1Δ, homologous LEU2 dots, ndt80Δ (A6917)
Wild-type, non-homologous LYS2/LEU2 dots, ndt80Δ (A11474)

B.

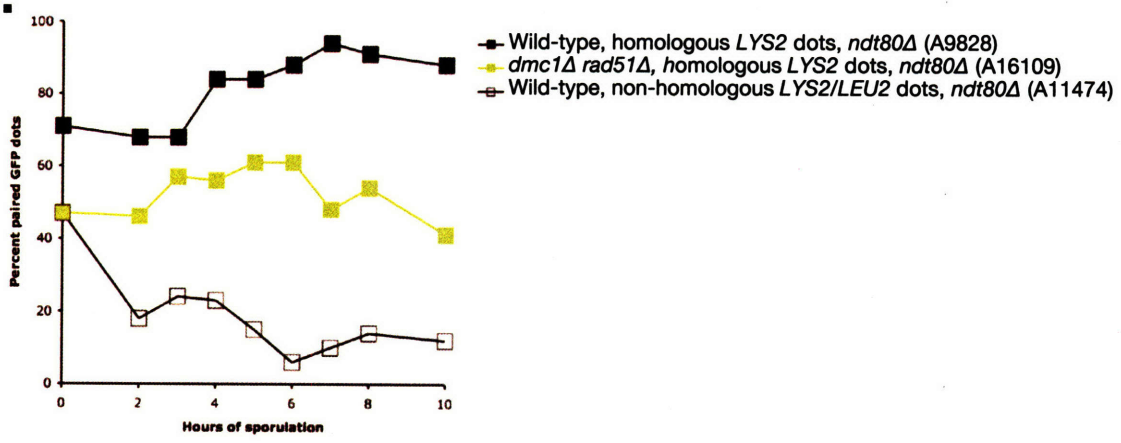
Percent paired GFP dots
Hours of sporulation
Wild-type, homologous LYS2 dots, ndt80Δ (A9828)
dmc1Δ rad51Δ, homologous LYS2 dots, ndt80Δ (A16109)
Wild-type, non-homologous LYS2/LEU2 dots, ndt80Δ (A11474)

Synaptonemal complex components and pairing

The SC assembles concomitant with recombination progression and is thought to be important to stabilize homolog interactions. Early SC is composed of lateral elements (LEs), consisting of components including Rec8 and Hop1. LEs are then linked by transverse elements (TEs) through the coiled-coil protein Zip1 (Zickler and Kleckner 1998); (Page and Hawley 2004). We found Hop1 to be essential for proper pairing at the *LYS2* locus in *ndt80Δ* cells, while Zip1 is unnecessary for pairing at this locus (Figure 10A). Zip1, however, is needed for full pairing at the *LEU2* locus (Figure 10B). Why is this the case? In addition to its role in TE formation, Zip1 is part of the synaptonemal initiation complex (SIC) that has been shown to mediate non-homologous centromere coupling interactions in early prophase (Tsubouchi and Roeder 2005). As *LEU2* is a centromere-proximal locus, while *LYS2* is centromere distal, it is possible that this centromere coupling specifically contributes to homologous pairing at centromeres. It will be important to examine the roles of other SIC and SC components in pairing to clarify this issue.

Figure 10: SC components contribute to pairing
(A) All strains shown are deleted for *NDT80* and carry homologous tandem TetO arrays at *LYS2.* Wild-type (solid black circles), *zip1Δ* (solid dark gray circles) and *hop1Δ* (solid light gray circles) were induced to sporulate. At the indicated times, samples were taken and assayed for pairing. 100 cells were counted per strain per timepoint. Wild-type cells with non-homologous tandem TetO arrays were induced to sporulate in parallel and are shown as open black circles.

(B) All strains shown are deleted for *NDT80* and carry homologous tandem TetO arrays at *LEU2.* Wild-type (solid black squares) and *zip1Δ* (solid gray squares) were induced to sporulate. At the indicated times, samples were taken and assayed for pairing. 100 cells were counted per strain per timepoint. Wild-type cells with non-homologous tandem TetO arrays were induced to sporulate in parallel and are shown as open black squares

Figure 10

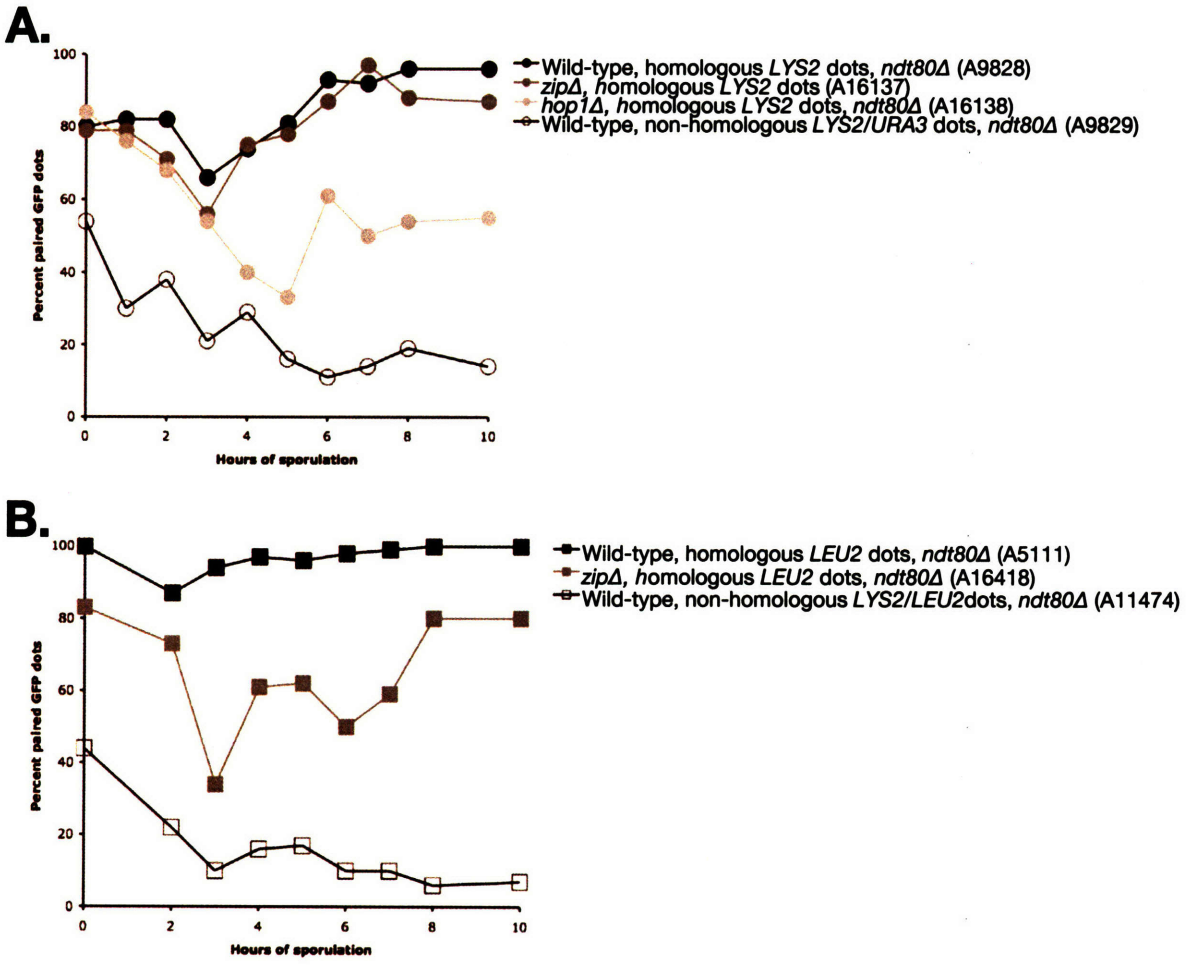
A.
Percent paired GFP dots
Hours of sporulation
Wild-type, homologous LYS2 dots, ndt80Δ (A9828)
zipΔ, homologous LYS2 dots (A16137)
hop1Δ, homologous LYS2 dots, ndt80Δ (A16138)
Wild-type, non-homologous LYS2/URA3 dots, ndt80Δ (A9829)
B.
Percent paired GFP dots
Hours of sporulation
Wild-type, homologous LEU2 dots, ndt80Δ (A5111)
zipΔ, homologous LEU2 dots, ndt80Δ (A16418)
Wild-type, non-homologous LYS2/LEU2dots, ndt80Δ (A11474)

DNA replication and pairing

In addition to recombination, and SC formation, another major early meiotic process is DNA replication. Meiotic DNA replication appears to utilize similar replication factors and origins of replication to mitotic DNA replication, but requires twice as much time to complete (Forsburg 2002). It has been suggested that this additional time is used to set up prophase events, including DSB formation.

I examined pairing ability of *ndt80Δ* cells carrying a meiosis-specific depletion of the pre-RC component, Cdc6, by placement of *CDC6* under the mitosis-specific promoter for sister chromatid cohesion component, *SCC1/MCD1*. This construct allows the strain to be maintained as mitotic replication is unaffected, but Cdc6 is not expressed in meiotic S-phase, leading to a block specifically in meiotic DNA replication (Hochwagen, Tham et al. 2005). I found these *pSCC1-CDC6* cells to have no obvious defect in pairing at either *LYS2* or *URA3* despite undergoing no DNA replication (Figure 11). Surprisingly, when I examined pairing in another replication-defective mutant, an *ndt80Δ* strain also deleted for S-phase cyclins *CLB5* and *CLB6*, I found cells also failed to replicate, but showed a severe pairing defect at *LYS2* and *LEU2* (Figure 12). Similarly, an *ndt80Δ* strain carrying an allele coding for a chemically-repressible Cdc28 (Benjamin, Zhang et al. 2003), the primary *S. cerevisiae* CDK, shows a defect in pairing at *LYS2* that is dose-dependent with CDK inhibitor (Figure13A).

The defect in this strain, however, is mild compared to that seen in *clb5Δclb6Δ* cells, likely due to incomplete inhibition of Cdc28. These experiments will need to be expanded to clarify this discrepancy.

Why do *clb5Δclb6Δ* cells show a severe pairing defect, whereas p*SCC1-CDC6* cells pair normally? Neither strain undergoes DNA replication, so the *pSCC1-CDC6* result suggests that both the process of DNA replication and the presence of a sister chromatid are dispensible for pairing. Recent work, however, suggests that Clb5-CDKs are responsible for phosphorylating Mer2 (Meiotic Recombination factor 2), a protein required for DSB formation, on Serine 30 (Henderson, Kee et al. 2006). *mer2-S30A* cells, in which this Serine is mutated to a non-phosphorylatable residue (Alanine), show a dramatic defect in pairing (Figure 13B), indicating that it is Clb5 and Clb6's roles in DSB formation, rather than their more established roles in DNA replication, that contribute to proper pairing. As expected based on this hypothesis, *clb5Δclb6Δndt80Δspo11Δ* cells and *clb5Δclb6Δndt80Δspo11-Y135F* cells show no additional pairing defect at *LYS2*, compared to *clb5Δclb6Δndt80Δ* cells (Figure 14A). The severe pairing defect in *clb5Δclb6Δ* or *spo11*, cells alone, however, could make an additive defect difficult to detect. We also find that p*SCC1-CDC6 spo11Δ* cells and p*SCC1-CDC6 spo11-Y135F* cells mimic the pairing defect seen in *clb5Δclb6Δ* strains at *LYS2* (Figure 14B), supporting the hypothesis that DSB formation, but not DNA replication or the presence of a sister chromatid, is essential for meiotic pairing.

Figure 11: Strains depleted for Cdc6 do not replicate, but are pairing competent

(A) Wild-type (solid blue diamonds) or *pSCC1-CDC6* (solid green diamonds) cells carrying homologous tandem TetO arrays at *LYS2* were induced to sporulate. At the indicated times, samples were taken and assayed for pairing. 100 cells were counted per strain per timepoint. Non-homologous array strains are shown by open diamonds as a control for array clustering.

(B) Wild-type cells were induced to sporulate. At the indicated times, samples were taken and assayed for DNA content by flow cytometry. The x-axis represents DNA content, y-axis represents number of cells and z-axis represents hours of sporulation. These samples are from the same experiment as (A).

(C) *pSCC1-CDC6* cells were induced to sporulate. At the indicated times, samples were taken and assayed for DNA content by flow cytometry. The x-axis represents DNA content, y-axis represents number of cells and z-axis represents hours of sporulation. These samples are from the same experiment as (A).

(D) All strains shown are deleted for *NDT80.* Wild-type (solid blue circles) or *pSCC1-CDC6* (solid green circles) cells carrying homologous tandem TetO arrays at *URA3* were induced to sporulate. At the indicated times, samples were taken and assayed for pairing. 100 cells were counted per strain per timepoint. Non-homologous array strains are shown by open circles as a control for array clustering.

(E) Wild-type cells were induced to sporulate. At the indicated times, samples were taken and assayed for DNA content by flow cytometry. The x-axis represents DNA content, y-axis represents number of cells and z-axis represents hours of sporulation. These samples are from the same experiment as (D).

(F) *pSCC1-CDC6* cells were induced to sporulate. At the indicated times, samples were taken and assayed for DNA content by flow cytometry. The x-axis represents DNA content, y-axis represents number of cells and z-axis represents hours of sporulation. These samples are from the same experiment as (D).

Figure 11

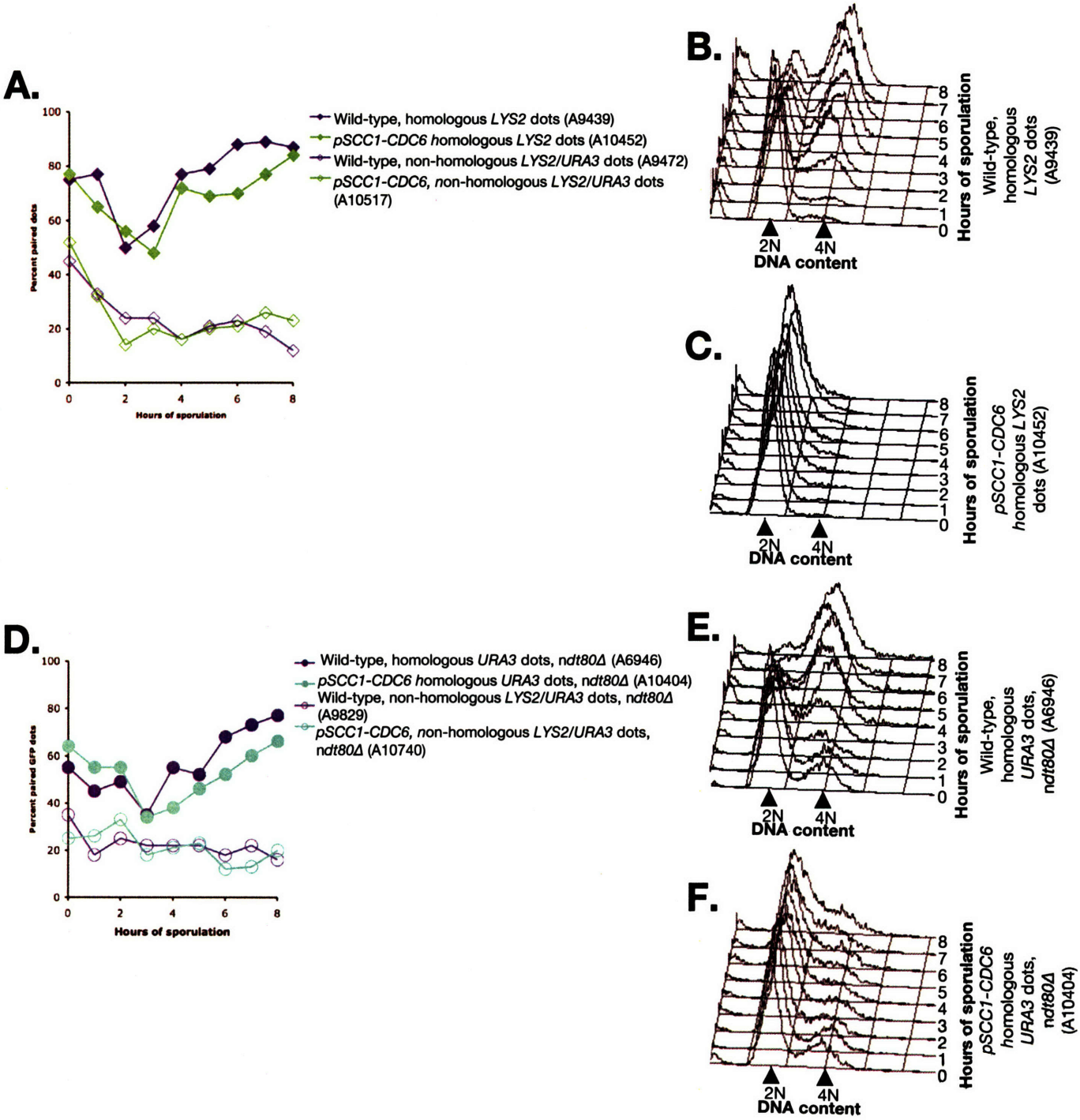
A.
Wild-type, homologous LYS2 dots (A9439)
pSCC1-CDC6 homologous LYS2 dots (A10452)
Wild-type, non-homologous LYS2/URA3 dots (A9472)
pSCC1-CDC6, non-homologous LYS2/URA3 dots (A10517)
Percent paired dots
Hours of sporulation
B.
Hours of sporulation
Wild-type, homologous LYS2 dots (A9439)
2N
4N
DNA content
C.
Hours of sporulation
pSCC1-CDC6 homologous LYS2 dots (A10452)
2N
4N
DNA content
D.
Wild-type, homologous URA3 dots, ndt80Δ (A6946)
pSCC1-CDC6 homologous URA3 dots, ndt80Δ (A10404)
Wild-type, non-homologous LYS2/URA3 dots, ndt80Δ (A9829)
pSCC1-CDC6, non-homologous LYS2/URA3 dots, ndt80Δ (A10740)
Percent paired GFP dots
Hours of sporulation
E.
Hours of sporulation
Wild-type, homologous URA3 dots, ndt80Δ (A6946)
2N
4N
DNA content
F.
Hours of sporulation
pSCC1-CDC6 homologous URA3 dots, ndt80Δ (A10404)
2N
4N
DNA content

Figure 12: Strains deleted for *CLB5* and *CLB6* do not replicate and do not pair

(A) All strains shown are deleted for *NDT80.* Wild-type (solid blue squares) or *clb5Δclb6Δ* (solid green squares) cells carrying homologous tandem TetO arrays at *LYS2* were induced to sporulate. At the indicated times, samples were taken and assayed for pairing. 100 cells were counted per strain per timepoint. Non-homologous array strains are shown by open squares as a control for array clustering.

(B) Wild-type cells were induced to sporulate. At the indicated times, samples were taken and assayed for DNA content by flow cytometry. The x-axis represents DNA content, y-axis represents number of cells and z-axis represents hours of sporulation. These samples are from the same experiment as (A).

(C) *clb5Δclb6Δ* cells were induced to sporulate. At the indicated times, samples were taken and assayed for DNA content by flow cytometry. The x-axis represents DNA content, y-axis represents number of cells and z-axis represents hours of sporulation. These samples are from the same experiment as (A).

(D) All strains shown are deleted for *NDT80.* Wild-type (solid blue diamonds) or *clb5Δclb6Δ* (solid green diamonds) cells carrying homologous tandem TetO arrays at *LEU2* were induced to sporulate. At the indicated times, samples were taken and assayed for pairing. 100 cells were counted per strain per timepoint. Non-homologous array strains are shown by open diamonds as a control for array clustering.

(E) Wild-type cells were induced to sporulate. At the indicated times, samples were taken and assayed for DNA content by flow cytometry. The x-axis represents DNA content, y-axis represents number of cells and z-axis represents hours of sporulation. These samples are from the same experiment as (D).

(F) *clb5Δclb6Δ* cells were induced to sporulate. At the indicated times, samples were taken and assayed for DNA content by flow cytometry. The x-axis represents DNA content, y-axis represents number of cells and z-axis represents hours of sporulation. These samples are from the same experiment as (D).

Figure 12

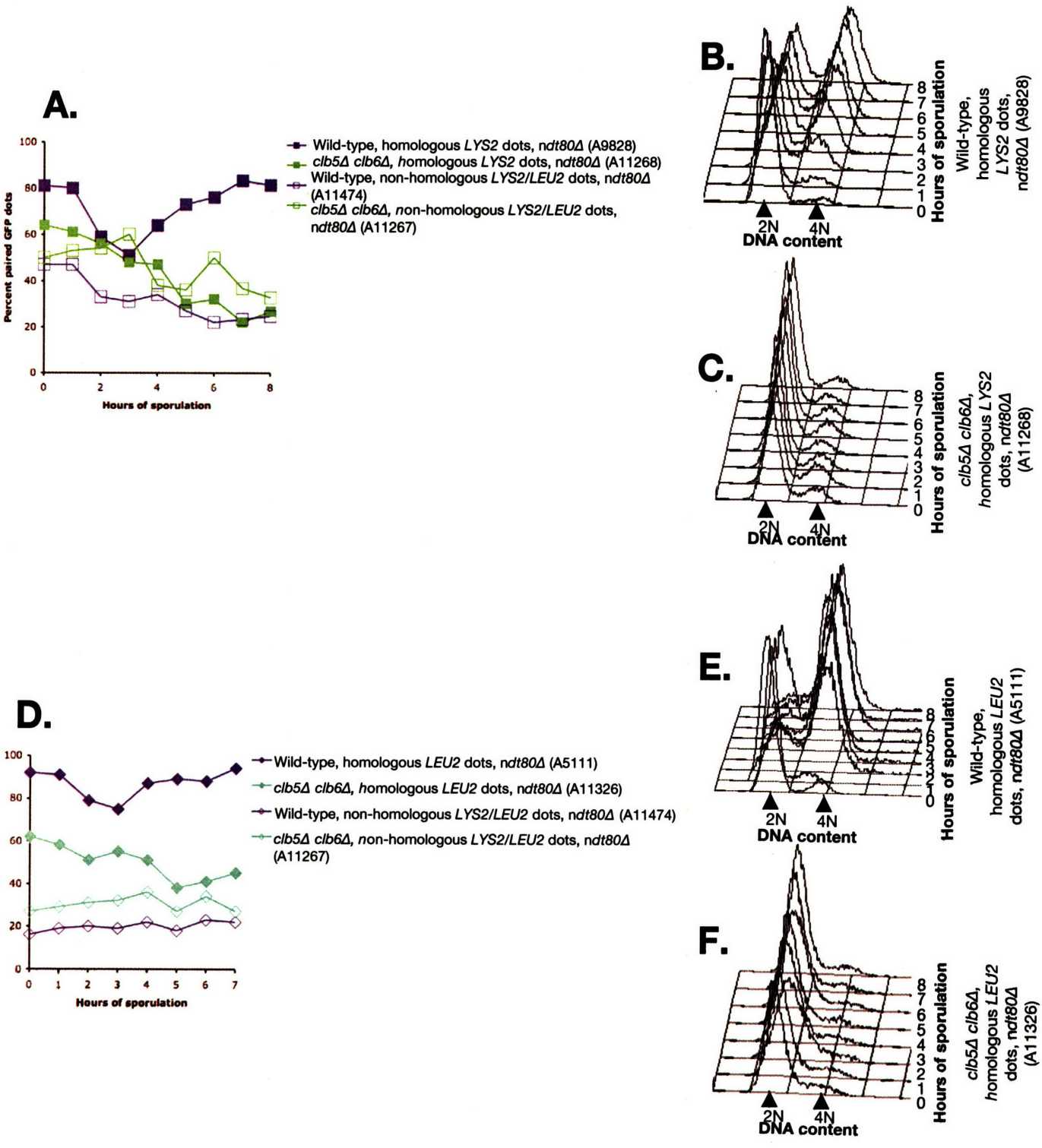
A.
Percent paired GFP dots
Hours of sporulation
Wild-type, homologous LYS2 dots, ndt80Δ (A9828)
clb5Δ clb6Δ, homologous LYS2 dots, ndt80Δ (A11268)
Wild-type, non-homologous LYS2/LEU2 dots, ndt80Δ (A11474)
clb5Δ clb6Δ, non-homologous LYS2/LEU2 dots, ndt80Δ (A11267)
B.
Hours of sporulation
DNA content
2N
4N
Wild-type, homologous LYS2 dots, ndt80Δ (A9828)
C.
clb5Δ clb6Δ, homologous LYS2 dots, ndt80Δ (A11268)
D.
Percent paired GFP dots
Hours of sporulation
Wild-type, homologous LEU2 dots, ndt80Δ (A5111)
clb5Δ clb6Δ, homologous LEU2 dots, ndt80Δ (A11326)
Wild-type, non-homologous LYS2/LEU2 dots, ndt80Δ (A11474)
clb5Δ clb6Δ, non-homologous LYS2/LEU2 dots, ndt80Δ (A11267)
E.
Wild-type, homologous LEU2 dots, ndt80Δ (A5111)
F.
clb5Δ clb6Δ, homologous LEU2 dots, ndt80Δ (A11326)

Figure 13: Cdc28 activity and phosphorylation of the DSB initiating complex factor Mer2 contribute to pairing through their roles in DSB initiation
(A) The strain shown is deleted for *NDT80,* carries tandem TetO arrays at *URA3* and carries the analog sensitive allele of *CDC28, cdc28-as*. Cells treated at 1 hour with a vehicle control (black circles), cells treated at 1 hour with 0.5μM *cdc28-as1* inhibitor 9 (dark gray circles), cells treated at 1 hour with 5μM *cdc28-as1* inhibitor 9 (light gray circles), cells treated at 4.5 hours with a vehicle control (black squares), cells treated at 4.5 hours with 0.5μM *cdc28-as1* inhibitor 9 (dark gray squares) and cells treated at 4.5 hours with 5μM *cdc28-as1* inhibitor 9 (light gray squares) were induced to sporulate. At the indicated times, samples were taken and assayed for pairing. 100 cells were counted per treatment per timepoint.

(B) All strains shown are deleted for *NDT80*. Wild-type cells carrying homologous tandem TetO arrays at *LYS2* (solid blue circles), *mer2-S30A* cells carrying homologous tandem TetO arrays at *LYS2* (solid red circles), and wild-type cells carrying non-homologous tandem TetO arrays (open blue circles) were induced to sporulate. At the indicated times, samples were taken and assayed for pairing. 100 cells were counted per strain per timepoint.

Figure 13

A.

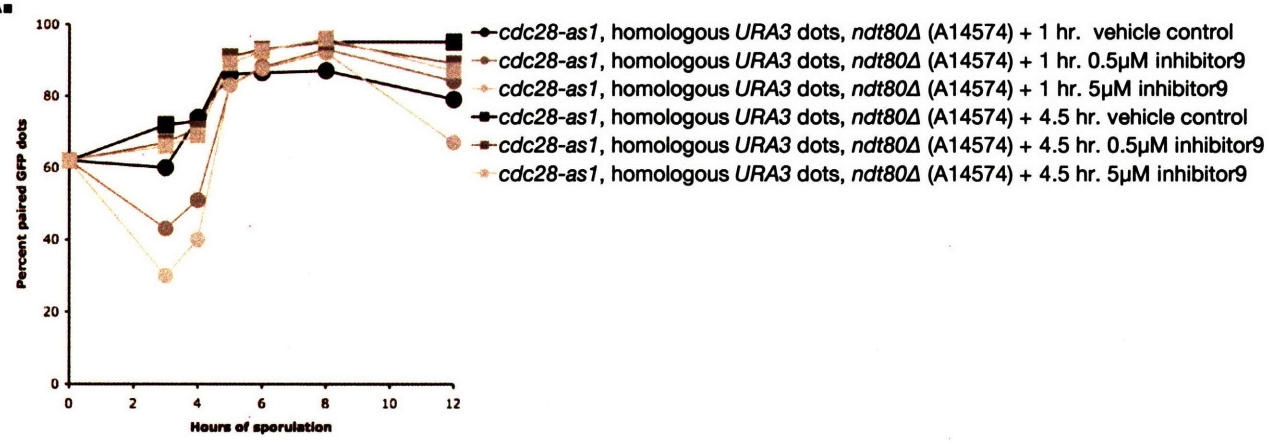
Percent paired GFP dots
Hours of sporulation
cdc28-as1, homologous URA3 dots, ndt80Δ (A14574) + 1 hr. vehicle control
cdc28-as1, homologous URA3 dots, ndt80Δ (A14574) + 1 hr. 0.5μM inhibitor9
cdc28-as1, homologous URA3 dots, ndt80Δ (A14574) + 1 hr. 5μM inhibitor9
cdc28-as1, homologous URA3 dots, ndt80Δ (A14574) + 4.5 hr. vehicle control
cdc28-as1, homologous URA3 dots, ndt80Δ (A14574) + 4.5 hr. 0.5μM inhibitor9
cdc28-as1, homologous URA3 dots, ndt80Δ (A14574) + 4.5 hr. 5μM inhibitor9

B.

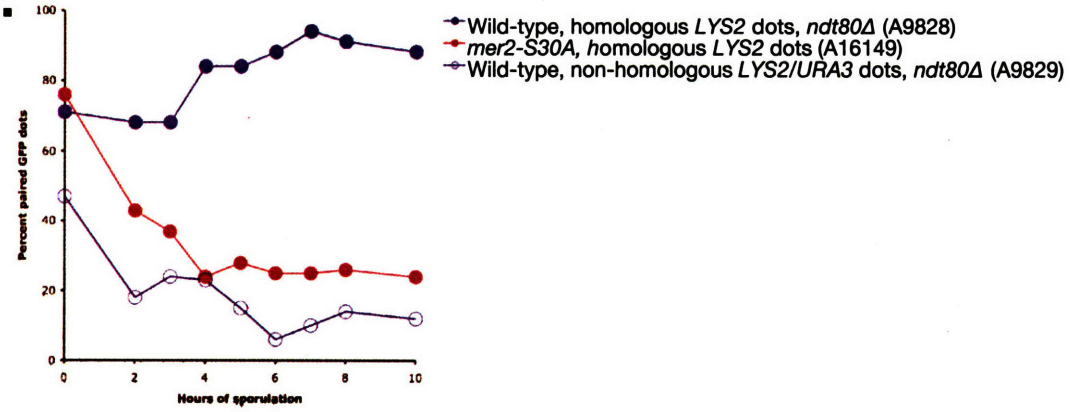
Percent paired GFP dots
Hours of sporulation
Wild-type, homologous LYS2 dots, ndt80Δ (A9828)
mer2-S30A, homologous LYS2 dots (A16149)
Wild-type, non-homologous LYS2/URA3 dots, ndt80Δ (A9829)

Figure 14: Eliminating DSBs eliminates pairing in replication defective strains

(A) All strains shown are deleted for *NDT80.* Wild-type cells carrying tandem TetO arrays at *LYS2* (solid black circles), *clb5Δ clb6Δ* cells carrying tandem TetO arrays at *LYS2* (solid purple circles), *clb5Δ clb6Δ spo11Δ* cells carrying tandem TetO arrays at *LYS2* (solid pink circles), and wild-type cells carrying non-homologous tandem TetO arrays (open black circles) were induced to sporulate. At the indicated times, samples were taken and assayed for pairing. 100 cells were counted per strain per timepoint.

(B) Wild-type cells carrying tandem TetO arrays at *LYS2* (solid black squares), *spo11Δ* cells carrying tandem TetO arrays at *LYS2* (solid green squares), *pSCC1-CDC6 spo11Δ* cells carrying tandem TetO arrays at *LYS2* (solid blue squares), and wild-type cells carrying non-homologous tandem TetO arrays (open black squares) were induced to sporulate. At the indicated times, samples were taken and assayed for pairing. 100 cells were counted per strain per timepoint.

Figure 14

A.

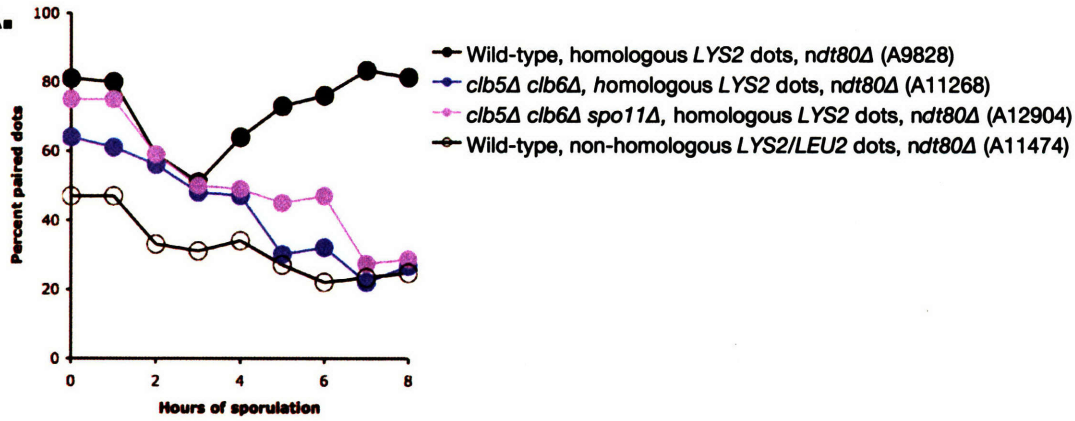
Percent paired dots
Hours of sporulation
Wild-type, homologous LYS2 dots, ndt80Δ (A9828)
clb5Δ clb6Δ, homologous LYS2 dots, ndt80Δ (A11268)
clb5Δ clb6Δ spo11Δ, homologous LYS2 dots, ndt80Δ (A12904)
Wild-type, non-homologous LYS2/LEU2 dots, ndt80Δ (A11474)

B.

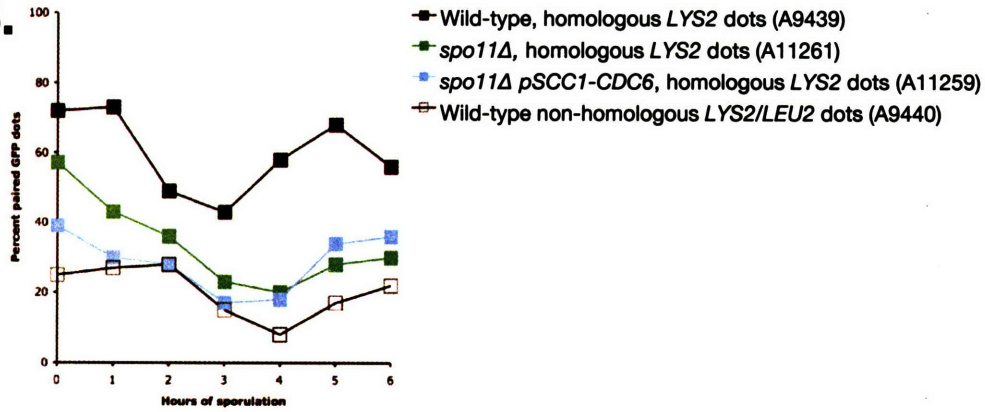
Percent paired GFP dots
Hours of sporulation
Wild-type, homologous LYS2 dots (A9439)
spo11Δ, homologous LYS2 dots (A11261)
spo11Δ pSCC1-CDC6, homologous LYS2 dots (A11259)
Wild-type non-homologous LYS2/LEU2 dots (A9440)

The role of the meiotic cohesin Rec8 in pairing

It is somewhat surprising that cells are capable of pairing in the absence of a sister chromatid, yet cannot pair normally in the absence of chromosome axes, as mediated by LE formation and Hop1. The meiotic cohesin, Rec8, is also a component of the LE that has been thought to depend on DNA replication for loading onto chromatin and it's well-established cohesive role in the meiotic divisions (Zickler and Kleckner 1998; Forsburg 2002). I wondered if cells deleted for *REC8* were capable of pairing normally. I observed that *rec8Δ* cells show a locus-specific pairing defect. Pairing in *rec8Δ ndt80Δ* cells is extremely defective at *LYS2*, but is nearly normal at *LEU2* (Figure 15A). When I examine all five loci for which we have GFP dots available, we find that *rec8Δ ndt80Δ* cells are capable of pairing relatively normally only at *LEU2*. Pairing at *CEN5, TEL5, URA3,* and *LYS2* is ablated in this background (Figure 15B).

Why Rec8 is needed for pairing at all sites examined besides *LEU2* is not clear, although, as shown in Figure 3 that *LEU2* naturally shows higher pairing than other loci and is very active for DSB formation. The relationship between this abnormally high baseline pairing, DSB formation and Rec8 merits further examination. Additionally, assessment of *rec8Δ* pairing at more loci would be informative.

Figure 15: *rec8Δ* cells show pairing defects at most loci examined
(A) All strains shown are deleted for *NDT80*. Wild-type cells with homologous tandem TetO arrays at *LEU2* (solid black squares), *rec8Δ* cells with homologous tandem TetO arrays at *LEU2* (solid dark blue squares), wild-type cells with homologous tandem TetO arrays at *LYS2* (solid gray squares), *rec8Δ* cells with homologous tandem TetO arrays at *LYS2* (solid lighter blue squares), wild-type cells with non-homologous tandem TetO arrays (open black squares) and *rec8Δ* cells with non-homologous tandem TetO arrays (open blue squares) were induced to sporulate. At the indicated times, samples were taken and assayed for pairing. 100 cells were counted per strain per timepoint.

(B) All strains shown are deleted for *NDT80*. Wild-type cells with homologous tandem TetO arrays at *TEL5* (solid black circles), wild-type cells with homologous tandem TetO arrays at *LEU2* (solid dark gray circles), wild-type cells with homologous tandem TetO arrays at *URA3* (solid medium gray circles), wild-type cells with homologous tandem TetO arrays at *CEN5* (solid light gray circles), *rec8Δ* cells with homologous tandem TetO arrays at *TEL5* (solid darkest blue circles), *rec8Δ* cells with homologous tandem TetO arrays at *LEU2* (solid dark blue circles), *rec8Δ* cells with homologous tandem TetO arrays at *URA3* (solid medium blue circles), *rec8Δ* cells with homologous tandem TetO arrays at *CEN5* (solid light blue circles), and wild-type cells with non-homologous tandem TetO arrays (open black circles) were induced to sporulate. At the indicated times, samples were taken and assayed for pairing. 100 cells were counted per strain per timepoint.

Figure 15

A.

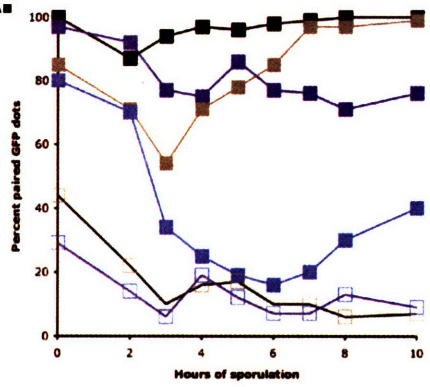

- Wild-type, homologous *LEU2* dots, *ndt80Δ* (A5111)
- *rec8Δ*, homologous *LEU2* dots, *ndt80Δ* (A16131)
- Wild-type, homologous *LYS2* dots, *ndt80Δ* (A9828)
- *rec8Δ*, homologous *LYS2* dots, *ndt80Δ* (A16108)
- Wild-type, non-homologous *LEU2/LYS2* dots, *ndt80Δ* (A11474)
- *rec8Δ*, non-homologous *LEU2/LYS2* dots, *ndt80Δ* (A16135)

B.

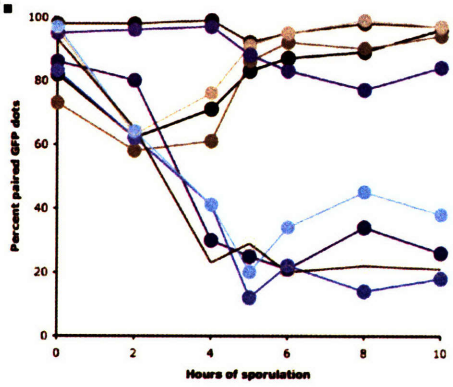

- Wild-type, homologous *TEL52* dots, *ndt80Δ* (A16366)
- Wild-type, homologous *LEU2* dots, *ndt80Δ* (A5111)
- Wild-type, homologous *URA3* dots, *ndt80Δ* (A6946)
- Wild-type, homologous *CEN5* dots, *ndt80Δ* (A16362)
- *rec8Δ*, homologous *TEL5* dots, *ndt80Δ* (A16535)
- *rec8Δ*, homologous *LEU2* dots, *ndt80Δ* (A16131)
- *rec8Δ*, homologous *URA3* dots, *ndt80Δ* (A16538)
- *rec8Δ*, homologous *CEN5* dots, *ndt80Δ* (A16537)
- Wild-type, non-homologous *LEU2/CEN5* dots, *ndt80Δ* (A16360)

Examining the relationship between DNA replication, Rec8 and pairing

To better understand Rec8's role in pairing, I compared pairing in *rec8Δ* cells with *pSCC1-CDC6* cells. It is discussed in Chapter 3 that DNA replication is required for Rec8's role in sister chromatid cohesion. DNA replication is not required, however, for Rec8's role in SC assembly, and appears to also be dispensible for homolog pairing. I wondered if *rec8Δ* cells might appear to be defective in pairing due to the presence of "loose" sister chromatids in this background, which would not be present in cells that don't undergo DNA replication. To investigate this issue, I examined pairing in *rec8Δ pSCC1-CDC6 ndt80Δ* cells. I find that chromosomes in *rec8Δ pSCC1-CDC6 ndt80Δ* cells show the same mild decrease in pairing seen in *rec8Δ ndt80Δ* cells alone at *LEU2* (Figure 16A), suggesting that this partial pairing defect is genuinely due to lack of Rec8 rather than free sister chromatids.

The situation at *LYS2* is slightly more complex. *rec8Δ pSCC1-CDC6 ndt80Δ* cells show a similar lack of pairing at early timepoints as seen in *rec8Δ ndt80Δ* cells, but some pairing is recovered at later timepoints (Figure 16B). Pairing at *LYS2* in *rec8Δ pSCC1-CDC6 ndt80Δ* cells does not recover to wild-type levels, but this result indicates that some of the perceived defect in arm pairing in cells lacking Rec8 is actually due to either loose sister chromatids interfering with pairing establishment, or the inability to accurately count GFP dots as separated sister chromatids (two GFP dots) look like separated

homologs (two GFP dots). This may indicate that Rec8 does not actually function to promote pairing in a locus-dependent manner and rather that Rec8 is partially responsible for pairing at all chromosomal loci. This issue will require further experiments to clarify.

Figure 16: *rec8Δ* cells show a pairing defect that is independent of the presence of sister chromatids

(A) All strains shown are deleted for *NDT80* and carry homologous tandem TetO arrays at *LEU2*. Wild-type (solid black circles), *rec8Δ* (solid blue circles), *pSCC1-CDC6* (solid red circles) and *rec8Δ pSCC1-CDC6* (solid purple circles) were induced to sporulate. At the indicated times, samples were taken and assayed for pairing. 100 cells were counted per strain per timepoint. Wild-type cells with non-homologous tandem TetO arrays (open black circles) and *rec8Δ* cells with non-homologous tandem TetO arrays (open blue circles) were induced to sporulate in parallel.

(B) All strains shown are deleted for *NDT80* and carry homologous tandem TetO arrays at *LYS2*. Wild-type (solid black squares), *rec8Δ* (solid blue squares), *pSCC1-CDC6* (solid red squares) and *rec8Δ pSCC1-CDC6* (solid purple squares) were induced to sporulate. At the indicated times, samples were taken and assayed for pairing. 100 cells were counted per strain per timepoint. Wild-type cells with non-homologous tandem TetO arrays (open black squares) and *rec8Δ* cells with non-homologous tandem TetO arrays (open blue squares) were induced to sporulate in parallel.

Figure 16

A.

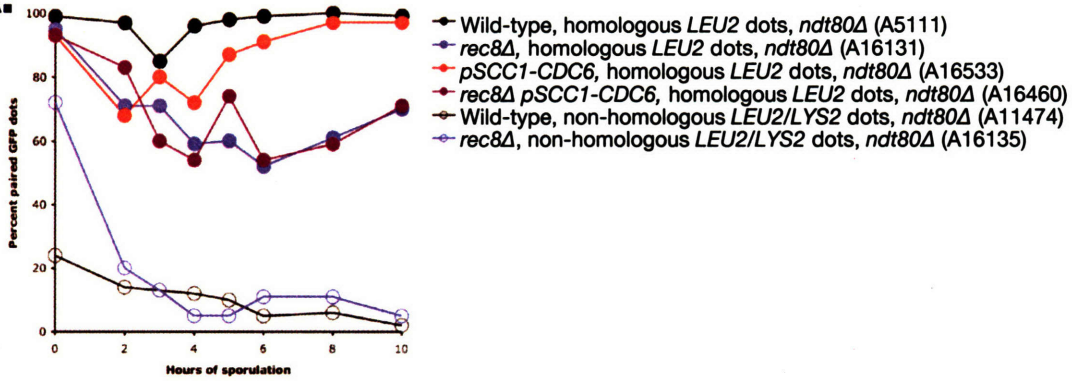
Percent paired GFP dots
Hours of sporulation
Wild-type, homologous LEU2 dots, ndt80Δ (A5111)
rec8Δ, homologous LEU2 dots, ndt80Δ (A16131)
pSCC1-CDC6, homologous LEU2 dots, ndt80Δ (A16533)
rec8Δ pSCC1-CDC6, homologous LEU2 dots, ndt80Δ (A16460)
Wild-type, non-homologous LEU2/LYS2 dots, ndt80Δ (A11474)
rec8Δ, non-homologous LEU2/LYS2 dots, ndt80Δ (A16135)

B.

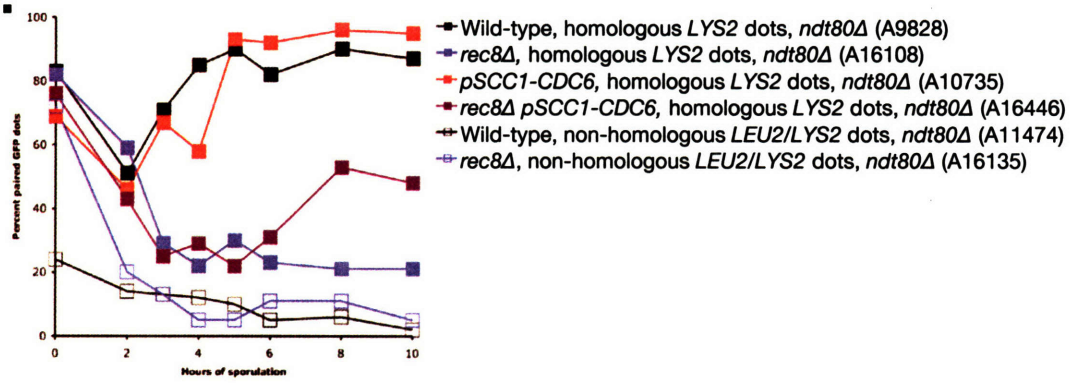
Percent paired GFP dots
Hours of sporulation
Wild-type, homologous LYS2 dots, ndt80Δ (A9828)
rec8Δ, homologous LYS2 dots, ndt80Δ (A16108)
pSCC1-CDC6, homologous LYS2 dots, ndt80Δ (A10735)
rec8Δ pSCC1-CDC6, homologous LYS2 dots, ndt80Δ (A16446)
Wild-type, non-homologous LEU2/LYS2 dots, ndt80Δ (A11474)
rec8Δ, non-homologous LEU2/LYS2 dots, ndt80Δ (A16135)

Genetic interactions between REC8 and ZIP1 in pairing

Of the mutants that I have discussed thus far, two showed locus-variable effects on pairing. *zip1Δ* cells paired normally at *LYS2*, but were defective in pairing at *LEU2*. The reverse result was seen in *rec8Δ* cells. I sought to clarify these locus-specific effects through double-mutant analysis. I find that deletion of *REC8* in *zip1Δndt80Δ* cells results in a complete loss of pairing at the *LYS2* locus (Figure 17B), indicating that genetically *REC8* acts downstream or parallel to *ZIP1* in its pairing function at chromosome arms. I find that deletion of *ZIP1* in *rec8Δndt80 Δ* cells results in a defect slightly less than seen in *rec8Δndt80Δ* cells and similar to that seen in *zip1Δndt80Δ* cells alone (Figure 17A), indicating that *ZIP1* genetically acts downstream of or in parallel to *REC8* in its pairing function at *LEU2*. Combining these results, it seems likely that, despite acting together to promote SC formation, Zip1 and Rec8 act in parallel in their respective pairing roles.

Figure 17: Examination of the locus-specific genetic interactions of *rec8Δ* and *zip1Δ* on pairing

(A) All strains shown are deleted for *NDT80* and carry homologous tandem TetO arrays at *LEU2.* Wild-type (solid black circles), *rec8Δ* (solid blue circles), *zip1Δ* (solid yellow circles) and *rec8Δ zip1Δ* (solid green circles) were induced to sporulate. At the indicated times, samples were taken and assayed for pairing. 100 cells were counted per strain per timepoint. Wild-type cells with non-homologous tandem TetO arrays (open black circles) and *rec8Δ* cells with non-homologous tandem TetO arrays (open blue circles) were induced to sporulate in parallel.

(B) All strains shown are deleted for *NDT80* and carry homologous tandem TetO arrays at *LYS2.* Wild-type (solid black squares), *rec8Δ* (solid blue squares), *zip1Δ* (solid yellow squares) and *rec8Δ zip1Δ* (solid green squares) were induced to sporulate. At the indicated times, samples were taken and assayed for pairing. 100 cells were counted per strain per timepoint. Wild-type cells with non-homologous tandem TetO arrays (open black squares) and *rec8Δ* cells with non-homologous tandem TetO arrays (open blue squares) were induced to sporulate in parallel.

Figure 17

A.

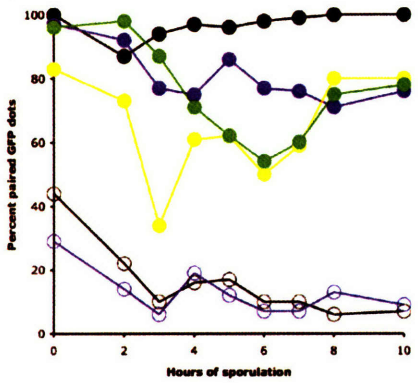

- Wild-type, homologous *LEU2* dots, *ndt80Δ* (A5111)
- *rec8Δ*, homologous *LEU2* dots, *ndt80Δ* (A16131)
- *zip1Δ*, homologous *LEU2* dots, *ndt80Δ* (A16418)
- *rec8Δ zip1Δ*, homologous *LEU2* dots, *ndt80Δ* (A16416)
- Wild-type, non-homologous *LEU2/LYS2* dots, *ndt80Δ* (A11474)
- *rec8Δ*, non-homologous *LEU2/LYS2* dots, *ndt80Δ* (A16135)

B.

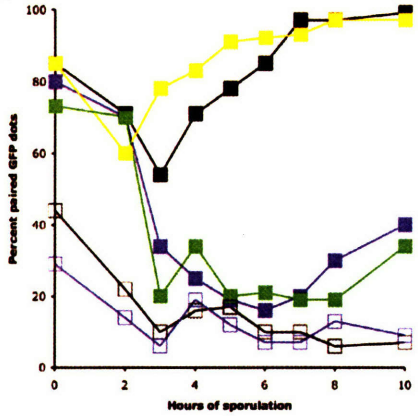

- Wild-type, homologous *LYS2* dots, *ndt80Δ* (A9828)
- *rec8Δ*, homologous *LYS2* dots, *ndt80Δ* (A16108)
- *zip1Δ*, homologous *LYS2* dots (A16137)
- *rec8Δ zip1Δ*, homologous *LYS2* dots, *ndt80Δ* (A16414)
- Wild-type, non-homologous *LEU2/LYS2* dots, *ndt80Δ* (A11474)
- *rec8Δ*, non-homologous *LEU2/LYS2* dots, *ndt80Δ* (A16135)

Discussion

Pairing at diverse chromosomal sites: findings and future studies

Preliminary characterization of the pheonomenon of meiotic pairing has yielded insight into connections between pairing and other early meiotic events. The five loci examined by population assays appear to pair with similar timing, indicating that chromosomes are not consistently "zipped up" from telomeres as has been suggested in some organisms (McKee 2004). More conclusive proof of this model may be obtained through the use of strains with multiple homologous fluorescent dots in the same strain. My attempts to generate such strains have been unsuccessful thus far, due to apparent instability of arrays other than the Tet Operators used in these studies in our strain background, but the utility of such strains merits further effort towards their construction.

Chromosome movement in pairing

The studies in this chapter additionally suggest that early pairing stages require ATP and actin filaments, but do not require telomere clustering in the bouquet formation. The basis for the requirements of ATP and actin filaments are not clear. Examination of the pairing consequences in strains disrupted for actin motor activity may clarify this requirement. Some preliminary time-lapse microscopy indicates that Latrunculin A treatment disrupts chromosome motion, while no mutants examined thus far share this phenotype (data not shown). *spo11* mutants, in fact, while massively defective for successful pairing, do not

show gross movement defects by live cell time-lapse microcopy, indicating that control over chromosome movement is achieved through a mechanism that is independent of DSBs and that perhaps chromosome movement and pairing specificity are independently regulated to achieve meiotic pairing (data not shown).

Dissecting the roles of cohesin and SC components in pairing

DNA replication and the presence of a sister chromatid are dispensible for proper pairing, but the meiotic factor Rec8, best characterized for its role in sister chromatid cohesion, also plays a role in pairing. Rec8 appears to contribute to proper pairing at most loci, though is less important for pairing at the *LEU2* DSB hotspot. Characterization of more sites will be important to determine the reason for the unusual pairing behavior at *LEU2.* Of the five loci examined in this chapter, *LEU2* is unusual not only in the mild pairing defect in *rec8Δ* cells, but also the generally high level of pairing at this locus even in early prophase. It will be important to assay other DSB hotspots for pairing behavior, as well as other loci surrounding *LEU2* on Chromosome 3 to determine the reason for these variations.

Synaptonemal complex components Hop1 and Zip1 also appear to contribute to successful pairing. These relationships require further study. Hop1 is, along with Rec8, a component of chromosome axes or LEs, structures formed as chromosomes compact in prophase. Both Hop1 and Rec8 show chromosome pairing defects. Utilization of various non-deletion mutants of

these factors, as well as examination of the roles of Hop1 and Rec8 at additional chromosomal loci will be helpful in this effort. Zip1, the major component of transverse elements of the SC, appears to contribute to pairing in a locus-specific manner. More precisely, Zip1 seems to promote pairing of a centromere-proximal locus, while not contributing significantly to pairing of an arm locus. It will be important to examine further examples of centromere-proximal and centromere-distal sites to determine if this is indeed a general pheonomenon. Further, if Zip1 is indeed important for centromere pairing specifically, other components of the SIC centromere coupling complex such as Zip2 and Zip3 should be examined for a potential role in pairing as well.

Time-lapse studies of chromosome movement during pairing

Movies generated by time-lapse microscopy of live meiotic cells represent a powerful tool for dissecting pairing mechanism. Thus far I have performed only a cursory analysis of such movies, but believe that this is an area of study that could contribute valuable insight into processes involved in pairing. Mathematical modeling of the paths followed by homologous loci as they pair will be necessary to further these studies as preliminary analysis suggests complex and indirect motion of homologs with respect to each other during this process.

DSBs and pairing: findings and future studies

The process examined thus far that appears to be most important to proper completion of pairing is DSB formation. There has been a general belief that DSBs contribute to meiotic pairing, but the extent of this contribution has been controversial. My studies indicate DSBs to be essential to proper pairing. *spo11* mutants and other DSB-defective strains (such as *clb5Δclb6Δ*) show the largest pairing defect of any strains examined here. Dissection of this role is difficult, however, as cells initiate hundreds of DSBs early in meiosis and the position of these DSBs is relatively random (Blitzblau, Bell et al. 2007). Thus for any single live cell, it is difficult to know where DSBs exist and which might be contributing to pairing.

These studies indicate that cells require only a fraction of the number of DSBs that are normally formed to initiate recombination. The significance of this finding is unclear. Do only a portion of DSBs contribute to homology search normally? How might these DSBs be special? As mentioned above, *spo11* cells are unable to achieve proper pairing, but by time-lapse microscopy, homologous sites do not show any gross movement defects compared to wild-type cells.

Taken together with the observations that strand-invasion of resected DSBs in recombination generally involves only a few hundred nucleotides, and the existence of repetitive DNA present in even the relatively simple budding yeast genome, it seems likely that there are multiple steps to the pairing process. In the first step, I propose that homologs are moved in proximity to

each other by processes requiring actin filaments and ATP. The ability of homologs to sort together is mysterious, but could involve the presence of generally similar chromosomal structure rather than DNA-DNA interactions. Once homologs have been sorted to the same region, strand invasion by newly resected DSBs might assist in alignment and locking of paired homologs together. The use of screens to identify factors that might contribute to the first, sorting step of this pairing model will be invaluable. In the concluding chapter of this thesis, I suggest two screens that might assist in this endeavor. I further discuss in the next chapter a study to probe the relationship between a single DSB and local and global pairing. The use of strains with one engineered DSB and a variety of GFP marked homologous loci will be useful for these studies (Neale, Ramachandran et al. 2002).

Conclusions and perspectives on pairing

Meiotic pairing is a process that I have found to be continuously fascinating and intermittently frustrating throughout my graduate career. This is also the process that I have worked on that I believe holds the most promise for discovery of novel cellular mechanisms and a deeper understanding of meiosis as a whole. Meiotic segregation is based on the ability of homologs to align, recombine, and then segregate apart reductionally as occurs uniquely in Meiosis I. While huge progress has been made in understanding recombination and Meiosis I chromosome segregation, this first step of homolog alignment remains remarkably mysterious. I have great hope that pairing mechanism will be

deconstructed in the near future and that the studies discussed in this thesis will be of some assistance to this goal.

Materials and Methods:

Strains and Plasmids:

The strains used in this study are all derivatives of SK1. All deletions are performed using one-step gene replacement (Longtine, McKenzie et al. 1998). The GFP dots were described in (Straight, Belmont et al. 1996; Michaelis, Ciosk et al. 1997; Klein, Mahr et al. 1999). *pSCC1-CDC6* is described in (Hochwagen, Tham et al. 2005). *mer2-S30A* is described in *(Henderson, Kee et al. 2006)* and *spo11* hypomorphic alleles are described in (Henderson and Keeney 2004).

Sporulation conditions:

Cells were grown to saturation in YPD (YEP + 2% glucose) for 24 hours, diluted into YPA (YEP + 2% KAc) at OD_{600} = 0.3 and grown overnight. Cells were then washed with water and resuspended in SPO medium (0.3% KAc [pH = 7.0]) at OD_{600} = 1.9 at 30°C to induce sporulation.

Pairing assay: This is diagrammed in Figure 1. Cells with homologous tandem TetO arrays and carrying a TetR-GFP fusion protein are visualized *in vivo* with a Zeiss Axioplan 2 microscope. The number of cells with one GFP dot (indicating closely aligned homologs) versus two GFP dots (indicating distant homologs) is used as a metric of pairing status.

Flow cytometry: Flow cytometric analysis of total cellular DNA content was performed as described in (Visintin et al., 1998).

Live cell microscopy: Cells are treated and imaged as described in (Nachman, Regev et al. 2007).

References:

Benjamin, K. R., C. Zhang, et al. (2003). "Control of landmark events in meiosis by the CDK Cdc28 and the meiosis-specific kinase Ime2." Genes Dev **17**(12): 1524-39.

Blitzblau, H. G., G. W. Bell, et al. (2007). "Mapping of meiotic single-stranded DNA reveals double-stranded-break hotspots near centromeres and telomeres." Curr Biol **17**(23): 2003-12.

Chikashige, Y., C. Tsutsumi, et al. (2006). "Meiotic proteins bqt1 and bqt2 tether telomeres to form the bouquet arrangement of chromosomes." Cell **125**(1): 59-69.

Diaz, R. L., A. D. Alcid, et al. (2002). "Identification of residues in yeast Spo11p critical for meiotic DNA double-strand break formation." Mol Cell Biol **22**(4): 1106-15.

Forsburg, S. L. (2002). "Only connect: linking meiotic DNA replication to chromosome dynamics." Mol Cell **9**(4): 703-11.

Henderson, K. A., K. Kee, et al. (2006). "Cyclin-dependent kinase directly regulates initiation of meiotic recombination." Cell **125**(7): 1321-32.

Henderson, K. A. and S. Keeney (2004). "Tying synaptonemal complex initiation to the formation and programmed repair of DNA double-strand breaks." Proc Natl Acad Sci U S A **101**(13): 4519-24.

Hochwagen, A. and A. Amon (2006). "Checking your breaks: surveillance mechanisms of meiotic recombination." Curr Biol **16**(6): R217-28.

Hochwagen, A., W. H. Tham, et al. (2005). "The FK506 binding protein Fpr3 counteracts protein phosphatase 1 to maintain meiotic recombination checkpoint activity." Cell **122**(6): 861-73.

Hochwagen, A., G. Wrobel, et al. (2005). "Novel response to microtubule perturbation in meiosis." Mol Cell Biol **25**(11): 4767-81.

Jin, Q. W., J. Fuchs, et al. (2000). "Centromere clustering is a major determinant of yeast interphase nuclear organization." J Cell Sci **113 (Pt 11)**: 1903-12.

Keeney, S. and M. J. Neale (2006). "Initiation of meiotic recombination by formation of DNA double-strand breaks: mechanism and regulation." Biochem Soc Trans **34**(Pt 4): 523-5.

Klein, F., P. Mahr, et al. (1999). "A central role for cohesins in sister chromatid cohesion, formation of axial elements, and recombination during yeast meiosis." Cell **98**(1): 91-103.

Lee, B. and A. Amon (2001). "Meiosis: how to create a specialized cell cycle." Curr Opin Cell Biol **13**(6): 770-7.

Longtine, M. S., A. McKenzie, 3rd, et al. (1998). "Additional modules for versatile and economical PCR-based gene deletion and modification in Saccharomyces cerevisiae." Yeast **14**(10): 953-61.

Marston, A. L. and A. Amon (2004). "Meiosis: cell-cycle controls shuffle and deal." Nat Rev Mol Cell Biol **5**(12): 983-97.

McKee, B. D. (2004). "Homologous pairing and chromosome dynamics in meiosis and mitosis." Biochim Biophys Acta **1677**(1-3): 165-80.
Michaelis, C., R. Ciosk, et al. (1997). "Cohesins: chromosomal proteins that prevent premature separation of sister chromatids." Cell **91**(1): 35-45.
Nachman, I., A. Regev, et al. (2007). "Dissecting timing variability in yeast meiosis." Cell **131**(3): 544-56.
Neale, M. J., M. Ramachandran, et al. (2002). "Wild-type levels of Spo11-induced DSBs are required for normal single-strand resection during meiosis." Mol Cell **9**(4): 835-46.
Page, S. L. and R. S. Hawley (2004). "The genetics and molecular biology of the synaptonemal complex." Annu Rev Cell Dev Biol **20**: 525-58.
Rockmill, B. and G. S. Roeder (1998). "Telomere-mediated chromosome pairing during meiosis in budding yeast." Genes Dev **12**(16): 2574-86.
Roeder, G. S. (1995). "Sex and the single cell: meiosis in yeast." Proc Natl Acad Sci U S A **92**(23): 10450-6.
Storlazzi, A., L. Xu, et al. (1995). "Crossover and noncrossover recombination during meiosis: timing and pathway relationships." Proc Natl Acad Sci U S A **92**(18): 8512-6.
Straight, A. F., A. S. Belmont, et al. (1996). "GFP tagging of budding yeast chromosomes reveals that protein-protein interactions can mediate sister chromatid cohesion." Curr Biol **6**(12): 1599-608.
Trelles-Sticken, E., M. E. Dresser, et al. (2000). "Meiotic telomere protein Ndj1p is required for meiosis-specific telomere distribution, bouquet formation and efficient homologue pairing." J Cell Biol **151**(1): 95-106.
Trelles-Sticken, E., J. Loidl, et al. (1999). "Bouquet formation in budding yeast: initiation of recombination is not required for meiotic telomere clustering." J Cell Sci **112 (Pt 5)**: 651-8.
Tsubouchi, T. and G. S. Roeder (2005). "A synaptonemal complex protein promotes homology-independent centromere coupling." Science **308**(5723): 870-3.
Weiner, B. M. and N. Kleckner (1994). "Chromosome pairing via multiple interstitial interactions before and during meiosis in yeast." Cell **77**(7): 977-91.
Yamamoto, A. and Y. Hiraoka (2001). "How do meiotic chromosomes meet their homologous partners?: lessons from fission yeast." Bioessays **23**(6): 526-33.
Zickler, D. and N. Kleckner (1998). "The leptotene-zygotene transition of meiosis." Annu Rev Genet **32**: 619-97.

Chapter 5:

Discussion and Future Directions

Recent developments in meiosis research

Meiosis research has advanced tremendously over the last several years, largely based on mechanistic studies in budding and fission yeast. There is now a general understanding of the regulation underlying step-wise loss of cohesion. The identification of Sgo1, the counterpart of *D. melanogaster MEI-S332* in yeast and humans has led to a model in which centromeric Rec8 is protected from cleavage in Meiosis I (Katis, Galova et al. 2004; Kitajima, Kawashima et al. 2004; Marston, Tham et al. 2004; Rabitsch, Gregan et al. 2004). The Sgo1-dependent protected region has been determined to be approximately 50 kilobases surrounding each centromere, and this region appears to depend solely on the presence of a core centromere sequence (Kiburz, Reynolds et al. 2005). At least a portion of Sgo1's protective activity depends on its ability to recruit the PP2A phosphatase to this centromere-proximal region (Kitajima, Sakuno et al. 2006; Riedel, Katis et al. 2006; Tang, Shu et al. 2006).

Recent work has also provided greater understanding of prophase events, including recombination mechanism, prophase chromosome dynamics and the meiotic recombination checkpoint. For example, identification of the Zmms aided in the understanding of the types of recombination pathways present in prophase and clarified inaccuracies in the classic Szostak recombination model (Borner, Kleckner et al. 2004; Lynn, Soucek et al. 2007). Identification of Mus81, the sHJ resolvase involved in one pathway of crossover

recombination, was a major breakthrough in understanding of recombination mechanism (Whitby 2005). Using advanced live-cell microscopy, work from several groups has shown the importance of telomere tethering and cytoskeleton to chromosome movement in meiotic prophase (M. Dresser and N. Kleckner, personal communication; Nachman, Regev et al. 2007). Additionally, details of recombination checkpoint signaling have been elucidated, including identification of Fpr3, a factor involved in allowing cells to "cut their losses" and adapt to this checkpoint under conditions of persistent damage (Hochwagen, Tham et al. 2005; Hochwagen and Amon 2006).

Summary of key conclusions of this thesis

In my thesis work, I have aimed to contribute to the ongoing elucidation of meiotic chromosome segregation mechanisms. Using *S. cerevisiae*, I have worked to address several basic questions. What role does Rec8 phosphorylation play in stepwise loss of cohesion in meiosis? How does Rec8 function to promote prophase progression? How do homologs pair? I will now summarize the results presented in this thesis that help clarify answers to these questions.

The roles of Rec8 phosphorylation and recombination in cohesin cleavage

The meiotic cohesin Rec8 has been reported to be heavily phosphorylated, with at least a portion of this phosphorylation being dependent on the Polo kinase Cdc5 (Lee and Amon 2003). We identified 25 *in vivo* Rec8 phospho-sites and determined 11 of these sites to be Cdc5-dependent. With these sites, we were able to determine the first *in vivo* Cdc5 phosphorylation motif. We find that Cdc5-dependent and non-Cdc5-dependent sites contribute to the efficiency of Rec8 cleavage at Meiosis I. Mutation of 17 Rec8 phospho-sites to Alanines results in a delay in the cleavage of Rec8 and accumulation of cells in metaphase I, indicating that phosphorylation primes Rec8 for cleavage. Mutation of fewer sites at once did not result in a metaphase I defect, indicating that it is likely bulk phosphorylation rather than individual phospho-sites that is important to promote Rec8 cleavage by Separase. Importantly, the cells that accumulate in metaphase I are largely positive for Securin, indicating that the defect is a direct result of a difficulty cleaving Rec8 and not in progression through the metaphase I to anaphase I transition.

The defect in Rec8 cleavage in *rec8-17A* cells is dependent on recombination initiation by Spo11. We find that this is a result of the regulation of arm cohesion loss in Meiosis I by recombination. It appears that homolog linkage through recombination creates tension that is necessary for satisfaction of the spindle checkpoint and cleavage of Rec8 in Meiosis I. In the absence of

recombination, all cohesin is removed in Meiosis II, where Rec8 cleavage is independent of Rec8 phosphorylation status. We were able to show that phosphorylation of Serine 521 is centromere-excluded at Meiosis I and not present at Meiosis II. This further supports the assertion that Meiosis I Rec8 cleavage (normally of arm cohesins only) is promoted by bulk phosphorylation, but that Meiosis II Rec8 cleavage (normally of centromere-proximal cohesins) is independent of phospho-status (See Figure 1 for a model).

Figure 1

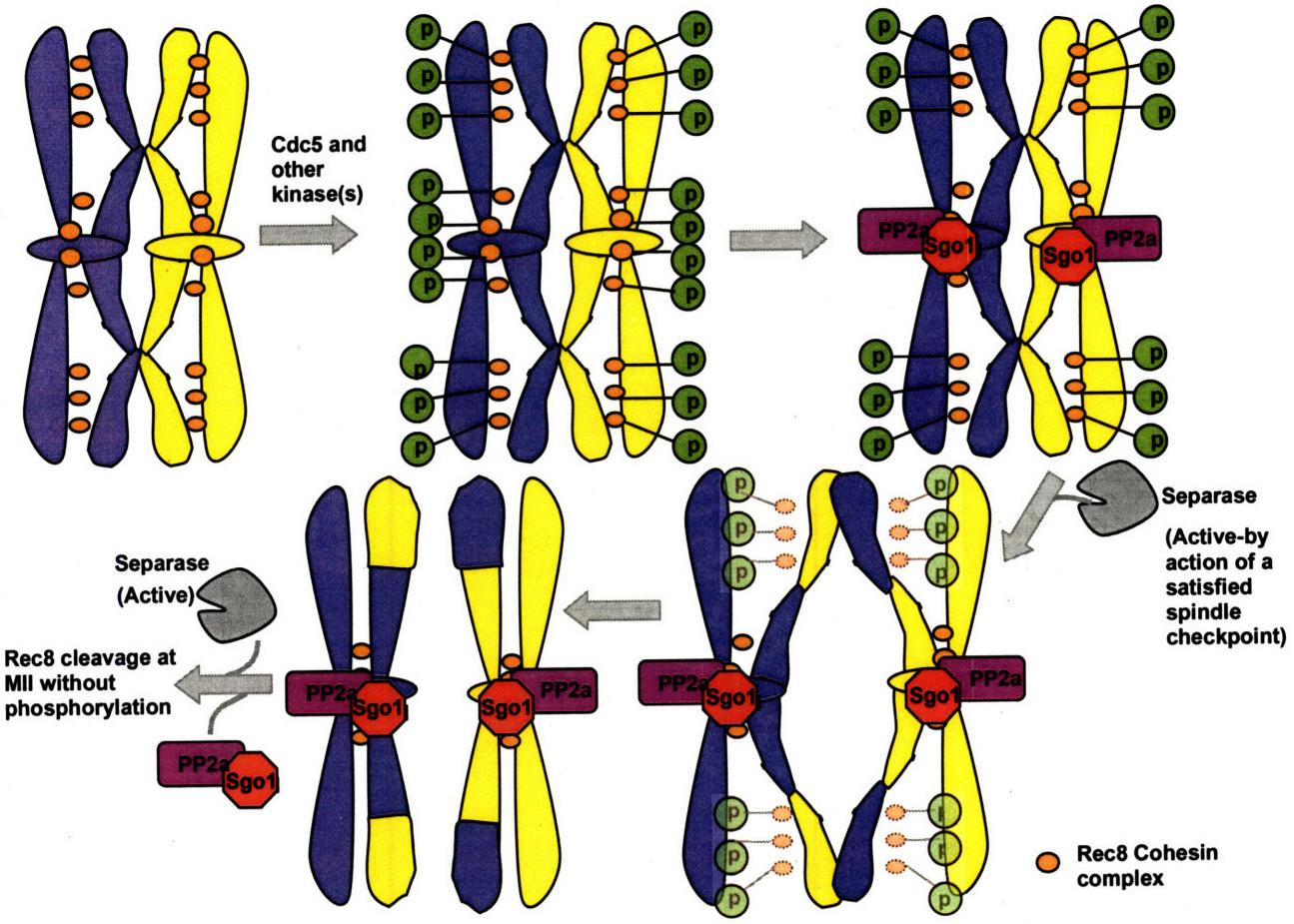

Figure 1: A model for stepwise loss of cohesion in meiosis
Rec8 is heavily phosphorylated by Cdc5 and other kinases at some point prior to metaphase I. It is not clear whether centromere-proximal Rec8 cohesin complexes are phsophorylated and then dephosphorylated by the action of Sgo1 and PP2a or whether arms are preferentially phosphorylated. In either case, by anaphase I, arm cohesins are phosphorylated. Separase is activated by a satisfied spindle checkpoint that senses homolog attachment through chiasmata. Separase preferentially cleaves phosphorylated arm cohesins at anaphase I, while centromere-proximal cohesins are protected by Sgo1. Sgo1 leaves chromosomes prior to anaphase II, at which point Rec8 cleavage is no longer influenced by its phosphorylation. The remaining cohesin is now removed by Separase that is again activated by a satisfied spindle checkpoint.

The role of Rec8 and its phosphorylation in prophase progression

Our work on the role of Rec8 phosphorylation in cohesin removal also identified combinations of phospho-sites that, when mutated to Alanines, resulted in prophase defects but no metaphase to anaphase transition defects. Based on the separation of Rec8 function provided by these mutants, we revisited the role of Rec8 in prophase, finding that this function of Rec8 is independent of DNA replication, Cdc5 phosphorylation, and Rec8 cleavage. We find that Rec8 protein and its phosphorylation contribute to assembly of the transverse elements of the SC, but that Rec8 protein and not its phosphorylation contribute to lateral element formation. We additionally determine that post-replicatively associated Rec8 and DSB formation are together capable of promoting SC assembly. We conclude that Rec8 performs functions at multiple meiotic stages, thus promoting linkage and directionality of the meiotic program.

A basic characterization of meiotic pairing

A final series of studies discussed in this thesis concerns the phenomenon of homolog pairing in meiotic prophase. I performed a basic characterization of pairing, finding the motion of pairing homologs to be

complex, indirect, and dependent on the presence of actin filaments. We find that pairing is an active process that is fully dependent on DSB formation, though cells may pair normally with 20-30% of normal DSBs present. Pairing is surprisingly independent of the presence of a sister chromatid or the process of DNA replication, though cohesin and SC components do appear to be important for this process.

Unanswered questions and future directions

Despite the recent significant progress in understanding cellular mechanisms that contribute to meiotic chromosome segregation, there are still many open questions. There exists a basic framework for understanding stepwise loss of cohesion, but mechanistic understanding is still weak. This is also the case for the regulation of sister coorientation, suppression of a second S-phase between MI and MII, and events that govern exit from the segregation phases. As for prophase, many details of recombination mechanism have been elucidated, but the question of coregulation of prophase processes remains mysterious. How does a DSB get sorted into a specific recombination pathway? How does the cell coordinate recombination and SC formation? What does the SC do? The biggest mystery remaining to be addressed in meiotic research, however, concerns pairing. How do cells effectively and reproducibly pair homologous chromosomes? In the following sections, I will discuss some of these open questions with a focus on approaches that may be useful to future research in these areas.

The mechanism of Sgo1 action in cohesin regulation

Stepwise loss of cohesion in meiosis has been an active area of research for several years. The existence of *MEI-S332* in *Drosophila* led many to speculate on the existence of a MI protector of centromeric Rec8 in yeast and other organisms before Sgo1 was identified by three groups in 2004 as playing this role (Kerrebrock, Moore et al. 1995; Katis, Galova et al. 2004; Kitajima, Kawashima et al. 2004; Marston, Tham et al. 2004; Rabitsch, Gregan et al. 2004). Subsequent research has shown Sgo1 to function partially through recruitment of PP2A phosphatase to centromeric regions prior to MII (Kitajima, Sakuno et al. 2006; Riedel, Katis et al. 2006; Tang, Shu et al. 2006). The extent to which Sgo1 function is mediated by PP2A, however, is controversial. While Riedel and colleagues find artifical tethering of PP2A to be sufficient for essentially full Rec8 protection, Kitajima and colleagues found Sgo1 to have protective activity that is independent of PP2A. My work is more consistent with the findings of Kitajima. Based on several experiments, I believe that it is likely that Sgo1 affects cohesin cleavage through mechanisms that are independent of PP2a. I will now discuss these experiments, propose a model for Sgo1 action, and suggest strategies to better elucidate Sgo1's mechanism in cohesion regulation.

Several experiments presented in Chapter 2 merit further discussion at this point. First, I presented an experiment in which I examined chromosome segregation in cells meiotically depleted for Cdc5 (*pCLB2-CDC5*) and also deleted for *SPO11* (Figure 3, Chapter 2). The rationale for this experiment was to look at metaphase I-arrested chromosomes. *SPO11* was deleted in order to remove any defects caused by incomplete recombination seen in meiotic *cdc5* mutants, in order to focus on chromosome segregation exclusively. Homologous chromosomal loci were visualized with the Tet-GFP dot system discussed previously with Tet Operators inserted on homologous chrosomes, adjacent to the centromere of chromosome 5. These cells arrest in metaphase I due partially to the inability to phosphorylate and cleave Rec8. I will discuss in greater detail in a later section the basis for this conclusion and additional functions of Cdc5 at the metaphase I to anaphase I transition.

pCLB2-CDC5 spo11Δ cells show a lack of homolog segregation, as judged by only a single GFP dot or two closely positioned GFP dots representing adjacent homologs in 85% of cells after 10 hours in sporulation conditions. In contrast, when isogenic cells were also meiotically depleted for Sgo1 (*pCLB2-SGO1*), homologs were seen to segregate apart, as judged by distant GFP dots in 51% of cells after 10 hours in sporulation conditions. Correlating with this apparent chromosome segregation in *pCLB2-CDC5 spo11Δ pCLB2-SGO1* cells, anaphase I spindles were observed in these cells in large numbers and cells achieved over 30% separated DAPI masses by 10

hours compared to essentially no anaphase I spindles or separated DAPI masses in *pCLB2-CDC5 spo11Δ* cells. Further, when these two strains were assayed for Rec8 cleavage, the delay seen in *pCLB2-CDC5 spo11Δ* cells compared to *spo11Δ* cells is alleviated in *pCLB2-CDC5 spo11Δ pCLB2-SGO1* cells. Finally, when cells were spread and analyzed for Rec8 localization, *pCLB2-CDC5 spo11Δ pCLB2-SGO1* cells showed an increased population with no Rec8 visible on chromosomes compared to *pCLB2-CDC5 spo11Δ* cells. It is important to note that in *pCLB2-CDC5 spo11Δ* cells Rec8 remains fully present along the length of the chromosomes and that chromosomes do not separate even at late timepoints. This contrasts significantly with the case where these cells are also depleted for Sgo1, resulting in decreased Rec8 visible on chromatin and substantial separation of chromosomes.

These results support a model in which Sgo1 regulates cleavage of arm and centromeric Rec8. If Sgo1 were merely protecting cleavage of centromeric Rec8, its removal might lead to separated centromeric GFP dots due to premature centromeric Rec8 cleavage. This scenario could also yield early Rec8 cleavage by Western blot analysis, where the early population of cleavage product seen in *pCLB2-CDC5 spo11Δ pCLB2-SGO1* cells solely represents centromeric Rec8. A simple role of Sgo1 as a protector of centromeric Rec8 would not, however, yield fully separated DAPI masses in *pCLB2-CDC5 spo11Δ pCLB2-SGO1* cells or an increase in the number of cells with no Rec8 on

chromosomes when compared to *pCLB2-CDC5 spo11Δ* cells. These two results imply that Sgo1 regulates the removal of **all** Rec8 from chromosomes.

A second series of experiments further support a model in which Sgo1 affects total cohesin cleavage. I described in Chapter 2 that cells in which 17 of Rec8's phosphorylation sites are mutated to non-phosphorylatable residues *(rec8-17A)* show a delay in Rec8 cleavage by Western blot analysis when compared to wild-type cells. When *rec8-17A* cells are also depleted for Sgo1, however, this cleavage delay is rescued (Figure 3, Chapter 2). Additionally, the metaphase I accumulation seen in *rec8-17A* cells is not present in *rec8-17A pCLB2-SGO1* cells. If Rec8 phosphorylation of arm cohesins promotes their cleavage in Meiosis I, as is the model supported by significant data presented in Chapter 2, and Sgo1 merely protects centromeric cohesin at Meiosis I, then depletion of Sgo1 in a *rec8-17A* background should not rescue the metaphase I delay in *rec8-17A* cells. These cells should still be unable to efficiently cleave arm cohesins and should thus remain delayed in metaphase I. These data are more consistent with a model in which Sgo1 regulates the cleavage of arm and centromeric cohesin.

How might Sgo1 regulate all cohesin cleavage? To begin to answer this question, it is useful to consider an experiment performed by Kiburz and colleagues, who found that depletion of Sgo1 rescued the metaphase I arrest seen in cells depleted for the APC/C subunit Cdc20. Cdc20 activates the APC to degrade Securin and therefore activate Separase at the metaphase to anaphase

transitions. Depletion of Cdc20 results in high levels of Securin, the absence of Rec8 cleavage and metaphase I arrest. Additional depletion of Sgo1 results in separated homologs, as judged by GFP dot analysis and the appearance of anaphase I spindles. Securin levels, however, remain high in this strain (Kiburz, Amon et al. 2008). Therefore, it appears that Sgo1 depletion rescues the metaphase I arrest in Cdc20 cells at a step downstream of Securin inhibition of Separase. These data would be consistent with models in which Sgo1 either inhibits Separase in a Securin-independent manner or directly regulates the "cleavability" of arm Rec8.

Which of these possibilities is more likely? A major reason that Sgo1 has been thought to specifically regulate centromeric Rec8 is that centromeres are the site of Sgo1 DNA localization (Katis, Galova et al. 2004; Kitajima, Kawashima et al. 2004; Marston, Tham et al. 2004; Rabitsch, Gregan et al. 2004). In fact, Sgo1 specifically colocalizes with the population of Rec8 that is maintained until Meiosis II (Kiburz, Reynolds et al. 2005). Therefore, it seems unlikely that Sgo1 could directly regulate arm Rec8. It is possible, however, that Sgo1 regulates Separase activity through a mechanism yet to be determined. This is the model that is most consistent with the body of data available on Sgo1 function. One can imagine that Sgo1 results in modification of Separase such that Separase preferentially cleaves phosphorylated Rec8, but is inhibited for cleavage of hypo-phosphorylated Rec8. This would then result in protection of centromeric Rec8 at Meiosis I. Sgo1 then leaves centromeres prior to metaphase II, at which

time Separase can now cleave all remaining Rec8, regardless of phosphorylation status.

Through such a mechanism, Sgo1 would act in two separate ways to protect centromeric Rec8. It would recruit PP2a to keep centromeric Rec8 in a hypo-phosphorylated state and enforce preferential cleavage of hyper-phosphorylated (arm) Rec8. It is interesting to note that PP2a has been suggested to have a role in regulation of mitotic exit, through both the MEN (Mitotic Exit Network) and the FEAR (Cdc Fourteen Anaphase Release) network (Wang and Ng 2006; Forester, Maddox et al. 2007). As Esp1 is a component of the FEAR network (Stegmeier, Visintin et al. 2002), it is possible that PP2a is involved in regulating Esp1 in this context as well, though the regulatory subunit of PP2a used in enforcing Sgo1 activity is different than the subunit apparently involved in mitotic exit.

In order to test this model for Sgo1 action, a number of experimental strategies would be informative. The simplest mode in which Sgo1 might regulate Separase would be through direct interaction. Co-immunoprecipitations (Co-IPs) of these two proteins would support this model. Development of an *in vitro* assay for Separase activity would also be useful in assessing the likelihood of modification of Separase protease activity by Sgo1. Additionally, structure/function analysis of Sgo1 could aid in understanding the mechanism of this protein. Thus far the majority of data regarding Sgo1 activity is genetic. Until the above-described or other experiments are performed to gain better

biochemical and molecular understanding of Sgo1, it is difficult to confirm or discard the model that I propose above for Sgo1 action.

Rec8 function

There are also still significant questions regarding the mechanisms by which Rec8 functions. Presumably Rec8's role in prophase is related to its status as a core component of chromosome axes and Lateral Elements (LEs). The fact that Rec8 phosphorylation appears to contribute to SC assembly, however, implies either that phosphorylation of Rec8 significantly alters the structure of the protein and thus the proper structure of LEs, or that Rec8 phosphorylation is involved in signaling that contributes to SC assembly and prophase progression. The fact that Hop1 appears to assemble normally in Rec8 phospho-mutants that show significant prophase delays supports a signaling role for some of these phosopho-sites, but much more analysis is necessary to make a conclusive statement on the matter. Structural studies could be very useful in understanding SC assembly in wild-type cells and various *rec8* mutant cells. Also, we do not yet know anything about the structure of Rec8.

The vast majority of studies of Rec8 phosphorylation that are described in this thesis involve analysis of multiple phospho-sites at once. This was done for two chief reasons. Firstly, with one exception, the few cases in which single

Rec8 phospho-sites were analyzed resulted in no discernable mutant phenotype by assays performed at that time. Additionally, the sheer number of *in vivo* phospho-sites identified on Rec8 made a detailed analysis of all single and small combinations of sites technically challenging. It would, however, be extremely informative to perform such experiments in order to better understand the mechanisms by which Rec8 phosphorylation influences its cleavage and prophase role. Further, I have described experiments that suggest that although Rec8 is heavily phosphorylated by Cdc5, this is likely not the only kinase responsible for regulation of Rec8 cleavage and is probably not at all responsible for regulation of Rec8's prophase role. Identification of the kinases responsible for Rec8's non-Cdc5 phospho-sites would be extremely helpful in further dissecting Rec8 regulation.

Cdc5 function at the metaphase I to anaphase I transition

While Rec8 is regulated by phosphorylation of kinases other than Cdc5, Cdc5 is also important for phosphorylation of factors other than Rec8. Cdc5 has been shown as important for resolution of dHJs to complete recombination and is also a component of the FEAR network that regulates mitotic exit and also the transition between meiotic divisions (Stegmeier, Visintin et al. 2002; Clyne, Katis et al. 2003). I have performed recent experiments that suggest Cdc5 has additional roles at the metaphase I to anaphase I transition. Work originally done

by Lee and Amon showed that meiotic depletion of Cdc5 results in metaphase I-arrested cells that are delayed in Rec8 cleavage. I have performed recent experiments that suggest that even in the absence of Rec8, Cdc5-depleted cells are still largely arrested in metaphase I (data not shown). Given the large number of cellular roles already attributed to Cdc5 activity, it is not surprising that Cdc5 might perform multiple roles at the metaphase I to anaphase I transition. Identifying these roles is challenging, however. Cdc5 is extremely promiscuous *in vitro,* making much traditional biochemical analysis of Cdc5 function difficult. The best way, then, to analyze Cdc5 cellular roles appears to be through well-designed genetic experiments. It will be important to carefully determine whether Securin is degraded in Cdc5-depleted, metaphase I-arrested cells to better place Cdc5's role at the metaphase I to anaphase I transition in relation to the spindle checkpoint. *In vivo* phosphorylation assays would also be very informative, although strategies to perform such experiments are still in their infancy.

The mechanism of meiotic pairing

Arguably the biggest challenge remaining in understanding basic meiotic principles is to elucidate pairing mechanism. This is an area that has been of major interest to me throughout my graduate career. I have worked to characterize the phenomena involved in pairing, but there are many more

experiments that should be done to elucidate the mechanisms behind pairing. The most informative experiments at this point fall into three categories. First, a well-designed screen should be able to identify pairing factors. Second, analysis of meiotic chromosome movement and processes involved in this movement would complement the third approach, which focuses on how DSBs promote homolog interactions.

Using screens to elucidate pairing mechanism

I propose two screens as potentially useful to identify pairing factors. The first screen is based on the concept that there are likely multiple levels of chromosome recognition. Due to the importance of DSBs and strand invasion factors to pairing, it seems that these early recombination steps are used to test homologous sites before stable pairing is established. It seems unlikely, however, that repeated, random invasion and searching for homologus sequences to each resected DSB site is the only method by which homologs are aligned.

One can imagine that it would be much simpler for cells to initially roughly align homologous chromosomes and then simply use localized strand invasion as a way of refining this alignment. This is especially true when one considers that the yeast genome contains repetitive elements such as transposons that would cause false alignment of homologs if local invasion were enough to lock homologs together. Additionally, in the case of more complex eukaryotes, the

sheer quantity of repetitive DNA would make homolog alignment based purely on local homology untenable. Therefore, with the assumption that homologs are first roughly aligned and then stabilized by invasion of resected DSB sites, a screen based on inappropriate alignment and ectopic recombination could identify factors involved in the first rough alignment.

For this approach (Figure 2), one would identify genes that when deleted result in an increase in association (and thus recombination) of non-homologously integrated heteroalleles of an auxotrophic marker. This background could be crossed into each strain of the yeast non-essential deletion collection. Complete strains could be induced to enter meiosis, allowed to "pair" and undergo recombination, then returned to mitotic growth and assessed for increased frequency of prototrophy for the given marker. It may be additionally informative to perform a similar screen, but using mutagenesis of a heteroallelic background as discussed above rather than systematic deletions of non-essential genes. This approach would allow identification of essential cellular components that may play a role in pairing. Using either mutagenesis or the deletion collection library, this screen has several caveats, most importantly its basis on the hypothesis that pairing is a chromosome-wide event rather than the sum of numerous local interactions.

A less-biased screen involves introducing homologous GFP chromosome tags into the approximately 4500 strains of the yeast non-essential deletion library and arresting cells in prophase with deletion of *NDT80*. One could then identify through microscopic screening and the pairing assay described in

Chapter 4, Alternatively, as discussed above, it may be useful to perform an unbiased screen using mutagenesis to create diverse mutant alleles, rather than relying on deletions of non-essential genes exclusively to provide insight into pairing mechanism.

Figure 2

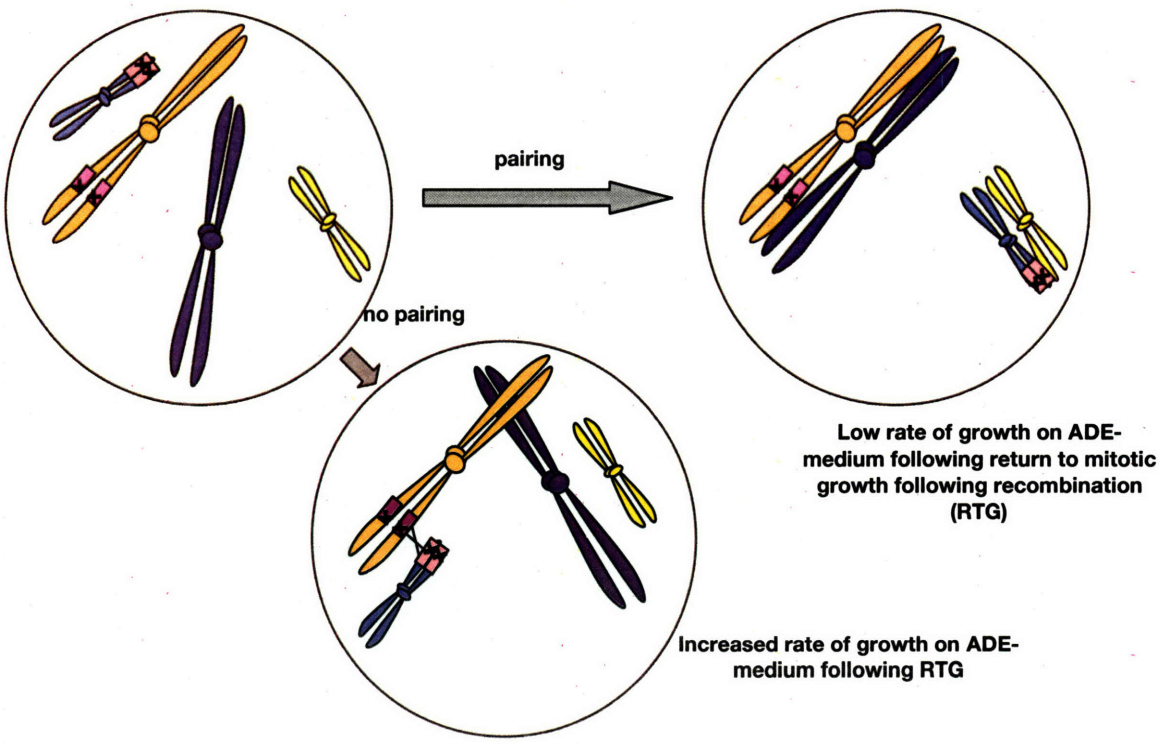

Figure 2: A screen to identify pairing factors
Cells containing heteroalleles of *ADE2* are made to initiate meiosis, complete recombination and are then returned to mitotic growth in rich medium lacking Adenine. Cells will form colonies if they experience recombination between the *ade2* heteroalleles, creating a functional *ADE2* gene and the ability to grow on medium lacking Adenine. As the heteroalleles are at non-homologous genomic sites, recombination between them is expected to be elevated in mutants that do not pair homologs correctly. Note that two pairs of homologs of different size are shown above, with "mom chromosomes" in blue and "dad chromosomes" in yellow.

and represent heteroalleles of auxotrophic marker (*ADE2*)

Investigation of chromosome motion and the cytoskeleton in pairing

From preliminary experiments, it appears that F-actin and microtubules play a role in pairing. Further characterization of these role, including investigation of candidate motors and kinetechore/microtubule interactions would be interesting to better understand how cytoskeletal elements influence pairing. Additionally, chromosome movement during pairing can be studied in more detail through expansion of preliminary live time-lapse microscopy investigations to include modeling of chromosome paths as they pair as well as comparison of these patterns at different chromosomal loci and under various mutant and drug-treatment conditions. Understanding of movement speeds and patterns may help elucidate the mechanisms responsible for these effects, as well as characterize the steps at which various pairing-associated genes might act.

Dissection of the relationship between DSBs and homolog pairing

Thus far, the single process that appears to most significantly contribute to pairing is DSB formation. In order to understand the essential role that DSBs play in allowing chromosomes to successfully align, utilization of strains carrying various single engineered DSBs, homologous GFP dots, and catalytically-inactive Spo11 (Neale, Ramachandran et al. 2002) could be used to answer a number of questions, including:

i. Is pairing initiated near a DSB which then allows the rest of the chromosome to "zip up" (Zipper model) or does creation of a DSB along a chromosome somehow license homologs to align simultaneously along their length (Snap model)?

ii. What are the positional effects of DSBs? Do centromere-proximal, telomere-proximal and arm DSBs show different abilities to induce pairing?

iii. Is there any global effect of a DSB on pairing? Does a break on one chromosome influence pairing on another?

iv. Are certain chromosomal regions more receptive to pairing in response to a DSB?

v. Does pairing occur in an "all or none" or graded fashion?

Using engineered breaks in simplified situations to answer these questions would provide a more detailed dissection of the relationship between DSBs and pairing and thus assist in constructing mechanistic models of the pairing process.

Concluding thoughts

Meiosis remains an exciting field of study, with unique biological problems that cells must solve in order to achieve the complex chromosomal dance that results in gamete formation. Recent work has shed significant light on mechanisms involved in meiosis, including notably recombination, step-wise

cohesion loss and coorientation of sister kinetechores. Much more work is needed to clarify these mechanisms, and to begin to address the more mysterious meiotic process of pairing. The apparent conservation of meiotic processes from yeast to plants to animals makes the study of meiotic mechanisms not only intellectually fascinating, but also potentially useful to the understanding of human conditions including infertility and mental retardation.

References:

Borner, G. V., N. Kleckner, et al. (2004). "Crossover/noncrossover differentiation, synaptonemal complex formation, and regulatory surveillance at the leptotene/zygotene transition of meiosis." Cell **117**(1): 29-45.

Clyne, R. K., V. L. Katis, et al. (2003). "Polo-like kinase Cdc5 promotes chiasmata formation and cosegregation of sister centromeres at meiosis I." Nat Cell Biol **5**(5): 480-5.

Forester, C. M., J. Maddox, et al. (2007). "Control of mitotic exit by PP2A regulation of Cdc25C and Cdk1." Proc Natl Acad Sci U S A **104**(50): 19867-72.

Hochwagen, A. and A. Amon (2006). "Checking your breaks: surveillance mechanisms of meiotic recombination." Curr Biol **16**(6): R217-28.

Hochwagen, A., W. H. Tham, et al. (2005). "The FK506 binding protein Fpr3 counteracts protein phosphatase 1 to maintain meiotic recombination checkpoint activity." Cell **122**(6): 861-73.

Katis, V. L., M. Galova, et al. (2004). "Maintenance of cohesin at centromeres after meiosis I in budding yeast requires a kinetochore-associated protein related to MEI-S332." Curr Biol **14**(7): 560-72.

Kerrebrock, A. W., D. P. Moore, et al. (1995). "Mei-S332, a Drosophila protein required for sister-chromatid cohesion, can localize to meiotic centromere regions." Cell **83**(2): 247-56.

Kiburz, B. M., A. Amon, et al. (2008). "Shugoshin Promotes Sister Kinetochore Biorientation in Saccharomyces cerevisiae." Mol Biol Cell **19**(3): 1199-209.

Kiburz, B. M., D. B. Reynolds, et al. (2005). "The core centromere and Sgo1 establish a 50-kb cohesin-protected domain around centromeres during meiosis I." Genes Dev **19**(24): 3017-30.

Kitajima, T. S., S. A. Kawashima, et al. (2004). "The conserved kinetochore protein shugoshin protects centromeric cohesion during meiosis." Nature **427**(6974): 510-7.

Kitajima, T. S., T. Sakuno, et al. (2006). "Shugoshin collaborates with protein phosphatase 2A to protect cohesin." Nature **441**(7089): 46-52.

Lee, B. H. and A. Amon (2003). "Role of Polo-like kinase CDC5 in programming meiosis I chromosome segregation." Science **300**(5618): 482-6.

Lynn, A., R. Soucek, et al. (2007). "ZMM proteins during meiosis: crossover artists at work." Chromosome Res **15**(5): 591-605.

Marston, A. L., W. H. Tham, et al. (2004). "A genome-wide screen identifies genes required for centromeric cohesion." Science **303**(5662): 1367-70.

Nachman, I., A. Regev, et al. (2007). "Dissecting timing variability in yeast meiosis." Cell **131**(3): 544-56.

Neale, M. J., M. Ramachandran, et al. (2002). "Wild-type levels of Spo11-induced DSBs are required for normal single-strand resection during meiosis." Mol Cell **9**(4): 835-46.

Rabitsch, K. P., J. Gregan, et al. (2004). "Two fission yeast homologs of Drosophila Mei-S332 are required for chromosome segregation during meiosis I and II." Curr Biol **14**(4): 287-301.

Riedel, C. G., V. L. Katis, et al. (2006). "Protein phosphatase 2A protects centromeric sister chromatid cohesion during meiosis I." Nature **441**(7089): 53-61.

Stegmeier, F., R. Visintin, et al. (2002). "Separase, polo kinase, the kinetochore protein Slk19, and Spo12 function in a network that controls Cdc14 localization during early anaphase." Cell **108**(2): 207-20.

Tang, Z., H. Shu, et al. (2006). "PP2A is required for centromeric localization of Sgo1 and proper chromosome segregation." Dev Cell **10**(5): 575-85.

Wang, Y. and T. Y. Ng (2006). "Phosphatase 2A negatively regulates mitotic exit in Saccharomyces cerevisiae." Mol Biol Cell **17**(1): 80-9.

Whitby, M. C. (2005). "Making crossovers during meiosis." Biochem Soc Trans **33**(Pt 6): 1451-5.